

Preparing to Resume a Permissive Left-Turn Task: Impact of Takeover  
Requests, Non-Driving Related Tasks, and Control Transitions on  
Traffic Operations and Safety

By

Lingqiao Qin

A dissertation submitted in partial fulfillment of the requirements for the degree of

Doctor of Philosophy

(Civil and Environmental Engineering)

at the

University of Wisconsin-Madison

2021

Date of final oral examination: 03/23/2021

The dissertation is approved by the following members of the Final Oral Committee:

David A. Noyce, Professor, Civil and Environmental Engineering

Soyoung (Sue) Ahn, Professor, Civil and Environmental Engineering

Bin Ran, Professor, Civil and Environmental Engineering

John D. Lee, Professor, Industrial and System Engineering

© Copyright by Lingqiao Qin  
All Rights Reserved

## **Abstract**

With the increase in the development efforts of vehicular automation, driving automation systems are expected to assist and replace human drivers to reduce traffic crashes due to human errors. Most driving automation systems to date make the task of driving a vehicle one that is shared between the system and the driver. This research aims to contribute by advancing the understanding of driver behavior in automated driving systems to develop more feasible and reliable driving automation systems when encountering permissive left-turn maneuvers. Specifically, this research examines the control transitions from automation systems to human drivers when approaching a signalized intersection and desired left-turn maneuver with permissive left turn operations in urban environments. Permissive left turns are selected because of the inherent complexities in gap selection and traffic signal phasing determination required to safely complete this maneuver.

Throughout the proposed research, two key issues associated with control transitions will be conquered, which are:

- (1) How drivers will resume control from the automation system and complete the left-turn task at permissive left-turn signal indications; and
- (2) How control transitions affect traffic operations and safety of a signalized intersection.

To thoroughly explore these two problems, the proposed research first examines the state-of-the-art of the levels of driving automation systems and their deficiencies. Recognizing that human drivers still need to intervene the control process and to resolve certain critical situations that currently are out of automation's limits, this research focuses on the human driver's role in a SAE Level 3 driving automation system. When the AI-powered driving automation system

encounters a permissive left-turn operation at a signalized intersection, it needs to traverse the intersection efficiently and safely, or at least as well as a human driver does. Building upon the knowledge gained regarding the behavior of driving automation systems at signalized intersections, this study further examined how the vehicle control will be switched from the automation system to the human drivers. There is a need to understand the timing and the sequence of driver behavior during the takeover and the left-turn maneuvers. Therefore, the delivery of takeover requests (TORs), drivers' situational awareness, supervision over driving automation system, and takeover performances will be closely studied.

Driving automation is expected to relieve drivers from the tedium of driving, opening new ways for drivers to spend their time on things of their own interest. Accordingly, non-driving related tasks (NDRTs) that could keep drivers physically and mentally occupied from driving tasks will be utilized in this research. However, making a left turn at a permissive left-turn signal indication is complex for human drivers when traffic coming from opposing direction is heavy, gaps between vehicles are tight, or the available acceptable gaps are few. The incorporation of NDRTs is intended to simulate a more realistic future situation in which distracted human drivers must resume control before or as the driving automation fails to make a left turn. Through meta-regression analysis, this research investigates how drivers would perform permissive left-turn maneuvers with different TOR lead times while engaging in NDRTs.

After investigating the effects that NDRTs and TORs have on takeover behavior in the circumstance of permissive left turns, this research then models drivers' takeover behavior in VISSIM. The impact that the occurrence of taking-over control has on traffic operations at an intersection remains unknown. Accordingly, the second component of the proposed research is to examine the impact of the control transitions from automation to driver when approaching a

signalized intersection where the driving automation planned to make a left turn and permissive left turn operations is detected. Multiple simulation tasks are accomplished to fill this knowledge gap.

This research focuses the discussion of potential impact of takeover on traffic efficiencies on the circumstance of signalized intersections that allow for permissive left-turn maneuvers. To evaluate the throughput, delay, and queuing at an intersection where left-turning movements with mixed manual vehicles and automated driving systems are permitted, three different penetration rates of the driving automation systems will be adopted with optimized cycle lengths and signal timings.

Based on the simulation results, this research identifies the impact of control transition from automation to drivers on traffic operations at a signalized intersection. The overarching goal is to identify how drivers would reclaim control from the system to complete a left-turn task and how this transition will affect the traffic speed, queue length, delay, and safety at signalized intersections.

This research utilized results from existing control-transition studies and extended it to predict takeover behavior in new disengagement scenarios. The results of this research show that operating speed of vehicle before automation disengagement, lead time, driver age, and NDRTs are four main factors that affect drivers' takeover response. A XGBoost model is also developed that uses the identified influencing factors to predict drivers' takeover behavior. Through meta-regression analysis, Driver-automation system (DAS) modeling, and VISSIM simulation, it is shown that even though triggering events of disengagements could be very different, drivers' response to TORs is only determined by when to take over control and how much longitudinal and

lateral control is needed. There is no previous research that has similarly combined the results of multiple studies and apply them to new scenarios. This research made a significant contribution by systematically assessing study-level results and then derive high-level summary measures of takeover behavior.

Methodologically, this research has demonstrated a statistical procedure that combined data from multiple studies focusing on the same question—takeover behavior in control transitions to consolidate research evidence into a quantitative estimates of drivers' takeover behavior. How learned knowledge and quantitative estimates of takeover behavior can be incorporated in simulation is also shown in this research. A model framework capturing the interactions of a DAS during control transition in the context of PPLT scenario is also presented in this research. The core problem of a DAS in PPLT scenario is how a driver might take back control from an automation system. Automation disengagement and driver takeover behavior can be simulated by an event-based approach in VISSIM. The methods used in this research including meta-regression analysis, DAS modeling, and VISSIM simulation serve as a general framework enabling comprehensive data consolidation and knowledge enhancement and expansion. The unique model calibration method and simulation analysis in this study have potential to be used in practical engineering applications for safety evaluations of signalized intersections.

## **Acknowledgements**

This dissertation has benefitted immensely from many people.

I want to express my gratitude to my advisor Dr. Noyce, for his invaluable guidance in my academic research and support throughout my graduate study. Dr. Noyce's dedication and rigorous attitude in safety set an example to my career.

I am also grateful to my faculty committee: Sue Ahn, John Lee, and Bin Ran, not only for their previous time serving in the exam committee, but for their constructive criticisms on this research. Their enthusiasm and encouragement have been of great help in the completion of the dissertation.

Thanks also goes to all colleagues in my research group for their assistance and help.

Finally, I would like to thank my parents and friends for their encouragement.

# Table of Contents

<b>Abstract.....</b>	<b>i</b>
<b>Acknowledgements .....</b>	<b>v</b>
<b>Table of Contents .....</b>	<b>vi</b>
<b>List of Figures .....</b>	<b>ix</b>
<b>List of Tables .....</b>	<b>x</b>
<b>Chapter 1 Introduction .....</b>	<b>1</b>
1.1 Driving automation.....	1
1.2 Research context .....	4
1.2.1 Intersection safety.....	4
1.2.2 Automation crash and disengagement .....	5
1.2.3 Traffic control .....	9
1.2.4 Traffic conflicts, protected, and permissive movements .....	11
1.2.5 Driving automation decision-making at intersections.....	13
1.3 Research scope and research gaps.....	17
1.4 Research questions and research goals.....	21
<b>Chapter 2 State-of-the-Art.....</b>	<b>25</b>
2.1 Driving Automation .....	25
2.1.1 Levels of automation .....	25
2.1.2 Human factors issues in Automation .....	31
2.2 Automation disengagement .....	34
2.2.1 Disengagement reporting.....	34
2.2.2 Causes of automation disengagements .....	38
2.3 Traffic control .....	54
2.4 Permissive left turns .....	64
2.5 Driver-Automation system .....	70
2.5.1 Defining Driver- Automation System.....	70
2.5.2 Driver’s role in DAS.....	70
2.5.3 Control transitions.....	72
2.6 Takeover behavior .....	72
2.7 Takeover request design .....	99
2.7.1 TOR design and lead time.....	100
2.7.2 HMI design .....	103
2.7.3 TOR and HMI examples in automobile industry.....	104
2.8 Non-driving related Tasks (NDRTs) .....	108
2.9 Summary.....	117
<b>Chapter 3 Meta-analysis of drivers’ takeover behavior .....</b>	<b>119</b>
3.1 Literature selection.....	119

3.2 Research results encoding .....	121
3.2.1 Takeover time, steering time, and braking time .....	122
3.2.2 TOR modality .....	124
3.2.3 Takeover measures .....	124
3.2.4 NDRTs summary .....	127
3.2.4 Driver gender and age .....	128
3.2.5 Missing data .....	129
3.3 Machine learning-based Meta-analysis .....	131
3.3.1 Takeover quality (TOQ) .....	131
3.3.2 XGBoost regression algorithm .....	133
3.3.3 XGBoost modeling .....	138
3.4 Estimation of Takeover behavior .....	141
3.5 Summary .....	145
<b>Chapter 4 Modeling takeover transitions .....</b>	<b>147</b>
4.1 Takeover behavior and automation system .....	147
4.2 DAS model contributing to evaluation of TOQ .....	149
4.1.1 Driver's out-of-the-loop state as a result of automation systems .....	149
4.1.2 Individual differences .....	150
4.1.3 Automation system limitations and automation disengagement .....	152
4.3 DAS model process .....	153
4.4 DAS model input I: automation attribute .....	156
4.5 DAS model component II: driver behavior .....	157
4.6 Summary .....	158
<b>Chapter 5 VISSIM Simulation: takeover in permissive left-turn scenarios .....</b>	<b>161</b>
5.1 Introduction .....	161
5.1.1 Overview of microscopic traffic simulation .....	161
5.1.2 Simulation Platform .....	162
5.2 Base model development .....	162
5.2.1 Geometric layout .....	163
5.2.2 Traffic inputs and other parameter settings .....	164
5.2.3 Signal optimization and capacity of intersection lane group .....	165
5.3 VISSIM traffic implementation .....	167
5.3.1 Speed distributions .....	168
5.3.2 Vehicle composition .....	168
5.3.3 Vehicle routes .....	168
5.4 DAS model implementation .....	169
5.4.1 Control transitions .....	170
5.4.2 Driving behavior .....	171
5.4.3 Takeover behavior .....	172
5.5 Evaluation setup .....	173
5.5.1 Seeding period, evaluation period, observations, and simulation run times .....	173
5.5.2 Baseline scenarios .....	174
5.5.3 Simulation data recording .....	174

5.6 Model calibration .....	176
5.6.1 Calibration method .....	177
5.6.2 Calibration results .....	178
<b>Chapter 6 Simulation results and discussions.....</b>	<b>179</b>
6.1 Delays and queues.....	179
6.2 Safety.....	187
6.2.1 Speed variation.....	187
6.2.2 Surrogate safety measures.....	191
6.3 Conclusions.....	195
<b>Chapter 7 Contributions and future research .....</b>	<b>198</b>
7.1 Theoretical contribution.....	198
7.2 Methodological contribution.....	199
7.3 Engineering significance .....	200
7.2 Limitations .....	203
7.3 Future research .....	204
<b>Appendix A Machine learning-based meta-analysis .....</b>	<b>206</b>
Global setting.....	206
1 Data preparation¶ .....	207
1.1 Training and testing .....	207
2 Model fitting and model selection .....	207
2.1 Train and compare multiple regression models .....	207
2.2 Fit XGBoost model with training data. ....	209
2.3 Feature selection using XGBoost .....	209
3 Fine tune XGBoost.....	210
3.1 Fix learning rate and number of estimators for tuning tree-based parameters .....	210
3.2 Tune max_depth and min_child_weight.....	211
3.3 Tune gamma.....	214
3.4 Tune subsample vs colsample_bytree.....	216
3.5 Tune Regularization Parameters.....	232
3.6 Tune learning rate and n_estimators .....	235
3.7 Save final model.....	238
4. Make predictions.....	239
<b>References .....</b>	<b>240</b>

## List of Figures

Figure 1-1 Vehicle-to-vehicle conflict points at an intersection.....	12
Figure 2-1 Number of participants in takeover studies.....	74
Figure 2-2 The TOR interface when the traffic jam pilot of Audi A8 request drivers to take back control (source: AUDI AG, Image No: A1710305) .....	105
Figure 2-3 The virtual cockpit display of Pilot Assist: (1) Pilot Assist is off when the steering wheel symbol is grey, and (2) Pilot Assist is on when the steering wheel symbol is green (Volvo, 2019).....	106
Figure 2-4 NDRTs used in takeover studies.....	111
Figure 2-5 Sample images of visually demanding search task (Kim et al., 2018) .....	114
Figure 3-1 Lead time, takeover time, steering time, and braking time during control transitions .....	122
Figure 3-2 Data imputation based on hierarchical clustering results.....	130
Figure 3-3 Takeover time versus driver ages, NDRTs, lead time, and TOR modality .....	130
Figure 3-4 Prediction results of different regression models.....	139
Figure 3-5 Feature importance score from XGBoost regression model .....	140
Figure 3-6 Workflow of takeover behavior estimation.....	142
Figure 3-7 Estimated TTC probability density .....	143
Figure 3-8 Estimated probability density of takeover time .....	143
Figure 3-9 Estimated probability density of deceleration rate.....	144
Figure 3-10 Estimated probability density of angular speed .....	144
Figure 4-1 Driver-automation feedback loop .....	149
Figure 4-2 Process of event-based driver behavior modeling during disengagement-trigger events .....	154
Figure 4-3 Variations and gaps in model congruence during a control transition.....	159
Figure 5-1 Roadway network in VISSIM simulation.....	163
Figure 5-2 Mechanism of DAS model in VISSIM .....	170
Figure 5-3 Driving behavior set-up in VISSIM simulation.....	172
Figure 6-2 Queue lengths in scenarios with different levels of traffic volume and penetration rate .....	181
Figure 6-2 Vehicle delays in scenarios with different levels of traffic volume and penetration rate.....	181
Figure 6-3 Differences in means of vehicle delays between scenarios with different penetration rate.....	185
Figure 6-4 Boxplot of vehicle delays in different simulation scenarios .....	186
Figure 6-5 Differences in means of queue lengths between scenarios with different penetration rate.....	187
Figure 6-6 Standard deviation of speeds with different flow rates.....	190
Figure 6-7 Standard deviation of speeds with different AV penetration rates .....	190
Figure 6-8 Traffic conflicts with different flow rate.....	194
Figure 6-9 Traffic conflicts with different penetration rates .....	195
Figure 7-1 Achieving safety and efficiency goal through efforts of stakeholders.....	201

## List of Tables

Table 2-1 Levels of driving automation systems (NHTSA, 2013; SAE International, 2018).....	29
Table 2-2 Driver's role in automation systems .....	32
Table 2-3 WeRide's autonomous miles and number of disengagements (WeRide, 2018) (gathered by author).....	43
Table 2-4 GM Cruise's autonomous miles and number of disengagements (GM Cruise, 2018) (gathered by author).....	43
Table 2-5 GM Cruise's reported FCDs (GM Cruise, 2018) (gathered by author) .....	43
Table 2-6 Phantom AI's reported FCDs (Phantom AI, 2018) (gathered by author) .....	44
Table 2-7 NVIDIA's autonomous miles and number of disengagements (NVIDIA, 2018) (gathered by author).....	45
Table 2-8 NVIDIA's reported FCDs (NVIDIA, 2018) (gathered by author).....	45
Table 2-9 Honda's reported FCDs (Honda, 2018) (gathered by author).....	46
Table 2-10 Summary of intersection control protocols .....	58
Table 2-11 Flashing Yellow Arrow configuration and signal sequence (recreated based on NCHRP 03-125). .....	66
Table 2-12 Flashing Red Arrow configuration and signal sequence (recreated based on NCHRP 03-125).....	67
Table 2-13 Pseudo-code for left-turn maneuvering when facing permissive left-turn signal .....	68
Table 2-14 Summary of takeover behavior studies .....	75
Table 3-1 Weighted average takeover time, braking time, and steering time .....	123
Table 3-2 Metrics used in driver takeover experiments based on selected studies .....	125
Table 3-3 The impact of NDRTs on Drivers' takeover behavior .....	127
Table 3-4 XGBoost regression algorithm .....	136
Table 3-5 Initial model selection for meta-regression analysis .....	138
Table 3-6 Driver age and NDRT categorization in XGBoost regression model .....	141
Table 4-1 Primary influencing factors of takeover behaviors .....	155
Table 5-1 Experiment variables in simulation .....	164
Table 5-2 Traffic demand inputs and optimized signal timings .....	165
Table 5-3 Parameter settings in signal optimization.....	165
Table 5-4 Specification of driving logics in different zones.....	173
Table 5-5 Calibration measures, data sources, and calibration threshold.....	177
Table 5-6 Summary of calibration results.....	178
Table 6-1 Delays and queue lengths by traffic volume and AV penetration rate.....	180
Table 6-2 ANOVA table for two-factor ANOVA analysis of vehicle delays .....	184
Table 6-3 Tukey Test results for Vehicle delays .....	184
Table 6-4 ANOVA table for two-factor ANOVA analysis of queue lengths.....	185
Table 6-5 Tukey Test results for Vehicle delays .....	186
Table 6-6 Standard deviation of speeds for different movements at intersection IB.....	188
Table 6-7 Simulated traffic conflicts in different experimental conditions.....	192
Table 6-8 Average traffic conflicts with different levels of traffic volume.....	193

# Chapter 1 Introduction

## 1.1 Driving automation

The use of automation technology and artificial intelligence (AI) has been witnessed in the fields of automobile and transportation engineering as safer and smarter ways of traveling. Vehicles are enabled to automatically adjust speed to maintain safe distances from vehicles ahead, to keep centered in the lane, and to automatically park. Nearly all major automobile manufacturers have introduced automated driving systems. Various advantages are promised by the advent of autonomous driving technologies, including improved traffic flow efficiency and increased highway capacity (Friedrich, 2016; Michael et al., 1998; Talebpour and Mahmassani, 2016), reduced parking demand (Zakharenko, 2016; Zhang et al., 2015), reduced fuel consumption and emissions (Barth et al., 2014; Brown et al., 2014; Mersky and Samaras, 2016), and greater social benefits for both commuters and those who are unable to drive (Fagnant and Kockelman, 2015; Tettamanti et al., 2016; Zakharenko, 2016). In fact, automated driving systems are believed to be capable of fundamentally changing the entirety of the future transportation through assisting and replacing human drivers to reduce traffic crashes brought about by human errors. Compared to human drivers, driving automation systems are expected to perform driving tasks better through quicker reaction times, better recognition, improved judgment, and the elimination of road rage, fatigue driving, distracted driving, and impaired driving.

Even though driving automation systems could assist and replace human drivers to reduce traffic crashes due to human error, there is still no consensus on their potential safety impacts. For example, semi-automated vehicles are expected to reduce speed limit violations and therefore

reduce speed related crashes by 50% (Pérez-Marín and Guillen, 2019). Forward collision warning (FCW) could reduce front-to-rear (FTR) crash by 27% and FTR injury crash by 20% (Cicchino, 2017). When combined with autonomous emergency braking (AEB), FCW could reduce FTR crashes and FTR injury crashes by 50% and 56% respectively (Cicchino, 2017). On the other hand, inherent safety and security challenges still remain at the forefront in the development of driving automation systems (Cui et al., 2018), given the fact that innovative methods to demonstrate safety and reliability of automated vehicles are lacking (Kalra and Paddock, 2016). As indicated in previous studies, a human-centered approach is more appropriate when introducing the next generation of driver assistance and intelligent vehicles to improve traffic safety (Bencloucif et al., 2019; Carsten and Martens, 2018; Goodrich and Boer, 2003, 2000; McCall et al., 2004; Moon and Yi, 2008; Nguyen et al., 2017; Ohn-Bar and Trivedi, 2016; Saito et al., 2018; Sentouh et al., 2018; Solís-Marcos et al., 2018; Wada, 2018; Z. Wang et al., 2019, 2018). As a matter of fact, the driving automation system still requires a human driver's adequate supervision and cooperation when reaching system limits. It is crucial that we gain a full comprehension on how drivers will perform when driving automated vehicles. It is likewise imperative to fully explore the effects on a driver's situational awareness, monitoring, and out-of-loop performance, with and without secondary tasks.

The Society of Automotive Engineers (SAE) International recommends using the terms “driving automation” and “driving automation systems” to convey the concept that the object of the automation is the driving, rather than the vehicles. Terms such as *autonomous*, *driving mode(s)*, *self-driving*, *unmanned*, and *robotic* are often misused to describe driving automation systems and vehicles equipped with them (SAE International, 2018). It is notable that the National Highway Traffic Safety Administration (NHTSA) prefers the term *automated driving system* in its documents to guide and aid the research and development of vehicle safety technologies. For the

sake of clear communication, the terms *driving automation systems* and *automated driving systems* are more appropriate for characterizing systems that perform part or all of given dynamic driving tasks. Therefore, *driving automation system* and *automated driving system* are used interchangeably in this research. The term autonomous vehicle is not used since it could prompt functional imprecision, confusion, misunderstanding, misjudgment, and decreased credibility.

There are broadly six levels of automation ranging from no driving automation to full driving automation as defined by SAE international (SAE International, 2018). Circumstances permitting automated driving and requiring human intervention are the main factors in defining these six levels. At the basic level (Level 0), human drivers are responsible for all dynamic driving tasks, and must have full control of the brakes, steering wheel, throttle, power, and so on. The driving tasks shift more and more from the driver to the automation system as the level of automation increases. Along with that, the automated functions expand from patricidal, to conditional, to high, and all the way up to full automation. At Level 4 and Level 5, all driving tasks are automated and human intervention is not required. However, driving automation at Level 4 is limited to specific driving circumstances and human supervision is still required when operating outside those circumstances. It is still in discussion whether the full driving automation (Level 5) under any driving circumstances can be achieved in the near future (Casner et al., 2016; Etemad, 2015; Glander and Rooij, 2018; Grace et al., 2018; Kirkpatrick, 2015; Koopman and Wagner, 2016).

A number of driving automation systems are actively being developed and tested under different levels of automation. The NHTSA encourages stakeholders involved in the development of automated driving systems to share insights into their approaches to safety in developing driving automation systems. Ten technological giants and automobile manufacturers to date, including

Waymo, Uber, Zoox, Nvidia, Nuro, Starsky Robotics, Navya, GM, Ford, and Mercedes-Benz/Bosch, have submitted their reports of Voluntary Safety Self-Assessments to NHTSA (Bosch and Mercedes-Benz, 2018; Ford Motor Company, 2018; Navya, 2018; Nuro, 2018a; NVIDIA, 2018; Starsky Robotics, 2018; Uber Advanced Technologies Group, 2018; Waymo, 2018a; Zoox, 2018a).

## **1.2 Research context**

### **1.2.1 Intersection safety**

Urban intersections probably represent the most challenging driving situations for drivers; where the drivers are most likely to be cognitively overloaded. Drivers must comprehend the traffic control rules, predict the intention of other road users, and evaluate and identify the best alternatives to complete their necessary driving tasks to get to their desired destinations. In the United States, around 27% of fatal crashes occur at intersections (FHWA, 2018) while 33% of police-reported crashes are related to intersections in Germany (Sander and Lubbe, 2018). Furthermore, left-turn crashes account for a high percentage of total crashes occurring at signalized intersections (Wang and Abdel-Aty, 2008). Take Florida for instance, 64.2% of left-turn crashes caused injuries, whereas the injury rate of other crashes was 50.1% (Wang and Abdel-Aty, 2008). Left-turning vehicles are more involved in pedestrian crashes at intersections, compared to right-turning and straight-through movements (Qi and Guoguo, 2017).

Unlike protected left-turns, driving automation systems may need to interact with other road users including opposing traffic while turning left at a permissive left-turn signal as oncoming vehicles are active agents having the right-of-way and making decisions for their own utility only. In other words, an automated driving system must negotiate and compete with the oncoming traffic

when it plans to turn left during a permissive left-turn signal. The speed, location, and behavior of the oncoming traffic must be detected and predicted by the driving automation system before starting the left-turn maneuver.

### **1.2.2 Automation crash and disengagement**

The world's first fatal crash involving a Level 2 driving automation (a Tesla Model S) occurred in China on January 20<sup>th</sup>, 2016 after Tesla's autopilot feature was first introduced to the Chinese market ([Lulu Chang and Luke Dormehl, 2018](#)). The vehicle was traveling in autopilot mode in the left lane of a two-way eight-lane divided highway. The car ahead of the Model S encountered a street sweeper in the left lane, and moved into the center lane, leaving the street sweeper directly on the victim's path. According to the video, no warnings were activated by the vehicle before it crashed into the back of the sweeper ([CGTN, 2016](#)). Counterintuitively, Tesla Model S manual stated that the Traffic-Aware Cruise Control would be unable to detect stationary objects at a high speed (50 mph) ([Tesla, 2016](#)).

About three months later, the first US fatal crash - which also happened to involve a 2015 Tesla Model S occurred on May 7<sup>th</sup>, 2016 in Florida ([NTSB, 2017](#)). In this crash, the Tesla vehicle was using Traffic-Aware Cruise Control and Autosteer lane-keeping, which Tesla refers to as Autopilot. It was traveling at 74 mph on the divided four-lane Highway 27A with a posted speed limit of 65 mph when it crashed into a tractor-semitrailer truck that was making a left turn onto the highway ([NTSB, 2017](#)). According to the crash investigation ([NTSB, 2017](#)), the probable causes of this crash were (1) the truck driver's failure to yield to the right-of-way to the Tesla vehicle, and (2) the Tesla driver's inadequate monitoring due to overreliance on the automation, which resulted in the driver's absence of reaction to the presence of the truck.

On March 18<sup>th</sup>, 2018, a pedestrian was fatally injured by an Uber driving automation test vehicle in Arizona (NTSB, 2018a). As the Uber test vehicle was traveling in the right-through lane, its right-front side struck a pedestrian who was walking a bicycle crossing Mill Avenue. According to the data retrieved from the crash vehicle, the vehicle first registered the pedestrian about 6 s before impact, when traveling at 43 mph. The pedestrian was initially classified as an unknown object, then as a vehicle, and lastly as a bicycle with uncertain future path. The system recognized the need for an emergency braking just 1.3 s before the impact. A safety driver was present, however the system was not designed to alert the safety driver (NTSB, 2018a). Uber stated that the developmental driving automation still relied on an attentive safety driver to facilitate safe testing and manage a number of types of risks (Uber Advanced Technologies Group, 2018).

Another fatal crash occurred on US Highway 101 in California on March 23<sup>rd</sup>, 2018 involving a 2017 Tesla Model X P100D using Traffic-Aware Cruise Control and Autosteer Lane-Keeping with the speed set at 75 mph. The Tesla vehicle approached a gore area dividing the travel lane and the exit ramp, then crossed the gore area and struck a damaged crash attenuator at a speed of 70.8 mph. A review of the performance data downloaded from the vehicle showed the following (NTSB, 2018b):

- In the 60 s before the crash, the driver's hands were detected on the steering wheel three times for an aggregate 34 s;
- At 8 s preceding the crash, the Tesla was following a lead vehicle at 65 mph;
- At 7 s preceding the crash, the Tesla started steering left while still following a lead vehicle;
- At 4 s preceding the crash, the Tesla was not following a lead vehicle anymore;
- At 3 s prior to the crash and until the time of impact, the Tesla increased its speed from 62 to 70.8 mph without braking or taking any evasive action.

When driving automation fails or reaches its limits, the automation mode disengages, and drivers are expected to resume manual control. All the driving automation tests on California public roads are mandated to be retrofitted to include a back-up driver by the California Department of Motor Vehicles (DMV). In addition, automation disengagement and crash data regarding driving automation on-road tests is required to be submitted and to become publicly available ([California Department of Motor Vehicles, 2017](#)) in California. Automation disengagement refers to the process that an automation system withdraws from actively performing driving tasks in a particular situation; either when it reaches its limits or when the safety driver of the system recognizes a need to take immediate control of the system. The outcome of an automation disengagement is the control of the vehicle switches from the system to the driver. The disengagements of automation mode can be classified into (1) passive disengagement, when the disengagement is initiated by the system when it is unable to cope with the current situation; and (2) active disengagement, when the driver actively resumes manual control though the system does not detect any failure ([Lv et al., 2018](#)). The dominant causes for both passive and active disengagements are software issues including inadequacies of perception, decision making, path planning, and vehicle control ([Lv et al., 2018](#)). The detailed causes of disengagement reported by manufacturers are reviewed in Chapter 2.

Based on the reported disengagement data ([Favarò et al., 2018](#)), system failure (hardware or software system failures) and human factors (human drivers deciding to initiate the disengagement due to discomfort, uneasiness, or a lack of trust in the system) are the major causes of automation disengagement, accounting for 52% and 30%, respectively. Similar results were also found in an earlier study in which 56.1 % of disengagement were caused by system failures and 26.57 % were driver- initiated ([Dixit et al., 2016](#)). It is noticed that Mercedes Benz was mostly

involved in the human factors-related disengagement data (Favarò et al., 2018). The disengagements of Delphi driving automation were more often caused by external conditions (such as fading lane markings, debris on the road, or excessive pedestrian traffic) (Favarò et al., 2018). After evaluating the cause, dynamics, and impact of automation disengagement across a wide range of manufacturers, Banerjee et al revealed that (Banerjee et al., 2018):

- Machine-learning-based systems for perception, decision making, and control led to 64% of automation disengagement;
- Driving automation systems are 15 to 4000 times worse than human drivers regarding crash per miles driven;
- Compared to other safety-critical automation systems, driving automation systems are 4.22 times worse than airplanes and 2.5 times better than surgical robots regarding reliability per mission; and
- Drivers of driving automation systems ought to be as vigilant as drivers driving conventional vehicles.

According to the California DMV rule regarding disengagement reporting, the reaction time of the safety driver is measured as the time elapsed from when the safety driver was alerted, to when he or she resumed manual control from the system. Based on the driving automation test data between September 2014 and November 2015, it was found that for Waymo and Mercedes Benz, when the disengagement occurred due to system failures, safety drivers' average reaction times are 0.83 and 0.84 s with standard deviations 0.53 and 0.9, respectively (Dixit et al., 2016). Considering all test situations, the reaction times of safety drivers in resuming control when automation disengagement occurred were actually quite stable, regardless of the disengagement causes. The disengagement reaction time data collected in (Dixit et al., 2016) reveals that the

average reaction time of a total of 1330 disengagement events is 0.85 s with a standard deviation of 0.70. However, ordinary drivers' reaction times are not as consistent as the safety drivers of those driving automation prototypes. In an experimental study using a driving simulator, reaction times of 100 regular drivers ranging from 0.81 s to 2.44 s with a mean of 1.33 s and a standard deviation of 0.27 s were discovered (Broen and Chiang, 1996). The perception-reaction times (PRT) seem to reveal more solid information regarding driver PRTs when further investigated along with age effect on PRTs. Based on on-road test results of 116 subjects (more than 200 subject in total) ranging from ages 20 to over 70 years old, during emergency braking (avoiding a crash barrel), most of the observed fast PRTs were from young people, with less than 1.25 s (Lerner, 1993). However, no differences were found in either central tendency (mean = 1.5 s) and upper percentile (85th percentile = 1.9 s) among the age groups (Lerner, 1993). The design value of 2.5 s for PRT was used for horizontal curves, vertical curves, approaches to intersections, sign placement, traffic signalization, and other roadway design elements in American Association of State Highway and Transportation Officials (AASHTO) (AASHTO, 2001).

### **1.2.3 Traffic control**

Various traffic controls have been developed to regulate traffic and to facilitate efficient and safe traffic movements. One of the earliest traffic signals consisting of only red and green indications was installed in Cleveland in 1914 and had to be operated manually. In 1917, yellow lights were added to the manual traffic lights in Detroit. Later, traffic indications for pedestrian crossing were added to the traffic control family in 1931. Looking back at the control mechanism of traffic signals, the evolution has been from manual control to partially automated, and finally to fully automated control. Meanwhile following the success of traffic signals at intersections, signal control was first introduced to the highway ramp on the I-290 Eisenhower Expressway in Chicago in 1963. The

development of computer and information technology has then further allowed for more advanced traffic control mechanism, including real-time adaptive control and corridor-wide, or city-wide coordinated control. In 1984, the first intelligent traffic light system was put into operation right before the Olympic Games in Los Angeles (Roper, 1987). A more comprehensive review on the invention, development, and evolution of traffic signal lights can be found in (Kellerman, 2019, 2018).

Traffic signals are the most fundamental type of traffic controls used in urban environments. On the other hand, traffic signs and pavement markings are usually used together to resolve conflicts at intersections for efficient and safe movements of vehicles, pedestrians, and bicyclists. Examples of traffic signs and pavement markings include warning signs, regulatory signs, guide signs, turning arrow markings, yield markings, lane-use markings (such as for bike lanes and for two-way center left-turn lanes). Intersections feature a variety of design elements to process the traffic stream in an efficient and safe way, requiring any agent traversing the intersection to comprehend and follow the rules. Depending on how traffic is controlled at an intersection, intersections can usually be categorized as signalized intersections and unsignalized intersections (such as Stop sign-controlled and Yield sign-controlled). Traffic lights at intersections can effectively resolve conflicts between vehicles, pedestrians, and bicyclists by assigning signal phases to all the crossing and turning movements of each moving entity.

The advent of automated driving technology has brought traffic control to the spotlight. Consequently, during the past decade we have witnessed a tremendous advance in traffic control research. Connected and autonomous vehicles (CAVs) are expected to fundamentally change our current traffic control mechanism. For example, a reservation-based control protocol has drawn a lot of attentions in traffic control research to alleviate congestion (Bashiri et al., 2018b; Carlino et

al., 2013; Dresner and Stone, 2007, 2005; Dukic et al., 2013; Fajardo et al., 2011; Guler et al., 2014; Hausknecht et al., 2011; Li et al., 2013; Middlesworth et al., 2008; Perdomo López et al., 2017; Schepperle et al., 2008; Schepperle and Böhm, 2008, 2007). The reservation-based control protocol allows driver agents to reserve the temporal-spatial resource from the intersection control agent when approaching an intersection. The control agent simulates the requested time-dependent path and accepts the reservation if the path is available or rejects it if conflicts exist in the request. Novel control protocols such as priority-based (Alonso et al., 2011; Gregoire et al., 2014; Hassan and Rakha, 2014; Qian et al., 2014), sequenced-based (Perronnet et al., 2013), demand responsive-based (Yang et al., 2016), optimized reservation-based (Levin and Rey, 2017), and synchronized arrival flow-based (Azimi et al., 2015) have been developed with the interest of harvesting the benefits from driving automation technology as well as from the technologies of vehicle-to-vehicle (V2V), Vehicle-to-Infrastructure (V2I), and Vehicle to both vehicles and the infrastructure (V2X) communications.

#### **1.2.4 Traffic conflicts, protected, and permissive movements**

In an urban environment, drivers often need to yield to other road users and to respond to unexpected events. It is often challenging for automated driving systems to handle these situations. Signal lights are often used to resolve conflicts between crossing and turning movements at intersections. Intuitively, path-crossing points are the spots where traffic conflicts can potentially occur. Usually, there are 32 vehicle-to-vehicle conflicting points at a generic four-leg intersection, including eight diverging points, eight merging points, and 16 crossing points (Figure 1-1). Procedures and software programs have been developed for automatic determination of conflicts points at an intersection dependent on lane configurations and traffic movement regulations (Lu et al., 2013; Pan et al., 2013). It is worth noting that diverging conflicts occur before entering an

intersection while merging and crossing conflicts occur after entering an intersection. The number and distribution of conflicting points are often used in evaluations of intersection safety (Ahn and Del Vecchio, 2018; Alhajyaseen, 2015; Chen et al., 2017; Essa and Sayed, 2018; Guo et al., 2018). In this research, to facilitate the discussion of protected and permissive movements, only merging and crossing conflicts are considered.

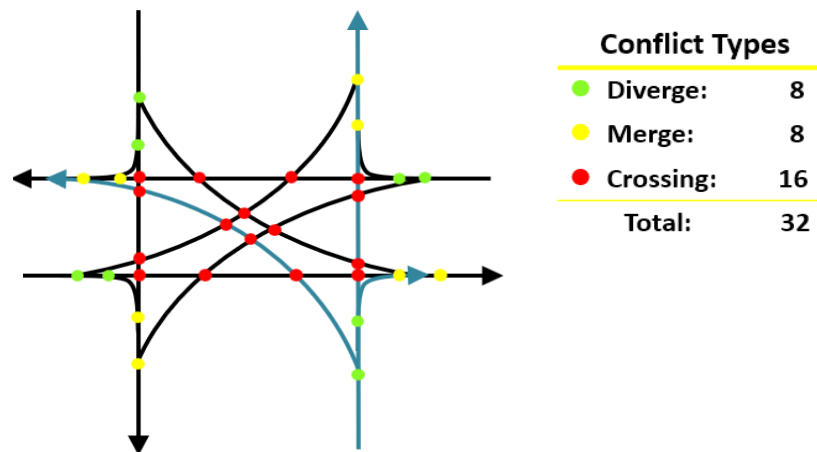


Figure 1-1 Vehicle-to-vehicle conflict points at an intersection

Intersection signal controls usually allow compatible traffic movements to simultaneously enter an intersection at a given time. *Protected movement* refers to the traffic movements that are granted the right-of-way by a dedicated green indication while any conflicting movements are required not to interfere the warranted moving agent. When facing an exclusive protected movement signal, driving automations' intersection traversal movements are warranted and other conflicting agents are stopped. For example, the left-turn movements are protected on a green left-turn arrow while other vehicular movements pedestrians and bicyclists must stop for the left-turning vehicles. *Permissive movement* refers to the traffic movements that must share the right-of-way with other protected movements while they execute their desired movements through gaps

in the conflicting traffic. For example, when turning right on a red indication, drivers must stop and yield to the oncoming vehicles and merge into the desired lane in a subsequent safe gap.

Permissive left-turns were added to traffic signals to allow for more left-turn maneuvers during a signal cycle. The prevalence of these permissive left-turn signals requires a driving automation to yield both to opposing traffic and to crossing pedestrians - while identifying a safe turning gap between oncoming vehicles to complete its left-turn maneuver. When facing permissive signals, the driving automation's trajectory planning must account for conflicting moving agents coming from the opposite direction, who actually have the right-of-way. It is also possible for a traffic signal cycle to have a dedicated phase to grant the right-of-way solely to left-turning movements, which would be *protected left turns* during this portion of the signal cycle. A permissive left-turn phase could be added through solid green or flashing yellow arrow during the remainder of the signal cycle, which would result in the commonly known *protected-permissive left-turn control* (Brehmer et al., 2003; Knodler et al., 2007a, 2005; Noyce et al., 2014). Intersections with permissive only or protected/permissive left-turn (PPLT) controls are nonetheless still challenging circumstances for driving automation. To turn left, the driving system must yield both to opposing vehicles and to pedestrians while trying to find a safe turning gap.

### **1.2.5 Driving automation decision-making at intersections**

Left-turn maneuvering is still a challenging task for a driving automation system. To make a left turn, a driving automation must thoroughly analyze the traffic situation at the intersection and follow the traffic rules. Localization, object detection, object tracking, mapping, path planning, and control are generally unraveled issues for automated driving systems (Chen et al., 2019b, 2019a; Fethi et al., 2018; H. Guo et al., 2019; Hu et al., 2018; Li et al., 2018; Nguyen et al., 2018; Saraoglu et al., 2018; Stern et al., 2018; Y. Wang et al., 2019; You et al., 2019). However,

challenges remain in regard to how driving automations can make decisions using the sensor data in complicated urban environments. Lane-changing (Bahram et al., 2014; Nilsson and Sjoberg, 2013; Noh and An, 2018; P. Wang et al., 2018; Wei and Dolan, 2009), car-following (Nilsson and Sjoberg, 2013; Wei and Dolan, 2009), highway on-ramp merging (Amezquita-Semprun et al., 2018; Rios-Torres and Malikopoulos, 2017a, 2017b; Wang and Chan, 2018; Zhou et al., 2018a, 2018b), and speed strategy on curvy sections (Bosetti et al., 2015; Chu et al., 2018, 2017; Xinli Geng et al., 2016; Zhang et al., 2013) have been extensively studied. In particular, the research on decision-making processes at intersections for driving automation is still at its developing stage (Noh, 2019). Socially acknowledged behaviors are expected from driving automation, even at complex urban intersections where traffic with uncertain intentions may exist. To understand how driving automations behave at intersections, current research and practices of available automation prototypes on decision-making at intersections are reviewed. It remains challenging for researchers and engineers to develop a decision-making framework for driving automation; particularly one that is capable of quickly analyzing an intersection situation and predicting the future movements of another moving agent within and near the intersection.

When solving the problem of automation decision-making in various traffic circumstances, the strategy learning from human drivers is often adopted. For example, a human-like decision-making algorithm was developed based on human driver recordings at unsignalized intersections and roundabouts (de Beaucorps et al., 2017). After reviewing human driver models, (Liu and Ozguner, 2007) also demonstrated an algorithm for a left-turn scenario at an unsignalized intersection. It is worth noting that this algorithm was based on rather simple assumptions of driver characteristics. The Partially Observable Markov Decision Process (POMDP) is often employed in decision-making frameworks of intersection traversal, in which the intentions of the other

agents at the intersection are not directly observable and are encoded as hidden variables (Hubmann et al., 2017; Kye et al., 2015; Liu et al., 2015; Sefati et al., 2017). However, the POMDP is usually intractable in real-time applications, making it difficult to solve for decision making at intersections.

One notable trend regarding driving automation's decision-making processes at intersections is the unsignalized intersection traversal. Some of the representative studies are listed as below:

- A human-like decision-making algorithm was proposed and validated at unsignalized intersections and roundabouts in an artificial environment (de Beaucorps et al., 2017). According to the algorithm, a decision must be made before a driving automation entered the decision zone 30 meters ahead of an intersection while a short-term prediction needs to be made about another moving agent during each time step (approximately 100 ms) with a time horizon of 2 s if the AV reaches the intersection within this horizon.
- A decision-making algorithm considering the interactions and the uncertainties of surrounding vehicles based on a POMDP was proposed and evaluated in an artificial environment, which included an unsignalized intersection and a T intersection (traffic control method was not specified) (Hubmann et al., 2017). The ego vehicle plans to turn left at the unsignalized intersection and the T intersection. However, more particles in the solver are needed if incorporating the existence of pedestrians.
- A generalized approach towards high-level decision-making based on POMDP was proposed. The model validation only considers longitudinal behavior planning (maneuvers that only involves accelerating, braking, or keeping a constant velocity) in varied unsignalized intersection scenarios (Sefati et al., 2017).

- A intention-aware decision-making model based on POMDP was proposed and evaluated at unsignalized intersections in the real world (Kye et al., 2015). The intention-aware model only makes decisions on longitudinal movement (go, stop, and undetermined).
- The first on-road demonstration of cooperative traversal at an unsignalized intersection was accomplished in France, in which three vehicles determined the turning order and successfully traversed an intersection without a collision (J. Baber et al., 2005).

The prototypes on roads present another picture about driving automation's decision-making at intersections. As was noticed earlier, automation disengagements occur so frequently that 52% of disengagements occurred due to system failure, and among all disengagements, 49% happened on streets (Favarò et al., 2018). One of Waymo's driving automation's technical flaws is its hesitation at the intersection (Efrati, 2018). According to (Efrati, 2018), Waymo's driving automations would stop at least three s at a Stop sign. It is stated that Waymo's automation have issues with unprotected left turns when a left-turning vehicle does not have the right-of-way at places where there are no left-turn lanes (Efrati, 2018). As a matter of fact, Waymo driving automations were often observed to have difficulties in traversing a Stop sign controlled intersection (Rapier, 2017): it would stop 10 s even when there is no crossing traffic and sometimes turned into the wrong lane. Waymo driving automation is designed to pause at a green light at an intersection. A Waymo vehicle was observed sitting at a flashing yellow light waiting to turn, and then the safety driver resumed control and ran the red light to complete the left-turn task (Waymo and whatasimpleton, 2018). There are countless examples of Waymo having difficulties in traversing an intersection. Therefore, this research aims to investigate how a driver collaborates with the driving automation system to complete an intersection traversal task especially making a left turn when encountering permissive left-turn signals.

### 1.3 Research scope and research gaps

The objective of this section is to define, limit, and motivate the present research. In this research, the terms autonomous vehicles and automated vehicles both refer to driving automation systems that require human drivers' backup when the system reach its limits. Recognizing that human drivers are still needed to resolve some critical situations that currently are out of automation's limits, this research focuses on the human driver's role in a SAE Level 3 driving automation system. Existing studies have demonstrated different ways to model the cognitive decision-making processes of driving automations when encountering different driving environments. To truly fulfill its potential, the AI-powered driving automation system must be able to use human-like reasoning about an intersection situation to traverse it efficiently and safely, or at least as well as a human driver does. Therefore, drivers' situational awareness, supervision over driving automation system, and takeover performances will be closely studied.

From the discussions and remarks presented in [Section 1.2](#), there is still a transition period before the fully automated driving system can efficiently and appropriately react to any driving circumstance including permissive left turns at signalized intersections. Recent advancement in sensors and communications also have made it possible to create advanced traffic control methods in the future. However, V2V-, V2I-, and V2X- based traffic control that allows for effortless intersection traversal seems distant due to the lack of necessary robust wireless communication and other technical barriers, and missing governmental regulations in the development of future traffic control methods. Efforts are still needed to study how driving automation copes with current common traffic controls. Extensive studies have been focusing on driving automation's Stop-sign controlled intersection maneuvering ([Jonathan Baber et al., 2005](#); [de Beaucorps et al., 2017](#);

Hubmann et al., 2017; Kye et al., 2015; Sefati et al., 2017) , while Waymo prototypes are still not able to traverse a Stop-sign controlled intersection as naturally as a human driver does (Efrati, 2018; Rapier, 2017). Permissive left-turn maneuvering at signalized intersections requires more reliable situation-aware and intention-aware decision-making of the automated driving system. When driving automation reaches its limits in a permissive left-turn situation, drivers need to take back control to safely and efficiently complete the left-turning task without causing delays or disturbances to other vehicles. Therefore, this research mainly focuses on the situation in which driving automation requests the human drivers to take back control and complete the left turn when facing a permissive left-turn traffic signal operation. Given the complexities of permissive left turns in gap selection and the potential for non-motorized (pedestrians and bicycles) interactions, the take back control message is required at every required permissive left turn. There is a need to understand the timing and sequence of driver behaviors during the takeover and the left-turn maneuvers.

Driving automation is expected to relieve drivers from the tedium of driving and thus open up new ways for drivers to spend their time on things of their own interest. A substantial number of non-Driving-related Tasks (NDRTs) were used in previous takeover behavior studies (Banks et al., 2018; Körber et al., 2016; Merat et al., 2012; Naujoks et al., 2018, 2016; Radlmayr et al., 2014; Schwalk et al., 2015; Shen and Neyens, 2017; Wan and Wu, 2018a; Wandtner et al., 2018c, 2018b; Zeeb et al., 2017, 2016). This research chooses to focus on NDRTs that could keep drivers physically and mentally occupied from driving tasks, with an increasing level of NDRT difficulty. In fact, making a left turn at a permissive left-turn intersection is even harder for human drivers when opposing traffic is heavy, gaps between vehicles are tight, or the available acceptable gaps are few. The incorporation of NDRTs is intended to simulate a more realistic future situation in

which distracted human drivers need to resume control when the driving automation fails to make a left turn. Through meta-regression analysis, this research attempts to investigate how drivers would perform a permissive left-turn maneuver when resuming control from the automation when engaging in NDRTs.

The driving automation developed by Waymo has been known for spending too much time in attempting to make a left-turn at intersections ([Rapier, 2017](#)). When an automation reaches its time budget in decision-making at an intersection, the Takeover Request (TOR) will be delivered to its human driver. Furthermore, fatal crashes involved in driving automations ([Lulu Chang and Luke Dormehl, 2018](#); [NTSB, 2018a, 2018b, 2018c, 2017](#)) could be avoided or at least the severities could be reduced through an effective TOR design. Various studies have explored different ways to effectively deliver the TOR message considering the effects that the format and the timing may have on driver reactions ([Bazilinskyy et al., 2018](#); [Dogan et al., 2017](#); [Epple et al., 2018](#); [Forster et al., 2017](#); [Gold et al., 2016](#); [Melcher et al., 2015](#); [Merat et al., 2014b](#); [Naujoks et al., 2018](#); [Petermeijer et al., 2017b](#); [Schwalk et al., 2015](#); [van den Beukel et al., 2016](#); [Yun et al., 2018](#); [Zeeb et al., 2017](#)). However, most of these TORs were tested on highways, few of them were in the context of an urban environment, and none of them focused on performing a left-turn task after reestablishing control from the automation. Driving experiment will be developed with different TORs to alert the human driver to resume control from the automation while approaching a signalized intersection. The message informs the human driver that the left-turn will be delivered at different locations along the urban street, giving drivers a varying range of times to complete the left-turn task.

As highlighted earlier, besides the uncertainties associated with drivers' engagement in NDRTs and how the TOR message should be delivered to drivers when approaching a signalized intersection, the implication of control transition before traversing an intersection on traffic operations is another equally important issue which needs to be studied. Though growing literatures focusing on the impact of CAVs on intersection capacities and efficiencies (Azimi et al., 2015; Chen and Englund, 2016; Dresner and Stone, 2008; Ilgin Guler et al., 2014; Levin and Rey, 2017; Li et al., 2013; Xu et al., 2018), how the occurrence of taking-over control before an intersection remains unknown. Multiple simulation tasks could be accomplished to fill this knowledge gap. In this research, we narrow down the discussion of its potential impact on traffic efficiencies to intersections allowing for permissive left-turn maneuvers.

In SAE Level 3 automation, a driver's main responsibility is to respond quickly and correctly when the driving automation system reaches its limits. During automated driving, drivers may shift their attentions away from information relevant to the driving task to one of non-driving related secondary tasks. The switch inattention could potentially affect drivers' ability to perceive, comprehend, and foresee events in the driving scene, thereby decreasing their situation awareness and readiness to resume control when the system triggers a TOR that a manual intervention is needed. An effective way to deliver the TOR is especially critical when driving in an urban environment and especially when a left-turn maneuvering is coming; there is still a need to fully understand the timing and sequence of driver performance during takeovers. The effect of drivers' NDRT engagement while resuming control from the automation to perform a left-turn maneuver in urban environment is rarely investigated. Solving traffic safety issues and the potential impact of driving automation on traffic operations where drivers are driving automated vehicles is rarely a simple task. The development of driving automation systems requires driver mental models for

better situation awareness shared between the system and the human driver. The takeover effect on traffic operation needs to be investigated to provide insight on how a human-automation driving entity would affect our future traffic operations and how we can find effective ways to accommodate their presences in urban driving environments.

#### **1.4 Research questions and research goals**

The automobile industry and the top technology companies have committed to the development of driving automation systems. Recognizing the advantages and potential benefits of V2V, V2I, and V2X communication, research on more advanced and more efficient traffic control methods has been developed to better manage future heterogenous traffic flow (manual vehicles, automated driving systems, and connected vehicles). What will be the role of human drivers in such a rapidly changing era? Clearly, before achieving full driving automation, a future driver of L2 – L4 driving automation systems will face two intelligent systems, one being the driving automation system, and the other being the traffic control system.

This research aims to advance the understanding of driver behavior in automated driving systems and develop more feasible and reliable driving automation systems when encountering permissive left-turn circumstances. When driving automation system is introduced, the role of the human driver becomes supervising and taking-over control in circumstances that are out of the system's limits. Most driving automation systems to date make the task of driving a vehicle shared between the system and the driver. To this end, the following research question needs to be answered:

Question 1: Are human drivers reliable and capable of cooperating with a shared automation system when encountering a permissive left-turn situation?

In fact, the amount of visual information available to drivers is found to be influential on how quickly drivers would resume control (Louw et al., 2017). Research also shows that the presence of NDRTs would affect drivers driving performance (Jamson et al., 2013; Merat et al., 2014a; Wandtner et al., 2018b; Zeeb et al., 2017, 2015). In particular, NDRTs are employed in the driving experiment to reflect the fact that drivers would take the advantage of driving automation and thus driving time is spent on other non-driving related activities. This research therefore aims to investigate the NDRTs' effect involved during the transition period by answering the following question:

Question 2: How would NDRTs affect drivers' performance during transition period and left-turning performance after resume control from the system when using a SAE L3 automaton?

Automation crashes reviewed in Section 1.2.2 (Lulu Chang and Luke Dormehl, 2018; NTSB, 2018a, 2018b, 2018c, 2017) have indicated that when and how to deliver the takeover-request (TOR) is critical when the human driver is decoupled from active control. A well-designed automation system should predict when it can no longer handle the driving situation, and ask the human driver to resume control simultaneously. Meanwhile, automation surprises exist in any shared automation system and have been studied extensively in the aviation domain (De Boer et al., 2017; De Boer and Hurts, 2017; Dehais et al., 2015; Landman et al., 2017a, 2017b; Mauro et

al., 2017; Rankin et al., 2016). This research also recognizes the importance of TOR design for safe takeover performance by raising the following three questions:

Question 3: How do different TORs affect drivers' reaction time (time-to-steering wheel, time to-brake) and takeover performance?

Question 4: How are different automation surprises associated with different lead time in TOR design in driving automation?

Question 5: How do different types of TORs affect drivers' subsequent permissive left-turn behavior in permissive left-turn circumstances?

After investigating the effects of NDRTs and TOR design on takeover behavior in permissive left turns, this research attempts to quantitatively identify critical NDRTs that could negatively affect drivers' driving behaviors in an urban environment. A good TOR timing design prompting good takeover performance in urban traffic situations will also be highlighted. With the knowledge gained in the driving experiment, this research then focuses on the impact of takeover behavior at the operational traffic level. Although traffic density has been shown to have an impact on drivers' takeover performance (Dogan et al., 2017; Gold et al., 2018, 2016; Jamson et al., 2013; Körber et al., 2018a, 2016; Radlmayr et al., 2014), few information is available as to what extent takeover could affect urban traffic flow especially intersection efficiency. In this respect, microsimulation of intersections with permissive left turns in VISSIM will be employed to investigate the takeover impact on traffic flow at signalized intersections. Longer cycle lengths are known to be more effective as traffic volume increases. To evaluate the throughput, delay, and

queuing of an intersection allowing for left-turning movements with mixed manual vehicles and automated driving systems, three different penetration rates will be simulated with three different cycle lengths. Then the following two questions can be answered:

Question 6: How does TORs affect the traffic efficiency at an intersection as the traffic volume increases or as the traffic cycle length increase?

By exploring these research questions above, this dissertation hopes to shed more light on some of the issues of shared human-automation control, driving safety, NDRT engagement, and on intersection efficiency when a driving automation switches to manual control.

## Chapter 2 State-of-the-Art

This chapter summarizes and discusses the state of the art for topics relevant to how a driver-automation system collaborates to complete the left-turn task at signalized intersections with permissive left-turn signal indications. First, the definitions of automation levels and human factors issues are reviewed; How automation system can disengage in different triggering conditions is then investigated; [Section 2.3](#) introduces a brief history of traffic signal control systems along with issues and challenges facing by driving automation at signalized urban intersections; [Section 2.4](#) highlights the functional requirements for a driver-automation system when facing a permissive left signal.

### 2.1 Driving Automation

#### 2.1.1 Levels of automation

The concept of levels of automation was first introduced in 1978 to illustrate how various automation modes could take over functions that were previously performed by humans ([Sheridan and Verplank, 1978](#)). In 2013, the first set of driving automation levels was established by the NHTSA, ranging from Level 0 with no automation to Level 4 with full self-driving automation ([NHTSA, 2013](#)). These five levels of automation definition were mainly based on what role a driver plays in the target system:

- In Level 0, drivers are responsible for all driving tasks.
- In Level 1, drivers can choose to use driving automation to aid him or her in driving.

- In Level 2, at least two driving controls are automated, but the driver is still fully responsible for monitoring the road.
- In Level 3, driving automation system allows the driver to cede control of the vehicle under certain environment. However, some critical situations still expect the driver to be available to resume control for safe operation.
- In Level 4, the driver becomes a true passenger. To complete a trip, the driver only needs to inform the driving automation system his or her destination.

Who is responsible for executing longitudinal and lateral control of the vehicle? Who is responsible for monitoring the driving environment? Who is supposed to back up the driving system when an automation disengagement occurs? And what driving modes of a driving automation are allowed? The definitions of NHTSA seem not explicit enough to answer these questions. In order to bring more clarity to the development of driving automation systems, the SAE International defined five levels of automation in 2014 based on the NHTSA's delimitations. In 2018, these levels were expanded to six levels, which are presented as follows ([SAE International, 2018](#)):

- At Level 0, all functions are manually controlled.
- At Level 1, most functions are still performed by the driver, but some specific functions can be controlled automatically by the vehicle.
- At Level 2, driver assistance system of steering and acceleration/ deceleration are automated using information about the driving. Therefore, driver starts getting disengaged from operating the vehicle by having their hands off the steering wheel or foot off the pedal.

However, driver still need to be alert and must always be ready to take over control of the vehicle.

- At Level 3, safety-critical functions are mostly shifted to vehicles under certain traffic or environmental conditions. Drivers are still present and will intervene if needed. However, drivers are not required to monitor the driving environment as are required by Level 2.
- At Level 4, vehicles are capable of all safety-critical driving functions and monitoring roadway conditions for the entire trip. However, the Operational design domain (ODD) of the vehicle at this level is limited since every possible driving scenario is not guaranteed.
- At Level 5: this level refers to a fully-autonomous system in which it is expected that the vehicle's performance to equal that of a human driver, in every driving scenario—including extreme environments like dirt roads that are unlikely to be navigated by driverless vehicles soon.

These levels defined by both NHTSA and SAE International have achieved standard and authority acknowledgement. In both sets, drivers in the automation Level 0 to 2 need to execute the driving task and monitor the driving situation with the help of driver assistance systems. In the rest of levels (NHTSA Level 3 and 4, SAE Levels 3 to 5), driving tasks and monitoring task are executed mainly by the driving automation system. It indicates that driving automation will gradually take on more and more driving tasks from human drivers until all the driving tasks are automated in all possible driving conditions and none needs to be done by drivers. NHTSA's automation definitions seem clearer in terms of drivers' role in each level of driving automation while SAE International's Level 4 and Level 5 complicates drivers' role and make full automation ambiguous.

To comprehend these levels, it is vital to have a detailed review on the definitions, functional features, drivers' responsibilities, and system capabilities of these automation levels. [Table 2-1](#) details all these automation levels considering the levels issued by both NHTSA and SAE international. It's also worth noting that most Advanced Driver Assistance Systems (ADAS) include Level 0 to Level 2 features, such as automatic emergency braking, adaptive cruise control, forward collision warning, blind spot detection, lane departure warning, lane keep assist, rear cross traffic alert, and highway assist.; automated driving systems (ADS) are features at Level 3 to Level 5 that might be able to operate a vehicle under limited conditions and will not operate when it is out of the operational design domain.

Table 2-1 Levels of driving automation systems (NHTSA, 2013; SAE International, 2018)

Level		Name	Definition	Execution of Steering and Acceleration/Deceleration	Monitoring of Driving Environment	Fallback Performance of Dynamic Driving Task	System Capability (Driving Mode)
NHTS	SAE						
0	0	No Automation	The full-time performance by the human driver of all aspects of the dynamic driving task, even when enhanced by warning or intervention systems	Human driver	Human driver	Human driver	N/A
1	1	Driver Assistance	The driving mode-specific execution by a driver assistance system of either steering or acceleration/deceleration using information about the driving environment and with the expectation that the human driver performs all remaining aspects of the dynamic driving task	Human driver and system	Human driver	Human driver	Some driving modes
2	2	Partial Automation	The driving mode-specific execution by one or more driver assistance systems of both steering and acceleration/deceleration using information about the driving environment and with the expectation that the	System	Human driver	Human driver	Some driving modes

			human driver performs all remaining aspects of the dynamic driving task				
3	3	Conditional Automation	The driving mode-specific performance by an automated driving system of all aspects of the dynamic driving task with the expectation that the human driver will respond appropriately to a request to intervene	System	System	Human driver	Some driving modes
3/4	4	High Automation	The driving mode-specific performance by an automated driving system of all aspects of the dynamic driving task, even if a human driver does not respond appropriately to a request to intervene	System	System	System	Some driving modes
	5	Full Automation	The full-time performance by an automated driving system of all aspects of the dynamic driving task under all roadway and environmental conditions that can be managed by a human driver	System	System	System	All driving modes

### **2.1.2 Human factors issues in Automation**

Important challenges need to be resolved while reaching for higher levels of automation in different driving environments. Though the key aspects of the levels of driving automation are outlined in [Table 2-1](#), foundational work concerning human factors in parallel is also critical for the development of driving automation. Therefore, potential human factors issues associated with each level of driving automation are presented in [Table 2-2](#) to provide insight into driver-automation interactions. What responsibilities do driving automation require drivers to undertake? [Table 2-2](#) presents the role of the driver at each level of automation.

Table 2-2 Driver's role in automation systems

Level		Automation level	Driver's role	Human factors issues
NHTSA	SAE			
0	0	No Automation	Full-time driver	The vehicle only provides warnings but not driving automation. Essentially, all human factors issues existing nowadays are challenges faced by Level 0 automation, including distracted driving, drunk driving, speeding, impaired driving, fatigued driving, aggressive driving, and road rage.
1	1	Driver Assistance	Driver with assistance	The vehicle starts to provide active assistance to enhance vehicle systems for safety and better driving. Many modern vehicles nowadays are equipped with advanced driver assistance system (ADAS), such as lane keeping assistance and cruise control to assist drivers have a better lateral and longitudinal control of the vehicle. Cruise control was developed to automate the driving task of headway maintenance. From a human factors perspective, cruise control need explicit activation and deactivation by drivers to allow them not to attend to headway and speed. Nevertheless, inadequate understanding towards it could lead to collision (Seppelt and Lee, 2015). Wu and Boyle also highlighted the danger of being distracted while using adaptive cruise control (Wu and Boyle, 2015). The Fitts's list of 11 statements, also known as the MABA-MABA list (refers to men are better at and machines are better at), were developed to determine whether humans or machines are better at certain tasks of a system (Fitts, 1951).
2	2	Partial Automation	Co-driver	Automation at this level starts to change drivers' typical role as a driver and the way how driving tasks are performed though the driver is still in control of the vehicle at all times. Simple tasks of longitudinal and lateral control are eliminated by automation. However, complex cognitive tasks and tasks superficially easy are left to drivers. The changes in the driving task structure leads to well-known effect of automation clumsy (Cook et al., 1991; Wiener, 1989). For example, drivers tend to take their attention away from the driving tasks as automation becomes increasingly capable at this level.

3	3	Conditional Automation	Backup driver	Drivers starts to be automated out of the control loop by automated driving functions, leading to the likelihood that drivers rationally disengage with the feedback of the current states of the vehicle, the road, and the traffic situation. The driving system is required to monitor the driving environment. Drivers' constant attention is not required while moving from high-engagement mode to low-engagement mode (riding to resuming control when requested). However, it is difficult for drivers to timely re-engage and to resume control of the vehicle (Beller et al., 2013a; Eriksson and Stanton, 2017; Gold et al., 2016; Körber et al., 2016; Louw et al., 2017; Merat et al., 2014b; Zeeb et al., 2015). Driving tasks are divided in such a way that drivers need to replace the automation when the driving system reaches it limits. As driving tasks and driving responsibilities are gradually shifted to the system, the role of a driver becomes a backup level of the driving process. Most feedback available to drivers from manual control is replaced by automation.
3/4	4	High Automation	Minimum driver	The diminished driving tasks that accompanies automation often has a negative impact on driving skills. Therefore, a trainer module was patented to prevent driving skill atrophy by disabling certain automated driving tasks based on the driver's current skill level, and forces the driver to utilize and sharpen his or her driving aptitudes (Chang, 2014). In fact, skills that were gained over a long time period may atrophy and may not be available when called upon with the increase in automation (Sheridan et al., 1983). Automation moves the feedback from raw data to prepared and integrated information. The absence of low-level information regarding the driving situation makes it difficult for the driver to properly and timely diagnose and respond to the system limits. After reviewing 32 studies, a proper feedback system is found to be critical regarding drivers situation awareness in driving automation (Joost C F de Winter et al., 2014).
	5	Full Automation	Full-time passenger	When traveling as a passenger in a vehicle, human don't need to responsible for driving safety at all(Koopman and Wagner, 2016).

## 2.2 Automation disengagement

### 2.1.1 Disengagement reporting

A driving automation system can disengage either initiated proactively by a safety driver or triggered because of design limitations regarding a particular circumstance. By January 2018, there were 50 manufacturers with valid permits to test driving automation prototypes with the presence of a safety driver on California public roads ([California DMV, 2018](#)). The California DMV mandates manufactures to report disengagement events during their testing on interstates, freeways, highways, rural roads, streets, and in parking facility in California ([California DMV, 2014](#)). There are requirements for a manufacturer to be qualified for testing their driving automation prototypes on California public roads. Title 13, Division 1, Chapter 1 Article 3.7 § 227 requires that driving automation prototypes to be tested must meet the standards of SAE Levels 3, 4, or 5. In addition, information regarding (1) testing permits on California public roads, (2) financial responsibility, (3) instrument of insurance, (4) surety bond, (5) self-insurance certificate, and (6) a copy of proof of insurance and a copy of bond, (7) identifications of driving automation prototypes, (8) requirements and qualifications for test drivers, (9) test driver training programs can be found in ([California DMV, 2014](#)). The information that manufactures need to report about each disengagement stated in Title 13 Article 3.7 § 227 include ([California DMV, 2014](#)):

- Whether the test vehicle is capable of operating without a test driver
- Total number of disengagements
- Total mileage each test prototype traveled in autonomous mode on public roads per month.

- Time duration between the time the system notifies a TOR and the time driver take back control of the vehicle.
- Testing locations at the time of the disengagements including interstate, freeway, highway, rural road, street, or parking facility.
- Facts causing disengagements (FCD) including weather conditions, road surface conditions, construction, emergencies, accidents or collisions, and whether the disengagement was the result of a planned test of the autonomous technology.

The California DMV leaves freedom to manufacturers on how the required information should be presented in their reports. For example, Apple's approach to assessing disengagements has advanced from categorizing causes of disengagement as manual takeovers and software disengagements (including perception, motion planning, controls, and communication) to adding more details about the causes since July 2018. In particular, certain disengagements were flagged as Important Disengagement that might lead to a safety-critical event or a violation of the traffic rules (Apple, 2018a). The facts that Honda reported on causing disengagements only show general information, including software discrepancy, hardware discrepancy, incorrect behavior of prediction, undesired motion planner, perception discrepancy, and reckless user (Honda, 2018). All the disengagements happened in Aurora were due to perception discrepancy, map discrepancy, planning discrepancy, and control discrepancy (Aurora, 2018). The description of facts causing disengagement provided by SAIC Motor included software discrepancy, decision-making discrepancy, and perception discrepancy (SAIC Motors, 2018). The lack of detail in the reported FCD makes it impossible to identify the exact technical bottlenecks in the development of higher levels of driving automation. The facts causing Nissan's 26 disengagements are presented in detail in section 2.4.2), which were also categorized as the following main types of causes (Nissan, 2018):

- System fails and requires driver to take over
- System does not recognize failure, but the needs to take over for safety
- Test vehicle is about to collide with another vehicle or obstacle due to self-steering

Though DMV mandates manufactures to provide the time elapsed between the disengagement and the safety driver resumes control, this information is still missing in some companies' 2018 disengagement reports ([Apple, 2018b](#); [AutoX, 2018](#); [BMW, 2018](#); [GM Cruise, 2018](#); [Honda, 2018](#); [Qualcomm, 2018](#); [Roadstar.ai, 2018](#); [SF Motors, 2018](#); [Uber, 2018](#); [Udelv, 2018](#); [Waymo, 2018b](#); [WeRide, 2018](#); [Zoox, 2018b](#)). Honda explained that automation disengagement - manual engagement (ADME) time duration was not measured due to the facts (1) that not all driving situations require measurable driver input, and (2) rigorous training and qualification required by Honda for their safety drivers enables them to be immediately alerted and to resume control if the system disengages from automation mode ([Honda, 2018](#)). Nissan did provide the ADME time duration in their disengagement report, with minimal 0 s and maximal 1 s ([Nissan, 2018](#)). NVIDIA stated that the average time of their test vehicles was less than 1 s ([NVIDIA, 2018](#)). Safety drivers in the case of Udelv's test vehicles were stated to be able to resume control within 1 s when a system failure or subpar execution of the automation technology was detected ([Udelv, 2018](#)).

Regarding whether the test vehicle is capable of operating without a safety driver, AutoX highlighted that one of their test vehicles is capable of operating without a safety driver ([AutoX, 2018](#)); Aurora reported that all of their test vehicles currently are not yet capable of operating without a driver and they always had a safety driver and copilot present ([Aurora, 2018](#)). Udelv's two test vehicles were reported as capable of operating without a driver with the fact that there

were 125 disengagements in 461 miles traveled resulting in 3.688miles per disengagement (MPD) (Udelv, 2018). Pony AI's all six test vehicles were reported as capable of operating without a safety driver with 1022.25 MPD (Pony AI, 2018). Nullmax's only one test vehicle was also reported to be capable of operating without a driver, which had 9.18 MPD and 44.65 MPD in 2017 and 2018 (Nullman, 2018). Telenav only had one test vehicle, and was reported as being capable of operating without a driver. It completed 30 miles test drive in a parking facility and had five disengagements (Telenav Inc, 2018). The requirement regarding whether an automation system is capable of operating without a driver in Title 13, Division 1, Chapter 1 Article 3.7 § 227 is incompetent to explain which automation level the test vehicle belongs to and its degree of reliability. On-road tests conducted by NIO USA have only been for Level 2 features between October 2016 and November 2017, thus having no automation disengagement of Levels 3, 4, and 5 to report (NIO USA, 2018). In Qualcomm's disengagement reports, it is stated that the all the FCDs in 2018 was due to "planned test of technology" (Qualcomm, 2018) , which Qualcomm interpreted as one type of probable causes while California DMV intended to decide if the disengagement was the result of a planned test or not. Majority of the other manufactures reported that their test vehicles were not capable of operating without a driver (AiMotive, 2018; Apple, 2018c; Baidu, 2018; BMW, 2018; GM Cruise, 2018; Honda, 2018; Mercedes Benz, 2018; Nissan, 2018; Phantom AI, 2018; PlusAi, 2018; Qualcomm, 2018; Roadstar.ai, 2018; SF Motors, 2018).

The disengagement reporting form also requests information regarding who initiated each disengagement (e.g., the automation system, the safety driver, the remote operator, or the passenger). Qualcomm stated that all their disengagements were initiated by safety drivers (Qualcomm, 2018). All the disengagements of the SAIC Motors were also initiated by the safety driver (SAIC Motors, 2018). BMW only used one of their test vehicles which had nine

disengagements in 41 miles drove in autonomous mode. Without exception, all these disengagements were initiated by safety drivers (BMW, 2018). Roadstar AI's all 43 disengagements were reported to be initiated by safety drivers with 175.33 MPD (Roadstar.ai, 2018). GM Cruise's all 86 disengagements were also initiated by safety drivers which all occurred on Street. Pony AI's 19 disengagements in an 18-month test period were initiated by safety drivers and the rest of one disengagement was initiated by the system while their four test vehicles were tested on Street (Pony AI, 2018). SF Motors' all 232 disengagements were reported to be initiated by safety drivers with 11.04 MPD (SF Motors, 2018). All of the Phantom AI's 200 disengagements were initiated by safety drivers and the disengagement locations were Street (Phantom AI, 2018). Telenav owned only one test vehicle which had five disengagements initiated by the safety driver within an accumulated test drive of 30 miles in autonomous mode (Telenav Inc, 2018). No further information was given that allows the readers to determine the exact system limits that lead to such a disengagement (SAIC Motors, 2018). Baidu had 88 disengagements including 86 initiated by the safety driver and the rest were initiated by the automation system (Baidu, 2018). Udelv had 15 disengagements initiated by the system and the rest of 110 were initiated by safety drivers (Udelv, 2018). Honda had 64 disengagements initiated by safety drivers and 13 disengagements initiated by the system (Honda, 2018). Pony AI had one disengagement triggered by the automation system and the rest of 15 were initiated by safety drivers in 2018 (Pony AI, 2018). AiMotive's all 17 disengagements were initiated by safety drivers (AiMotive, 2018).

### **2.2.2 Causes of automation disengagements**

The automation disengagement investigated at an aggregated level (Dixit et al., 2016; Favaro et al., 2018) results in a loss of the details on which component or element of the system fails to fulfill

its role that caused the disengagement. This section provides the specific causes of automation disengagement reported across all companies.

Waymo owned 111 test vehicles which resulted in 114 disengagements between December 1<sup>st</sup>, 2017 and November 30<sup>th</sup>, 2018. Specifically, 91 of the disengagements occurred on Street, 16 of them occurred on Highway, 5 of them occurred on Freeway, and 2 of them occurred on Interstate. It is also noted that, 8% of the disengagements were initiated by the system. The reported FCDs are presented as follows (Waymo, 2018b):

- Hardware discrepancy caused by a potential performance issue either related to hardware component of the automation system or a component of the base vehicle.
- The perception system failed to detect an object correctly causing a perception discrepancy.
- Unwanted maneuver of the vehicle that was not desirable under the circumstances.
- Incorrect behavior prediction of other traffic participants.
- Adverse weather conditions during testing.
- Reckless behavior of other road users.

Zoox stated that more progress has been made in 2018 by completing more miles during the daytime, nighttime, in fog and rain, in dense downtown San Francisco and freeways (Zoox, 2018b).

The disengagements captured in Toyota's report fall into four categories, which include (Toyota, 2018):

- Safety driver decided that extra braking should be applied to maintain an appropriate gap to the lead vehicle.

This type of disengagements was initiated by safety drivers when the path established by the automation system was inappropriate or when manual intervention was requisite for safe and comfortable braking.

- Automatic disengagement due to perception fault.

This type of disengagements was initiated by the system when a camera or a sensor was not functioning within internal tolerance or issued a fault. By doing so, the system chooses not to rely on the remaining cameras and sensors but returns control back to the safety driver.

- Automatic disengagement due to localization fault.

This type of disengagements was initiated by the automation system when the localization system was unable to determine the vehicles' exact location within a set time.

- Automatic disengagement due to system integrity check.

This type of disengagements was initiated by the automation system when a potential malfunction was detected in one of the redundant autonomy engagement mechanisms.

Apple's test vehicles completed 24,604 miles in automation mode, during which 40,198 manual takeovers and 36,359 software disengagements occurred between April 14, 2017 to November 30, 2018 ([Apple, 2018a](#)). The details about manual takeovers and software disengagements are presented as below ([Apple, 2018a](#)):

- Manual takeovers refer to circumstances that the safety driver decides to take back control from the vehicle software. Operational constraints such as emergency vehicles,

construction zones, or unexpected objects in and around the roadway usually will trigger manual takeovers. Safety drivers of Apple was also instructed to take back control anytime they feel imperative to do so.

- Software disengagements refer to circumstances that the monitoring system detect an issue with the input, output, or decision-making capability of the automation system, which is further categorized as the following categories:
  - Disengagements due to perception: when the sensing system cannot sufficiently localize, detect and classify an object, or track the objects in the surrounding environment.
  - Disengagements due to motion planning: when the path planning system is unable to generate a motion plan.
  - Disengagements due to control: when vehicle or the actuator systems does not respond appropriately or as expected within the designed plan.
  - Disengagements due to Communication: when there are timing issues or dropped messages between processes.

With five vehicles that are licensed for autonomous-driving test, WeRide have completed 19,067 autonomous miles and a total of 251 reportable disengagements during the test period. The MPD has improved from 3 in 2017 June to over 600 in November 2018 (WeRide, 2018). The descriptions of FCDs are divided into five categories. The frequency and percentage of each FCD category is presented in [Table 2-3](#). Examples of each type of FCDs are presented as follows:

- Discrepancy in planning: the planning system determines and calculates the trajectory that the vehicle should maintain to negotiate obstacles or the driving circumstance.

- Improper braking or acceleration during a right turn on red traffic signal.
- Failed to promptly or safely pass an obstacle or object on the roadside.
- Discrepancy in perception: the perception system detects other road agents and objects in the driving environment. Perception issues may occur when the system is unable to detect an object, detects an object but classifies it incorrectly, or late detection.
  - Detected a bicyclist but classified it as a pedestrian.
  - Late detection of traffic lights due to lighting conditions or algorithm insufficiency.
- Irregularity in control: the control system refers to the software program that dwells closest to the hardware that initiates the manipulate of the vehicle brake, steering, throttle, gear shift, turn signals, and so on.
  - Sudden vehicle acceleration or deceleration.
  - Excessive or insufficient turning during a driving maneuver.
- Irregularity in hardware: the hardware system consists of the vehicle, computing unit, sensors, wiring, fasteners, or anything that is not related to the software.
  - Inappropriate camera angle or insufficient calibration resulting in erroneous or delayed traffic light detection
  - Mechanical failure of a sensor because of wear and tear.
- Irregularity in the system: the system is defined as the middleware and auxiliary software components of the test vehicle that are liable for logging, monitoring, and coordinating data transfers between other subsystems such as control system and perception system.
  - Irregular or unsynchronized data flows in the subsystem
  - The state or performance of the subsystem is suboptimal or unsafe.

Table 2-3 WeRide's autonomous miles and number of disengagements (WeRide, 2018) (gathered by author)

<b>Facts Causing Disengagements</b>	<b>Counts</b>	<b>Percentage</b>
Discrepancy in planning	86	34.40%
Discrepancy in perception	63	25.20%
Irregularity in control	40	16.00%
Irregularity in hardware	33	13.20%
Irregularity in the system	28	11.20%
<b>Total</b>	<b>250</b>	<b>100%</b>

During the period from December 1<sup>st</sup>, 2017 to November 30<sup>th</sup>, 2018, GM Cruise's automation performance has improved a lot in terms of total autonomous miles driven as well as automation disengagements. Table 2-4 summarizes the total autonomous miles driven by GM Cruise's test vehicles as well as their disengagements.

Table 2-4 GM Cruise's autonomous miles and number of disengagements (GM Cruise, 2018) (gathered by author)

<b>Year</b>	<b>Autonomous Miles</b>	<b>Number of Disengagements</b>	<b>MPD</b>
2017	129764	105	1236
2018	447621	86	5205

According to the disengagement report of GM Cruise (GM Cruise, 2018), there are primarily four causes of disengagements, including planning related issues, perception related issues, control related issues, and other road users behaving poorly. Examples of disengagements caused by the first three include the test vehicle took too long to realize that the road was clear, the planned turns were too tight, and the vehicle accelerated too quickly. Examples of other road users caused disengagements could be other vehicles were not yielding to the test vehicle, other vehicles drifting into the test vehicle's lane, and other vehicles running stop signs. It is noticed from Table 2-5 that almost 50% of the disengagements were caused by other users' poor behaviors.

Table 2-5 GM Cruise's reported FCDs (GM Cruise, 2018) (gathered by author)

<b>Facts Causing Disengagements</b>	<b>Counts</b>	<b>Percentage</b>
-------------------------------------	---------------	-------------------

Another road user behaving poorly	41	47.67%
Precautionary takeover to address planning	36	41.86%
Precautionary takeover to address perception	8	9.3%
Precautionary takeover to address controls	1	1.16%
<b>Total</b>	<b>86</b>	<b>100%</b>

Phantom AI provided a detailed explanation when reporting FCDs. According to the disengagement report, invalid object detection results, invalid traffic light results, invalid decision-making results, and invalid high definition (HD) map results are found to be the primary causes of automation disengagements (Phantom AI, 2018). Table 2-6 presents each FCD along with its frequency.

Table 2-6 Phantom AI's reported FCDs (Phantom AI, 2018) (gathered by author)

<b>Facts Causing Disengagements</b>	<b>Counts</b>	<b>Percentage</b>
Hardware error	6	3%
Vehicle control problem	4	2%
Failed lane change maneuver	16	8%
Invalid HD map information	26	13%
Invalid motion planning result	5	2.5%
Invalid traffic light result	34	17%
Invalid localization result	8	4%
Invalid object detection result	43	21.5%
Invalid decision-making result	29	14.5%
Invalid perception result (Unexpected pedestrian)	10	5%
Invalid prediction result (Other vehicle unexpected or violated traffic rule)	19	9.5%
<b>Total</b>	<b>200</b>	<b>100%</b>

With seven licensed test vehicles, NVIDIA completed 4142 autonomous miles resulting in 206 disengagements during December 1<sup>st</sup>, 2017 to November 30<sup>th</sup>, 2018. All the tests were conducted on freeways as well as on- and -off ramps (NVIDIA, 2018). About 8.74% of those disengagements were initiated by the system and the rest were initiated by safety drivers. NVIDIA's MPD has increased from 4.6 in 2017 to 201.1 in 2018 (See Table 2-7). The FCDs reported are categorized into four types and no detailed explanations of each category were

provided. [Table 2-8](#) presents each FCD that NVIDIA reported along with their frequencies and percentages.

Table 2-7 NVIDIA's autonomous miles and number of disengagements ([NVIDIA, 2018](#))  
(gathered by author)

Period	Autonomous Miles	Number of Disengagements	MPD
12/01/2016 -11/30/2017	505	109	4.6
12/01/2017- 11/30/2018	4142	206	20.1

Table 2-8 NVIDIA's reported FCDs ([NVIDIA, 2018](#)) (gathered by author)

Facts Causing Disengagements	Counts	Percentage
Disengaged due to operator discomfort	147	71.36%
Disengaged due to perception mismatch	22	10.68%
Disengaged due to software discrepancy	18	8.74%
Disengaged due to operating outside Operational Design Domain (ODD)	19	9.22%
<b>Total</b>	<b>86</b>	<b>100%</b>

Drive AI owned 13 licensed test vehicles which had completed 4616.19 autonomous miles. There were 55 disengagements in 2018 either due to a failure of the automation technology or because that the safe operation of the vehicle required the safety driver to take back control of the vehicle. Drive AI presented definitions and descriptions of the FCDs in their disengagement report, which included the following three categories ([Drive AI, 2018](#)) :

- Motion planning discrepancy

Deviation from the planned motion behavior is regarded as an error of the path planning system. Examples of disengagements caused by this error could be insufficient clearance when passing other vehicles or late braking for pedestrians and bicyclists.

- Perception discrepancy

Discrepancy or errors in the information collected by the perception system about the attributes of other agents, static obstacles, and traffic signals are regarded as perception discrepancy. Examples of disengagements caused by this may include false perception of traffic light caused the test vehicle to proceed at red light, poor perception of red light caused the test vehicle not to stop, poor braking for pedestrian with intent to cross protected crosswalk, and so on.

- Localization divergence

Errors that cause the vehicle to become uncertain about its location are regarded as localization divergence. Examples of disengagements caused by this may include poor lane placement, uncomfortable proximity to static objects, and failed to stop outside of crosswalk for pedestrians while making a right turn.

Honda had 77 disengagements and the reported FCD are presented in [Table 2-9](#).

Table 2-9 Honda's reported FCDs (Honda, 2018) ([gathered by author](#))

<b>Facts Causing Disengagements</b>	<b>Counts</b>	<b>Percentage</b>
Incorrect behavior prediction	29	37.66%
Perception discrepancy	20	25.97%
Undesired motion planner	6	7.79%
Hardware discrepancy	13	16.88%
Software discrepancy	8	10.39%
Reckless user	1	1.30%
<b>Total</b>	<b>77</b>	<b>100%</b>

SF Motors owned one test vehicle and accumulated 2561.8 miles in autonomous mode on both urban streets and highways ([SF Motors, 2018](#)). In the report, Longitudinal Control was used to portray the relevant components of the system that control the cruising speed and Lateral Control is used to describe the relevant components of the system that control the vehicle's lateral position for path tracking. The FCDs reported by SF Motors were in great detail ([SF Motors, 2018](#)):

- Perception issue:
  - Test vehicle failed to detect red traffic light
  - The perception system failed to detect the vehicle ahead of it due to Lidar hardware or software issue
  - The performances of both Longitudinal Control and Lidar perception system were not ideal and fine tuning for safe operation is needed so the safety driver disengaged to log issues for further investigation.
  - The Lidar system failed to detect object.
  - Lane detection of the Perception system was not ideal, affecting Lateral Control performance and causing the test vehicle to oscillate within the lane.
  - The perception system failed to detect poor lane markings.
  - The perception system did not detect the edges of the traveling lane due to missing lane markings.
  - The perception system failed to detect the edges of the traveling lane due to sunlight reflections of the road surface.
  - The perception system mis-detected over-hanging bridges as an Object in the path so the test vehicle attempted to brake while the test driver take back control to avoid causing hazards in traffic.
  - The perception system failed to detect the lane markings due to foggy weather conditions.
  - The perception system failed to detect the lane markings due to wet roadway conditions.
  - The perception system failed to detect the lane markings due to rainy weather.

- The perception system mistook a bridge as a vehicle ahead of it and braked harshly.
- Lane-changing maneuver failed since the perception system was not able to detect adjacent lane
- Planning issue
  - The test vehicle lost planned trajectory due to planning software froze
  - The planning system froze causing the test vehicle unresponsive to the traffic situation.
  - The planned path was too close to adjacent lanes causing the test vehicle to be off-centered.
- Control issue:
  - Test vehicle drove too close to the right of the lane, so the safety driver disengages the automation mode to center the vehicle.
  - The performance of Longitudinal Control was not ideal and fine tuning for safe operation is needed so the safety driver disengaged to log issues for further investigation.
  - The Lateral Control performance was not ideal, causing the test vehicle to oscillate within the lane
  - The test vehicle was programmed to keep a predefined time headway while following a lead vehicle. Other vehicles cut in and the safety driver applied harsh braking to accommodating the other vehicles.
  - The test vehicle did not decelerate adequately.
- Hardware and software issue

- Planning software encountered issues, so the safety driver disengaged to reset hardware to address the issue.
- Planning software exited unexpectedly.
- Sensor delays caused delays in braking
- Precautionary takeover
  - Safety drivers disengaged the automation system due to difficult road conditions such as a tight curve.
  - The test vehicle was not performing optimally in heavy traffic condition.
  - The test vehicle was going at the speed limit but slow than the traffic stream, so the driver took over control and sped up to avoid causing unnecessary disturbances in traffic flow.
  - Another overtaking vehicle cut in too closely, so the safety driver took back control to address the unanticipated event.
  - The test vehicle was too close to the edge of the traveling lane while going downhill on a tight curve.
  - The test vehicle was not decelerating enough, so the safety driver applied the brake to keep a safe distance to the lead vehicle.
  - The traffic lights turned red and the vehicle was not decelerating enough. Therefore, the safety driver braked cautiously.
- GPS issue:
  - The GPS location of the test vehicle was not accurate.

Pony AI provided detailed descriptions of the FCDs regarding the test performance of their four test vehicles. The reported FCDs are adopted and slight altered to assist the readers have an understanding about the technical limits that hinder the development of higher levels of driving automation systems (Pony AI, 2018):

- Delayed perception for a fast-approaching vehicle
- The test vehicle drove too close to vehicles parked on the side of a street.
- GPS lost connection, impairing localization accuracy.
- The test vehicle lost traffic light status while creeping forward at an unprotected left turn
- Poor GPS signal resulting in a failure of the localization module
- The perception system detected an incoming car in a close distance at an unprotected right-turn signal
- Reckless cut-in from a neighboring vehicle
- The test vehicle was not reacting to a reckless behavior of another vehicle
- Poor yielding to U-turn cars due to a map issue
- The test vehicle did not detect the existence of a truck until it was close to it
- The test vehicle turned to the middle of the road at starting point
- The test vehicle attempted to proceed at a red traffic signal while a large truck blocked the view of the traffic signal
- The test vehicle failed to yield to pedestrians due to map issues
- The test vehicle was not ready for autonomous driving due to on-board engineering error
- The test vehicle was not yielding to pedestrians on crosswalks

- The test vehicle failed to yield to another vehicle which was attempting to merge into the lane.
- The test vehicle stalled in the middle of the intersection due to the lead vehicle and crossing traffic
- The test vehicle lost sensor data and the perception system timed out
- The localization system failed sounds to match points due to two large neighboring vehicles.
- Poor lane change maneuver when traffic light turned green

There were only five disengagements occurred during Telenav's test in a parking facility.

The FCDs were presented as following ([Telenav Inc, 2018](#)):

- Localization discrepancy:
  - The test vehicle deviated 2 meters away from its driving lane when traveling at a low speed.
  - The safety driver took back control since the back of the test vehicle was 2 meters from a wall when the vehicle was performing a parking maneuver.
  - When performing a parking maneuver, the safety driver took back control since the localization system notified the driver that it was no longer updating its location due to power cord was disconnected from one of the computers.
- Perception discrepancy:
  - The safety driver took back control since there was a pedestrian within 10 meters close to the vehicle and the visual system misclassified the subject as non-pedestrian object.

Nuro completed 24679.3 autonomous miles during December 1<sup>st</sup>, 2017 to November 30<sup>th</sup>, 2018, during which 24 disengagements had occurred (Nuro, 2018b). Significant advancement was made between 2017 and 2018 with an increase of MPD from 476 in 2017 to 1028 in 2018. There were both a safety driver and a co-driver on the test vehicle throughout all those driving tests. Safety drivers were expected to be receptive to TORs delivered by the on-board system. Co-drivers are expected to ensure the safety driver was notified by the system to resume control of the vehicle. The detailed FCDs presented in the disengagement report include the following:

- Object perception
  - The test vehicle briefly lost track of the vehicle stopped on the road resulting in an inadequate spacing between the planned trajectory and the stopped vehicle.
  - The object perception failed to detect a vehicle backing out of an occluded driveway resulting in an inadequate braking of the planned trajectory.
  - Erroneous sensor data caused the planned trajectory to diverge from the lane resulting in a potential contact with the median.
  - The late identification of a bicyclist resulting in a planned trajectory with inadequate time to yield.
  
- Onboard map:
  - The inaccuracy of the onboard map resulted in a planned trajectory that could have contacted the curb while turning right.
  
- Agent prediction

- The prediction failed to anticipate another reckless vehicle's sudden lane change which pulled across the test vehicle's lane to get to a left-turn lane.
  - The prediction failed to anticipate another reckless driver pulled out from a driveway and was pulling into the test vehicle's right-of-way.
  - Another vehicle pulled out of a driveway across the planned path.
  - A reckless driver pulled out from an unmapped driveway leading to late perception and prediction
  - The agent prediction was unable to provide an accurate prediction regarding a child ride a scooter in circles on the road, resulting in an inadequate planned trajectory.
  - After coming around a sharp bend, the prediction erroneously identified a vehicle as parked which was actually reversing from a driveway.
  - The agent prediction failed to have an accurate prediction about a bicyclist resulting in inadequate yield in a planned right-turn trajectory.
  - The agent prediction failed to anticipate a reckless vehicle running a Stop sign.
- Planning logic
    - The planned trajectory yielded late to on-coming vehicles during a unprotected left-turn maneuver.
    - The planned trajectory failed to yield to on-coming vehicles during a right-turn onto a narrow road.
    - The planned trajectory failed to leave adequate space for parked car on a narrow road.
    - The planned trajectory failed to leave enough space for a parked vehicle.

- The planned trajectory failed to leave adequate room to vehicles in the adjacent lane during a right turn.
- The planned trajectory executed erroneous sharp braking.
- The planned trajectory inadequately brakes when a reckless driver pulled out from an occluded driveway of a parking lot.
- The planned left-turn trajectory crossed the path of an oncoming vehicle at a four-way Stop-sign controlled intersection.
- The planned trajectory contacted the curb during a right-turn maneuver
- The planned trajectory did not sufficiently slow down or nudge for a construction worker on the road.

The detailed review on causes of automation disengagement provides the reader with a broad picture regarding what causes disengagements, how often it occurs, and where it usually occurs. Based on the reports covering December 1st, 2017 to November 30th, 2018 submitted pursuant to California Code of Regulations, Title 13, Article 3.7, Section 227.50, it is observed that almost everything regarding the automation system, including perception system, planning system, localization system, and prediction system, could trigger an automation disengagement. When automation disengages, human drivers need to reclaim control of the vehicle.

## **2.3 Traffic control**

The growing vehicular traffic in the United States has contributed to the development and evolution of traffic signal lights. In the past decades, numerous efforts have been devoted to improving the efficiency of the traffic control system to meet the ever-growing traffic demands.

This section aimed to focus on the how traffic signal control systems have been improved, the new and advanced control that attempt to utilize the advantages that driving automation provides. More importantly, the issues and challenges driving automation faces at signalized urban intersections will also be highlighted.

According to information used in current traffic control systems, there mainly three types of traffic signal control methods, including (1) fixed-time traffic signal control, (2) actuated traffic signal control, and (3) adaptive traffic signal control. The detailed information regarding each type of signal control is presented as follows:

- Fixed-time traffic signal control does not use any real-time information to configure its signal timing and phasing. It is often used to provide pedestrians with regular and consistent intervals to cross the street in the urban area. Its maintenance cost is usually lower than actuated signal control.
- Actuated traffic signal control needs real-time data collected through loop detectors installed at the road sections upstream of the intersection. It is often used in light traffic situation while the movements on the primary corridor is prioritized. Pedestrians and turning vehicles on the minor street need to use the push button and the loop detector, respectively, to activate the signal.
- Adaptive traffic signal control uses real-time traffic state measures of approaching vehicles to adapt to the actual real-time traffic demand. It is often used to efficiently move traffic through a busy corridor.

Innovations and advancement in the field of computer and communication technologies have motivated studies to develop more efficient next generation of traffic control methods. In the

past decade, various control automation methods have emerged with different optimization objectives to improve traffic efficiency at intersections. Minimizing the total delay becomes the most popular objective in prevalent studies, although with different constraints and optimization methods (Dresner and Stone, 2008; Li and Zhou, 2017; Müller et al., 2016; Zohdy et al., 2012). Specifically, (Li and Zhou, 2017) formulated the intersection control problem to be a CAV scheduling problem in which CAV are treated as jobs and intersections are taken as machines to process these jobs. The intersection automation method developed in this research could also be deployed network-wide to proactively schedule CAV's paths. On the other hand, the control protocols such as First-in-First-out (FIFO) were also often used in intersection control automation to minimize either time headway or both space-time resources (Dresner and Stone, 2008; Kolodko and Vlacic, 2003; Müller et al., 2016; Zohdy and Rakha, 2016). Simply put, most of the existing algorithms developed in intersection control automation employ V2V or V2I or both to improve intersection efficiency, which are presented as below:

- Reservation-based control protocol (Bashiri et al., 2018b; Carlino et al., 2013; Dresner and Stone, 2007, 2005; Dukic et al., 2013; Fajardo et al., 2011; Guler et al., 2014; Hausknecht et al., 2011; Li et al., 2013; Middlesworth et al., 2008; Perdomo López et al., 2017; Schepperle et al., 2008; Schepperle and Böhm, 2008, 2007);
- Priority-based (Alonso et al., 2011; Gregoire et al., 2014; Hassan and Rakha, 2014; Qian et al., 2014);
- Synchronized arrival flow or platoon-based (Azimi et al., 2015; Bashiri et al., 2018b; Yu et al., 2018; K. Zhang et al., 2018; Zhao et al., 2018);
- Consensus-based (Mirheli et al., 2019; Olfati-Saber et al., 2007; Peng et al., 2015; Qiu, 2018; Tsianos et al., 2012);

- Cooperative-based (Alonso et al., 2011; Bichiou and Rakha, 2018a; Lee et al., 2013; Lee and Park, 2012; Ren et al., 2018; Rodrigues de Campos et al., 2017; Xu et al., 2018; Zohdy and Rakha, 2016);
- Auction-based (Carlino et al., 2013; Levin and Boyles, 2015; Schepperle and Böhm, 2008)
- Sequenced-based (Perronnet et al., 2013);
- Demand responsive-based (Yang et al., 2016);
- Optimized reservation-based (Levin and Rey, 2017) ; and
- and others (J. Baber et al., 2005; Barthauer, 2019; Chen et al., 2018; Du et al., 2018; Feng et al., 2018, 2015; Mirheli et al., 2018; Wu et al., 2012).

As an improvement to the current traffic control approaches, however, these aforementioned control algorithms have involved limitations and assumptions, such as non-cooperative agents in the control system and equity problems when granting right-of-way. On the other hand, some of these algorithms also heavily rely on robust V2I, V2V, or V2X communication for their proper operation. Despite the significantly high cost of installing V2I control equipment, the V2I-based traffic control is usually a centralized system in which the intersection is a single point of failure. Once it fails, vehicles will have no other ways to coordinate their movements with other road users at the intersection. Another thing worth noting is that research has shown that traffic signal lights coexist with these newly proposed control automations to serve for human drivers (Barthauer, 2019; Dresner and Stone, 2007; Levin and Boyles, 2016; Sharon and Stone, 2017; Yang et al., 2016; Zhao et al., 2018). Table 2-10 presents some of the representative intersection control methods.

Table 2-10 Summary of intersection control protocols

<b>Study</b>	<b>Control protocol</b>	<b>Network control</b>	<b>Traffic composition</b>	<b>Communication</b>	<b>Novelty and Limitations</b>
(Azimi et al., 2015)(Beller et al., 2013b)	Synchronized arrival and passage at an intersection	Decentralized	Autonomous vehicles	V2I is required to synchronize the arrival flow. During intersection traversal, no V2I is required	The proposed control protocol allowed continuous flow of vehicles entering the intersection to utilize the maximum intersection capacity. However, this method enforced synchronized arrival of vehicles.
(Azimi et al., 2013)	Concurrent Crossing-Intersection protocol and Maximum Progression intersection protocol	Decentralized	Autonomous vehicles	V2V	The proposed method introduced Route Network Definition Files and constructing roundabout routes based on the GPS coordinates extracted from digital map databases.
(Middlesworth et al., 2008)	Reservation-based	Decentralized	Autonomous vehicles	V2V	No arbiter agent is required and Collision free is only achievable when all vehicles respect the protocol
(Hausknecht et al., 2011)	Reservation-based and Multiagent-based approach	Centralized	Autonomous vehicles	V2X	The control protocol based on multi-intersection optimization enabled novel, fine-grained, and dynamic control of autonomous vehicles through a grid of intersections
(Sharon and Stone, 2017)	Reservation-based	Decentralized	Manual, connected, and automated vehicles	Traffic light for drivers and V2I for connected and autonomous vehicles	The modified system could accommodate human-operated vehicles using traffic lights.

(Dresner and Stone, 2005)	Reservation-based	Decentralized	Connected vehicles	V2I	The proposed method allowed vehicles to accelerate while turning or traversing the intersection.
(Dresner and Stone, 2008)	Reservation-based	Decentralized	Autonomous vehicles	V2I	The proposed control mechanism significantly outperformed current intersection control methods -- traffic lights and stop signs. However, how turning movements would affect the efficiency of the proposed control protocol remains unclear.
(Li et al., 2013)	Reservation-based	De-centralized	Autonomous vehicles	V2I	Evaluated the control protocol on a standard simulation platform allowing for reliable comparisons between different control mechanism
(Ilgin Guler et al., 2014)	Reservation-based	Centralized	Connected vehicles	V2V	The proposed control algorithm can be used for penetration rates lower than 100%.
(Bashiri et al., 2018a)	Reservation-based	Centralized	Connected vehicles	V2V and V2I	A simple communication protocol was designed for V2I communication and two policies were introduced for the controller to minimize total delay and delay variance.
(Gregoire et al., 2014)	Priority-based	Decentralized but also possible for distributed			The priority graph is used to develop collision free and deadlock free control protocol. However, Fixed path assumption; Priority law lacks the consideration of sensing and control uncertainty
(Qian et al., 2014)	Priority-based	Decentralized	Manual and autonomous vehicles	Traffic light for drivers V2I for	Special priority policy to accommodate manual vehicles.

				autonomous vehicles	
(Scheppele and Böhm, 2008)	Reservation-based	Decentralized	Connected vehicles.	V2V	The design of effective mechanisms for intersection control, i.e., mechanisms which can reduce the average waiting time weighted by the driver valuations.
(Roozbehani et al., 2009)	A feedback formation protocol	Decentralized	Autonomous vehicles	V2V	A flexible, computationally efficient, decentralized algorithm was developed to resolve conflicts among autonomous vehicles with simple internal dynamics at intersections.
(Makarem and Gillet, 2011)	Energy optimization approach	Decentralized	Autonomous vehicles	Doesn't require long range communication and robust to various communication failures	Heavier vehicles have a priority to allow energy optimization for intersection crossing.
(Hassan and Rakha, 2014)	Priority-based	Distributed	Autonomous vehicles	V2X	The distributed algorithm enables vehicles in the vicinity of an intersection continuously cooperate with each other to develop a schedule that safe traversing of intersections while incurring minimum delays.
(Yang et al., 2016)	Demand responsive-based	Decentralized	Manual, connected, and automated vehicles	V2X	The proposed control protocol could modify automated vehicles' trajectories to reduce delay and stops. The fast branch and bound algorithm were used to improve computational efficiency.
(Levin and Rey, 2017)	Optimized reservation-based by developing a	Decentralized	Autonomous vehicles	V2I	This study provided justification for using conflict region model to approximated traffic control protocols

	subset of vehicles to move at each time step				that uses tile-based reservation approach and also developed more system-efficient policies for reservation-based control.
(Sun et al., 2017)	Optimized reservation-based	Decentralized	Manual, connected, and Automated vehicles	Traffic light for drivers and V2I for connected and autonomous vehicles	The proposed control protocol is able to serve bi-directional traffic in one signal phase and maximizes the intersection capacity by utilizing all lanes at any time. Right-turn traffic is not considered in this research. The proposed method is limited to theoretical analysis. Field implementation would not be possible unless enough CAVs are available in the real world.
(Yu et al., 2018)	Optimized reservation-based	Decentralized (isolated urban intersections)	Manual, connected, and automated vehicles	Traffic light for drivers and V2I for connected and autonomous vehicles	Vehicle trajectory planning is integrated into traffic signal optimization in a unified framework to minimize vehicle delays. All vehicles are assumed to be controllable which restricts the implementation of the proposed model. The uncertainties in driving behaviors and traffic environment needs to be addressed when implementing the proposed control protocol.
(Bichiou and Rakha, 2018a)	Sequenced-based	Decentralized: only single lane intersections are considered	Automated Connected Vehicles	V2V, V2I for autonomous vehicles (Perfect communication between the vehicles themselves and between the	The proposed algorithm outperforms the other intersection control strategies producing lower delays and CO <sub>2</sub> emissions with reductions of up to 80 % and 40 %, respectively, relative to the best intersection control strategy (in this case the roundabout). High

				scheduler is assumed.)	computational cost associated with the nonlinear optimization makes it difficult for. real-time applications
(Bichiou and Rakha, 2018b)	Sequenced-based	Decentralized: only single-lane intersections are considered	Automated vehicles	V2V, V2I for autonomous vehicles (perfect communication between the vehicles and between the scheduler is assumed)	The proposed method used optimal control theory to formulate the complete dynamic model to provides optimality and/or sub-optimality with a guaranteed low computational burden.
(Feng et al., 2018)	Two-level optimization approach	Decentralized: isolated intersections	CAV environment	Communication between the vehicles themselves and between the scheduler is assumed	This paper provides a joint control framework for controlling vehicle trajectories and traffic signals simultaneously to improve the efficiency of intersection operation as well as reduce vehicle emissions in a CAV environment. The control is extended from one dimension (either spatial or temporal) to two dimensions (spatiotemporal). The mixed traffic condition where not all vehicles are controllable is not considered
(Fayazi and Vahidi, 2018)	Optimization-based approach	Decentralized	A mix of autonomous and human-controlled connected vehicles.	V2V, V2I (the controller resides on a computational server and receives information of all subscribing vehicles and then schedules the intersection access time for each vehicle)	The proposed method not only significantly reduced intersection delay and number of stops compared to pre-timed intersection benchmarks, but also ensured that no crash occurred and did not compromise travel time. More modifications are required to make the proposed control scheme applicable to situations with purely manual vehicles that have no wireless

					connectivity. Left- and right-turning vehicles were not included in this research.
(Y. Guo et al., 2019)	Optimize CAV trajectories and intersection controllers: shooting heuristic algorithm is used to efficiently construct trajectories for a stream of traffic and dynamic programming algorithm to obtain an optimal signal timing plan	Decentralized but possible for distributed implementation	CAV	V2V, V2I for autonomous vehicles (Perfect communication between the vehicles themselves and between the scheduler and vehicles is assumed.)	The proposed algorithm method can be applied and adapted to busy physical urban signalized corridors. Compared to the adaptive signal control, it reduces the average travel time and reduce fuel consumption. The issues associated with parallel computation algorithms, feedback control, and distributed computation need to be taken into further consideration.
(Mirheli et al., 2019)	Dynamic optimization of acceleration to maximize intersection throughput	Distributed coordinated	Connected and automated vehicles	V2V	The distributed vehicle-level solutions were sent towards global optimality. The control protocol can be applied to a wide range of large-scale problems to assess its solution quality and computation efficiency. The effect of stochasticity on the performance of the proposed control protocol should be considered.

## 2.4 Permissive left turns

Traffic engineers have adopted permissive left-turns to improve traffic control efficiency as a driver has fewer available gaps in the opposing traffic to execute a left turn safely. During a protected left-turn interval, the left-turning vehicle has the exclusive right-of-way and faces no conflicts. During a permissive left-turn interval, the left-turning vehicle can turn only after yield to conflicting traffic, pedestrians, and bicyclists. Permissive left-turn intervals can be communicated to drivers by different traffic signal indications, which include circular green (CG), flashing circular red (FCR), flashing circular yellow (FCY), flashing red arrow (FRA), and flashing yellow arrow (FYA) indications. Using different indications to communicate the same message to drivers appeared to be a significant issue considering their impact on driver behavior and driving safety. It is worth highlighting that FYA was found to be the most effective way to communicate permissive left turns (Brehmer et al., 2003; Knodler et al., 2007b; Noyce et al., 2014). The usage of FYA was approved by FHWA and was documented in the Manual of Uniform Traffic Control Devices (MUTCD) (MUTCD, 2009). According to (MUTCD, 2009), left-turning movements could be controlled by one of the following methods:

- Protected only mode: left turns are only made during a left-turn green arrow signal indication
- Protected/Permissive mode: both modes are used on an approach within one signal circle
- Permissive only mode: left turns must be made on a circular green or a flashing left-turn yellow arrow
- Variable left-turn model: control mode of left-turning movements could be above three modes and changes as the traffic condition changes.

Agency practitioners from 50 states have been surveyed regarding the yellow change and red clearance intervals (NCHRP 03-125). According to the survey results, the usage of FYA and FRA indications were presented as follows (NCHRP 03-125):

- Most of the respondents (82%) only use FYA indications;
- Maryland and Delaware only used FRA indications for permissive intervals; and
- Alabama, Arizona, Florida, Georgia, New York, Michigan, and Virginia used both FYA and FRA indications.

In addition, most of the respondents (86%) reported that FYA or FRA indications were typically required at new signal installations where PPLT intervals were used (NCHRP 03-125). Regarding the future trend of permissive left-turn indications, the survey revealed that (NCHRP 03-125):

- More than half of the respondents (61%) reported that they had a plan to replace PPLT indications with FYA or FRA indications;
- Only 36% respondents had no plans to address FYA usage; and
- 3% of the respondents had already converted PPLT indications to FYA or FRA.

The application context affects the organizations' decisions on the implementation of FYA and FRA for permissive left-turn movements. The contextual factors may include the following (NCHRP 03-125):

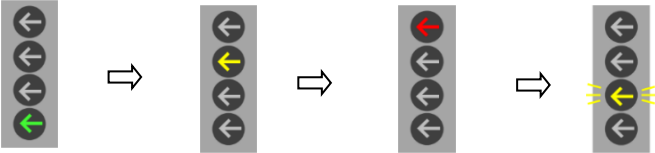
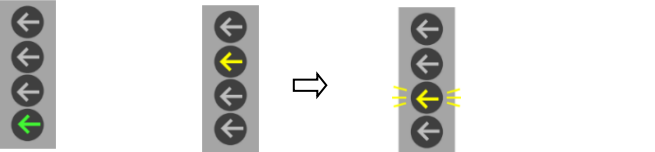
- Urban, suburban, and rural environments;
- Locations with high volumes of pedestrians;
- Near at-grade rail crossings; and

- Intersections with preemptions (such as emergency service or rail).

The signal head configurations and signal phase sequences when using FYA and FRA indications were also investigated extensively (NCHRP 03-125). Table 2-11 and 2-12 presents the surveyed results regarding the signal head configurations and signal phase sequences when using FYA and FRA. Multiple configurations could be selected by respondents according to their actual situation. According to Table 2-11 and 2-12, the following can be concluded:

- Majority of the respondents (77.7 %) use four-section signal heads when applying FYA;
- Only 20.5% of the respondents use three-section signal heads;
- Doghouses are still being used, though with a very low percentage of 1.4%;
- Majority of the respondents (76.5%) use a red clearance before transition to FYA;
- Majority of the respondents (70%) use three-section signal heads when applying FRA; and
- Majority of the respondents (80%) use a red clearance before transition to FRA.

Table 2-11 Flashing Yellow Arrow configuration and signal sequence (recreated based on NCHRP 03-125).

Display Type	Signal Sequence	Percentage
Four-Section Displays		61%
		16%

		0.7%
Three-Section Displays		6.5%
		0.7%
		9%
		4.3%
		0.7%
Doghouse display		0.7%
		0.7%

Table 2-12 Flashing Red Arrow configuration and signal sequence (recreated based on NCHRP 03-125)

Display Type	Signal sequence	Percentage
Three-section display		60%

		10%
Four-section display		20%
		10%

The automated driving system need to have a robust perception and planning system to be able to perform left-turn tasks at permissive left-turn signals. As is indicated by [Tables 2-11 and 2-12](#), there are various types of permissive left-turn signal indications. The variations of change intervals and clearance intervals used in various permissive left-turn indications also complicate the situation for driving automation system to properly react to it. To successfully perform a permissive left-turn task, the driving automation system needs to be able to perform the procedures presented in [Table 2-13](#).

Table 2-13 Pseudo-code for left-turn maneuvering when facing permissive left-turn signal

---

**Algorithm 1.** Left-turn manoeuvring: LTM

---

Input:

- Intersection lane related

lane\_position: Move to the correct lane to prepare for the coming left-turn maneuver

turn\_time: The estimated time to completely execute the left-turning maneuver

- Traffic signal related

signal\_type: The retrieved information on the type of traffic signal control;

signal\_phase : The recognized signal phase at the moment;

- Traffic condition related

gap: the calculated gaps from on-coming traffic flow  $f$  in second

pedestrian: the pedestrian existence on crosswalk

pedestrian = 0: no pedestrian or all pedestrians are out of the critical zone

pedestrian = 1: at least one pedestrian is in the critical zone

---

Output: The final decision-making of the left-turn execution

---

**Initialize:**

```
lane_position = left_turn
signal_type = permissive_only
select_gap = 0
pedestrian_safe = False
```

**# Check signal**

```
While t ≤ tmax
  if signal_type ≠ flashing_yellow:
    t += 1
  else
    signal_phase = flashing_yellow
end while
```

**# Check gap**

```
While t ≤ tmax
  gap = get.gap(t, f)
  for i in index(gap)
    if turn_time > gap(i)
      i += 1
    else
      select_gap = gap(i)
  end while
```

**# Check pedestrian**

```
While t ≤ tmax
  if pedestrian = 1:
    t += 1
  if pedestrian = 0
    pedestrian_safe = True
```

**# check time budget**

```
if t ≤ tmax and signal_phase = flashing_yellow and select_gap and pedestrian_safe
  ego vehicle execute left – turn
else
  request to intervene
```

---

When the driving automation is indicated to have system limits, as is case with SAE Level 3, the driver should be able to detect or reminded by the automation system about the following critical situations:

- When what the automation system is doing is not in line with what drivers considered to be safe;
- When the automation system is incapable of completing the necessary tasks (either because of a lack of human-like reasoning about the driving situation or a lack of logic for strategic reasoning) to follow the planned path; and
- When the automation system is deviating from the current planned trajectory.

When these three situations occurred during a left-turn task at a permissive left-turn signal, drivers need to reclaim control and complete the left-turn task.

## **2.5 Driver-Automation system**

### **2.5.1 Defining Driver- Automation System**

The scope of automated vehicle technology is presented [Section 2.1](#). The Driver-Automation System (DAS) in this research is defined as a system in which the functions of a driver and automated features are integrated. The DAS is treated as a single entity that interacts the external environment appropriately to complete all necessary driving tasks. While automation technologies at all levels are expected to provide a safety benefit, there are still human factors issues associated with them (see [Table 2-2](#)). The DAS entity takes full responsibilities of lateral and longitudinal control, monitoring of the other road users and the environment, and ensures safety.

### **2.5.2 Driver's role in DAS**

Automation is often used to improve system efficiency and safety by lessening the degree of human involvement. To achieve a safe driving automation, a cross-domain set of challenges must

first be solved as identified in [Section 2.2](#). As driving automation assists and even supplants drivers, the capability of automation to communicate and cooperate with human drivers becomes more important. As presented in [Section 2.1](#), drivers continue to have a role in driving automation either as a controller, co-pilot, supervisor, or a backup figure before all the driving tasks become fully automated. Many cognitive factors are involved in when drivers interacting with an automated driving system. For the purpose of modeling control transition in a PPLT scenario, drivers' visual scanning, attention selection, and response time will be reviewed.

First, drivers need to visually monitor the traffic condition and the driving environment, which includes where is the ego vehicle's current position and speed, other road users' intention, positions, and speed, potential static objects on the road, location of off-road objects, traffic signals, and road surface conditions.

With all the visual and other information collected, drivers need to select relevant information and neglect less relevant information to make decisions. Inattention can lead to degraded lane keeping, poor speed maintenance, delayed reaction time, missed traffic signs and traffic signals, and unsafe following distance.

[Section 1.2.2](#) touches on safety drivers' and ordinary drivers' reaction times: (1) the average reaction time of a total of 1330 disengagement events is 0.85 s with a standard deviation of 0.70; ordinary drivers' reaction times in an experimental study ranges from 0.81 s to 2.44 s with a mean of 1.33 s and a standard deviation of 0.27 s ([Broen and Chiang, 1996](#)). More information can be found in [Section 2.6](#) about drivers' response time with regard to TOR. Lead time or time budget is another important concept in the studies of control transitions in an DAS. [Section 2.7.1](#) highlighted related studies investigating driver performance following a TOR. The motivation of

thoroughly understanding driver responses given different lead times arises from a need to identify operational parameters for DAS. See more details in [Section 2.7.1](#). How a DAS should be designed to ensure reliable and safe behavior adaption is highly affected by how drivers react given different lead times.

### **2.5.3 Control transitions**

When the driving automation system detects that the current driving situation is out of its operational design domain, it will issue a TOR to driver. Control transitions of a vehicle is a state transition of the vehicle control between the automated system and the human drivers. When an automated system requests the driver to resume control, meaning a resumption of responsibilities on lateral and longitudinal control, monitoring of the traffic and road conditions, and interacting with the vehicle displays and automated systems correctly. Influencing factors on the quality of drivers' driving task execution after resuming control from automated driving systems are reviewed in [Section 2.6](#).

## **2.6 Takeover behavior**

This section attempts to carefully examine how drivers would resume control from various levels of driving automation in different situations with and without secondary tasks. It can be observed that takeover behavior in an automation system is a very important issue, especially in ensuring the overall safe driving performance of the shared-control system. In the following discussion, the relations between experimental factors and takeover performance, and the actual measures of takeover performance will be presented. Firstly, how drivers take back manual control over the automated system is investigated with the consideration of (1) whether drivers are engaged in a

NDRT, (2) what is the unfolding driving situation, and (3) what is the physical and mental condition when the automation request drivers to intervene.

Regarding the effect of on-going situation on takeover performance, traffic density was found to have a significant impact on drivers' takeover performance (Dogan et al., 2017; Gold et al., 2018, 2016; Jamson et al., 2013; Körber et al., 2018a, 2016; Radlmayr et al., 2014). Drivers experienced a longer reaction time in response to TOR with the presence of traffic (Gold et al., 2016). Regarding the effect of drivers' characteristics on takeover performance, drivers' ages were found to have a definite effect on their takeover performance (Körber et al., 2016). As a matter of fact, more than one hundred of experiment-based studies have been conducted to investigate how drivers will perform when the automation system requests the drivers to reclaim control in both critical and non-critical situation, on highways, on rural roads, around work zones, with high density traffic and with no traffic on the road. Similarly, how the drivers' ages, alcohol intake, sleep deficiencies, and overall fatigue affect drivers' takeover performance were also examined by the driving experiment-based studies. Figure 2-1 shows that a large number of participants were included in takeover studies. A total of 6339 subjects were included in those reviewed studies, including one survey-based study which had 3000 subjects from 102 countries (Bazilinsky et al., 2018). However, very few studies investigated takeover situations in urban scenarios especially on

taking back control at a signalized intersection. More detailed information regarding takeover behavior during various traffic situations is presented in [Table 2-14](#).

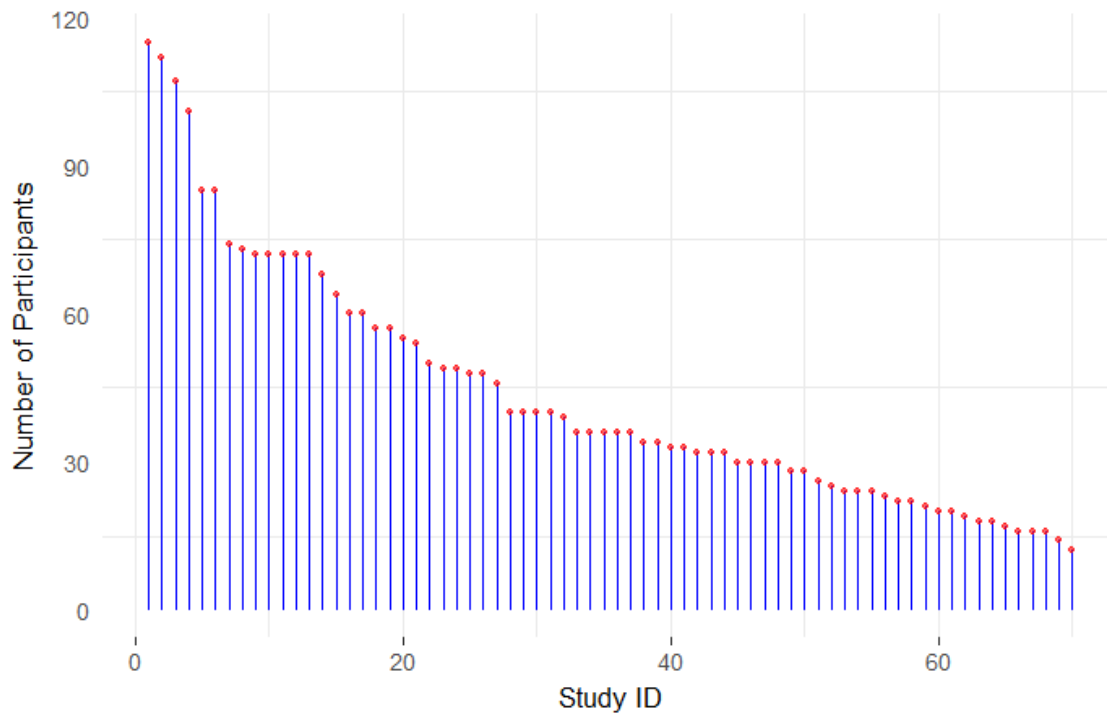


Figure 2-1 Number of participants in takeover studies

Table 2-14 Summary of takeover behavior studies

Study	Experiment	Measures	Conclusions
(Boelhouwer et al., 2019)	<ul style="list-style-type: none"> <li>• Apparatus: a driving simulator</li> <li>• Objective: the effect of system information on takeover decisions.</li> <li>• Participants: 28</li> </ul> <p>Scenarios: urban environment. Sharp curves, roadwork, T-junction, speed bumps, left-turns, non-signalized intersection, pedestrians, tunnel, crosswalk, dead end, small object, stranded vehicles, dirt road, and zone end were all included in the driving scenarios</p>	<ul style="list-style-type: none"> <li>• The timing of the takeover</li> <li>• Correct and incorrect takeovers</li> <li>• Percentages of drivers that correctly decide to rely on the vehicle when possible and to take back control when necessary</li> </ul>	<ul style="list-style-type: none"> <li>• At present, drivers in partially automated vehicles, in which the system still needs driver interaction in some cases, do not seem to have been prepared for a new role. After reading the system information, drivers ' mental models were not more accurate</li> </ul>
(Seppelt and Lee, 2019)	<ul style="list-style-type: none"> <li>• Apparatus: a fixed-based driving simulator</li> <li>• Number of participants: 48</li> <li>• Objective: to evaluate the benefits and costs associated with providing drivers continuous feedback on the limits and behavior of vehicle control automation</li> <li>• Scene: four-lane urban and freeway roads with a jersey barrier separating opposing lanes of traffic. Traffic in the oncoming and passing lanes passed at a rate of 12 to 18 cars per minute. A continuous light fog and light rain was simulated with a limited sight distance of 1300 m Participants followed a lead vehicle that varied its speed according to a sum of two sine waves</li> </ul>	<ul style="list-style-type: none"> <li>• Reaction time (brake response)</li> <li>• Time-to-collision</li> <li>• Frequency of responses prior to the event</li> <li>• Mental model accuracy</li> <li>• Proactive response behavior</li> <li>• Subjective trust and self-confidence</li> <li>• Secondary task performance</li> </ul>	<ul style="list-style-type: none"> <li>• Drivers responded earlier when provided with continuous display information than discrete warnings, and of the three forms, earliest with the multi-modal feedback</li> <li>• The comparison of the discrete and continuous information displays also confirmed the response benefit of auditory information over visual information in event-critical situations</li> <li>• The experimental results also demonstrated the response</li> </ul>

	<ul style="list-style-type: none"> <li>• NDRTs: roadside billboard detection task</li> <li>• Lead time: not mentioned</li> </ul>	<p>benefit of auditory information over visual information in critical scenarios. and also revealed the importance of including visual information when communicating the TOR to drivers</p> <ul style="list-style-type: none"> <li>• Continuous feedback helped inform drivers the evolving relationship between the system performance and the operating limits</li> </ul>	
(Wu et al., 2019)	<ul style="list-style-type: none"> <li>• Apparatus: a driving simulator</li> <li>• Number of participants: 115</li> <li>• Objective: to study the linear correlation between age and takeover-performance</li> <li>• Scene: drivers encountered three types of driving situation including automated driving for 3 minutes, automated driving for approximately 31 minutes, and automated driving for 10 minutes followed by 10-minute of manual driving and then followed by another automated driving</li> </ul>	<ul style="list-style-type: none"> <li>• Time consumed after takeover-request until the steering wheel is turned right by 1°</li> <li>• Time consumed until the brake pedal is pressed to 10 percent of full braking</li> <li>• Reaction time</li> <li>• Standard deviation of the steering wheel angle after lane change</li> <li>• Time-to-collision</li> <li>• Eye blink duration</li> <li>• Karolinska Sleepiness Scale</li> </ul>	<ul style="list-style-type: none"> <li>• Timely manual driving requires the driver to switch between manual and automated driving twice</li> <li>• Older drivers tend to be more vulnerable to the mental fatigue caused by the task switching that requires a functionality shift, and thus they react more slowly</li> </ul>
(Jarosch et al., 2019)	<ul style="list-style-type: none"> <li>• Apparatus: a driving simulator</li> <li>• Number of participants: 73</li> <li>• Objective: to investigate the effects of task-induced fatigue in prolonged</li> </ul>	<ul style="list-style-type: none"> <li>• PERCLOS: percentage of eyelid closure over the pupil over time</li> <li>• KSS: Karolinska Sleepiness</li> </ul>	<ul style="list-style-type: none"> <li>• An engagement in monotonous monitoring tasks in conditional automated driving affects drivers' state</li> </ul>

	<p>conditional automated driving on takeover performance</p> <ul style="list-style-type: none"> <li>• Scene: a three-lane highway with hard shoulders. The traffic density was low and there were two elongated curves and hardly any overtaking situations during the ride</li> <li>• NDRTs: a monotonous monitoring task (Pqpd task) and quiz tasks</li> <li>• Lead time: 7 s</li> </ul>	<p>Scale</p> <ul style="list-style-type: none"> <li>• Center-of-road fixation time</li> <li>• Hands-on time</li> <li>• First steering maneuver</li> <li>• First braking maneuver</li> <li>• Maximum longitudinal acceleration</li> <li>• Maximum lateral acceleration</li> </ul>	<p>and takeover performance when it comes to takeover situations</p> <ul style="list-style-type: none"> <li>• An adequate driver state is necessary for safety reasons especially in prolonged automated driving</li> </ul>
(Eriksson et al., 2019)	<ul style="list-style-type: none"> <li>• Apparatus: a driving simulator</li> <li>• Number of participants: 25</li> <li>• Objective: to investigate driver behavior in takeover scenarios with different stages of supports including baseline, sphere, carpet, and arrow HMI interfaces</li> <li>• Scene: the automated vehicle drove in the right lane of a two-lane highway at 110 km/h (68.4 mi/h) and approached a slow-moving vehicle (e.g., truck, tractor, or moped) driving at 58 km/h (36.0 mi/h)</li> <li>• NDRTs: played “Angry Birds” as a non-driving task</li> <li>• Lead time: 12s</li> </ul>	<ul style="list-style-type: none"> <li>• Success Rate</li> <li>• Braking Rate</li> <li>• Eyes-on-Windshield Reaction Time</li> <li>• Hand-on-Wheel Reaction Time</li> <li>• Steer Move Time</li> <li>• Brake Reaction Time</li> <li>• Lane Change Time</li> <li>• Head Angle</li> <li>• The NASA-TLX</li> <li>• A nine-item technology acceptance questionnaire</li> </ul>	<ul style="list-style-type: none"> <li>• The HMIs had no significant effect on drivers’ initial reaction to the takeover request</li> <li>• When drivers experienced the carpet or arrow interface, improvements were found in drivers’ correct decisions (for example, to brake or to change lane)</li> <li>• Visual HMIs can assist drivers in making a correct braking or lane change maneuver in a takeover scenario</li> </ul>
(Naujoks et al., 2019)	<ul style="list-style-type: none"> <li>• Apparatus: On-road experiment with a BMW 520d Touring</li> <li>• Number of participants: 34</li> <li>• Objective: to investigate the driver’s takeover performance when switching from working on different NDRTs</li> </ul>	<ul style="list-style-type: none"> <li>• Takeover time</li> <li>• Standard deviation of lateral position</li> <li>• Standard deviation of the steering wheel angle</li> <li>• Velocity</li> </ul>	<ul style="list-style-type: none"> <li>• The takeover times varied in a range of median values of 2.71 s to 4.90 s in noncritical situations</li> <li>• The effects of different NDRTs on takeover</li> </ul>

	<p>while driving with a conditionally automated driving function (SAE L3)</p> <ul style="list-style-type: none"> <li>• Scene: the driving wizard kept a constant speed of about 100 km/h while driving mostly on the right lane of the freeway, except for overtaking slower vehicles</li> <li>• NDRTs: reference task, audio book, search task, reading, and playing Tetris</li> <li>• Lead time: not mentioned</li> </ul>	<ul style="list-style-type: none"> <li>• The vehicle's lateral position</li> <li>• Rating scale for the assessment of driving and traffic situations</li> <li>• The level of drowsiness: the 9-point Karolinska Sleepiness Scale</li> </ul>	<p>performance could be shown to some extent</p> <ul style="list-style-type: none"> <li>• The adverse effects of taking back control from the driving automation on vehicle control were only visible during the first 5 s after the transfer of control</li> <li>• Drivers managed to regain control over the vehicle safely, nevertheless they needed more time to prepare for the manual takeover when the NDRTs caused motoric workload</li> </ul>
<p>(Pampel et al., 2019)</p>	<ul style="list-style-type: none"> <li>• Apparatus: a driving simulator</li> <li>• Number of participants: 16</li> <li>• Objective: to investigate the impact of short (unplanned, five s) and long (planned, 50 s) TORs on drivers' takeover performance while drivers were playing and were not playing an engaging tablet game</li> <li>• Scene: a busy UK motorway and the traffic slowed down to 40 mph and became a moving traffic jam.</li> <li>• NDRTs: an immersive game (Tetris) on a tablet</li> <li>• Lead time: not mentioned</li> </ul>	<ul style="list-style-type: none"> <li>• Speed</li> <li>• Lateral stability</li> <li>• Mean fixation duration</li> <li>• Number of fixations on HMI</li> <li>• Percentage to road center</li> <li>• Spread of search</li> </ul>	<ul style="list-style-type: none"> <li>• Comparisons of the 60-second period of manual driving following automation suggested better longitudinal vehicle control as well as more appropriate SA following the long TOR, and automation periods without the game</li> <li>• Following no engaging game, lateral performance was worse during the first 10 s of manual driving</li> <li>• Control-level visual search patterns did not change with TOC time or the game.</li> </ul>

<p>(Jarosch Oliver and Bengler, 2019)</p>	<ul style="list-style-type: none"> <li>• Apparatus: a driving simulator</li> <li>• Number of participants: (study 1) 52 valid /56 in total, (study 2) 68 valid / 73 in total</li> <li>• Objective: to compare two takeover situations that just differed in the duration of the automated driving</li> <li>• Scene: a three-lane highway with a hard shoulder, a crash in the lane of the ego vehicle</li> <li>• NDRTs: Quiz-task, PQBD-task</li> <li>• Lead time: 7 s</li> </ul>	<ul style="list-style-type: none"> <li>• Takeover control rating</li> <li>• Takeover categories</li> <li>• Mean scores of takeover control rating</li> <li>• Reactions of the drivers</li> </ul>	<ul style="list-style-type: none"> <li>• Takeover performance strongly differs among individuals</li> <li>• In conditional automated driving the human driver needs to be supported in takeover situation</li> <li>• The influence of the duration of the ride was stronger than that of the non-driving related task.</li> <li>• The TOC rating barely affects takeover performance if there are multiple options for a driver's response</li> </ul>
<p>(Vogelpohl et al., 2018)</p>	<ul style="list-style-type: none"> <li>• Apparatus: a driving simulator</li> <li>• Number of participants: 60</li> <li>• Objective: to investigate the progression of fatigue during automated driving and its effects on the ability to take back manual control after a TOR</li> <li>• Scene: a three-lane highway</li> <li>• NDRTs: not allowed</li> <li>• Lead time: 10 s</li> </ul>	<p>Reaction time</p> <ul style="list-style-type: none"> <li>• Eyes on Road</li> <li>• Hands On</li> <li>• Feet On</li> <li>• Automation Off</li> <li>• Brake Reaction</li> <li>• Gaze Side Mirror</li> <li>• Gaze Speed</li> </ul> <p>Situation awareness</p> <ul style="list-style-type: none"> <li>• The time taken to look at the side mirror and at the speed display for the first time after the takeover request/warning signal</li> <li>• The type of reaction (braking and staying in the lane vs. steering and</li> </ul>	<ul style="list-style-type: none"> <li>• Drivers of automated vehicles will likely be more prone to fatigue in the presence of a previously acquired lack of sleep than manual drivers</li> <li>• Fatigued drivers can be slow to react to takeover requests.</li> <li>• Drivers with automation needed longer to check their speed on a speed display after a takeover request</li> <li>• After a takeover request or a warning signal drivers tend to brake and stay in the lane behind a braking lead vehicle, compared to the manual drivers who often overtook</li> </ul>

		overtaking) (takeover modes)	the braking lead vehicle without braking
(Cramer and Klohr, 2019)	<ul style="list-style-type: none"> <li>• Apparatus: On-road experiment</li> <li>• Car: Audi A5 (construction year: 2012), partially automated driving</li> <li>• Number of participants: 39</li> <li>• Objective: to evaluate active vehicle roll motions as feedbacks for the driver to announce automated lane changes to obtain knowledge about the preferred roll motion design</li> <li>• Scene: a three-lane oval test track. The maximum speed of the test vehicle was 60 km/h on the straight part and 22 km/h in the curves of the test track</li> <li>• NDRTs: participants were instructed to supervise the system and no NDRTs were allowed</li> </ul>	<ul style="list-style-type: none"> <li>• Questionnaires were chosen with increasing intensity from 1 to 5</li> <li>• First impression of the intensity of roll motions</li> <li>• Direction of roll motions</li> <li>• Angle of roll motion</li> <li>• Announcement time for lane changes</li> <li>• Roll profiles</li> <li>• Motion sickness</li> <li>• System awareness</li> <li>• Acceptance</li> <li>• General attitude</li> </ul>	<ul style="list-style-type: none"> <li>• Active roll motions as a feedback for announcing automated lane changes should be perceptible and not misleading to support drivers to maintain their mode or system awareness</li> </ul>
(Yoon et al., 2019)	<ul style="list-style-type: none"> <li>• Apparatus: a driving simulator</li> <li>• Number of participants: 20</li> <li>• Objective: to investigate the influences of TOR modalities on a drivers' takeover performance after they engaged in NDRTs in highly automated driving</li> <li>• Scene: a four lanes two-way highway with no traffic and mostly consisted of straight roads</li> <li>• NDRTs: no-task, phone conversation, smartphone interaction, and video watching tasks</li> <li>• Lead time: 7 s</li> </ul>	<ul style="list-style-type: none"> <li>• Takeover time</li> <li>• Hands-on time</li> <li>• Time to fixation</li> <li>• Questionnaire: participants' subjective attitude towards the TOR</li> </ul>	<ul style="list-style-type: none"> <li>• Takeover and hands-on times varied significantly between modalities, especially for phone conversations and smartphone interaction tasks.</li> <li>• Participants failed to takeover control of the vehicle when they were given visual TORs for phone conversation and smartphone interaction tasks.</li> <li>• The perceived safety and satisfaction varied for the NDRTs</li> </ul>

			<ul style="list-style-type: none"> <li>• NDRTs significantly affected the takeover time, but there was no significant interaction effect between the TOR modalities and the NDRTs</li> </ul>
(Dogan et al., 2019)	<ul style="list-style-type: none"> <li>• Apparatus: a driving simulator</li> <li>• Number of participants: 44</li> <li>• Objective: to investigate the effect of different types of NDRTs and takeover situations on driver performance</li> <li>• Scene: a three-lane highway with a speed limit of 130 km/h and was modeled after a real highway around the city of Clermont-Ferrand, France.</li> <li>• NDRTs: writing emails and watching videos</li> <li>• Lead time: 10 s</li> </ul>	<ul style="list-style-type: none"> <li>• Takeover time (sec)</li> <li>• Lane change time (sec)</li> <li>• Lane change speed (m/s)</li> <li>• Maximum deceleration (m/s<sup>2</sup>)</li> <li>• Minimum time-to-collisions (sec)</li> <li>• Frequency analysis of steering wheel angle (Hz)</li> <li>• Standard deviation of speed (m/s)</li> <li>• Minimum time headway (sec)</li> <li>• Mental workload: Rating Scale Mental Effort (RSME)</li> </ul>	<ul style="list-style-type: none"> <li>• Regardless of the type of NDRTs, the takeover situation had an effect on drivers' takeover time and drivers had a shorter time in obstacle avoidance situation.</li> <li>• The criticality of the situation had an impact on takeover time and mental workload, while NDRT did not have a clear role</li> <li>• Measures of driver performance in the obstacle avoidance situation did not differ among manual and automated driving conditions, except for minimum TTC</li> <li>• Regardless of NDRTs that drivers engaged in, driving mode influenced both lateral and longitudinal control as well as minimum time headway in the missing lane situation</li> </ul>
(Yoon and Ji, 2019)	<ul style="list-style-type: none"> <li>• Apparatus: a driving simulator</li> <li>• Number of participants: 27</li> <li>• Objective: to investigate the influence</li> </ul>	<ul style="list-style-type: none"> <li>• Gaze-on time</li> <li>• Fixation time</li> <li>• Hands on steering wheel</li> </ul>	<ul style="list-style-type: none"> <li>• For both visual performance and takeover capability, there was a significant difference based on the task carried out.</li> </ul>

	<p>of NDRTs on takeover performance in a highly automated driving context and the effect of workload on driver's takeover performance</p> <ul style="list-style-type: none"> <li>• Scene: a 15 km long track. The participants were asked to take over control of the vehicle at three locations along the overall track (after approximately 3.5, 8, and 14 km)</li> <li>• NDRTs: (1) interacting with an entertainment console, (2) watching a video, and (3) interacting with a smartphone</li> <li>• Lead time: not mentioned</li> </ul>	<p>time</p> <ul style="list-style-type: none"> <li>• Takeover time</li> <li>• NASA-TLX</li> </ul>	<ul style="list-style-type: none"> <li>• Drivers' reaction times when reaching for the steering wheel did not differ among NDRTs</li> <li>• The types of NDRTs had a significant effect while a positive correlation between the performance dimension and takeover was found</li> <li>• Takeover performance for interaction with the entertainment console had a positive correlation, whereas watching a video or interacting with a smartphone had negative correlation with workload dimensions</li> </ul>
<p>(Feldhütter et al., 2019)</p>	<ul style="list-style-type: none"> <li>• Apparatus: a driving simulator</li> <li>• Number of participants: 42</li> <li>• Objective: to investigate how prolonged periods of conditionally automated driving affect passenger fatigue level and their takeover performance and how both are affected by NDRTs</li> <li>• Scene: a 60 mins drive with conditional automation on a three-lane highway at a constant speed of 120 km/h</li> <li>• NDRTs: play games on a computer tablet, listen to podcasts or watch videos, as well as read current</li> </ul>	<ul style="list-style-type: none"> <li>• PERCLOS (percentage of eyelid closure)</li> <li>• Blink frequency</li> <li>• Takeover time</li> <li>• Maximum longitudinal accelerations</li> <li>• Maximum lateral accelerations</li> <li>• Minimal time-to-collision</li> <li>• Securing behavior</li> </ul>	<ul style="list-style-type: none"> <li>• Twenty-five percent of the drivers in the fatigue encouraging condition temporarily showed strong evidence of fatigue or they fell asleep</li> <li>• The time of occurrence of fatigue phases varied among individuals (occurrence mainly after 20 to 40 mins of automated driving)</li> <li>• Drivers' takeover performance in the takeover situation after 60 mins of conditional automated driving did not deteriorate in the</li> </ul>

	<p>newspapers/journals or use the radio device that was provided</p> <ul style="list-style-type: none"> <li>• Lead time: 6 s</li> </ul>		<p>fatigue condition compared to the alertness condition</p>
(C. Guo et al., 2019)	<ul style="list-style-type: none"> <li>• Apparatus: a driving simulator</li> <li>• Number of participants: 12</li> <li>• Objective: to investigate the design of an override mode for automated driving systems and to explore a shared control framework for driver's override of automatic steering control</li> <li>• Scene: a ramp track and a highway mainline track. The ego vehicle first encountered Scenario A - passing a work zone. After Scenario A, the ego vehicle merged to the mainline of a two-lane highway. The speed limit was 90 km/h. However, vehicles in the right lane were purposely drive at 70 km/h to trigger overtaking</li> <li>• NDRTs: not mentioned</li> <li>• Lead time: not mentioned</li> </ul>	<ul style="list-style-type: none"> <li>• The root-mean-square of the driver's steering torque</li> <li>• The number of steering wheel reversals</li> <li>• A questionnaire related to their experiences with this configuration, rate their efficiency, feeling of comfort, perceived safety, and ease of trajectory control</li> </ul>	<ul style="list-style-type: none"> <li>• The proposed shared control framework allowed the driver to regain control with ease while ensuring the smoothness of control transition</li> <li>• Drivers' steering efforts were not affected with system's assistance during lane-changing maneuvers</li> </ul>
(Li et al., 2019)	<ul style="list-style-type: none"> <li>• Apparatus: a driving simulator</li> <li>• Number of participants: 24</li> <li>• Objective: to explore the design of age-friendly human-machine interactions in highly automated vehicles and highlights the importance of considering the older drivers' requirements when designing and developing automated vehicles</li> <li>• Scene: two types of roads including an urban road and a motorway in which</li> </ul>	<ul style="list-style-type: none"> <li>• Self-reported driving behavior of older drivers.</li> <li>• Older drivers' opinions towards the automated vehicles</li> <li>• Physical and potential control of the highly automated vehicles</li> <li>• Physical and potential control of the highly automated vehicles</li> </ul>	<ul style="list-style-type: none"> <li>• Older drivers had a positive attitude towards highly automated driving and welcomed the hands-on experience with highly automated driving</li> <li>• Older drivers wanted to retain physical and potential control over the highly automated vehicles and would like to perform a range of NDRTs in</li> </ul>

	<p>the ego vehicle will encounter a stationary car</p> <ul style="list-style-type: none"> <li>• NDRTs: monitoring driving and reading</li> <li>• Lead time: 20 s</li> </ul>	<ul style="list-style-type: none"> <li>• Human-machine interaction during automated driving in highly automated vehicles</li> <li>• Human-machine interaction during taking over control in highly automated vehicles.</li> <li>• Driving style of highly automated vehicles</li> </ul>	<p>highly automated vehicles.</p> <ul style="list-style-type: none"> <li>• Older drivers required an information system and a monitoring system to support their interactions with highly automated vehicles</li> <li>• Older drivers also expected the takeover request to be adjustable, explanatory, and hierarchical and the driving styles of the highly automated vehicle to be imitative and corrective</li> </ul>
<p>(Madigan et al., 2018)</p>	<ul style="list-style-type: none"> <li>• Apparatus: a driving simulator</li> <li>• Number of participants: 29/30</li> <li>• Objective: to investigate the effects of vehicle automation on drivers' behavior during non-critical takeover situations, such as driver-initiated lane-changing or overtaking</li> <li>• Scene: a three-lane motorway including straight and curved sections of road. There was a continuous stream of slow-moving traffic on the inside lane (left-hand lane) and no traffic in the outside lane (right-hand lane). The speed limit was set at 70 mph</li> <li>• Scenarios: In partially automated driving (PAD), drivers were required to resume control from an automated driving system to overtake a slow-moving vehicle. While in conditional</li> </ul>	<ul style="list-style-type: none"> <li>• Response time</li> <li>• Inverse time to collision and forward headway</li> <li>• Automation disengagement method</li> <li>• Lateral position</li> <li>• Speed profiles</li> <li>• Lateral acceleration</li> <li>• Subjective evaluation: drivers preferred automated system.</li> <li>• Subjective evaluation: ratings of system acceptance</li> </ul>	<ul style="list-style-type: none"> <li>• While drivers' acceptance of both the PAD and CAD systems was high, they generally preferred CAD</li> <li>• A comparison of overtaking positions showed that drivers initiated overtaking maneuvers slightly later in PAD than in manual driving or CAD</li> <li>• When compared to conventional driving, drivers had higher deviations in lane positioning and speed, along with higher lateral accelerations during lane changes following PAD</li> <li>• Even in situations which are not time-critical, drivers' vehicle control after</li> </ul>

	<p>automated driving (CAD), the driver used the indicator lever to initiate a system-performed overtaking maneuver</p> <ul style="list-style-type: none"> <li>• NDRTs: No. Drivers were required to monitor the system and the driving scene</li> </ul>		<p>automation is degraded compared to conventional driving</p>
(Ko and Ji, 2018)	<ul style="list-style-type: none"> <li>• Apparatus: a driving simulator</li> <li>• Number of participants: 32</li> <li>• Objective: investigated the flow experience of a driver who concentrated on NDRTs that induce mental workload under conditional automation</li> <li>• Scene: not given but the vehicle was traveling at 80 km/h before takeover.</li> <li>• NDRTs: watching a video, reading an article, N-Back task (2-back)</li> <li>• Lead time: not mentioned</li> </ul>	<ul style="list-style-type: none"> <li>• NASA task load index</li> <li>• The flow short scale</li> <li>• Perceived demand level</li> <li>• Gaze-on time</li> <li>• Road-fixation time</li> <li>• Hands-on time</li> <li>• Takeover time</li> </ul>	<ul style="list-style-type: none"> <li>• Participants had the longest reaction time when they indicated the highest flow score, and had the longest gaze-on time, road-fixation time, hands-on time, and takeover time under the fit condition</li> <li>• No significant difference existed between drivers' reaction times in the fit condition and the situation with N-Back tasks</li> <li>• Performing NDRTs that induce a high flow experience could influence driver reaction time similar to performing tasks with a high mental workload</li> </ul>
(Bourrelly et al., 2018)	<ul style="list-style-type: none"> <li>• Apparatus: a driving simulator</li> <li>• Number of participants: 30</li> <li>• Objective: to provide new insight on the impact of one hour of autonomous driving on takeover performance.</li> <li>• Scene: a highway loop with a speed of</li> </ul>	<ul style="list-style-type: none"> <li>• Driver's drowsiness state self-reported by a 5-point Likert scale</li> <li>• Action times</li> <li>• Car trajectories</li> <li>• Time from the TOR until the</li> </ul>	<ul style="list-style-type: none"> <li>• One hour of autonomous driving negatively affects drivers' takeover behavior. A decline in the takeover performance and an increase of the drowsiness state was observed</li> </ul>

	<p>110 km</p> <ul style="list-style-type: none"> <li>• NDRTs: watching a movie</li> <li>• Lead time: not mentioned</li> </ul>	<p>driver put hands on the steering wheel</p> <ul style="list-style-type: none"> <li>• First feet application on the pedals (brake or accelerator)</li> <li>• Time from the TOR until the drivers changed lane and returned on the right lane</li> <li>• Distance and time to collision (DTC and TTC, respectively)</li> <li>• Lateral deviation at the level of the accident</li> <li>• Minimal and maximal lateral speeds</li> <li>• Steering angle</li> <li>• Longitudinal and lateral speed</li> </ul>	<ul style="list-style-type: none"> <li>• Relatively frequent TORs could be beneficial to assist drivers to better resume control from the automation system</li> </ul>
<p>(Schartmüller et al., 2018)</p>	<ul style="list-style-type: none"> <li>• Apparatus: a driving simulator</li> <li>• Number of participants: 20 valid /21 in total</li> <li>• Objective: to investigate how drivers perform in a text transcription task when interrupted by imminent takeover notifications</li> <li>• Scene: on the center lane of a 3-lane highway, an obstacle was hidden due to road curvature</li> <li>• NDRTs: text</li> <li>• Lead time: 7 s</li> </ul>	<ul style="list-style-type: none"> <li>• Existing typing skills</li> <li>• Reaction time</li> <li>• Steering reversal rate</li> <li>• Time-To-Collision on lane change</li> <li>• Typing performance: words per minute and total error rate</li> <li>• NASA-TLX</li> <li>• Post-test Simulator Sickness Questionnaire (SSQ)</li> </ul>	<ul style="list-style-type: none"> <li>• The windshield alternative positively affects takeovers, while heads-down feedback lead to better typing performance</li> <li>• Text difficulty (two levels) had no significant impact on drivers' takeover time</li> </ul>
<p>(Politis et al., 2018)</p>	<ul style="list-style-type: none"> <li>• Apparatus: a driving simulator</li> <li>• Number of participants: 49</li> <li>• Objective: to evaluate users'</li> </ul>	<ul style="list-style-type: none"> <li>• Perceived Workload (PW, using Task Load Index – NASA-TLX)</li> </ul>	<ul style="list-style-type: none"> <li>• The desired interaction during takeover needs to be concise</li> </ul>

	<p>performance and views when exposed to the dialogue-based takeover interfaces</p> <ul style="list-style-type: none"> <li>• Scene: an about ten-mile long straight rural roads, and a motorway with no major curves.</li> <li>• NDRTs: using a 10-inch tablet</li> </ul> <p>Lead time: not mentioned</p>	<ul style="list-style-type: none"> <li>• Perceived acceptance (PA, using the Acceptance Scale)</li> <li>• Perceived Usability (PU, using the System Usability Scale – SUS)</li> <li>• Perceived Situation Awareness (PSA, using the Situation Awareness Rating Technique – SART)</li> <li>• Dialogue Performance (DiP)</li> <li>• Time to Takeover (TT)</li> <li>• Driving Performance</li> <li>• Speed</li> <li>• Longitudinal Acceleration</li> <li>• Absolute Angle Input</li> </ul>	<p>and under participants’ timing control</p> <ul style="list-style-type: none"> <li>• The simplicity and personal choice of a count-down interface regarding when to takeover was appreciated the most.</li> <li>• The interface requiring response to questions about the road helps engage the driver the most.</li> <li>• The interfaces with repetition of phrases were the least preferred, even when multi-modality was used</li> </ul>
(Kraft et al., 2018)	<ul style="list-style-type: none"> <li>• On-road experiment</li> <li>• Scenarios: two different in-vehicle displays in a partially automated vehicle and no display of a manual vehicle while driving on congested highway segment</li> <li>• Participants: 33</li> <li>• Scenarios: three consecutive drives of approximately 40 minutes</li> </ul>	<ul style="list-style-type: none"> <li>• Total glance durations</li> <li>• Single glance duration</li> <li>• Glance frequency</li> <li>• Ratings on trust and helpfulness of the system</li> <li>• Ratings on strain and safety of the drives</li> </ul>	<ul style="list-style-type: none"> <li>• Driving in partial automation mode could lead to a shift in drivers’ attention distribution</li> <li>• Drivers tend to spend more time looking at the in-vehicle display compared to manual driving mode</li> <li>• A simplified in-vehicle display could reduce glance duration and thus less distraction from it</li> </ul>
(Banks et al., 2018)	<ul style="list-style-type: none"> <li>• On-road experiment conducted using a right-hand drive Tesla Model S P90 equipped with the Autopilot version 7.x software</li> </ul>	<ul style="list-style-type: none"> <li>• Inter-rater reliability</li> <li>• Driving performance during system warnings</li> </ul>	<ul style="list-style-type: none"> <li>• Drivers are not properly support in complying with their new monitoring responsibilities and show</li> </ul>

	<ul style="list-style-type: none"> <li>• Scene: In the experiment drivers would drive along public roads and highways (B4100, M40, M42) within Warwickshire</li> <li>• NDRTs: none</li> </ul>	<ul style="list-style-type: none"> <li>• Drivers' intentional testing the limits of the automated functionality</li> <li>• Drivers' mode confusion on</li> <li>• Engagement in non-driving related secondary tasks</li> </ul>	<p>behavior that is indicative of complacency and over-trust.</p> <ul style="list-style-type: none"> <li>• These characteristics can encourage drivers on the road to take more risks</li> </ul>
(Bellem et al., 2018)	<ul style="list-style-type: none"> <li>• Apparatus: a driving simulator</li> <li>• Number of Participants:</li> <li>• Objective: to identify comfortable driving strategies in highly automated vehicles</li> </ul>	<ul style="list-style-type: none"> <li>• Personality traits</li> <li>• Self-reported driving style</li> <li>• Lane-changing, acceleration, and deceleration variations</li> </ul>	<p>An automated driving style which is perceived as comfortable can be identified regardless of subjects' personality</p>
(Belwadi et al., 2018)	<ul style="list-style-type: none"> <li>• Apparatus: a driving simulator</li> <li>• Number of participants: 11/16</li> <li>• Objective: to investigate the influence of age on takeover time from automation system (Level 3) in an emergency scenario</li> <li>• Scene: a two-way road with opposing traffic, a head-on crash event where the opposing vehicle crossed the dividing line and was traveling towards the subject vehicle</li> <li>• NDRTs: not mentioned</li> <li>• Lead time: not mentioned</li> </ul>	<ul style="list-style-type: none"> <li>• Max yaw Rate (deg/s)</li> <li>• Reaction time (s)</li> <li>• Stabilization time (s)</li> </ul>	<ul style="list-style-type: none"> <li>• Older drivers (0.7 s) react slightly faster than younger drivers (1 second)</li> <li>• For reaction and recovery times, younger drivers have a slightly quicker reaction time (12 s) as compared to adults (14 s)</li> <li>• Younger drivers oscillated or overcorrected immediately after takeover</li> <li>• For both age groups, about 10% of the drivers collided during the takeover in the presence of other road users, underscoring the difficulty of taking over in traffic</li> </ul>

<p>(Wan and Wu, 2018b)</p>	<ul style="list-style-type: none"> <li>• Apparatus: a driving simulator</li> <li>• Objective: to examine the effect of lead time and nondriving tasks on takeover behavior and driver acceptance to driving automation.</li> <li>• Participants: 36</li> <li>• Scenarios: in the middle lane of a five-lane freeway scenario</li> <li>• NDRTs: one of the six nondriving tasks, including reading, typing, watching videos, playing games, taking a nap, and monitoring during the experiment</li> </ul>	<ul style="list-style-type: none"> <li>• takeover reaction time</li> <li>• Minimum TTC</li> <li>• Maximum lateral acceleration</li> <li>• Maximum longitudinal deceleration</li> <li>• Perceived loudness of warning messages</li> <li>• Automation acceptance</li> <li>• Workload</li> </ul>	<ul style="list-style-type: none"> <li>• The optimal performance of drivers' takeover occurs when the lead time of the takeover request is 10 to 60 s</li> <li>• Furthermore, drivers' takeover performance is significantly influence by non-driving tasks.</li> <li>• When the lead time was relatively long, verbal message of takeover requests wa better to deliver specific information to drivers</li> </ul>
<p>(Wandtner et al., 2018b)</p>	<ul style="list-style-type: none"> <li>• Apparatus: a driving simulator</li> <li>• Objective: how drivers voluntarily schedule a secondary task based on the availability and predictability of automated driving modes</li> <li>• Participants: 20</li> <li>• Scenarios: two-lane highway with a total length 72km and with alternating sections of manual and highly automated driving. Drivers were requested to resume control when approaching a sharp horizontal curve bending to the left.</li> <li>• TOR lead time: 8 s</li> <li>• NDRTs: A texting task prior to takeover situations to was also used to evaluate how drivers would perform in both manual and highly automated</li> </ul>	<ul style="list-style-type: none"> <li>• Number of accepted tasks in dependence of the current driving mode</li> <li>• Disengagement from secondary tasks (task canceled vs. task continued) in takeover situations</li> <li>• Time until first gaze on road, time until hands were back at the steering wheel, time until system deactivation, and time until initiating steering</li> <li>• Variability of lateral position, lane exceedances, and maximum accelerations</li> </ul>	<ul style="list-style-type: none"> <li>• Drivers accepted significantly more tasks during highly automated driving compared to manual driving. Drivers continued texting after being prompted to take over</li> <li>• Drivers also interacted less with NDRTs during demanding or critical driving situations</li> <li>• Once engaged in a NDRT, drivers tend to continue texting even in takeover situations</li> <li>• More critical tasks prior to takeover situations are rejected by drivers when they</li> </ul>

	driving modes		could anticipate upcoming takeover situations
(Naujoks et al., 2018)	<ul style="list-style-type: none"> <li>• Apparatus: a driving simulator with patricidal and high automation modes</li> <li>• Number of Participants: 64</li> <li>• Objective: to study the effect of non-driving related tasks and drowsiness on takeover performance</li> <li>• Scene: the overall test course is a three-lane highway with only a little traffic. Drivers had to resume manual control in three different situations, including a construction site, a section of road missing lane markings, and a sudden sensor failure</li> <li>• NDRTs: smartphone reading, smartphone testing, smartphone video, smartphone social media, smartphone gaming, smartphone gaming, smartphone music, and magazine</li> </ul>	<ul style="list-style-type: none"> <li>• Takeover reaction time</li> <li>• Minimum time-to-Collision (TTC)</li> <li>• Subjective rating of criticality</li> <li>• Fatigue</li> <li>• Visual workload</li> <li>• Mental workload</li> <li>• Motor workload</li> <li>• Motivation</li> </ul>	<ul style="list-style-type: none"> <li>• Drivers readily engaged in various NDRTs on during a one or two hours partially or highly automated drive</li> <li>• Despite a long-automated drive, drowsiness stayed on a relatively low level, presumably as a result of stimulating interactions with the smartphone.</li> <li>• The duration of the automated drive did not influence the driver's takeover performance, during both partially and highly automated driving.</li> <li>• Drivers' drowsiness levels and interest in NDRTs had a negative impact on their takeover performance. In highly automated driving, no carry-over effects from NDRTs or drowsiness level on driver's braking performance were observed</li> </ul>
(Wiedemann et al., 2018)	<ul style="list-style-type: none"> <li>• Apparatus: a driving simulator</li> <li>• Number of participants: 36</li> <li>• Objective: effect of different levels of</li> </ul>	<ul style="list-style-type: none"> <li>• Takeover time</li> <li>• The standard deviation of lateral position</li> </ul>	<ul style="list-style-type: none"> <li>• A 0.08% BAC increases the time needed to re-engage in the driving task and impairs</li> </ul>

	<p>blood alcohol concentrations on takeover time and quality was assessed</p> <ul style="list-style-type: none"> <li>• Scene: one-hour drive on a three-lane motorway with low traffic density, in which seven takeover situations were encountered by the ego vehicle</li> <li>• NDRTs: a RSVP (rapid serial visual presentation) task</li> </ul>	<ul style="list-style-type: none"> <li>• The standard deviation of the steering wheel angle</li> <li>• The standard deviation of velocity</li> <li>• Minimum time-to-collision</li> <li>• Minimum headway to the broken-down vehicle</li> <li>• The criticality of the situation: rating scale for the assessment of driving and traffic situations</li> </ul>	<p>several aspects of longitudinal and lateral vehicle control</p> <ul style="list-style-type: none"> <li>• This study also cannot conclude that a BAC level of 0.05% does not impair takeover performance in automated driving</li> </ul>
(Yang et al., 2018)	<ul style="list-style-type: none"> <li>• Apparatus: a driving simulator</li> <li>• Participants: 32</li> <li>• Objective: relaxing “non-driving postures (NDPs)” influence takeover performance</li> <li>• Independent Variables: Torso angle, Knee angle</li> <li>• Relaxing NDPs are built by manipulating the driver’s knee angle (133°) and torso angle (38°) via seat adjustments</li> <li>• NDRTs: 1-back task</li> </ul>	<ul style="list-style-type: none"> <li>• Reaction time (Hands-on time, Takeover time)</li> <li>• Maximum longitudinal deceleration</li> <li>• Maximum absolute lateral acceleration</li> <li>• Time to collision</li> <li>• Standard deviation of lateral position</li> </ul>	<ul style="list-style-type: none"> <li>• The torso angle is identified as a significant impacting factor</li> <li>• The reclined driver takes over more poorly</li> <li>• A larger relaxing knee angle does not affect takeover performance if the heel is able to contact the pedal</li> </ul>
(Epple et al., 2018)	<ul style="list-style-type: none"> <li>• Driving simulator and interview data</li> <li>• Participants: 40</li> <li>• Scenarios: 100 km/h automated driving</li> <li>• Objective: examines driver behavior when experiencing a two-step TOR procedure in different modalities</li> </ul>	<ul style="list-style-type: none"> <li>• Drivers’ reaction time</li> <li>• Minimum time to collision (<math>TTC_{min}</math>)</li> <li>• Maximum change of steering wheel angle (<math>SWA_{max}</math>).</li> </ul>	<ul style="list-style-type: none"> <li>• A large number of drivers resumes controls after the second step, resulting in a higher number of crashes</li> <li>• Driving and interview data suggest that step two of the TOR should be presented earlier</li> </ul>

	<ul style="list-style-type: none"> <li>• NDRTs: Questions-and-answers game</li> </ul>		<ul style="list-style-type: none"> <li>• A multistep TOR could be used to increase drivers' situational awareness</li> <li>• Auditory TORs are associated with shorter reaction times than visual-auditory TORs</li> </ul>
(Borojeni et al., 2018a)	<ul style="list-style-type: none"> <li>• Apparatus: a driving simulator</li> <li>• Number of participants: 16</li> <li>• Objective: to investigate the effect of motion on TOR responses</li> <li>• Scene: the ego vehicle was traveling at a speed of 80 km/h on a single lane track with no traffic</li> <li>• NDRTs: a complex reading span task</li> <li>• Lead time: The TORs were presented in random intervals between 1 to 2 minutes</li> </ul>	<ul style="list-style-type: none"> <li>• NASA TLX questionnaire</li> <li>• Motion realism questionnaire</li> <li>• Reaction time</li> <li>• Lateral deviation from the center of the lane</li> <li>• Performance in reading span task</li> </ul>	<ul style="list-style-type: none"> <li>• Drivers responses to TORs vary depending on the road context where TORs are issued</li> <li>• While previous work showed that drivers are fast to respond to urgent cues, this study further confirmed that this is true only when TORs are presented on straight roads</li> <li>• Urgent cues issued on curved roads incurred slower responses than non-urgent cues on curved roads</li> <li>• TORs should be designed to be aware of road context to accommodate natural driver responses</li> </ul>
(Borojeni et al., 2018b)	<ul style="list-style-type: none"> <li>• Apparatus: a driving simulator</li> <li>• Number of participants: 18</li> <li>• Objective: we investigated the role of decision priming cues as TORs across different levels of NDRT engagement.</li> </ul>	<ul style="list-style-type: none"> <li>• Overall workload ratings (NASA TLX)</li> <li>• Reaction time</li> <li>• Time to collision to obstacle (TTC)</li> <li>• Number of collisions</li> </ul>	<ul style="list-style-type: none"> <li>• Priming drivers with upcoming maneuvers had faster responses and longer time to collision to obstacles</li> <li>• However, the level of engagement in NDRTs does</li> </ul>

	<ul style="list-style-type: none"> <li>• Scene: a two-lane highway with light traffic density. In the driving scenario, the highly automated ego vehicle was following a lead car with a speed of 27.0 m/s (approximately 100 km/h) and a time-headway of 1.6 s (equivalent to a distance of 44.4 m). In regular intervals of approximately one minute, the lead vehicle suddenly braked: in case of the two braking scenarios the speed was reduced from 27 to 21.0 m/s and for the two overtaking situations from 27 to 22.5 m/s</li> <li>• NDRTs: reading span task</li> <li>• Lead time: 9.9s, 9.6s, and 8.9s</li> </ul>	<ul style="list-style-type: none"> <li>• Number of alternative maneuvers</li> <li>• Eye-gaze behavior: the number and duration of glances</li> <li>• Performance in reading span task</li> </ul>	<p>not affect drivers' responses to TORs</p>
<p>(Sportillo et al., 2018)</p>	<ul style="list-style-type: none"> <li>• Apparatus: a driving simulator</li> <li>• Number of participants: 60</li> <li>• Objective: the effectiveness of a light Virtual Reality training program for acquiring interaction skills in automated cars was investigated</li> <li>• Scene: a straight two-lane road with guardrails. No traffic was implemented. Only trees were placed on the roadside</li> <li>• Scenarios: (a) a 10s TOR caused by a road narrowing provoked by a stationary; (b) a 10s TOR caused by a loss of road marking; (c) a 5s TOR caused by a sensor failure. car on the right lane</li> </ul>	<ul style="list-style-type: none"> <li>• A demographic questionnaire (containing questions about driving habits, familiarity with Virtual Reality, and previous experiences with driving simulators)</li> <li>• Questions survey to evaluate graphical and physical realism of the Virtual Environment</li> <li>• Simulator Sickness Questionnaire</li> <li>• Reaction time</li> <li>• Maximum deviation from the lane center</li> </ul>	<ul style="list-style-type: none"> <li>• The training system affects drivers' takeover performance.</li> <li>• Self-reported measures indicated that light VR training is preferred with respect to the other systems.</li> <li>• Virtual reality plays a strategic role in the definition of the set of metrics for profiling proper driver interaction with the automated vehicle</li> </ul>

	<ul style="list-style-type: none"> <li>• NDRTs: using a tablet to watch a video of a TEDx Talk in French</li> <li>• Lead time: 5s and 10s</li> </ul>	<ul style="list-style-type: none"> <li>• TTC</li> <li>• Stress and confidence in the vehicle</li> </ul>	
(Clark et al., 2018)	<ul style="list-style-type: none"> <li>• Apparatus: a driving simulator (2 drivers in 1 car)</li> <li>• Number of participants: 40</li> <li>• Objective: to investigate the concept of a vocal handover assistant by exploring information delivered in naturalistic vocal handover between two drivers</li> <li>• Scene: a motorway junction exit where the vehicle needed to move into the left lane exit</li> <li>• NDRTs: not mentioned</li> </ul>	<ul style="list-style-type: none"> <li>• Three questionnaires: the NASA-TLX, the SUS, and the SAS.</li> <li>• Mean percentage of handovers involving information transmission before and after pre-defined conditions</li> <li>• Longitudinal speed post-handover</li> <li>• Lateral velocity following handover</li> <li>• Qualitative feedback</li> </ul>	<ul style="list-style-type: none"> <li>• An efficient way to confirm information transfer so that drivers do not become frustrated with handover interactions</li> <li>• Drivers receive the information they require without unnecessary information being received</li> <li>• A degree of personalization in the information delivery to facilitate individual differences and preferences</li> </ul>
(Naujoks et al., 2017b)	<ul style="list-style-type: none"> <li>• Apparatus: a driving simulator</li> <li>• Objective: driver performance during system limits of partially automated driving</li> <li>• Scenarios: missing lane markings, temporary lines, and high curvature that may lead to failures of lateral guidance functionality are chosen as the test scenarios. During the experiment, a relatively stable traffic flow in low speed driving condition was designed</li> <li>• Independent variables: three levels of automation including hands-free driving possible for 120s, and hands-</li> </ul>	<ul style="list-style-type: none"> <li>• Deactivate method</li> <li>• Time-to- Deactivation</li> <li>• Velocity</li> <li>• Standard deviation of lateral position</li> <li>• Maximum lateral deviation</li> <li>• Lane exceedances</li> <li>• Subjective rating of situation criticality</li> <li>• Subjective rating of the Helpfulness the takeover control</li> </ul>	<ul style="list-style-type: none"> <li>• Regardless of the level of automation, all participants could control the situations safely</li> <li>• Even when they were able to take their hands off the steering wheel for longer periods, all participants kept the vehicle in the lane</li> <li>• The situations were therefore mostly rated as 'harmless.' No negative influence of secondary tasks on the driving performance measures was observed under the experimental conditions of</li> </ul>

	free for 10s, and manual reference drive were considered		this study
(Shen and Neyens, 2017)	<ul style="list-style-type: none"> <li>• Apparatus: a driving simulator</li> <li>• Objective: quantify drivers' response to a safety critical event during automated driving while engaging in a non-driving secondary task</li> <li>• Number of participants: 48</li> <li>• Scene: two levels of automated driving: (a) driving with no automation, and (b) driving with adaptive cruise control and lane keeping systems engaged; NDRTs: two levels of a non-driving task (a) watching a movie and (b) no non-driving task</li> </ul>	<ul style="list-style-type: none"> <li>• Level of engagement in non-driving tasks</li> <li>• Effects of automation on drivers' glance durations during non-driving tasks</li> <li>• Drivers' responses to the lane departure events</li> <li>• Reaction time</li> <li>• Lane departure duration</li> <li>• Maximum steering wheel angle</li> </ul>	<ul style="list-style-type: none"> <li>• Drivers using the automated systems responded worse than those manually driving in terms of reaction time, lane departure duration, and maximum steering wheel angle to an induced lane departure event</li> <li>• In the automated driving condition, drivers' responses to the safety critical events were slower, especially when engaged in a non-driving task</li> </ul>
(Forster et al., 2017)	<ul style="list-style-type: none"> <li>• Driving simulator and follow-up interview</li> <li>• Participants: 17</li> <li>• Scenarios: emerging secondary lanes</li> <li>• Objective: compares the effects of different auditory outputs in form of (1) generic warning tone and (2) Speech + generic warning tone</li> <li>• NDRTs: reading a magazine</li> </ul>	<ul style="list-style-type: none"> <li>• Reaction time</li> <li>• Complete HMI regarding usefulness, ease of use and perceived visual workload</li> <li>• Ratings on usability and acceptance</li> </ul>	<ul style="list-style-type: none"> <li>• Reaction times showed that hands-on-the-steering wheel, the termination of NDRT were shorter for 'Speech + generic' compared to 'Generic' situation.</li> <li>• While reaction time, reflecting allocation of attention (i.e., first glance ahead), did not show any difference</li> <li>• Subjective ratings were in favor of the system with additional speech output</li> </ul>

(Petermeijer et al., 2017a)	<ul style="list-style-type: none"> <li>• Apparatus: a driving simulator</li> <li>• Number of participants: 24</li> <li>• Objective: investigate the effects of TOR modality and left/right directionality on drivers' steering behavior when facing a head-on collision without having received specific instructions regarding the directional nature of the TORs</li> <li>• Independent variables: 3 session with different TOR modality (auditory, vibrotactile, and auditory-vibrotactile).</li> <li>• 6 TORs/session (2 left, 2 right, and 2 both left and right)</li> <li>• scenarios: 120km/h, 21.9 km, about 11.5 min. A total of six stationary cars in the middle lane, 7s lead time</li> <li>• sec-tasks: SURT</li> </ul>	<ul style="list-style-type: none"> <li>• A questionnaire on usefulness and satisfaction</li> <li>• NASA Task Load Index(NASA-TLX)</li> <li>• Steer touch: absolute steering wheel velocity greater than 1deg/s.</li> <li>• Steer initiate: absolute steering wheel angle greater than 0.25 deg</li> <li>• Steer turn: absolute steering wheel angle greater than 2 deg</li> <li>• Car avoid</li> <li>• Absolute deviation from the lane center greater than 1.00 m</li> <li>• Lane change: absolute deviation from the lane center greater than 2.00 m</li> <li>• Brake: pedal depression greater than 0%</li> </ul>	<ul style="list-style-type: none"> <li>• between the three TOR modalities tested, the multimodal approach is preferred.</li> <li>• Moreover, directional auditory and vibrotactile stimuli do not evoke a directional response in uninstructed drivers</li> <li>• More salient and semantically congruent cues, as well as explicit instructions, may be needed to guide a driver into a specific direction during a takeover scenario.</li> </ul>
(Petermeijer et al., 2017c)	<ul style="list-style-type: none"> <li>• Apparatus: a driving simulator</li> <li>• Participants: 101</li> <li>• Scenarios: two-lane motorway with a speed limit of 120 km/h, 6 Takeover Scenarios: breakdown car, breakdown truck, lane closed, roadworks, traffic jam, off-ramp</li> </ul>	<ul style="list-style-type: none"> <li>• Eyes-on-road reaction time</li> <li>• Steer initiation time</li> <li>• Steer turn time</li> <li>• Self-reported usefulness (usefulness and satisfaction questionnaire)</li> </ul>	<ul style="list-style-type: none"> <li>• Auditory and tactile takeover requests yielded overall faster reactions than visual takeover requests</li> <li>• The expected interaction between takeover modality and the dominant modality of the non-driving task was not</li> </ul>

	<ul style="list-style-type: none"> <li>• Objective: investigated the interaction between takeover request modality and type of non-driving task, regarding the driver's reaction time.</li> <li>• Independent variable: non-driving task (Video, Call, Reading)</li> <li>• NDRTs: reading (visual task), calling (auditory task), or watching a video (visual/auditory task)</li> </ul>	found	
(Eriksson and Stanton, 2017)	<ul style="list-style-type: none"> <li>• Apparatus: a driving simulator</li> <li>• Number of participants: 26</li> <li>• Objective: to determine the time it takes drivers to resume control from a highly automated vehicle in noncritical scenarios</li> <li>• Scenarios: noncritical scenarios, 70 mph on a 30-km, three-lane highway with some curves</li> <li>• NDRTs: read a newspaper, or monitor the system</li> </ul>	<ul style="list-style-type: none"> <li>• Reaction time</li> <li>• Standard deviation of steering angular rate (degrees per second)</li> <li>• Workload score (NASA-TLX)</li> </ul>	<ul style="list-style-type: none"> <li>• Drivers take longer to resume control when under no time pressure compared with that reported in the literature</li> <li>• Drivers occupied by a NDRT exhibited larger variance and slower responses to requests to resume control</li> <li>• Workload scores implied optimal workload</li> </ul>
(Happee et al., 2017)	<ul style="list-style-type: none"> <li>• Apparatus: a driving simulator</li> <li>• Participants: 48</li> <li>• Scene: a three-lane highway with a speed limit of 120 km/h and two stationary vehicles with flashing warning lights appeared at their current lane at a distance of 233 m representing a time budget of 7 s</li> <li>• Traffic settings: Participants were in the middle lane with traffic on the left</li> </ul>	<ul style="list-style-type: none"> <li>• Minimum time to collision (TTC)</li> <li>• Minimum clearance towards the obstacle</li> <li>• Lane position</li> <li>• Extended time-to-collision (ETTC)</li> </ul>	<ul style="list-style-type: none"> <li>• Effect of cognitive distraction was similar to visual distraction for the intervention time with effects on the surrogate safety metric TTC being larger with visual distraction</li> <li>• However, the precision of the evasive maneuvers was hardly affected with a similar clearance towards the</li> </ul>

and right lanes with a density of approximately 30 vehicles/km; no traffic existed, and participants were in the right, left, and middle lane, respectively

- NDRTs: n-back task, SuRT

obstacle, similar overshoots and similar excursions to the hard shoulder

## 2.7 Takeover request design

Automated driving systems will also entail significant evolution of the communication system between vehicles and drivers. The level of safety of a safety-critical human-automation system directly relies on the appropriate level of drivers' attention and intervention, which is closely related to the design of delivering TORs to drivers. A TOR is when the system initiates a control transition from automated driving to manual control. There is a well-developed body of knowledge about drivers' takeover performance when the driving automation system requests the driver to intervene. As presented in [Section 2.5](#), there has been a substantial number of studies dedicated to the issues of driver takeover performance when the driving automation was not able to provide full automation. As is highlighted by previous studies ([Harris and Li, 2017](#); [Parasuraman and Riley, 1997](#)), automation fundamentally changes the nature of the cognitive demands and obligations of the human operators of the system. A plethora of experimental and evaluative methods are therefore also presented to investigate drivers' takeover performance in the case of different TOR designs (See [Table 2-11](#)).

Driver attention and intervention can be activated in a timely manner by a good TOR design. The Highway Code of the United Kingdom also clearly requires drivers not to rely on driver assistance systems, such as cruise control and lane departure warnings, which are means to assist but not to reduce drivers' concentration levels ([Department for Transport, 2018](#)). When working with automation systems, it is an essential prerequisite for the driver to be aware of not only what automated functionalities are provided by the system, but also what is expected from the driver in terms of supervision of the automation status and readiness in resuming control. During the automated driving mode with no need for driver intervention, drivers may disengage from driving by attending some NDRTs. When takeover is needed, the system should have the programming to

responsibly alter the driver. It is vital to develop effective notification to elicit swift driver intervention.

### **2.7.1 TOR design and lead time**

Overall requirements and general principles on Human-Machine Interface (HMI) design have been explored extensively in the research community. For example, (Naujoks et al., 2017a) presented a prototypical HMI, which was evaluated by experts in the cognitive engineering field, to facilitate drivers to develop a better cooperative perception of the driving environment when TORs were delivered. The concept cooperative perception refers to the information perception completed by the ego vehicle and then reinforced by the advance information collected by other road users. With the help of cooperative perception, TORs thus can be delivered in advance, giving the driver more time to come back to the control loop before the system reaches the critical situation. Furthermore, a substantial of studies have reported the usage of TOR design in their studies on takeover behavior under various driving circumstances (Bazilinsky et al., 2018; Epple et al., 2018; Forster et al., 2017; Melcher et al., 2015; Naujoks et al., 2018, 2017a; Petermeijer et al., 2017a; Wu et al., 2019; Yang et al., 2018; Yoon et al., 2019).

The effectiveness of TORs is usually determined by two factors: timeliness and the modality of the request message. The lead time of TORs is defined as the time budget available until the critical event of interest is reached. Recent studies have used a TOR lead time in a range of 0 to 60 s to investigate takeover behaviors. A review on TOR lead times based on 25 studies from 2012 to 2016 revealed the mean of the lead time was 6.37 s with a standard deviation of 5.36 s (Eriksson and Stanton, 2017). In this study, the lead times used in the most recent studies on takeover behavior are highlighted as below:

- A lead time of 7 s was given drivers to respond to the TOR triggered by a broken, stopped vehicle 233 m ahead of the subject vehicle (Gold et al., 2016). However, it worth noting that lead times of 5 s, 5.5 s, 6.1s, 7 s, and 7.78 s were utilized by Gold et al in their preivous takeover behavior studies (Gold et al., 2015a, 2014, 2013).
- A lead time of 4 s was given drivers to take over vehicle control when the TOR was triggered by a curve on the simulated highway and the traveling speed of the subject vehicle was 60 km (Zeeb et al., 2016).
- A lead time of 7 s was designed before the subject vehicle collide with the obstacle on a simulated six-lane highway at 120 km/h (Körber et al., 2016).
- A lead time of 3.5 s was given drivers to resume control when the automation system failed to detect the lane markings while traveling at 130 km/h on the simulated three-lane highway (Zeeb et al., 2017).
- According to the experiment set-up that a stationary car ahead on the simulated highway while the automation system approaching it at a speed of 120 km/h, it can be calculated that a lead time of 6.69 s was used to study the takeover behavior while vibrotactile seat was used as one part of TOR delivery (Petermeijer et al., 2017b).
- A lead time of 7 s was used as in all test scenarios with varying NDRTs and varying fog conditions to investigate drivers' takeover reactions (Louw et al., 2017).
- A lead time of 10 s was used to deliver TORs to drivers with different levels of blood alcohol concentrations during takeover transitions (Wiedemann et al., 2018).
- A lead time of 8 s was used as the driving automation system approaching an braking vehicle on the simulated highway and needed the driver to take back control from the driving simulator (Naujoks et al., 2018) .

- A varied lead time between 60 s to 120 s was used in an investigation of control transitions when the automation traveling at 80 km/h on a simulated single lane track with no traffic was approaching curves on a highway (Borojeni et al., 2018a)
- Controlled lead times of 3 s, 6 s, 10 s, 15 s, 30 s, and 60 s were used to evaluate drivers' takeover behavior while involving in realistic NDRTs in a simulated five-lane freeway environment (Wan and Wu, 2018b).

From a safety point of view, it is found that drivers crashed more frequently when time budgets are 4 s, 5 s, 6 s but not 8 s (Damböck et al., 2012). Gold et al. (2013) compared drivers' response following an auditory TOR at either 5 s or 7 s TTC with a stationary vehicle ahead to a control group that performed the same task but in manual driving. It is found that drivers were able to react faster with a 5 s time budget than a longer time budget of 7 s. Nevertheless, drivers with 5 s time budget tend to have fewer glances at the rear and side mirrors before a lane change and were also less likely to use indicators. Hence, drivers who were given 5 s time budget tend to be more erratic following a TOR. In a similar rear-end near-crash situation, 47.5% and 12.5% of drivers were found to be unable to avoid collisions with a braking lead vehicle when the lead time is 1.5 s and 2.8 s, respectively (Van Den Beukel and Van Der Voort, 2013). Similar results were found in a later study where 45% of drivers when given a 4.9 s time budget collided with a lead vehicle while 15% of drivers when given a 6.6 s time budget crashed (Zeeb et al., 2015). These studies show that it is more difficult for drivers to resume control under time-pressured takeover scenarios.

Regarding the TOR modality, a substantial study has utilized different ways to present TORs to drivers. In general, TORs could be auditory, visual, haptic, or a mix of these three features. Compared to the effect that NDRTs have on takeover performance, the modality of TORs has a

more significant effect on drivers' reaction times to TORs (Petermeijer et al., 2017c). (Petermeijer et al., 2017c) found that auditory and tactile TORs were more effective than the visual ones after analyzing 666 takeover events in six different takeover situations.

### 2.7.2 HMI design

HMI's are used to provide feedback to users which is argued to be important for appropriate human-automation interactions. Insufficient or incorrect feedback in a DAS could lead to insufficient or inaccurate mental models of drivers, which could further lead to errors in decisions. To eliminate potential hazards caused by HMI design, Norman 1990 suggested four design criteria for automation HMI's, which are (Norman, 1990):

- Assume the existence of errors;
- Continually provide feedback;
- Interact with operator in an effective manner; and
- Allow for worst of situations

The driver feedback and warning systems for automated driving systems to communicate with drivers typically include different modalities (see [Section 2.6](#)). The design of HMI has been found to have a mediating effect on driver performance following a TOR. For instance, the usefulness of TORs was investigated via a simulator study with 101 participants (Petermeijer et al., 2017c). It is found that that auditory and tactile TORs yielded overall faster reactions than visual TORs. Auditory and tactile takeover requests yielded higher scores than visual ones in terms of self-reported usefulness. The authors also concluded that auditory and tactile stimuli are equally effective as TORs regardless of the NDRTs. It is also found that auditory warnings elicited

significantly shorter braking time regardless of whether drivers were distracted or not (Lee et al., 2002). Symbols of automation uncertainty was used as well to study if it can improve driver-automation interactions (Beller et al., 2013a). The authors found that when providing drivers with automation uncertainty, TTC is increased. Again, these studies demonstrate the importance of feedback during control transitions in improving driver performance.

### **2.7.3 TOR and HMI examples in automobile industry**

After reviewing the designs of TOR used in the research community, it would be beneficial to have an overview about actual TOR designs used in the automobile industry. The Audi AI traffic jam pilot on the new A8 was claimed to be the world's first automation system that meets the SAE Level 3 definition (Audi, 2017) (See Figure 2-2). When the traffic jam pilot engages, continuous monitoring of the vehicle and the road is not required from the driver. Drivers just need to stay alert and be ready to resume control in case a TOR is prompted. The speed of the vehicle is limited to 60 km/h (37.3 mph) when the traffic jam pilot is in use. When the traffic jam pilot requests drivers to resume manual control of the vehicle, the driver is given about 10 s to respond (Audi, 2017). When the automation system needs drivers to take back control, the TOR is delivered to drivers through three phases:

- Phase I: when the TOR is initially delivered

A red AI icon lights up at the lower right corner of the virtual cockpit and the digital instrument cluster is highlighted with red light. A subtle audio warning signal is also present in Phase I.

- Phase II: when the driver overlooks the prompt delivered in Phase I

The TOR warning signal becomes more salient and the warning text message “Traffic jam pilot: ending. Please resume full control of the vehicle” appears at the center of the virtual cockpit. Concurrently, the vehicle slows down, gently at first, then with a jolt, and then the safety belt will be tightened gently three times.

- Phase III: when the driver still remains nonresponsive after Phase II’s warning

The Emergency Intervention will start in Phase III. The warning signal becomes piercing and the safety belt is fully tightened. The vehicle slows down and stops in its current lane and simultaneously switches on the hazard lights. The system activates the parking brake, shifts the Tiptronic to P position, unlocks the doors, turn on the interior lights, and initiates an emergency call if there is still no response from the driver.



Figure 2-2 The TOR interface when the traffic jam pilot of Audi A8 request drivers to take back control (source: AUDI AG, Image No: A1710305)

Volvo's Pilot Assist is a SAE Level 2 driving automation, which, as itself claims, is not a substitute for drivers' attention and judgment (See Figure 2-3). Pilot Assist provides steering assistance to adaptive cruise control by having the vehicle keep up with the traffic, maintain

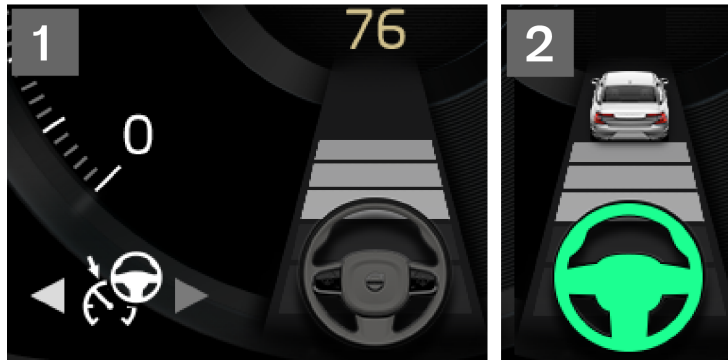


Figure 2-3 The virtual cockpit display of Pilot Assist: (1) Pilot Assist is off when the steering wheel symbol is grey, and (2) Pilot Assist is on when the steering wheel symbol is green (Volvo, 2019)

appropriate lateral position in the current lane, and stop completely if necessary. In Volvo's HMI design, green is used to indicate that steering assistance is active, and gray means it is deactivated. According to Volvo's manual (Volvo, 2018a, 2018b), Pilot Assist can toggle between on and off without prior notice if anything makes the Pilot Assist unable to clearly interpret the lane markings. Volvo also highlights that Pilot Assist is supplementary driver support and cannot handle all traffic, weather, and road conditions. Only if the driver puts his or her hands on the steering wheel does Pilot Assist function. If drivers' hands are not detected on the steering wheel, a symbol and text message will appear to require drivers to steer the vehicle; if their hands are still not detected after a few seconds, the TOR will be repeated along with an audible signal; if drivers still don't have their hands on the steering wheel after a few more seconds, the audible signal will become more intense and the Pilot Assist steering function will become inactive. Additionally, Volvo's Lane Keeping Aid also functions only if drivers have their hands on the steering wheel.

Tesla AutoPilot will periodically prompt drivers to reclaim control by flashing a lighted ring around the digital instrument cluster. The hands-off steering wheel time varies based on different sources : (1) drivers could remove their hands from the steering wheel of Tesla for 60 s (Solís-Marcos et al., 2018); (2) the hands-off steering wheel time was 3 minutes before a text message “hold steering wheel” was shown without acoustic warnings (Carsten and Martens, 2018); (3) the Tesla autosteer requires drivers to always keep their hands on the steering wheel, the system will deliver a warning signal after three to five minutes if drivers’ hands were not detected (Endsley, 2017). (Endsley, 2017) further revealed that there was no pressure sensor in the steering wheel. The system relies on the left- and right- inputs of the steering wheel to detect if drivers’ hands are on the steering wheel.

As is observed, the TOR design varies across different automobiles. Nevertheless, the regulators in Europe have amended existing regulations by explicitly stating that:

- A system failure shall be signaled to the driver by an optical warning signal only except when the system is manually deactivated by the driver.
- The automation system should be able to detect if the driver is holding the steering control when the system is active with a speed in the range of  $\max((V_{smin}, 10), V_{smax})$  km/h.
- An optical warning signal possibly accompanied by explanatory text shall be delivered if the driver is still not holding the steering wheel after a period no longer than 15 s.
- If the driver is not holding the steering control after a period of no longer than 30 s, the pictorial information of the optical warning signal can be highlighted in red and an acoustic warning signal can be provided.

- The system will automatically switch off in 30 s after the acoustic warning signal has begun. The system also needs to inform the driver that the system is deactivated using a different an acoustic signal than the previous one.

## 2.8 Non-driving related Tasks (NDRTs)

It is found that the absence of NDRTs, the execution of simple NDRTs, and the involvement of more complex NDRTs could affect drivers' takeover performance differently (Banks et al., 2018; Körber et al., 2016; Naujoks et al., 2018, 2016; Radlmayr et al., 2014; Schwalk et al., 2015; Shen and Neyens, 2017; Wan and Wu, 2018a; Wandtner et al., 2018d, 2018b; Zeeb et al., 2017, 2016). In particular, (Wandtner et al. (2018a) have investigated how drivers would self-regulate their engagement in NDRTs from the perspectives of planning level, decision level, and control level. Engaging in NDRTs requires some judgment regarding the relative utility of the NDRTs. Drivers may strategically schedule their NDRTs during or after automated driving periods (planning level). After evaluating the traffic situation and the status of the automation system, drivers will decide if current situation allows for an engagement in NDRTs (decision level). Once a NDRTs is initiated, drivers would regulate current NDRTs to accommodate potential TORs from the driving automation system (control level). Other research has also shown that the presence of NDRTs would affect drivers visual attention which further affects drivers driving performance (Jamson et al., 2013; Merat et al., 2014a; Wandtner et al., 2018b; Zeeb et al., 2017, 2015). Interestingly, it was found that drivers' reaction time was not affected by NDRTs engagement but the quality of takeover performance degraded (Gold et al., 2016). When investigating NDRTs in driving automation, drivers' level of responsibility can be determined on the basis of the level of automation. As a matter of fact, NDRTs can only affect drivers' takeover performance in drivers'

monitoring responsibility at Level 2 and fallback responsibility at Level 3 and Level 4. It has been found that drivers operating Adaptive Cruise Control (ACC) and other highly automated driving systems were much more likely to engage NDRTs (Joost C.F. de Winter et al., 2014).

The advances in vehicle automation may change the role of a driver from being actively controlling the vehicle to monitoring the automation system and the driving environment. Studies have suggested that driving automation might affect the propensity of drivers to involve in NDRTs. Driving tasks operated through automations instead of drivers might lead to a perceived reduction in cognitive workload. This, consequently, is likely to result in increased NDRT engagements (Joost C F de Winter et al., 2014). Drivers' willingness to engage in NDRTs while driving with different levels of automation has been investigated through on-road tests (Naujoks et al., 2016). It was found that drivers who were familiar with the ACC increased the frequency of engaging in an in-vehicle NDRT when the subjective and objective driving safety were not affected by the levels of automation. Drivers also adjusted their level of engagement in NDRTs according to the traffic situation (Naujoks et al., 2016). In addition, drivers' tactical decisions regarding whether to engage in a NDRT were distinctive during assisted and non-assisted driving (Naujoks et al., 2016). More interestingly, this study also revealed that increased NDRT engagement may indicate both positive consequences of driving assistive technologies, such as decreased workload and negative consequences such as decreased situation awareness.

How drivers would voluntarily schedule NDRTs on the basis of the availability and predictability of automated driving modes was also investigated through driving simulator-based experiment (Wandtner et al., 2018b). Similar to the prior study (Naujoks et al., 2016), there was a clear distinction in drivers' preferences for NDRT engagement during highly automated and

during manual driving (Wandtner et al., 2018b). More specifically, there was an increase in the level of NDRT engagement with partial automation such as an ACC (Wandtner et al., 2018b). However, drivers started to focus their attention on the primary driving task when speed increased (Wandtner et al., 2018b). (Wandtner et al., 2018b) also proposed the concept of *situation-adaptive behavior* to demonstrate how NDRT engagement was associated with both the driving automation mode and driving situation. (Wandtner et al., 2018d) found that the task modalities of NDRTs significantly affect drivers' takeover performance as well. For example, a task of visual-manual texting could degrade the takeover performance the most. Interestingly, (Wandtner et al., 2018d) suggested that the effect of an auditory-vocal task was similar to taking back control without any NDRTs.

Conversely, (Stanton, 2019) stated that if drivers didn't engage in a NDRT, they may suffer from reduced attentional resources and may result in being unable to reclaim control from the automation system in emergency. It was suggested that engagements in NDRTs had a protective effect on drivers' attentional resources by invoking a quicker takeover time (Stanton, 2019). In an earlier study based on driving simulator experiments in 1997, (Stanton et al., 1997) also found that one third of drivers failed to resume control of the vehicle before a collision occurred. Stanton and his colleague also revealed that there was a reduction in mental workload, within a NDRT paradigm, associated with certain forms of automation (Stanton et al., 1997; Stanton and Young, 1998). The concept of *malleable attentional resources theory* (MART) was developed to explain that the pool of attentional resources is dynamic and strongly affected by task demands (Young and Stanton, 2002). According to the MART, as the task demand reduces due to vehicle automation, drivers' pools of attentional resources also decrease (Young and Stanton, 2002). The MART challenges traditional beliefs of fixed attentional resource pools and the expectation that automated

driving grants drivers spare cognitive capacity for other NDRTs. The most recent review by (Stanton, 2019) emphasized the automation dilemma that driving automation needs to keep drivers busy with other activities if they are developed to replace human drivers. By keeping drivers busy, it could make drivers well-placed to reclaim control of the vehicle when automation reaches its limits. One of the advantages of driving automation is the plausibility to engage in NDRTs amid driving. Figure 2-4 illustrated NDRTs that were used in takeover studies.

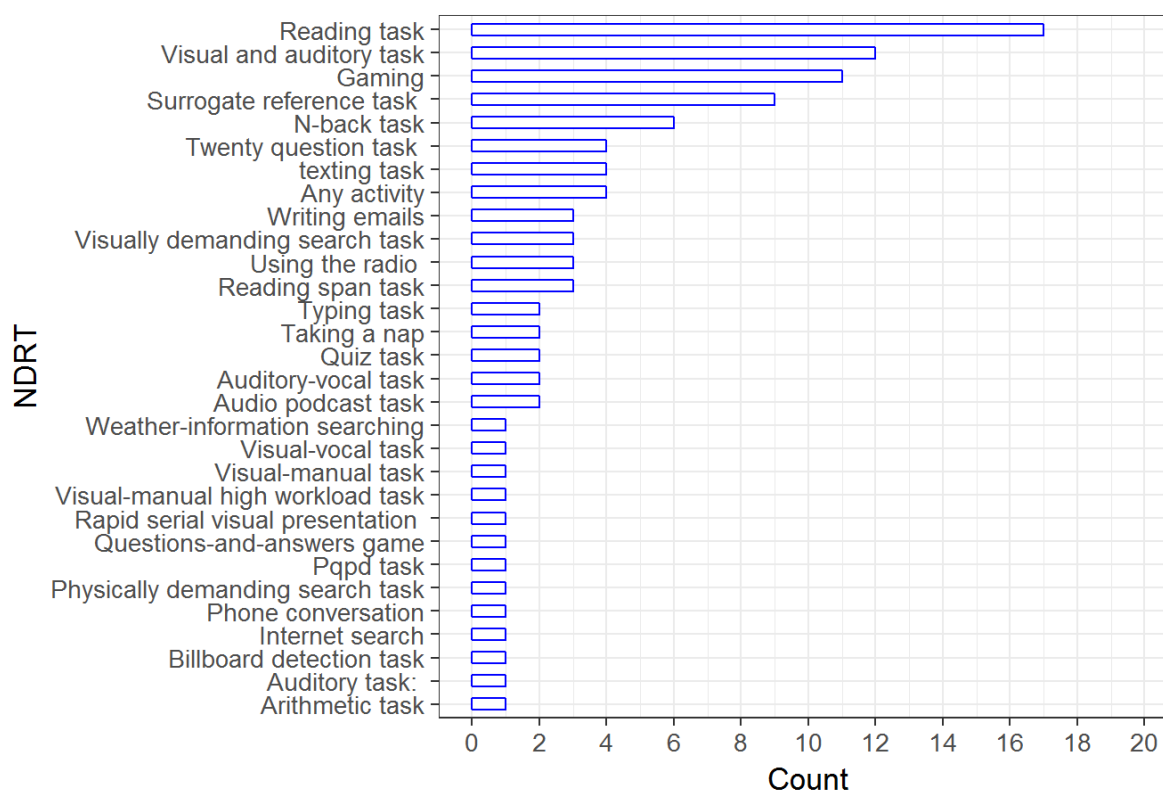


Figure 2-4 NDRTs used in takeover studies

Based on the reviewed studies on takeover performance during automation disengagements (Table 2-14), the NDRTs include the following:

1. Any activity: drivers could engage at their own will in any activities that are not related to the driving task (Banks et al., 2018; Jamson et al., 2013; Naujoks et al., 2018, 2016). For example, drivers were instructed to bring and use their own smartphones to engage in various NDRTs in a study investigating the relationship between NDRTs, drowsiness, and takeover performance (Naujoks et al., 2018).
2. Gaming: drivers played Angry Bird, Tetris, the “1-50” game that requires pressing the numbers from 1 to 50 as fast as possible, or other games on smartphones, iPads, or tablet (Eriksson et al., 2019; Feldhütter et al., 2019; Jamson et al., 2013; Naujoks et al., 2019, 2018; Olaverri-Monreal et al., 2018; Pampel et al., 2019; Schwalk et al., 2015; Wan and Wu, 2018b, 2018a; Yoon and Ji, 2019).
3. Surrogate reference task (SuRT): drivers were required to detect a target of a larger circle among smaller distractor circles. (Beller et al., 2013a; Gold et al., 2018; Happee et al., 2017; Kalb et al., 2018; Kerschbaum et al., 2014; Körber et al., 2018b, 2015; Lorenz et al., 2014; Petermeijer et al., 2017a).
4. Twenty question task (TQT): this task required drivers to guess an item from within an overriding category by asking a maximum of twenty questions (Gold et al., 2018, 2015b; Körber et al., 2016; Merat et al., 2012).
5. N-back task: the n-back task required drivers to respond to a series of stimuli, such as spatial locations, visual objects, and letters if the current stimulus is the same as the one seen n trials back (Cools, 2010). Takeover performance studies that used 1-back tasks (Borojeni et al., 2016; Yang et al., 2018); that used 2-back tasks (Heikoop et al., 2018) ; and that used n-back tasks (Happee et al., 2017; Petermeijer et al., 2017b).

6. Questions-and-answers game: drivers were required to select one of three possible answers to a question at a time (Epple et al., 2018) while in autonomous driving mode.
7. Arithmetic task: drivers were encouraged to do the NDRTs as many as possible. The arithmetic tasks include addition, subtraction, multiplication, and division of two-digit numbers (Wang and Soffker, 2018).
8. Auditory task: drivers make a phone call (Petermeijer et al., 2017c).
9. Visual and auditory task: drivers were instructed to watch a video from an entertainment, the first episode of “Brooklyn Nine-Nine”, a video of a group of people passing a ball, movie clips, an excerpt from a scientific television show, a collection of films and TV programs chose by drivers or other video clip showed on a tablet, a smartphone, or a DVD player (Braunagel et al., 2015; Dogan et al., 2019; Feldhütter et al., 2019; Jamson et al., 2013; Petermeijer et al., 2017c; Shen and Neyens, 2017; Sportillo et al., 2018; Wan and Wu, 2018b, 2018a; Wu et al., 2018; Yoon and Ji, 2019; Zeeb et al., 2016).
10. Visually demanding search task: drivers were instructed to search for a distinctive feature among several similar images on an iPad mounted to driver’s left side on the simulator’s dashboard (Kim et al., 2018; Körber et al., 2018b; Solís-Marcos et al., 2018). For instance, drivers were instructed to decide whether an arrow point upward was present in a 4 by 4 matrix of arrows on a tablet placed to the right of the steering wheel. Figure 3-5 also presents examples of images used as visually demanding search tasks in (Kim et al., 2018).

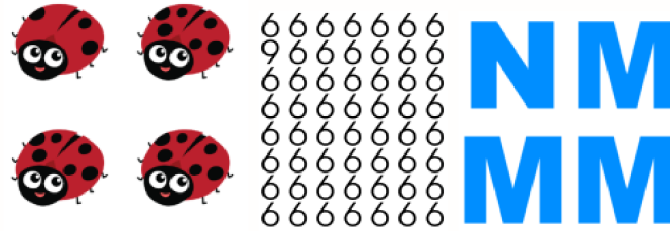


Figure 2-5 Sample images of visually demanding search task (Kim et al., 2018)

11. Rapid serial visual presentation (RSVP) task: drivers were presented with a series of letters on a head-down display at the lower half of the middle console. Some numbers appeared randomly between letters with a probability of 20%. Drivers had to react to the appearance of numbers by pressing a button positioned at the arm rest. Real-time feedback regarding drivers responses were also presented on the same head-down display (Wiedemann et al., 2018)
12. Auditory-vocal task: drivers were asked to repeat sentences read out by a text-to- speech software (Wandtner et al., 2018d, 2018a).
13. Visual-vocal task: drivers needed to read the sentences aloud that were displayed on a tablet computer mounted in the center console (Wandtner et al., 2018d).
14. Visual-manual task: drivers were required to transcribe sentences displayed on a handheld tablet computer using the virtual keyboard of the device (Wandtner et al., 2018a).
15. Reading task: reading tasks might include reading books, magazines, journals, a piece of newspaper, internet webpages emails, or texts on a smartphone (Braunagel et al., 2015; Buckley et al., 2018; Eriksson and Stanton, 2017; Feldhütter et al., 2019; Forster et al., 2017; Jamson et al., 2013; Li et al., 2019; Louw et al., 2015; Naujoks et al., 2019, 2018; Petermeijer et al., 2017c; Schwalk et al., 2015; Wan and Wu, 2018a, 2018b; Wright et al.,

- 2018; Zeeb et al., 2017, 2016). For example, in one study, drivers were instructed to read preselected articles in a weekly German print magazine. Experimenters also informed the drivers that they would be examined about the content of the article at the end of the experiment to ensure that drivers would actively engage in the NDRT (Forster et al., 2017).
16. Reading span task: drivers were required to read unconnected sentences in their native language (German) and to determine whether they semantically made sense on a Surface Pro 2. There was a single word placed at the end of each sentence. Drivers were asked to recall these words and type them in the correct order (Borojeni et al., 2018b, 2018a). This task is a standardized cognitive task that is similar to reading, writing text messages, and having conversations in an automated driving context (Pfleging et al., 2016).
  17. Writing emails: the emailing task required drivers to reply emails sent by the experimenter (Braunagel et al., 2015; Dogan et al., 2019; Zeeb et al., 2016). For example, the emails could be an invitation to a meeting which the driver had to reply to and the email was 100 words long (Zeeb et al., 2016).
  18. Typing task: drivers were required to type via a smartphone (Wan and Wu, 2018a, 2018b).
  19. Texting task: the texting task could be asking the drivers to complete the missing word of a saying or copying a given sentence (Zeeb et al., 2015), fill-in-the-blank text (Gold et al., 2018), asking drivers to decide when and whether or not to engage in self-paced short-sentence and long-sentence texting tasks during highly automated driving (Wandtner et al., 2018b), or to read and replicate different messages from the Enron Mobile dataset (translated to German) on a Windows phone 10 with the disabled word suggestion function (Wintersberger et al., 2018).

20. Phone conversation: drivers were asked to call the experimenter to finish a twenty-question task. Drivers had to hold the phone during the conversation (Yoon et al., 2019).
21. Audio podcast task: drivers listened to podcasts (Feldhütter et al., 2019) chose one of three podcasts before the drive. During the drive, drivers were instructed to listen to the podcast carefully (Naujoks et al., 2019).
22. Using the radio : drivers are permitted use the radio device (Feldhütter et al., 2019; Jamson et al., 2013; Yoon and Ji, 2019). For example, the interaction task with the radio device involved continuously searching for a radio station. Once a radio station was found, the driver was asked to search for the next radio station (Yoon and Ji, 2019).
23. Taking a nap: drivers were instructed to relax and take a nap (Wan and Wu, 2018a, 2018b).
24. Pqpd task: drivers were instructed to perform a monotonous monitoring task that might induce task-related fatigue. In the Pqpd task, the letters P, q, p, and d were randomly presented for a varying time period of 10 to 15 s. On average, the letter p appeared once a minute. Whenever the letter p was presented, the driver had to touch the screen (Jarosch et al., 2019).
25. Quiz task: drivers were instructed to finish a quiz task similar to quiz applications like Quizduell or Quizup (Jarosch et al., 2019). Correct and incorrect answers were highlighted in green and red, respectively, a total score was also displayed to motivate the quiz task (Jarosch et al., 2019). A game of quiz question on a mobile phone was also employed as a quiz task (Melcher et al., 2015).
26. Physically demanding search task: drivers had to turn around to reach a bag with building blocks and figures behind the central console of the vehicle. Then they had to pick specific items and place them in the cup holder of the vehicle (Naujoks et al., 2019).

27. Internet search: examples of internet search non-driving related tasks might be going to a mobile site or using a search engine ([Zeeb et al., 2015](#)).
28. Billboard detection task: drivers engaged in a pattern detection task of 8\*19 ft billboards on both sides of the road at a spacing of approximately 200 meters ([Seppelt and Lee, 2019](#)). During the experiments, drivers were required to press a button on the steering wheel when they observed two consecutive dice (dots arranged from one to six) that were identical ([Seppelt and Lee, 2019](#)).
29. Weather-information searching: drivers were informed to voluntarily search for weather information on a touch screen that was installed at a fixed position at the upper part of the central information display ([Naujoks et al., 2017b, 2016](#)).

## 2.9 Summary

With the increase in vehicular automation, automated driving systems are expected to assist and potentially replace human drivers to reduce traffic crashes due to human errors. Most driving automation systems to date make the task of driving a vehicle shared between the system and the driver. [Chapter 1](#) and [Chapter 2](#) identify critical issues in a new transportation system where vehicles are developed with different levels of automation, drivers are expected to take over control when the automation system reaches the limits of its operational design domain, and the traditional traffic signals at intersections might remain because of human-driven vehicles. Emerging trends and challenges in the development of driving automation systems were represented in [Chapter 1](#) and [Chapter 2](#).

Future trend and challenges of traffic control is briefly discussed in [Section 1.2.3](#) and is further reviewed in [Section 2.3](#). When the AI-powered driving automation system encounters a

permissive left-turn situation at a signalized intersection, it needs to traverse the intersection efficiently and safely, or at least as well as a human driver does. Recognizing the limitations of the driving automation systems at signalized intersections, this study further investigated how vehicle controls will be switched from the automation system to the human driver. The development of more feasible and reliable driving automation systems when encountering permissive left-turn circumstances cannot be separated from the understanding of drivers' behaviors in automated driving systems.

[Chapter 2](#) contributes with the following aspects:

- (1) Critical issues and challenges in the development of driving automation systems are identified;
- (2) Technical barriers and governmental regulations in the development of future traffic control methods are discussed; and
- (3) The characteristics and implications of delivery of takeover requests and drivers' takeover performances are presented.

## Chapter 3 Meta-analysis of drivers' takeover behavior

Previous chapters showed that automated driving systems have the potential to improve driving efficiency and safety. However, a limit of this potential could occur in the control transition process, and a model of DAS (see [Section 2.5](#)) in takeover process is dispensable for assessing the impact of control transitions on traffic flow. Three main challenges in using a DAS model for ensuring traffic safety and in assessing the impact of control transitions include:

- Identifying factors that may affect drivers' takeover behavior;
- Modeling the impact of those identified influential factors; and
- Validating the effect that influencing factors have on takeover behavior.

[Chapter 2](#) presented past research as narrative summaries. This chapter aims to address the first two challenges based on reviewed studies in Chapter 2 by conducting a meta-analysis on control transitions and driver takeover behavior. Meta-regression uniquely offers critical insights into the current stage of knowledge of how control transitions affect takeover behavior and how it affects traffic operations and safety. Specifically, [Section 3.1](#) and [Section 3.2](#) serve to derive a comprehensive list of factors that may affect drivers' takeover behavior. In [Section 3.3](#), a new effect metric called takeover quality (TOQ) is presented to replace various study effects reported in previous studies and a meta-regression model is developed to predict drivers' takeover behavior.

### 3.1 Literature selection

Previous studies mostly focus on one aspect when trying to identify factors that affect drivers' takeover behavior, which include (1) triggering event of the control transitions, (2) lead time of TOR, (3) TOR design, (4) driver age and gender, (5) alcohol impact, (6) NDRTs, and (7) the road

and traffic situation. An extensive literature review was conducted in [Chapter 2](#) to ensure that sufficient studies are included to reflect the aforementioned seven factors. Publications in leading journals including Accident Analysis & Prevention, International Journal of Human–Computer Interaction, Human Factors: The Journal of the Human Factors and Ergonomics Society, International Journal of Human-Computer Studies, Transportation Research Part F: Traffic Psychology and Behavior, IEEE Transactions on Human-Machine Systems, along with dissertations and conference proceedings are included if the study is related to control transition. Studies that meet the following criteria were included in the meta-analysis:

- The study focused on a control transition from partially, conditionally, or highly automated driving system to manual driving mode;
- The study hypothesized certain triggering events could cause control transitions;
- The study presented how TOR is communicated to drivers;
- The study measured how drivers react to the TOR stimulus and triggering event on the road; and
- The study investigated how takeover behavior is affected by the engagement of NDRTs.

An examination of selected studies showed similar results. A majority of studies used a full-scale driving simulator, several studies used a desktop driving simulator, four studies used a self-designed vehicle, and five studies used a Tesla Model S P90, 2017 Volvo S90, BMW 520d Touring F11, Audi A5 2012, and a 2013 Mercedes-Benz E-class, respectively, in their control transition experiments. Driver related data including driving behavior, takeover quality, driver physiological data, and NDRT performance data, vehicle kinematic data (such as steering wheel speed and lateral speed), driver history related information (such as motion sickness and crash history), and time related data that is derived from direct driver and vehicle measures are collected

from these selected studies though they used simulators of different levels of fidelity and different vehicles different triggering events, TOR designs, and different NDRTs. The selected studies provide an informative basis for assessing how drivers may resume control from the automated system when encountering a PPLT scenario. A preliminary analysis showed that there were 6,339 subjects involved in all reviewed control transition studies, including a few large sample studies having more than 100 subjects, some moderate-sized studies with more than 60 subjects, and some normal size studies consisting of more than 30 subjects.

### **3.2 Research results encoding**

Based on the related work that attempted to solve similar questions using comparable research design in [Chapter 2](#), a significant problem still remains when one seeks to encode the research findings into a database that can meaningfully support practical design in industry and theoretical analysis in academia. Hence, a standardized survey protocol was adopted to survey selected studies.

This section focuses on the aggregation and comparison of the findings of research studies presented in [Chapter 2](#). Coding the studies and entering the data into one dataset is a large task in this research. It is challenging to summarize effects in the context of the heterogeneity arising among diverse study designs, analysis approaches, and various variable categorizations. Through results encoding, the raw data of selected studies becomes manageable as a single database. It is necessary that those findings can be meaningfully compared. The results of each selected study including effect types and sizes are coded along with the study characteristics that affect the accuracy of their results (such as the sample size and reliability of key measures). The process of results encoding can be divided into four major steps, including:

1. Conducting systematic reviews of the related work

2. Extracting results from selected studies
3. Synthesizing individual study estimates to a common scale
4. Estimating a summary estimate using a weighted average of individual study results

### 3.2.1 Takeover time, steering time, and braking time

Metrics such as takeover time, steering time, and braking time are often used to measure driver's takeover behavior during the control transition. After examining the experiment conditions and reported data of 21 valid studies containing 2,056 subjects, the mean takeover time, steering time, and braking time given different lead times are presented in [Figure 3-1](#).

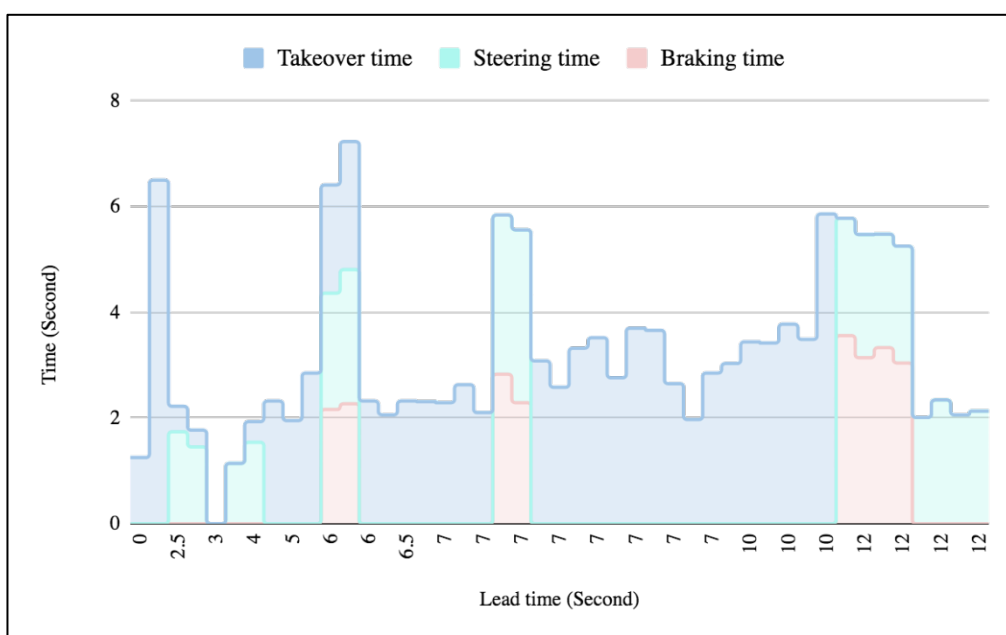


Figure 3-1 Lead time, takeover time, steering time, and braking time during control transitions

The lead time can be further classified into four levels (see [Table 3-1 column 1](#)). Weighted mean takeover time, braking time, and steering time are computed considering the weight of sample size from each study. Besides lead time, there are other confounding factors that affect drivers' response time when an automation system disengages and drivers need to take back

control, which include involvement of NDRTs, TOR modality, and urgency of the triggering events. The weighted means of takeover time, braking time, and steering time are presented in [Table 3-1](#).

Table 3-1 Weighted average takeover time, braking time, and steering time

Lead Time (s)	Takeover time(s)	Braking time(s)	Steering time(s)
<b>Critical (<math>1.5 \text{ s} \leq \text{LT} \leq 2.8 \text{ s}</math>)</b>	2.11	--	1.60
<b>Low (<math>3\text{s} \leq \text{LT} \leq 6 \text{ s}</math>)</b>	1.89	2.22	1.93
<b>Moderate (<math>6 &lt; \text{LT} \leq 8 \text{ s}</math>)</b>	2.98	2.56	3.14
<b>High (<math>\text{LT} &gt; 8 \text{ s}</math>)</b>	3.67	3.27	2.18

Braking time with a critical lead time cannot be calculated since it was not reported in any of the selected studies. 2,056 involved subjects from studies reported both lead times and at least one type of response times (i.e., takeover time, braking time, and steering time). The valid sample sizes for calculating weight mean takeover time, weighted mean braking time, and weighted mean steering time are 1623, 462, and 888, respectively. According to [Table 3-1](#), it is noticed that:

- The minimum weighted mean steering time is identified when lead time is critical;
- The minimum weighted mean takeover time happened when lead time is low;
- The maximum weighted mean takeover time happened when lead time is high;
- The maximum weighted mean steering time happened when lead time is moderate; and
- The maximum weighted mean braking time happened when lead time is high.

A new metric *response time to TOR* is defined as the time it takes for a driver to respond to a given TOR or triggering event. Then TOR response time is the minimum value of takeover time, braking time, or steering time if any of them exists for the following reasons:

- It can provide more information and impute the missing values for later analysis; and

- It indicates the shortest time they need to react to triggering event that causes automation disengagement.

Additionally, based on reported disengagement events, the reaction times of safety drivers in resuming control when automation disengagement occurred were quite stable, regardless of the disengagement causes which include system failure, adverse weather conditions, road users, construction zones, streets, and highways. The average reaction time of a total of 1330 disengagement events is 0.85 second with a standard deviation of 0.70 (Dixit et al., 2016).

### **3.2.2 TOR modality**

Depending on the modality of the TOR designs, its effectiveness in engaging drivers increases as more modalities are used. Accordingly, the effect of TOR design is presented as following:

- Low (only visual or only audio)
- Moderate (visual and audio)
- High (visual, audio, and haptic)

### **3.2.3 Takeover measures**

The selected studies in the meta-analysis are considered as multiple-endpoint studies since they often measure multiple outcomes for each subject. To describe driver behavior and resulting vehicle behavior, metrics used in reviewed studies are categorized into the following classes:

1. Vehicle kinematic related
2. Time related
3. NRDT related
4. Human Physiological related

5. Situation awareness related
6. Simulator sickness related
7. After experiment effect
8. Collision in experiment
9. Quality related
10. Automation trust and self-confidence
11. Human-automation interaction related

Table 3-2 shows the detailed metrics that are included in each class. Metrics extraction and variable coding in Table 3-2 are based upon reviewed results in Table 2-3. The categorization of takeover measures allows further categorization of takeover studies so that missing values in independent variables can be computed.

Table 3-2 Metrics used in driver takeover experiments based on selected studies

Human physiological related	Quality related	Time related	Vehicle kinematic related	Situation awareness related
Fatigue (1)	Takeover action (18)	Takeover time (25)	Velocity (10)	Side mirror (1)
Loudness of warning messages (1)	Minimum clearance towards the obstacle (1)	Minimal distance and time headway to leading vehicle (1)	Absolute angle input (1)	Glances on latent hazard (1)
Glance Frequency (5)	Correct and false detection (6)	Average braking time (1)	Car trajectories (4)	Brake application (1)
Head Angle (1)	Daimler lane change performance (1)	Lane change time (2)	Steering Reversal Rate (2)	Point-of-no-return (1)
Standard deviation of lateral position (5)	Percentage of drivers making a right decision (1)	Minimal time to lane crossing (1)	Roll profiles (1)	System awareness (1)
Eye blink duration (1)	Standard deviation of speed (2)	Time to first steer (1)	Lane Change Speed (1)	Spread of search (1)
Karolinska Sleepiness Scale (4)	Maximal deviation of the ego-vehicle from the center of the ego-lane (1)	Percentage time with PA2 (1)	Absolute steering wheel velocity (3)	Situation Awareness Rating Technique (SART) (1)

Eye- and head-tracking (1)	Maximum longitudinal acceleration (7)	Time to steering peak (1)	Longitudinal Acceleration (1)	<b>Driving history related</b>
Center-of-road fixation time (2)	Inter-rater reliability (1)	Extended time-to-collision (1)	Lane position (2)	SUS (1)
Short Stress State Questionnaire (1)	Maximum lateral deviation (1)	Reaction Time (81)	Lateral Position (3)	SAS (1)
Mean fixation duration (1)	Lane exceedances (3)	Time-to-Collision (23)	Lateral acceleration (1)	Workload (5)
Percentage to road center (1)	Physical and potential control (1)	Stabilization Time (1)	Road wheel angle (1)	Flow Short Scale (1)
Eye-gaze number (1)	Steering wheel reversals (2)	Time-to-Deactivation (1)	Steering Angle (3)	Perceived demand level (1)
Number of Fixations on HMI (2)	Number of alternative maneuvers (1)	Glance duration (11)	Deceleration rate (1)	Rating Scale Mental Effort (1)
Glances at the central display (1)	RMS of the driver's steering torque (1)	Eyes-off-road time (1)	Lateral Deviation (3)	<b>Human-automation related</b>
Pupil diameter (1)	Lateral deviation (3)	<b>NDRT related</b>	Lateral Speed (4)	Deactivation method (1)
First gaze at the road (2)	Maximum steering wheel angle (1)	Number of accepted tasks (1)	Longitudinal speed (3)	Number of off-switches (1)
Percentage time on the left lane (1)	Standardized brake pedal travel (1)	Disengagement from secondary task (1)	Braking Rate (2)	Automation trust and confidence (1)
Horizontal gaze deviation (1)	Frequency control of steering (1)	Performance in reading span task (2)	Direction of roll motions (1)	Human-machine interaction (1)
Percentage of eyelid closure over the pupil over time (2)	Frequency of responses prior to the event (1)	Number of trials completed per minute (1)	Lateral acceleration (1)	Handovers involving information transmission (1)
Gaze accumulation (3)	Rates of lane change errors (1)	Recall accuracy (1)	Lateral Speed (4)	Subjective trust and self-confidence (2)
Galvanic skin responses (1)	Steering wheel angle after lane change (8)	NDRT performance (1)	Braking Rate (2)	Securing Behavior (1)
Percentage of Time on Area of Interest (1)	Percentage of drivers making a right decision (1)	Subjective measures (1)	Direction of roll motions (1)	Number of drivers disengaging the automated system (1)
Bio-signals (1)	Mental model accuracy (1)	Success Rate (1)	<b>Simulator sickness related</b>	<b>Questionnaire related</b>
Proportion of gaze fell within road center area (2)	Maximum longitudinal deceleration (3)	Level of engagement in non-driving tasks (1)	Post-test Simulator Sickness Questionnaire (2)	Questionnaire after Experiment (37)

Attention allocation (1)	RMS steering speed (1)	Secondary task performance (2)	Motion sickness (1)	Questionnaire before experiment (28)
Glance location probability (1)	Maximum lateral acceleration (13)	Typing Performance (3)	<b>Collision related</b>	
Perceived vibration intensity (1)	Maximum deceleration (2)	Dialogue Performance (1)	Number of Collision (4)	
Percentage eyes closed (1)	Minimum time headway (3)	Multitasking performance (1)		
Blink Frequency (2)	Proactive response behavior (1)	Flow Short Scale (1)		
Angle of roll motion (1)	Maximum yaw rate (1)			
Head and eye tracking data (1)	Maximum acceleration (2)			
NASA-TLX (19)	Average lateral acceleration (1)			
Gaze heading (1)	Average absolute acceleration (1)			
Lateral Stability (1)	Average deviation from lane center (1)			
Sight patterns (1)				

*\*Note, numbers in the bracket represents number of times this metric has been used in selected publications.*

### 3.2.4 NDRTs summary

The impact of NDRTs on takeover behavior is discussed from three perspectives in [Section 2.8](#). Evidence from both theoretical and applied research showed that NDRTs might lead to impaired takeover performance. The reviewed results are presented in [Table 3-3](#).

Table 3-3 The impact of NDRTs on Drivers' takeover behavior

Absence of NDRTs	<b><i>Malleable attentional resources theory</i></b> (Young and Stanton, 2002): the pool of attentional resources is dynamic and strongly affect by task demands.
------------------	--

	<p>If drivers don't engage in a NDRT, they may suffer from reduced attentional resources and may result in being unable to reclaim control from the automation system in emergent situations.</p> <hr/> <p>Traditional beliefs of fixed attentional resource pools</p> <p>Automated driving grants drivers spare cognitive capacity for NDRTs.</p>
Simple NDRTs	<p>Driving automation might affect the propensity of drivers to involve in NDRTs.</p> <p>Drivers would voluntarily schedule NDRTs on the basis of the availability and predictability of automated driving modes.</p> <hr/> <p><b><i>Situation-adaptive behavior</i></b> (Wandtner et al., 2018d)</p> <p>NDRT engagement is associated with both driving automation mode and driving situations. Levels of NDRT engagement increase with levels of automation (Wandtner et al., 2018b). However, drivers started to focus their attention on the primary driving task when speed increases (Wandtner et al., 2018b).</p>
Complex NDRTs	<p>Complex NDRTs prolongs the time it takes drivers to take back control over the vehicle and there might be performance deficits after a control transition.</p>

### 3.2.4 Driver gender and age

There was a total of 6,339 subjects participated in all selected studies, including 1,677 male and 1,070 female participants (some of these studies didn't report subject gender in their experiments). A new variable called *male percentage* is created to reflect the potential effect from subject gender in takeover behavior. If gender information was available in a study, the *male percentage* is calculated as the number of male subjects divided by the total number of subjects in the study.

For all selected studies, the grand mean male percentage is 58.2%. The mean ages of subjects in selected studies range from 19 to 72 years old, indicating a good coverage of age groups. In addition, the mean ages of subjects in selected studies with no missing values in other variables

range from 21 to 45 years old. Drivers ages are transformed to be categorical variable according to the following rules:

- Young ( $\text{age} \leq 30$ )
- Middle aged ( $31 \leq \text{age} \leq 64$ )
- Old ( $\text{age} > 64$ )

### 3.2.5 Missing data

It is inevitable that some selected studies contributing to the meta-analysis have missing data. The intention of this section is to outline missing data issues and illustrate how missing values of independent variables are computed since input to regression models can be null. Independent variables extracted from selected studies include sample size, mean and standard deviation of subject ages, male percentage, NDRT, lead time, TOR modality, and operating speed before disengagement. Dependent variables include takeover time, steering time, braking time, TTC, deceleration rate, lateral acceleration, and angular velocity. All variables of categorical types are treated as nominal variables and the rest are treated as numeric variables. A hierarchical clustering model is applied to those studies with complete attribute information, then the mean values of each corresponding groups are used to impute the missing values. According to the tree plot (Figure 3-2), 30 studies with complete independent variable information are categorized into four groups. Finally, after using hierarchical clustering to infer those missing values from the existing data, the relationships of influencing factors and response variables in complete data are presented in Figure

3-3. The determination of the effects that lead time, driver ages, NDRTs, and TOR modality have on takeover time is presented in [Section 3.3](#).

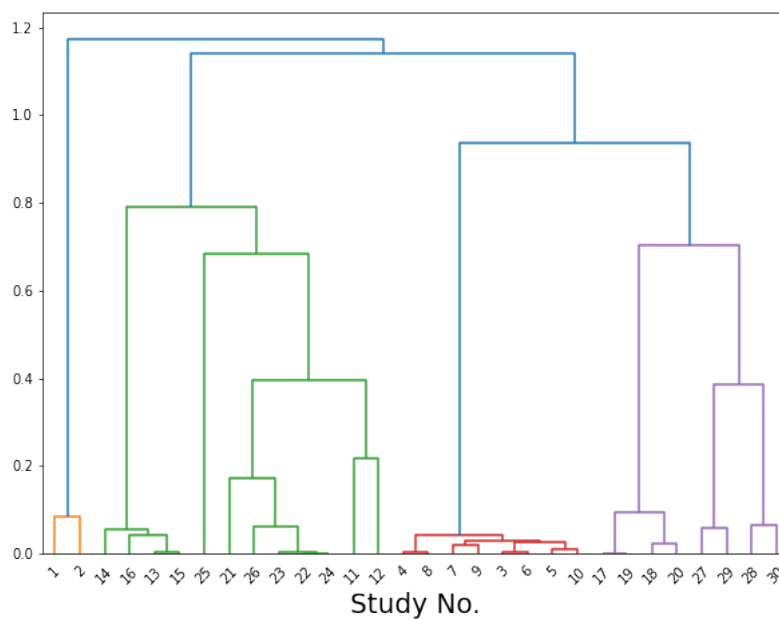


Figure 3-3 Data imputation based on hierarchical clustering results

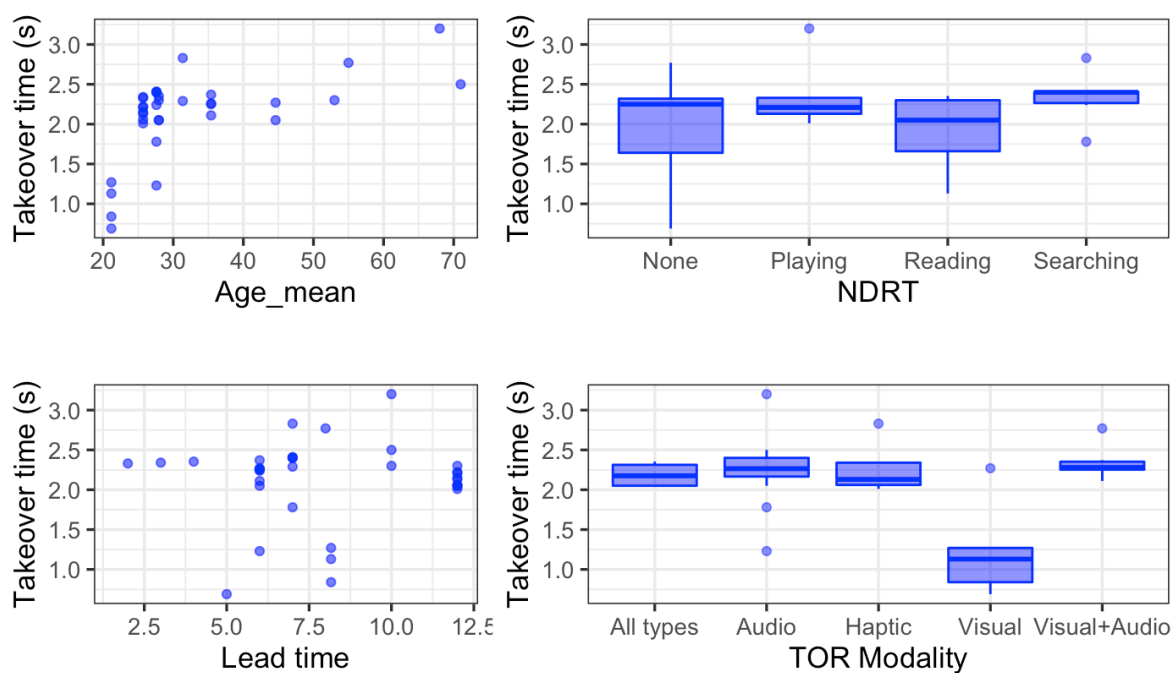


Figure 3-2 Takeover time versus driver ages, NDRTs, lead time, and TOR modality

### 3.3 Machine learning-based Meta-analysis

Based on the summaries in [Section 3.1](#) and [Section 3.2](#), this section consolidates the findings from previous studies into requirements needed by a DAS model using a regression technique from machine learning. In fact, meta-regression is often used in meta-analysis as a tool to evaluate the impact of moderator variables on study effects. As presented in [Chapter 2](#), there is substantial heterogeneity over the selected studies. Possible causes of the heterogeneity need to be considered. In the context of meta-analysis, this can be addressed by covariates on the study level that explains the differences between studies and covariates on the subject level. In this research, a new metric, *Takeover quality (TOQ)*, is designed to estimate the outcomes of selected studies.

Machine learning -based meta-analysis integrates research findings across studies, which is an improved approach to analyze multiple end-point studies. This section is organized as follows. In [Section 3.3.1](#), a new study effect metric is designed to represent different study effects presented in selected studies. [Section 3.3.2](#) presents a general introduction of XGBoost regression method with more than one covariate. In [Section 3.3.3](#), the results of a meta-regression model (i.e., XGBoost model) is presented.

Finally, through quantitative estimating findings across diverse studies, the machine learning -based meta-analysis can bring new knowledge to light and facilitate the DAS modeling work in [Chapter 4](#).

#### 3.3.1 Takeover quality (TOQ)

Since more than one metric are often reported in selected studies (see [Table 3-2](#)), a novel metric, *TOQ*, is created and designed to replace diverse study effects reported in selected studies. *TOQ* is defined as follows:

$$TOQ = \lambda * a_{-} + (1 - \lambda) \frac{v * \tan(q)}{TTC - TOT} \quad (3-1)$$

Where

$\lambda$  is a penalty parameter (unitless)

$a_{-}$  is the magnitude of deceleration rate ( $m/s^2$ )

$v$  is velocity when driver first taking back control (m/s)

$q$  is the absolute steering wheel angular input from the driver (deg)

$TTC$  is the measured time-to-collision (s)

$TOT$  is drivers' takeover time (s)

TOQ is Takeover Quality ( $m/s^2$ )

There are two terms in the TOQ definition with the intention that deceleration rate, speed, steering wheel angular input, and time difference between TTC and TOT can be translated into a single measure on how well a driver responds to a TOR. The first term in the TOQ metric is a penalty parameter times deceleration rate. The main logic behind  $TOQ$  is that higher deceleration rate will cause more discomfort to the driver and passengers, indicating lower takeover quality. It is also possible that higher deceleration rate is needed when the driver first takes back control because of the urgency or criticality of the situation. The penalty parameter,  $\lambda$ , varies from 0.0 to 1.0. The optimal value of  $\lambda$  is identified as 0.8, since gives the minimal RMSE when using all candidate values of  $\lambda$ .

The second term in the TOR metric is a penalty parameter multiplied by a scaled rate of velocity change. The numerator is the product of velocity  $v$  and a scale factor that converted from steering wheel angular input  $q$ . When both takeover velocity  $v$  and steering wheel angular input  $q$  are high given a fixed difference between TTC and TOT, the resulting acceleration is also high, and vice versa; When both takeover velocity  $v$  and steering wheel angular input  $q$  are fixed, an increased difference between TTC and TOT results in a reduced acceleration. It is expected that when TTC is greater than TOT, the resulting scaled rate of velocity change should be less given a takeover velocity.

$q$  is the absolute steering wheel angular input from the driver reported in selected studies. Some studies had more detailed metrics related lateral takeover. For instance, [Petermeijer et al., \(2017\)](#) measured steer touch, steer initiate, and steer turn in their experiment, which are defined as following:

- Steer touch: absolute steering wheel velocity greater than 1 deg/s. The steer-touch reaction time was also a measure of how quickly participants touched the steering wheel after receiving a TOR.
- Steer initiate: absolute steering wheel angle greater than 0.25 deg, which is also the minimum that could be reliably detected by the steering sensor as being different from the steering angles that were measured during automated driving.
- Steer turn: absolute steering wheel angle greater than 2 deg.

### 3.3.2 XGBoost regression algorithm

[Section 3.1](#) and [3.2](#) have demonstrated that Challenge One presented in the beginning of Chapter 3 can be essentially addressed by meta-regression as the statistical combination of study results.

There are many regression analysis methods that can be used in the meta-regression analysis, including linear regression, decision tree regression, random forest regression, Adaboost regression, and XGBoost regression. In this research, the XGBoost regression is adopted to analyze drivers' takeover behavior as XGBoost is a powerful tool for building regression models. The details on the model selection and model tuning can be found in [Appendix A](#). By using metrics defined in equation 3-5, 3-6, and 3-7, the performance of each model candidate is compared in [Table 3-4](#).

XGBoost is an ensemble of decision trees in which new trees are grown to minimize errors produced by previous trees ([Chen and Guestrin, 2016](#)). New trees are added until the error can no longer be improved in the model. The reasons why XGBoost is selected include:

- XGBoost is well known to have better results than other machine learning algorithms. In fact, it has been used in many different fields on structured dataset of various topics since its initial release in 2015. It has consistently outperformed other machine learning algorithms.
- XGBoost is a boosting algorithm using gradient boosting framework at its core. It builds a set of weak learners and provides an improved prediction accuracy. When building tree  $i$ , the model output is weighted based on the result of previous tree  $i - 1$ .
- XGBoost is designed with efficient parameter tuning for cross-validation, regularization, user-defined objective functions, and tree parameters.

More technical details about XGBoost can be found in ([Chen and Guestrin, 2016](#)). Algorithm 3.1 demonstrates how to build XGBoost trees for regression. Let  $D = \{(x_i, y_i): i = 1 \dots n, x_i \in \mathbb{R}^m, y_i \in \mathbb{R}\}$  represent the dataset collected from Section 3.2, which include  $m$

features and  $n$  observations and a corresponding response variable  $y$ . Let  $\hat{y}_i$  represent the output of the XGBoost regression model, which can be expressed as below:

$$\hat{y}_i = \sum_{k=1}^k f_k(x_i), f_k \in F \quad (3-2)$$

Where

$f_k$  represents a regression tree

$f_k(x_i)$  represents Similarity Score given by the  $i^{th}$  observation

$F$  is the space of regression trees.

In order to learn a set of functions, the following regularized objective function should be minimized:

$$L(\phi) = \sum l(\hat{y}_i ; y_i) + \sum \Omega(f_k) \quad (3-3)$$

$$\Omega(f_k) = \gamma T + \frac{1}{2} \lambda ||w||^2 \quad (3-4)$$

Where

$l$  is a differentiable convex loss function that measures the difference between the prediction  $\hat{y}_i$  and the target  $y_i$

$\Omega$  penalizes the complexity of the regression tree functions to prevent overfitting and to simplify the model produced by the algorithm

$\gamma$  regulates the minimum loss reduction required to make a further partition on a leaf node

$T$  is the number of leaves in the tree

$w$  is the leaf weight and  $w_i$  represents the score of the  $i^{th}$  leaf

$\lambda$  regulates the magnitude of leaf weight  $w$

Table 3-4 XGBoost regression algorithm

---

**Algorithm 3.1** XGBoost regression trees

---

**Definitions:**

Residuals: the difference between the observed and predicted values

SRS: sum of residuals, squared

$l$ : regularization parameter, which is intended to prevent overfitting by reducing prediction's sensitivity to individual observations.

$\gamma$ : tree complexity parameter

$\varepsilon$ : learning rate

Similarity Score(SS):  $SS = \frac{SRS}{Number\ of\ residuals + 1}$

Gain:  $Gain = Left_{similarity} + Right_{similarity} - Root_{similarity}$

**Output:**

$$Output\ value = \frac{Sum\ of\ Residuals}{Number\ of\ residuals + 1}$$


---

**Initialize:**

initial prediction: : 0.5

$l = 0$

$\gamma = 0$

$\varepsilon = 0.3$

**Process:**

1. All samples in the training set are grouped into the same partition (root);
2. Allocate the data into two partitions using all possible binary split according to percentiles of feature distribution;
3. Compute Similarity Score and Gain and select the split that minimizes SS;
4. Repeat the splitting rule to each of the new branches;
5. Repeat step 4 until each node reaches a minimum node size and becomes a terminal node;
6. Prune the tree by calculating the differences between Gain and  $\gamma$  according to:

$$Gain - \gamma = \begin{pmatrix} \geq 0, & don't\ prune \\ < 0, & prune \end{pmatrix}$$


---

It is worth noting that the output value is different from the Similarity Score and is the sum of residuals that are not squared. In addition, when  $l > 0$ , then it will reduce the amount that this

individual observation adds to the overall prediction, preventing over fitting the training data. When  $l = 0$ , there is no regularization.

The model performance is evaluated by comparing predicted and observed TOQ values using the Root Mean Squared Error (RMSE), the Mean Absolute Error (MAE), and  $R^2$ . The key difference is that RMSE penalizes large errors more harshly than MAE. Let  $y_1, \dots, y_n$ ,  $n \geq 1$  denote observed TOQ values,  $\hat{y}_1, \dots, \hat{y}_n$ ,  $n \geq 1$  represent the predicted values, and  $\bar{y}$  be the mean of observed values.

The RMSE is defined as:

$$RMSE = \sqrt{\frac{1}{n} \sum_1^n (y_i - \hat{y}_i)^2} \quad (3-5)$$

The MAE is defined as:

$$MAE = \frac{1}{n} \sum_1^n |y_i - \hat{y}_i| \quad (3-6)$$

$R^2$  is the proportion of variance explained by the model, which can be calculated as follows:

$$R^2 = 1 - \frac{\sum_1^n (y_i - \hat{y}_i)^2}{\sum_1^n (y_i - \bar{y})^2} \quad (3-7)$$

Five machine learning models were compared for takeover behavior analysis before finalizing on using XGBoost in this study. By comparing RMSE, MAE, and  $R^2$ , all candidate

models are compared. The results are shown in [Table 3-5](#). It is evident that XGBoost model outperforms the other four models.

Table 3-5 Initial model selection for meta-regression analysis

Model	RMSE	MAE	R <sup>2</sup>
<b>Linear regression</b>	2.409	1.457	0.781
<b>Decision tree regression</b>	0.826	0.537	0.927
<b>Random forest regression</b>	0.868	0.587	0.945
<b>AdaBoost regression</b>	0.752	0.513	0.925
<b>XGBoost regression</b>	0.620	0.336	0.979

### 3.3.3 XGBoost modeling

The Scikit-Learn python package is used to train a XGBoost model ([Open source, 2020](#)). A detailed training process can be found in ([Jason Brownlee, 2018](#)). An example of python code is given in [Appendix A](#), which details each step of the model training and parameter tuning.

The model trained using 32 studies with 1,295 subjects can be used to predict how a driver would take back control when the automation system disengages while approaching a signalized intersection with the signal phase being PPLT. The detailed model training and model tuning process is also presented in [Appendix A](#). Generally, the XGBoost modeling tuning process can be summarized as following:

- Start with a relatively high learning rate the model tuning process;
- Determine the optimal number of trees for the initial learning rate;
- Tune tree-specific parameters including `max_depth`, `min_child_weight`, `subsample`, `colsample_bytree` for decided learning rate and number of trees. Note that we can choose different parameters to define a tree;

- Tune regularization parameters (gamma, lambda, alpha) for XGBoost which can help reduce model complexity and enhance performance; and
- Lower the learning rate and decide the optimal parameters.

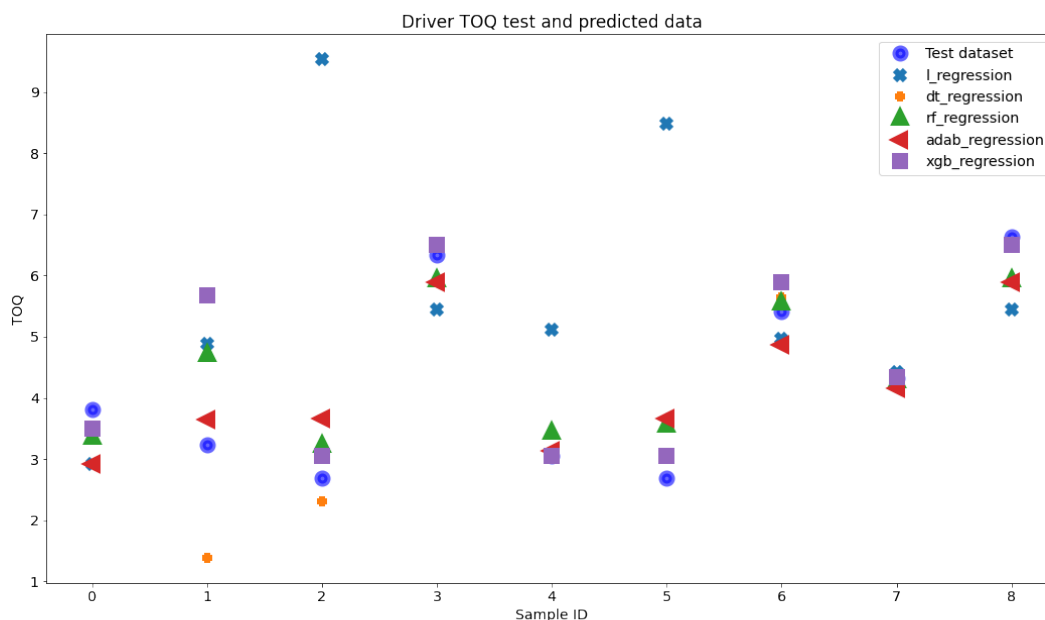


Figure 3-4 Prediction results of different regression models

One comparison of all candidate models' prediction on test dataset can be visualized in [Figure 3-4](#). It is evident that tree-based regression is generally better than linear regression model in addressing takeover behavior issues. The value of tree-based regression and its superiority can be explained as follows. By tracing the sample ID to the original publication where linear regression result is very different from the tree-based models, the actual scenario described by independent variables and response variables can be reviewed. It is possible that cases of large difference between linear regression result and ground truth is caused by its nature – always fits to a linear relationship between response variable and independent variables. Predictions from tree-based models are always an average of the predictions by all trees built in the forest. Tree-based regression essentially splits sample data over different combinations of features using objective

function that minimize the loss, step by step. Unlike linear regression, tree-base regression models are capable of capturing the non-linear interactions between the feature (used as the split node) and the response variable. Specifically, each tree that is constructed in XGBoost model is done by recursive partitioning the node (random sampled at each step) to identify the best split point with that feature. Tree-based models when trained properly is quite robust to noise even on a small training dataset.

The results for the trained XGBoost predictive model can be obtained after loading the saved model in Python. After the model selection and model tuning process presented in [Appendix A](#), it is found that AdaBoost (RMSE = 0.752, MAE = 0.513,  $R^2 = 0.925$ ) and XGBoost (RMSE = 0.620, MAE = 0.336,  $R^2 = 0.979$ ) have comparable predictive performance on the training dataset. However, XGBoost has more accurate prediction on test dataset than Adaboost.

Based on an initial trained XGBoost model, the importance of all features is presented in [Figure 3-5](#). It is found that vehicle operating speed at the moment when automation system disengages and lead time of TOR are comparatively the most important features in determine drivers' takeover behavior among all covariates.

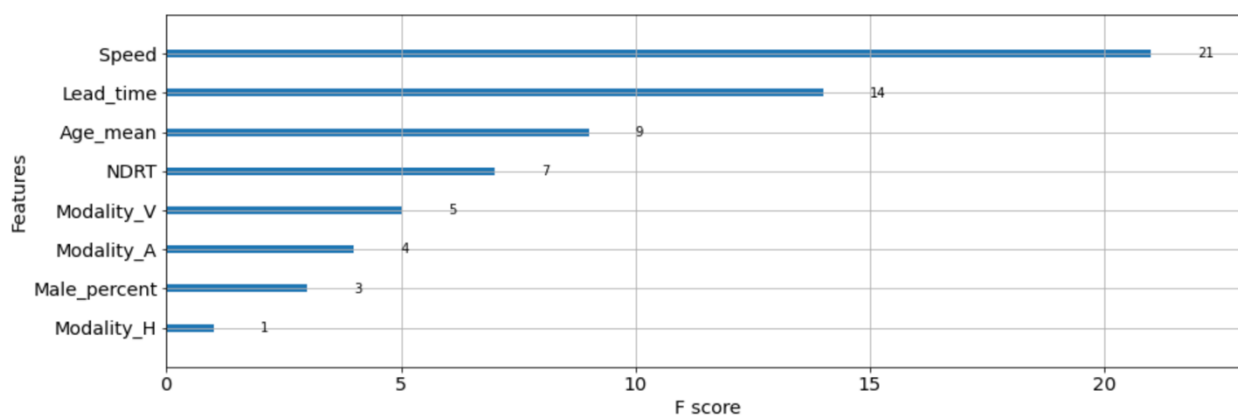


Figure 3-5 Feature importance score from XGBoost regression model

Furthermore, driver age, TOR modality and driver gender are less important compared to vehicle operating speed before automation disengagement, lead time, driver age, and NDRT involvement. This allows us to parameterize driver models that is implemented in VISSIM to truly reflect driver's takeover reaction when affected by different factors analyzed in [Section 3.2](#). Table 3-5 summarizes how driver age and different NDRT activity are categorized by XGBoost model in predicting TOQ. It has been suggested that potential inter-individual differences might exist in takeover behavior and imply that the difference should be investigated in future studies ([Körber et al., 2015](#)). Parameters in VISSIM are tuned to model drivers' takeover time, braking deceleration rate, and steering wheel control. More details are presented in [Chapter 4](#) and [Chapter 5](#). Once a XGBoost model is obtained, its parameters are tuned to minimize the RMSE, resulting in an optimized penalty coefficient  $\gamma$  in TOQ, which is 0.8. For more robust and reliable future predictions, the trained model parameters and  $\gamma = 0.8$  in equation 3-1 is used.

### 3.4 Estimation of Takeover behavior

Samples that cover all 48 combinations of cases ([Table 3-6](#)) are generated and takeover behavior is then estimated by XGBoost model. Increasing samples to ensure that there is at least one sample in each case reduces the limitation in the original dataset obtained in [Section 3.2](#) and also allows for a more comprehensive presentation of the drivers in takeover scenarios.

Table 3-6 Driver age and NDRT categorization in XGBoost regression model

Driver	Values	Levels
Speed	35mph	1
Lead time	Critical, Low, Moderate, High	4
Driver age	Young, Middle-aged, Old	3
NDRT involvement	None, Reading, Searching, Playing	4

Figure 3-6 highlights the key points presented in [Chapter 3](#), starting from takeover experimental data collection, XGBoost regression model training that minimizes the RMSE of TOQ, then resampling more input variables to have a better coverage of takeover settings, next using the trained XGBoost model to get takeover behavior. The last step after getting the output is to use distribution tests to identify the distribution of takeover behavioral data. Then, the probability distributions of the outputs including takeover time, TTC, deceleration rate, and steering wheel angular speed of the XGBoost model are obtained to ensure that models implemented in VISSIM can reflect how drivers might respond to TOR at a PPLT intersection. Examples of estimated probability densities are presented in [Figure 3-7](#) to [Figure 3-10](#).

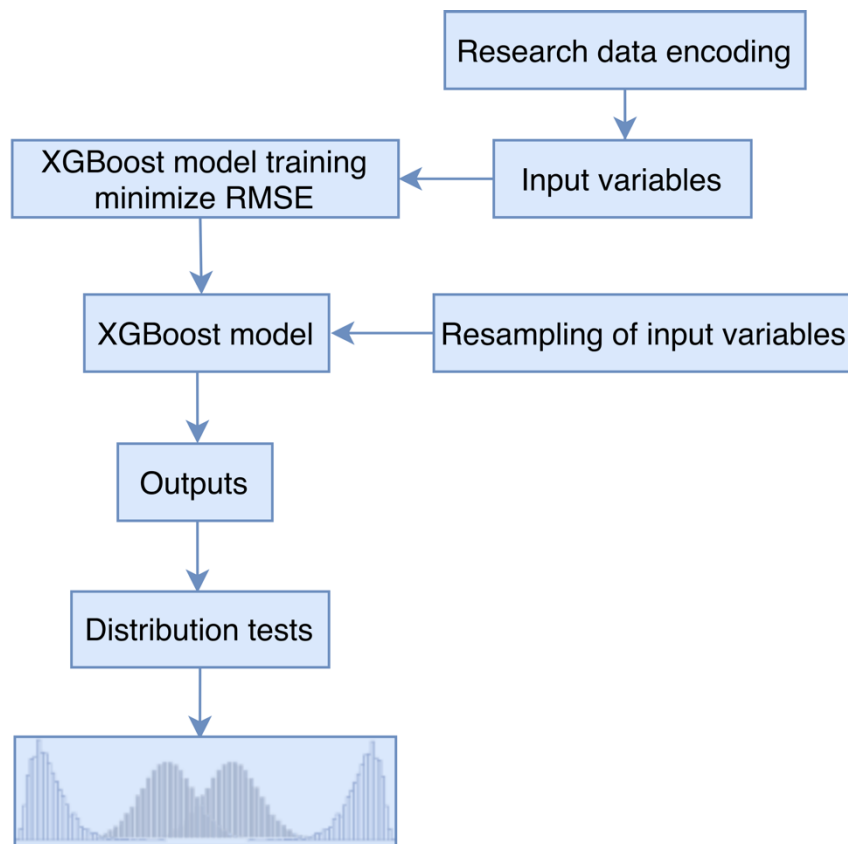


Figure 3-6 Workflow of takeover behavior estimation

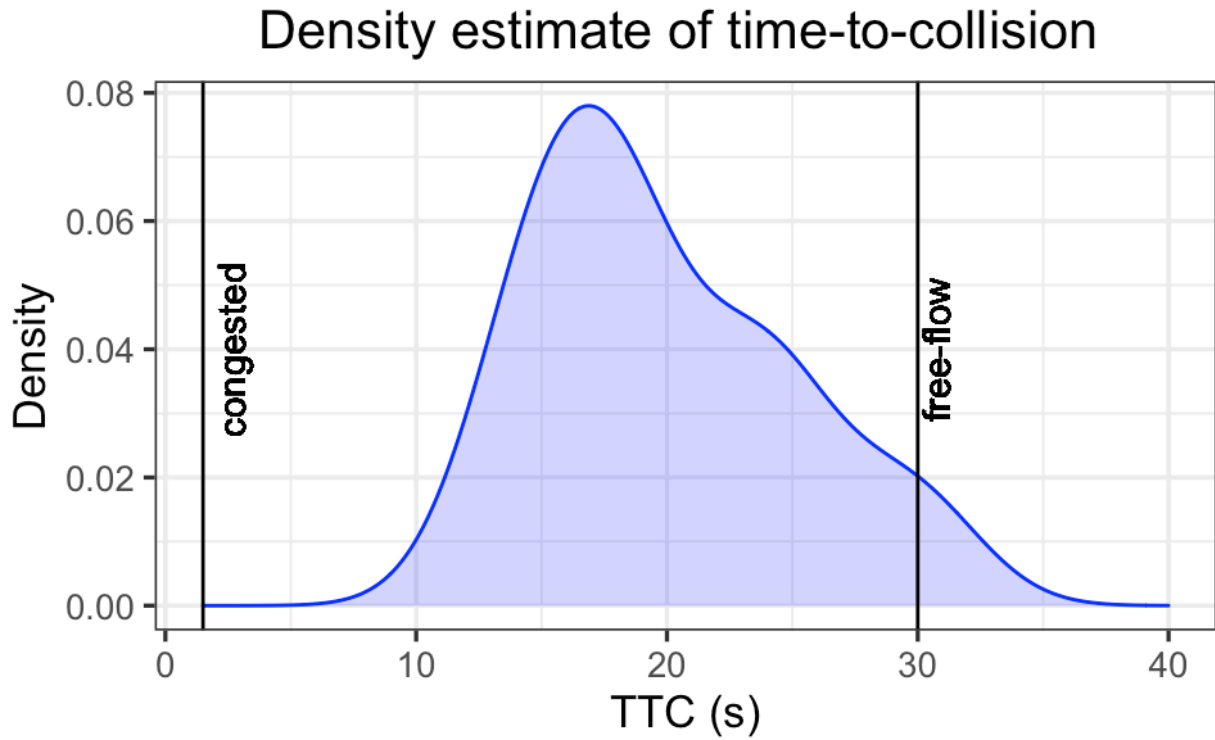


Figure 3-7 Estimated TTC probability density

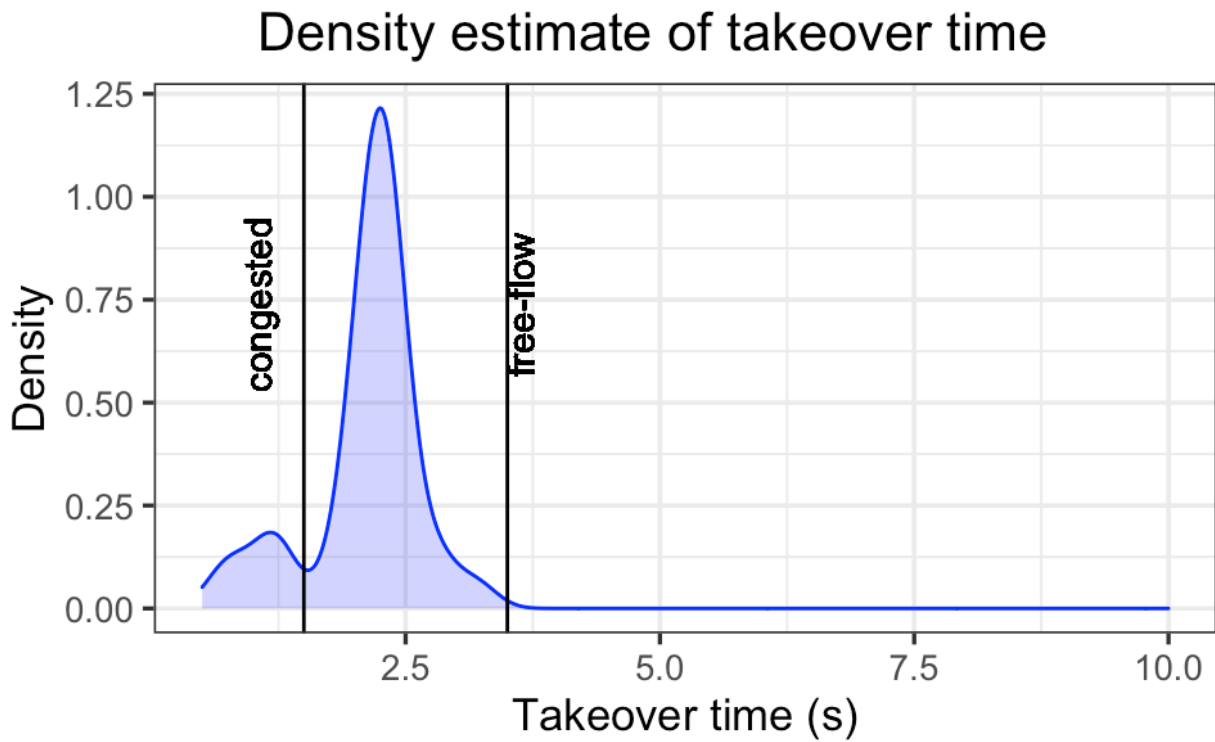


Figure 3-8 Estimated probability density of takeover time

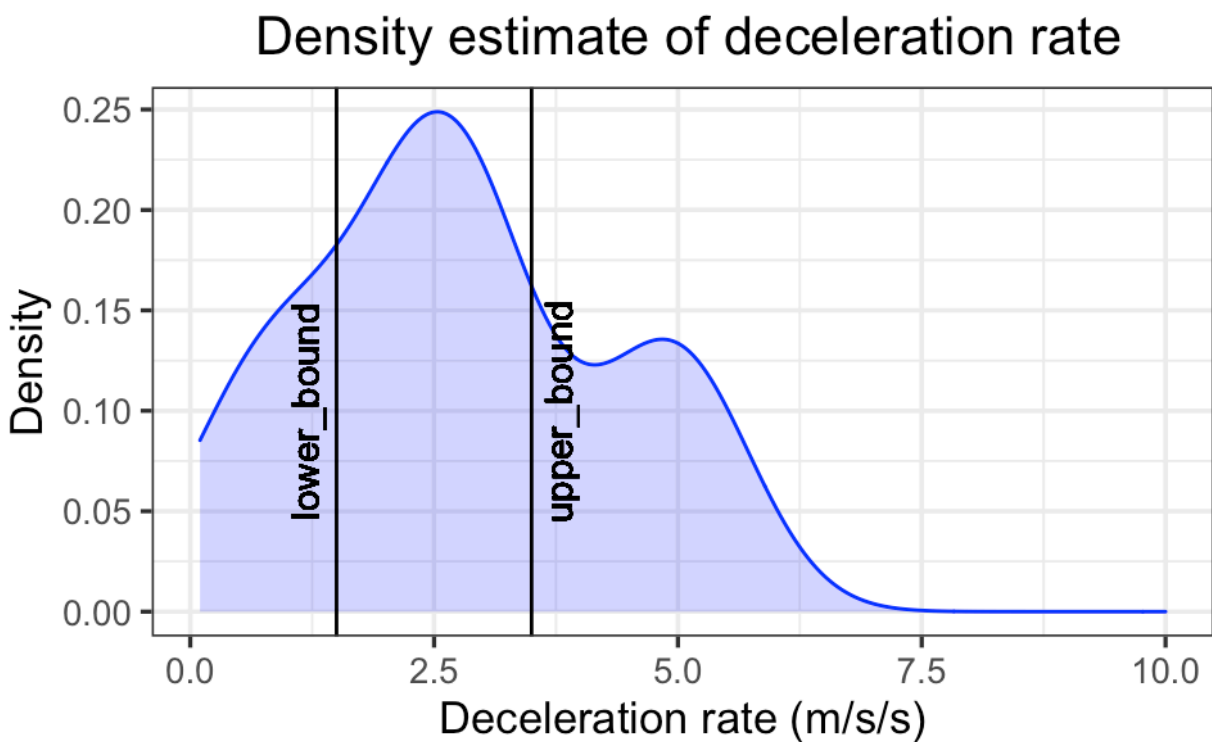


Figure 3-9 Estimated probability density of deceleration rate

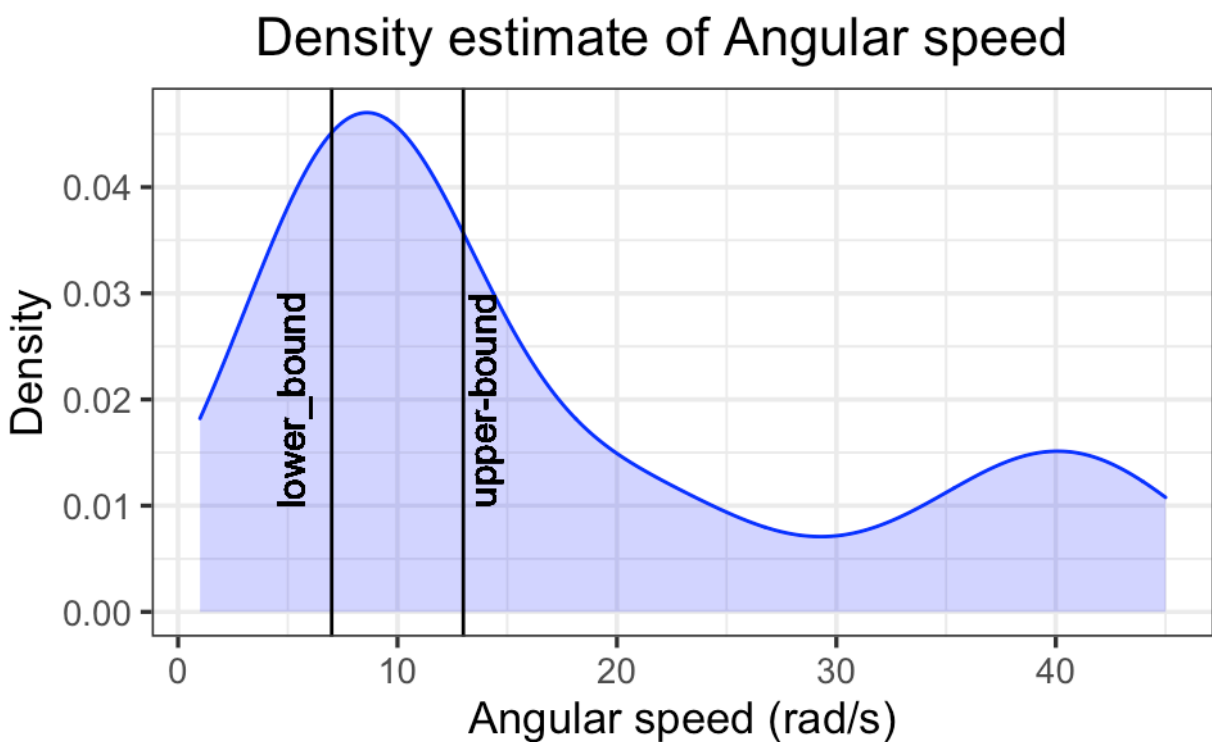


Figure 3-10 Estimated probability density of angular speed

Taken together, meta-regression analysis of disengagement events and takeover behaviors ensure that the outputs of the human-automation model are acceptable, which is based on two types of data:

- data that was used in the construction of the model; and
- data that was created to extend the scenario space.

Validations based on the collected data from related studies involves analyzing the goodness-of-fit of the model. Whether the model's predictive performance decreases when applied to pertinent new dataset was used as the validations of the hypothesized data. Finally, the XGBoost model that has been validated by two different approaches then is used to estimate drivers' takeover behavior in PPLT-induced disengagement events. The output for the XGBoost model is then transformed to probability densities and implemented in a VISSIM simulation on drivers' responses to disengagement events when approaching a signalized intersection.

### 3.5 Summary

Three main challenges in using a DAS model for ensuring traffic safety and in assessing the impact of control transitions were highlighted in [Chapter 3](#). The main contributions of [Chapter 3](#) are summarized as below:

- (1) Summarized key factors that may affect drivers' takeover behavior ([Section 3.1](#) and [Section 3.2](#));
- (2) Defined a unique TOQ metric that can assess driver takeover behavior during control transitions and the RMSE of TOQ can be optimized when the penalty factor is 0.8.

- (3) Presented a XGBoost regression algorithm to assess the impact of those identified influential factors on takeover behavior ([Section 3.3](#));
- (4) Identified that operating speed before disengagement, lead time, driver age, and NDRT engagement are more significant factors that affect driver's takeover behavior ([Section 3.3.3](#))
- (5) Highlighted the extensive and unique computer code ([Appendix A](#)) developed to complete the required analysis.
- (6) Demonstrated a sound process from data collection of takeover behavior, XGboost regression model training, and data resampling, to making predictions of drivers' takeover time, TTC, deceleration rate, and steering wheel angular speed to reflect how drivers might respond to TOR at a PPLT intersection.
- (7) Made generalizable estimates and validated the effect that influencing factors has on takeover behavior ([Section 3.4](#))

## Chapter 4 Modeling takeover transitions

Most previous studies of automation disengagement have focused on capturing the behavior differences in various disengagement-triggering events. Nevertheless, takeover time, braking time, TTC, and other non-time related response measures do not detail the quality of vehicle control after a human driver resumes control from the automation counterpart. Chapter 4 develops a DAS model that describes the interactions between automation systems and human drivers in a PPLT scenario. The DAS model generates driver takeover time, deceleration rate, and steering wheel speed to a PPLT disengagement event. The DAS model is then included in VISSIM simulation where different percentage of left-turn movements disengages due to permissive left-turn signal and a human driver needs resume vehicle control from the automation system. As mentioned throughout, the complexities of permissive left-turn decision making likely requires disengagement under nearly all conditions.

### 4.1 Takeover behavior and automation system

This chapter describes a model framework to capture the interactions of a DAS during control transition in the context of PPLT scenario. First, drivers in a DAS are modeled according to a set of states based on reviews in [Section 2.5](#) and [Section 3.2](#). The core problem of a DAS in PPLT scenario is how a driver might take back control from an automation system. As noted in preceding narrative reviews and meta-regression analysis, effective modeling of DAS interactions must be developed according to the following requirements:

- Requirement 1: Functions allocated to each agent (a driver or an automation system) must be within their reasonable capability; and

- Requirement 2: Each agent's functionality must be compatible with the dynamics of the DAS entity.

To satisfy *Requirement 1*, drivers' takeover time, braking deceleration rate, steering wheel speed, and overall TOQ must be within a reasonable range, which can be compared with previous takeover studies as well. When allocating driving tasks to drivers, the impact of driver ages on their takeover behaviors also must be considered. Similarly, how much lead time can an automation system provide to the driver must be reasonable for certain disengagement scenarios. For instance, if a system is known to have limited capability on PPLT handling, then it usually gives drivers enough lead time to take back control. Further, to address *Requirement 2*, a model of DAS interactions must be able to reflect the dynamic aspects of tightly coupled driver and automation system since their tasks are interdependent.

In case of DAS, the driver manages the longitudinal and lateral control of the loop to minimize the discrepancy between the actual and targeted driving goal (such as speed and lateral position). The automation part takes over the task of vehicle control so that the driver becomes out of the feedback loop. To successfully undertake the driving task, the driver needs to continuously observe the external environment and re-calibrate his or her driving tasks at the moment. A more complete illustration of the driver-automation feedback loop is shown in [Figure 4-1](#).

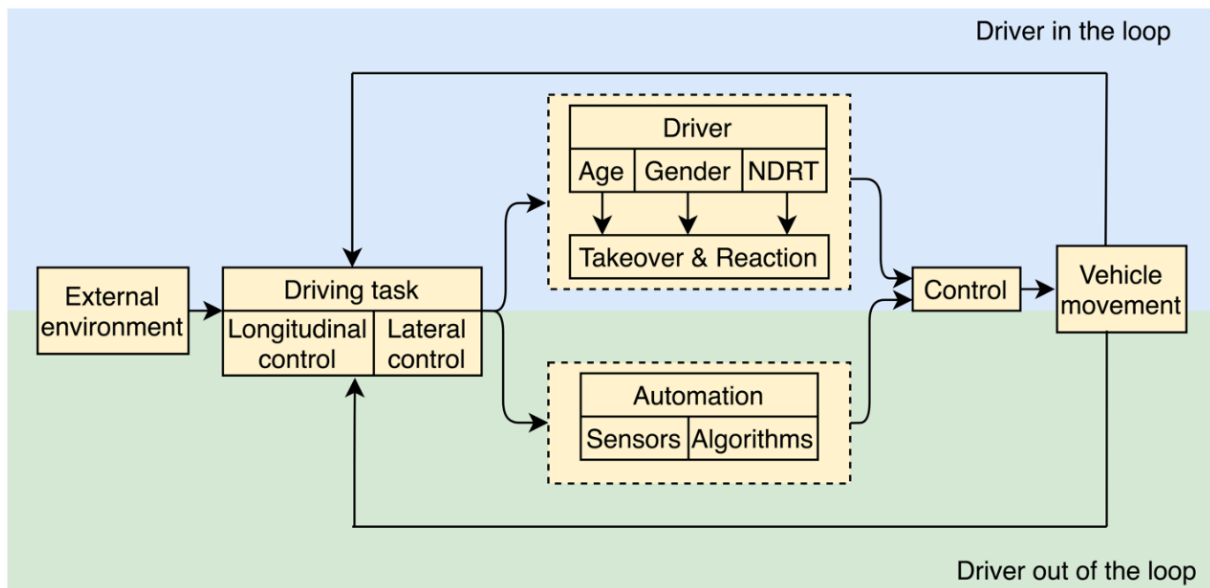


Figure 4-1 Driver-automation feedback loop

## 4.2 DAS model contributing to evaluation of TOQ

In Section 4.1, three aspects that should be considered in the DAS model are described, which enable a description of the DAS model that can be implemented in VISSIM.

### 4.1.1 Driver's out-of-the-loop state as a result of automation systems

First, drivers' out-of-the-loop state is defined as a driver's state of readiness to timely take back control from the automation. When a driver is in the out-of-the-loop state, he or she needs some time to have the up-to-date knowledge of the vehicle state and the external environment, such as vehicle operating speed, position, speed of headway vehicle, and road conditions, and the like. The driver also needs time to predict the driving situation and to develop a safe driving strategy to react to current driving situation or a disengagement event. Depending on the level of readiness, a driver

can also be in the in-the-loop state even though the automation system takes full control of the vehicle. Overall, drivers can be out-of-the loop at different levels. A deeper out-of-the-loop state can result in longer reaction times (Eriksson et al., 2019; Naujoks et al., 2019) and inaccurate situation awareness (Köhn et al., 2019; Strand et al., 2014). A driver can be in a high out-of-the-loop state as a result of different causes, such as engagement in a NDRT.

Contrary to out-of-the-loop state, when drivers are in-the-loop, their attentions on the external environment and current vehicle state are constantly required. When automation starts to take over certain driving tasks from time to time, the driver allocates a part of his or her attention to a NDRT and no longer takes full charge of driving tasks including collecting information on external environment, and thus reaches the out-of-the-loop state.

#### **4.1.2 Individual differences**

It has been shown that there might be potential inter-individual differences in takeover behavior. Körber et al. (2015) suggested that the difference should be investigated in future studies. To keep the driver at a low out-of-the-loop state, he or she needs to update external environment (such as road and other vehicles) and vehicle state for driving safety while being engaged in a NDRT at the same time. Impact of NDRTs on drivers' takeover behavior is discussed from three different perspectives in [Section 2.8](#). Evidence from both theoretical and applied research showed that NDRTs might lead to impaired takeover performance. The reviewed results in [Section 2.8](#) are summarized in [Table 3.1](#)

It has been shown that drivers' engagement in NDRT varies by the complexity of those tasks. Therefore, their potential to reach a critical out-of-the-loop state due to NDRT engagement also might differ. Meta-analysis in [Section 3.3](#) reveals that when drivers are not engaged in any NDRTs, their takeover time is generally shorter than when they are engaged in some reading, monitoring and searching, and playing tasks. Out-of-the-loop state leads to longer reaction times when compared to in-the-loop state. Thus, it is safe to expect that NDRT engagement is directly related to how long it may take a driver to take over control of the vehicle from automation systems.

The impact of driver ages on takeover behavior has also been investigated through experiment-based studies which included 36 older drivers (greater than 60 years old) and 36 younger drivers ([Körber et al., 2016](#)). In the experiment, how drivers perform in a critical traffic event when automation disengaged were investigated with an addition of a verbal NDRT and with different levels of traffic density (no traffic, medium, and high). Older drivers reacted as fast as younger drivers in critical events. Furthermore, older drivers braked more often and much harder and maintained a higher TTC ([Körber et al., 2016](#)). ([Körber et al. \(2016\)](#)) also observed deteriorated takeover time and quality due to increased traffic density and engagement in a NDRT on the same level for both age groups. Likewise, 30 participants in ages from 61 to 79 years old (mean 68.4, SD = 5.2) were recruited to study whether explanation on the traffic scenes where the driving automation system may fail to detect a hazard has an impact on drivers' takeover behavior ([Liu et al., 2018](#)). It is suggested that drivers that were explained the possible system failures in certain scenes can deal well and it might be necessary for car makers or dealers to explain to drivers on possible scenes where the driving automation system may fail to detect a hazard ([Liu et al., 2018](#)). Subjects of the majority of takeover studies included in meta-regression analysis belongs to the young (age  $\leq 30$ ) to middled age ( $31 \leq \text{age} \leq 64$ ). The XGBoost regression revealed that driver age

actually is one of the significant features that determine TOQ. If needed, an appropriate assumption can be made on how an older driver performs in a traffic event that causes automation disengagement compared to younger drivers while holding the other factors the same (such as event type, TOR modality, NDRT engagement, traffic density, and operating speed before disengagement)

Individual reaction time has also been suggested as another factor influencing takeover time (Körber and Bengler, 2014). This seems intuitive and Section 2.5.2 highlights that the average reaction time of safety drivers during 1,330 automation disengagement is 0.85 second with a standard deviation of 0.70. Beyond this, ordinary drivers' reaction times in an experimental study range from 0.81 s to 2.44 s with a mean of 1.33 s and a standard deviation of 0.27 s (Broen and Chiang, 1996). Here in the DAS model, it is appropriate to adopt a positive correlation between individual reaction time and takeover time. Accordingly, no additional parameters will be added to capture this positive correlation in the DAS interaction model. Implementing a DAS interaction model in VISSIM which can reflect the positive correlation between reaction time and takeover time is not in the scope of this research.

#### **4.1.3 Automation system limitations and automation disengagement**

When an automation system reaches its limitation, it will disengage and the vehicle control will be transitioned to a driver from the automation system. If the human model of control contradicts or deviates from the external environment to be controlled, it will result in a mismatch during the control transition. Automation system reduces feedback from the controlled external environment when driver is out-of-the-loop. Meta-regression analysis in Chapter 3 reveals that compared to

driver age, gender, operating speed, lead time, and NRDT engagement, the TOR modality is least important in predicting drivers' TOQ. It is therefore reasonable that the impact of TOR modality on drivers' takeover behavior in PPLT-induced disengagement event is not directly considered in microscopic simulation. When developing a representation matrix of the automation system for VISSIM simulation, accordingly, only lead time is considered as an input that affects driver takeover behavior.

### **4.3 DAS model process**

[Section 4.1](#) presents the key aspects that must be addressed in the DAS model. In this research, the modeling of driver takeover behavior is event-based. Only when automation disengages when encountering a PPLT scenario, driver behavior will be described in the DAS model and then implemented in VISSIM simulation. This section aims to describe how the driver behavior component and the automation component are modeled during a disengagement-triggering event. [Figure 4-2](#) shows the detailed steps on DAS modeling and how DAS model can be incorporated into VISSIM simulation.

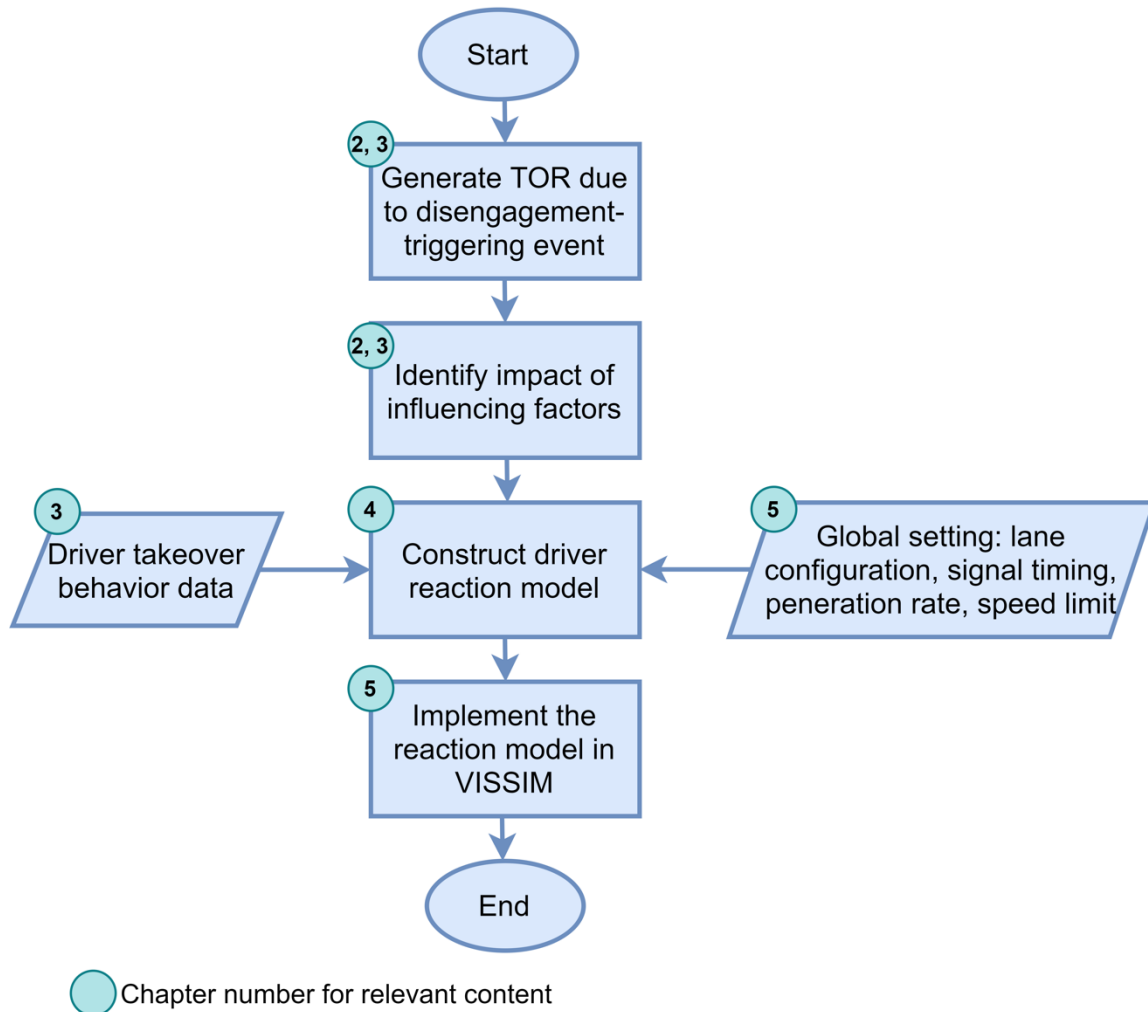


Figure 4-2 Process of event-based driver behavior modeling during disengagement-trigger events

The first step in the modeling process is TOR generation, which differs in different cases. In the DAS model, TOR is represented primarily by lead time. As highlighted in [Section 3.2.1](#), the lead time before an automation system issues a TOR could be very short, short, moderate, and long. When implementing the DAS model in VISSIM, the effect that lead time of TORs has on takeover behavior can be realized through adding vehicle attribute decisions on links.

Besides lead time, other influencing factors of takeover behavior also must be addressed when parameterizing driver behaviors during control transitions. [Table 4-1](#) highlights those influencing factors that are identified and analyzed in [Chapter 2](#) and [Chapter 3](#). It needs to be pointed out that the conclusions and findings of [Chapter 3](#) is not a direct input for VISSIM simulation. Nevertheless, their effect, or in other words, the resulting takeover behavior is one of the primary components in the DAS model. Through the simulation of takeover behavior in VISSIM and the analysis of the simulation results, the DAS model further empowers the author to interpret the impact of those influencing factors on overall traffic operations.

Table 4-1 Primary influencing factors of takeover behaviors

Lead time	NDRT	Age
Critical ( $1.5 \text{ s} \leq \text{LT} \leq 2.8 \text{ s}$ )	None	Young (age $\leq 30$ years old)
Low ( $3 \text{ s} \leq \text{LT} \leq 6 \text{ s}$ )	Reading	Middle aged ( $31 \leq \text{age} \leq 64$ years old)
Moderate ( $6 < \text{LT} \leq 8 \text{ s}$ )	Searching	Old ( $> 64$ years old)
High ( $\text{LT} > 8 \text{ s}$ )	Playing	--

The driver takeover behavior data in the event-based driver behavior modeling indicates when and how a driver takes back control. The behavior data in a PPLT-induced disengagement event is parameterized as takeover time, deceleration rate, and vehicle steering wheel speed. The behavior data is determined by the XGBoost modeled trained in [Chapter 3](#). Once takeover behavior data is determined, it is then implemented through driver behavior parameters in VISSIM. The detailed relationship from takeover data to driver behavior in VISSIM is presented in [Section 5.4](#).

In addition, driver reaction model in PPLT-induced disengagement is not independent of global settings of the traffic conditions. The geometric layout including number of lanes, lane

widths, turning bay length, speed limits, and traffic signal optimization are presented in [Section 5.2.1](#). The traffic inputs and parameter setting, and signal optimizations for three intersections in the simulated network is presented in [Section. 5.2.2](#) and [5.2.3](#).

In general, TOR generation and impact from influencing factors on takeover behavior can capture driver' reaction to PPLT-induced disengagement event, and drivers' during behavior during the control transition also relates current traffic conditions. To sum up, this section discusses the process of modeling takeover behavior so that an applicable model can be implemented in VISSIM to demonstrate these relations.

#### **4.4 DAS model input I: automation attribute**

The purpose of describing reasonable attributes that an automation system havee when disengagement occurs is to enable more specific analysis of control transitions in VISSIM simulation. The attributes summarize information useful for the modeling of control transitions from automation system to human drivers and forms a basis for inputs that reflect system characteristics during a disengagement event, which is dependent on particular response strategy based on TOQ value.

In case of PPLT-induced disengagement event, the automation system is treated as a component that knows ahead about the characteristics of approaching intersection. Lead times of four levels presented in Table 4-1 are all attributes of the automation part in the DAS. The maximal lead time in collected data is 12 s. Different lead times are considered such that automation system might disengagement at different locations when approaching a signalized intersection.

## 4.5 DAS model component II: driver behavior

The reaction to TOR during a disengagement event is mostly about when to and how to take over. Most event-based problems are modeled as a binary compliance problem. However, as indicated by meta-regression results in [Section 3.3](#), drivers' takeover strategy is more complicated than a single compliance rate. In this research, drivers' reactions to TORs or to disengagement-triggering events are mainly modeled using a probabilistic approach. When the lead time and operating speed are fixed and the driving scenario is set (such as lane configuration, intersection signal timing, and so on), drivers' takeover behavior will be treated as a discrete choice model to reflect driver decisions as a function of disengagement-scenario parameters and traffic characteristics.

Drivers' takeover time to PPLT-induced disengagement event is calculated from the point of system disengagement to the point driver takes back control. Each takeover strategy is determined by TOQ based on driver, automation, and scenario parameters.

Most simulation studies of driver behaviors such as car-following and lane-changing modeling assume all the vehicles would act as the same according to the rules defined in the model. DAS modeling enables the addition of subtle differences of individual drivers when some events occur. The interactions of a driver and an automation system are realized by input variables of the XGBoost model representing a disengagement event and response variables describing how drivers might respond to.

## 4.6 Summary

The automation component in the DAS model describes when a disengagement event will occur. The driver component of the AS model generates TTC, takeover time, deceleration rate, and steering wheel angular speed to a PPLT disengagement event. Since the determination of TOQ involves TTC, it indirectly allows the DAS model to reflect the relationship between the driver's vehicle and the lead vehicle regarding velocity and relative position.

As outlined in [Figure 3-7](#) to [Figure 3-10](#), there are uncertainties in automation system when disengagement occurs resulting in a variety of lead times. How drivers take back control to complete following driving tasks is also stochastic. [Chapter 3](#) summarized previous disengagement studies from an analytical approach. The insights learned from [Chapter 3](#) forms the basis for the modeling of DAS interactions. An important finding from [Section 3.2.1](#) is that, despite different lead times from critical to high, there is no significant variations in drivers' takeover time. The development of an effective driver-automation decision-making model is necessary to demonstrate not only how each sub-function is carried out by each agent in the process of turning left when encountering a PPLT signal at intersections.

Taken together, the variations in automation component and drivers' takeover response must be accommodated by the DAS model. As shown in [Figure 4-3](#), the uncertainties in automation component and stochastic takeover when disengagement occurs lead to the incongruence to the external environment. The vertical axis in [Figure 4-3](#) represents the degree of congruence ranging from ideal to low. The horizontal axis presents the dynamic process of control transitions. [Figure 4-3](#) is not intended to establish exact measure of variations in each DAS

components, but to illustrate more clearly that variations exist in DAS components regardless of the level of congruence between vehicle control and external environment. Gaps A and B in [Figure 4-3](#) are examples of how model congruence could appear when driver states vary during a disengagement event. From the previous problem descriptions and discussions above, it follows that the inputs of automation component and driver components in DAS model must be sufficiently complex to detect and act on possible variations.

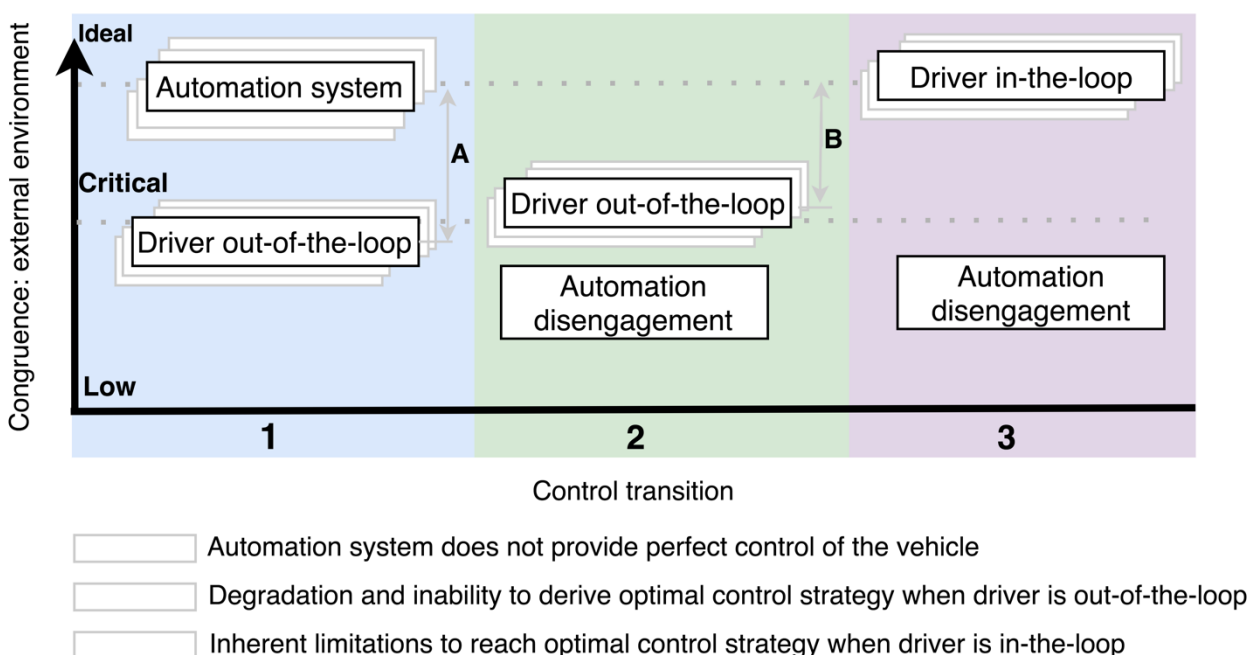


Figure 4-3 Variations and gaps in model congruence during a control transition

Variations in automation component and drivers' takeover response must be accommodated by the DAS model. Uncertainties in automation component and stochastic takeover when disengagement occurs lead to the incongruence to the external environment. Inputs of automation component and driver components to the DAS model described in [Chapter 4](#) are

sufficiently complex to detect and act on possible variations during control transitions. The output from the XGBoost model is transformed to probability densities which are then implemented in VISSIM simulation as drivers' responses to disengagement events when approaching a signalized intersection. The key contributions of [Chapter 4](#) are as follows:

- (1) Presented a unique and feasible approach to incorporate uncertainties in automation component and stochasticity of takeover behavior during control transitions;
- (2) Elaborated on how different influential factors including driver age, gender, operating speed, lead time, NRDT engagement, and TOR modality are treated in a DAS model. Specifically, TOR modality is least important in predicting drivers' TOQ, which is therefore reasonable that the impact of TOR modality on drivers' takeover behavior in PPLT-induced disengagement event is not directly considered in microscopic simulation;
- (3) When developing a representation matrix of the automation system for VISSIM simulation, accordingly, only lead time is considered as an input that affects driver takeover behavior; and
- (4) Described detailed steps about the implementation of DAS model into VISSIM simulation.

## **Chapter 5 VISSIM Simulation: takeover in permissive left-turn scenarios**

### **5.1 Introduction**

#### **5.1.1 Overview of microscopic traffic simulation**

Microscopic traffic simulation software has become increasingly popular to analyze traffic operations in various traffic conditions. Traffic simulation models usually use stochastic processes to model traffic conditions given a set of geometric layouts, signal controls, traffic demand, and driver behavior inputs. Most previous studies regarding the impact of driving automation systems on traffic operations relied heavily on self-developed simulation tools to implement and evaluate their algorithms. Nevertheless, the usage of unstandardized simulation platforms makes it really hard to evaluate the effect of the existence of driving automation systems in traffic streams. This research explores a way to model automated-to-manual transitions when approaching a signalized intersection where the automation system planned to make a left turn. Standardized simulation software such as VISSIM provides standard modeling parameters and enables standard outputs to reveal the impact of control transitions when approaching a signalized intersection. There has been a number of studies us VISSIM as the simulation platform for the modeling of connected and automated vehicles (Le Vine et al., 2015; Li et al., 2013; Mirheli et al., 2018; Papadoulis et al., 2019; Rahman et al., 2019; Shao et al., 2019).

### 5.1.2 Simulation Platform

The traffic simulation PTV VISSIM 10.00-05 was used to evaluate the operational impact of driving automation systems that requires human drivers to regain control of the vehicle to complete a left-turn task at signalized intersections in an urban environment. When considering the circumstance that a driving automation disengages before executing a left-turning task at an intersection, the operational performance of mixed traffic consisting of both manual vehicles and automated vehicles under different traffic demand levels was evaluated. To investigate the traffic impact when a driver is requested to resume control and complete the left-turning task, the simulation models must be calibrated. *Model calibration* refers to the adjustment of model settings and parameters such that the developed model is capable of accurately reflecting certain prevailing conditions of the roadway network. In VISSIM, adjustable model parameters may include car following behavior, drivers' lane changing aggressiveness, lane change gap acceptance, vehicle route choice, vehicle speed distributions, and vehicle acceleration distributions.

## 5.2 Base model development

This section provides the detailed design regarding the development of the VISSIM traffic simulation model. The geometric layout including number of lanes, lane widths, turning bay length, speed limits, and traffic signal optimization will be presented.

### 5.2.1 Geometric layout

In this research, a simple two-way two-lane urban street was developed to model the automation-to-manual transitions. Specifically, the roadway network featured three signalized intersections, four sections of two-way two-lane roadways with one dedicated left-turn lanes, called as *Major street I*, and six sections of two-way two-lane roadways without dedicated left-turn lanes, called as *Minor streets A, B, and C*. The intersections in this network are referred as intersections *IA, IB, and IC*. [Figure 5-1](#) provides an illustration of the roadway network used in the VISSIM simulation. It is worth mentioning [Figure 5-1](#) does not reflect the actual dimensions of those roadway design elements. The roadway sections of *Major street I* between intersections were set as 1000 ft. Left-turn, though, and right-turn movements were all allowed at all three simulated intersections *IA, IB, and IC* in VISSIM. Specifically, each of these three intersections had one dedicated left-turn lane and one shared through-and-right lane at all eastbound and westbound approaches along *Major street I*. All the northbound and southbound approaches had only one lane for all intersections.

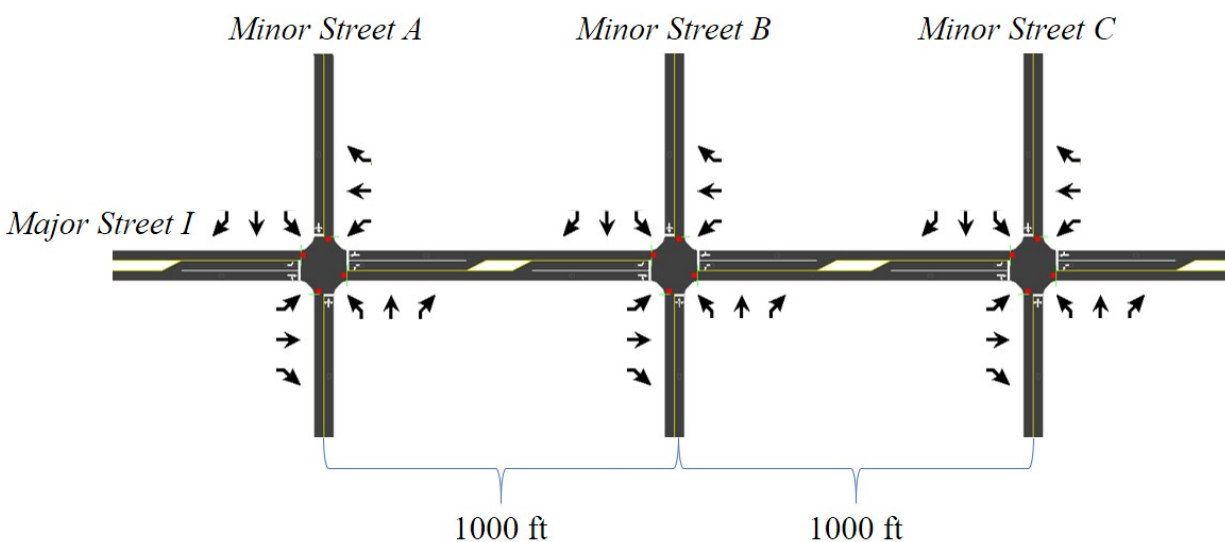


Figure 5-1 Roadway network in VISSIM simulation

### 5.2.2 Traffic inputs and other parameter settings

Traffic demand used in microscopic traffic simulations in urban streets varies depending on study issues and objectives. For instance, to study the safety impact of driving automations, an intersection of two three-lane arterial roads with bus routes were implemented according to the actual scene in Melbourne, Australia (Morando et al., 2018). The traffic volume per intersection lane groups ranges from 760 to 2,260 vph. Li et al. (2013) increased the traffic demand per approach from 150 veh/hr up to 2,850 veh/hr of a four-way six-lane intersection was increased. In (Sharon and Stone, 2017), the traffic demand was simulated from 100 veh/hr/ln to 900 veh/hr/ln. The percentages of turning movements kept consistent throughout all simulations. According to the analysis of four plausible future developments for automated vehicles in the Netherlands for 2030 and 2050, the penetration rates of driving automation systems were expected to be between 1% and 11% (mainly conditional driving automation at NHTSA Level 3) in 2030 and between 7% to 61% (mainly fully automated driving automation at NHTSA Level 4) (Milakis et al., 2017) in 2050. The adoption rates of CAV technologies in the United States were predicted to be 24% pessimistically and 87% optimistically at Level 4 by 2045 (Bansal and Kockelman, 2017). When studying the effectiveness of an intersection control protocol, (Sharon and Stone, 2017) used CAV penetration rates of 0% (baseline scenario), 1%, 5%, 10%, and 50% for a four-way intersection case. According to Table 5-1, there will be 6\*7\*1 distinctive simulation scenarios to investigate the impact of takeover transitions when approaching a signalized intersection.

Table 5-1 Experiment variables in simulation

Traffic Characteristics	Values	Levels
Traffic demand of Major street I	400, 500, 600, 700, 800, 900	6
Penetration rates of driving automations	0%, 10%, 30%, 50%, 70%, 100%	7

Table 5-2 Traffic demand inputs and optimized signal timings

Traffic demand per intersection approach (pc/hr/ln)	Demand by movement (pc/hr/ln)			*Optimal cycle length (s)	Timings of Signal phasing (s)		Capacity of an intersection lane group (pc/hg/ln)
	*LT	*Thru	*RT				
400	80	280	40	40	16	16	1520
500	100	350	50	40	16	16	1520
600	120	420	60	46	22	16	1569
700	140	490	70	50	24	18	1596
800	160	560	80	50	26	16	1596
900	180	630	90	75	44	23	1697

*\*Note: 1. LT: left turn, 2. Thru: through, 3. RT: right turn, 4. The optimized cycle lengths and signal timings for various traffic demand was obtained with the speed limits of 35 mph*

### 5.2.3 Signal optimization and capacity of intersection lane group

Based on the geometric design and varying traffic demands in [Sections 5.2.1](#) and [5.2.2](#), the traffic signals at each intersection of the simulated urban network need to be optimized. In this research, the signal timings of these three signalized intersections were optimized using Synchro 10. This section presents the procedures and parameter settings for the coding and development of Synchro models and traffic simulations of those three intersections and ten road sections. [Table 5-3](#) represents the parameter settings when using Synchro to optimize the cycle lengths and signal timings of intersections IA, IB, and IC. The results of the Synchro signal optimization at nine different levels of traffic demand are then implemented in in VISSIM. The optimal cycle length and timings of signal phasing for each demand scenario are presented in [Table 5-2](#).

Table 5-3 Parameter settings in signal optimization

Item	Parameter	Value
------	-----------	-------

Lanes	Lane width (ft)	12
	Flow Rate (vphpl)	1900
	Stored Passenger Car Length (ft)	25
	Allow Right Turns On Red	√
	Travel Speed (mph)	35
	Critical gap for permitted left turn (s)	4.5
	Follow-up time for permitted left turn (s)	2.5
	Stop threshold speed (mph)	5.0
	Critical merge gap (s)	3.7
Volumes	Peak Hour Factor	0.92
	Growth Factor	1.00
	Heavy Vehicles (%)	0
	Conflicting Pedestrians (#/hr)	0
	Pedestrian Walking Speed (ft/s)	4.0
Timings	Analysis Period (min)	15
	Cycle Length (s)	40.0
	Maximum Cycle Length (s)	150.0
	Allow Lead/Lag Optimization	√
	Yellow Time (s)	3.5
	All Red Time (s)	0.5
	Lost Time Adjust (s)	0.0
	Reference Phase	2+6
	Offset Style	Begin of Green
	Minimum Split Thru (s)	20.0
	Minimum Split Left (s)	8.0
Phases	Control Type	Pretimed
	Minimum Initial (s)	4.0
	Vehicle Extension (s)	3.0
	Minimum Gap (s)	3.0
	Predestine Phase (Through Phase)	√
	Fixed Forceoffs	√
Simulation	Yield Point	Single
	Taper Length	25
	Crosswalk Width	16
	Simulation Left Turn Speed (mph)	15
	Simulation Right Turn Speed (mph)	9

According to HCM 2010 (HCM, 2010), *intersection capacity* is determined by the critical lane group that requires the most amount of green time. Equation 5-1 is used to calculate the capacity of an intersection lane group:

$$c_i = s_i \left( \frac{g_i}{C} \right) \quad (5-1)$$

Where

$c_i$  is the capacity of lane group  $i$ , veh/h

$s_i$  is the saturation flow rate for lane group  $i$ , veh/hg

$g_i$  is the effective green time for lane group  $i$ , s

$C$  is the signal cycle length, s

Saturation flow rates vary widely with a variety of prevailing conditions, including lane widths, heavy-vehicle presence, approach grades, parking conditions near the intersection, bus presence, pedestrian demands, and others. The current ideal saturation flow rate included in [HCM 2010](#) is 1900 pc/hg/ln ([HCM, 2010](#)). When saturation headway is 2 s, then the saturation flow rate of a lane group is 1800 veh/hg/ln. By using [Equation 5-1](#), cycle length, and signal timing in [Table 5-2](#), flow rate, yellow time, all-red time in [Table 5-3](#), and set start-up lost time and clearance lost time to be 2 s, the theoretical capacity of an intersection approach for different scenarios in [Table 5-2](#) can be then be obtained, which are presented in the last column of [Table 5-2](#).

### 5.3 VISSIM traffic implementation

The VSSIM traffic model files for both baseline scenario and experiment scenarios were created by setting speed distributions, vehicle composition, and vehicle routes. This section details the experiment set-up of traffic stream in VISSIM.

### 5.3.1 Speed distributions

Desired speed distributions were set based on a posted speed limit of 35 mph in the simulation design for road sections. In addition, desired speeds for right turns and left turns were set as 7.5 mph to 15.5 mph and 12.4 to 18.6 mph, respectively.

### 5.3.2 Vehicle composition

In this research, only two vehicle classes were considered: cars and *cars with automation systems* (denoted as AV in VISSIM file) to better concentrate on the core problem and reduce additional work required if other vehicle types were included. Uniform vehicle composition and basic behavior was set network wide in all simulation scenarios.

### 5.3.3 Vehicle routes

The traffic network ([Figure 5.1](#)) is balanced in terms of both geometric design and traffic volumes. For all scenarios, there are  $8 \times 7$  possible routes, and routes are defined so that the traffic volumes for all possible origin-destination pairs are homogeneous. Two fixed routes are designated to model the movement of *cars with automation systems* which will disengage when approaching intersection IB.

## 5.4 DAS model implementation

The purpose of DAS model implementation in PPLT scenarios in VISSIM is to reveal how human-automation interactions affect the overall traffic operations at an urban signalized intersection. In VISSIM, there are four ways to implement driver behaviors in the simulation of automation disengagement events, which are:

1. Modification of driver behavior parameters;
2. VISSIM COM;
3. Using External Driver Model DLL; and
4. A mixture of the above

In [section 4.2](#), the event-based driver takeover behavior is described by a set of parameters. Modification of driver behavior parameters is suitable to model most of the TOR generation during a disengagement-triggering event. VISSIM COM needs complicated computations to obtain certain attributes of the traffic flow, which is not a necessity for event-based behavior modeling. Continuous events such as platooning or CV research are generally more complicated than one-time event-based event modeling, which can be realized by VISSIM COM, External Driver Model, or a mixture of these two. In this research, drivers' reaction to TOR is implemented by modifying driver behavior parameters in VISSIM.

### 5.4.1 Control transitions

The Driving Behavior module of VISSIM allows the author to implement takeover behavior defined by the proposed DAS model for some or all vehicles in simulation. During a simulation run, VISSIM processes the DAS parameters for each DAS-equipped vehicle at each simulation time step to determine its behavior. Specifically, VISSIM passes the current state of the vehicle and surrounding vehicles to the DAS. Then the DAS computes the longitudinal and lateral behavior and passes these values back to VISSIM. [Figure 5-2](#) shows how the DAS model is incorporated in VISSIM simulation.

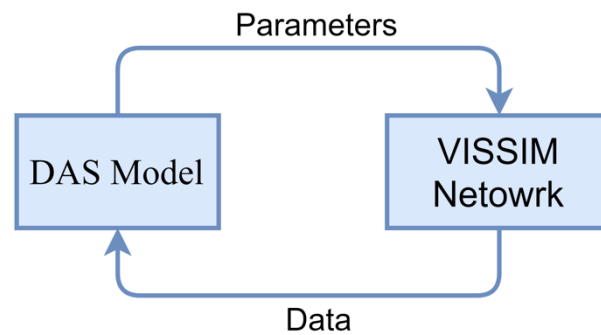


Figure 5-2 Mechanism of DAS model in VISSIM

The DAS model is achieved for vehicles equipped with automation systems in VISSIM simulation by checking the vehicle composition box as “AV” in the Vehicle Input tab. The independent variables presented in [Table 4-3](#) are used to simulate disengagements. Drivers’ takeover behavior when approaching an intersection are estimated by XGBoost model. The section below describes how estimated takeover behavior can be incorporated in VISSIM simulation.

### 5.4.2 Driving behavior

Vehicle class-specific driving behaviors are allowed for each link and connector in VISSIM simulation, which allows a vehicle from vehicle class *cars with automation systems* behave differently than a conventional car that are simulated by vehicle class *car* in all simulation runs. There are predefined driving behaviors such as *Urban (motorized)*, *Right-side rule (motorized)*, *Freeway (free lane selection)* that can be adjusted to represent a specific driving behavior. Default values of parameters in driving behavior model proposed by PTV VISSIM are based on empirical studies. Conventional cars in VISSIM representing normal traffic flow are defined by default driving behavior which is called as *Urban (motorized)*.

In the list of Link behavior types, driving behavior to be used can be specified for each link. The behavior of a *car with automation systems* will be determined by three models: (1) *car with automation systems* will behave as good as human drivers before it approaches a permissive left-turn intersection and its behavior is modeled as “AV”; (2) when it enters a critical area triggered by a predefined lead time, the *car with automation systems* keeps its current driving speed and lateral position, and (3) a human-control behavior model will be activated according to the takeover time, deceleration rate, and steering wheel angular speed. [Figure 5-3](#) provides an example of how to set different driving behaviors to urban traffic in the VISSIM simulation.

Link Behavior Types / Driving Behaviors By Vehicle Class			
Select layout...			
Count: 4	No	Name	DrivBehavDef
1	1	Urban (motorized)	1: Urban (motorized)
2	2	AV_capable	6: AV
3	3	AV_challenging	7: AV_disengaged
4	4	Human_takeover	8: Human_control

Count: 4	VehClass	DrivBehav
1	10: Car	1: Urban (motorized)
2	70: AV	6: AV
3	80: AV_disengaged	7: AV_disengaged
4	90: Human_takeover	8: Human_control

Figure 5-3 Driving behavior set-up in VISSIM simulation

Some assumptions of autonomous vehicles in VISSIM simulation are adopted for driving behaviors of *cars with automation systems* in this research, which include:

- *Cars with automation systems* keeps smaller standstill distance;
- *Cars with automation systems* keeps smaller headway; and
- *Cars with automation systems* keeps the desired speed strictly.

Lastly but not least, lane-changing logic in VISSIM is used to decide if it is possible to change to the decided lane. A vehicle's lane selection process for lane changes is based on gap acceptance. More detailed information about lane-changing logic in VISSIM can be found in (Sukennik, 2018).

### 5.4.3 Takeover behavior

In both of a real-world disengagement scenario and a simulation scenario, the study area is spatially divided into four zones where different driving behavior models are needed. In the *AV\_capable* zone, the *car with automation systems* could use normal driving logic; In the *AV\_challenging* zone, the *car with automation systems* will disengage because of its limitation in handle permissive left-turn tasks; In the *Human\_takeover* zone, a *human\_control* behavior model will be activated to

resume the remaining driving tasks; For other regular cars in *urban (motorized)* zone, the link behavior is defined as default one. As a result, driving behaviors of one vehicle could be modeled using different driving logics in different areas of a network. [Table 5-3](#) illustrates how different logics are determined for each zone.

**Table 5-4** Specification of driving logics in different zones

Zone	Driving logic		
	AV_normal(N)	AV_disengaged (D)	Human_takeover(HT)
AV_capable: urban street	N	--	--
AV_challenging: disengagement-triggering area	--	D	--
Takeover zone: control transition	--	--	HT
Intersection area: links and connectors within intersections	N	--	--

## 5.5 Evaluation setup

### 5.5.1 Seeding period, evaluation period, observations, and simulation run times

This section presents different evaluation methods and the evaluation parameters to measure the control transitions in a PPLT scenario. Firstly, each simulation run consists of a 600 s seeding period and a 3000-to-13500 s evaluation period. A seeding period is required to initialize the model to match with the network conditions ([Figure 5-1](#)) by the time the evaluation period starts. Once the simulation configuration and input of driver behavior model are ready, the Evaluation Configuration Window in VISSIM is used to set the simulation time periods. Accordingly, traffic measurements are only collected during the evaluation period which is set in the Result Attributes tab through “From time” to “To time” attributes. An evaluation period of 50 minutes to 900 minutes are used based on the fact that left turn values range from 80 to 180 veh/hr/ln to ensure at

least 30 observations are collected for each simulation experiment. The optimal cycle lengths are 40, 46, 50, and 75 s corresponding to different traffic demands in all simulation experiments, which allows takeover behavior data to be collected for 75, 65, 60, and 40 times in a 3,600-second simulation. Lastly, each simulation experiment was run 10 times to obtain representative data.

### **5.5.2 Baseline scenarios**

Baseline scenarios are when all vehicles are human driving vehicles in the simulation and there will be no control transitions when approaching a signalized intersection. Conversely, experimental scenarios are when the *cars with automation systems* are present but their autonomous functions are disengaged when approaching a signalized intersection. Their operating and control transition characteristics can be individually compared to the baseline scenarios. There are a total of six baseline scenarios corresponding to six levels of traffic volumes. Without *cars with automation systems*, vehicles are operating as human driving using calibrated VISSIM's driver model.

### **5.5.3 Simulation data recording**

There are various kinds of data that can be collected from VISSIM simulation to evaluate traffic operations from different perspectives: intersection, route, and network. Results Attributes in Evaluation Configuration can be used to determine which attributes to be recorded during each simulation run in VISSIM, including:

- Area measurements
- Areas & ramps
- Data collections

- Delays
- Links
- Nodes
- Queue counters
- Vehicle travel times
- Vehicle network performance
- And others

Node evaluation results are exploited to evaluate the impact that takeover behaviors have on intersections. In this research, a Node boundary is constructed around the intersection under study (IB in [Figure 5.1](#)) to collect traffic measurements, which primarily include volume, stopped delay, queue length, and number of stops. Queue length estimated through Node evaluation is calculated as the arithmetic mean length of the queue at each time step.

The Node evaluation settings can also be adjusted in the embedded Queue counter so that queues at the intersection under study (IA) are measured from the downstream position of the Queue counter to the furthest upstream vehicle in the queue. Two Queue counters were placed 180 ft upstream at the dedicated left turn lane of the westbound and eastbound approaches, respectively. Another two Queue counter were placed 500 ft at the shared through-and-right lane of the westbound and eastbound approaches, respectively. The second set of Queue counters were added in case uneven lane utilization or queue spillover from the turn lane occur. The following queue metrics are collected:

- Maximum queue length: the longest distance from the first vehicle in the queue to the last vehicle entering the queue during a simulation run;
- Average queue length: a queue length is recorded for each timestamp, and an average queue length is the average length of the queue during a simulation run.

Travel Time can also be collected by specifying a starting and an end point, which is calculated as the average time it takes for vehicles to traverse the specified segment during a selected time period of a simulation run. Considering the output from VISSIM simulation is stochastic, the travel times, speed, and queue lengths recorded in each simulation will be different. The averages of travel times, speed, and queue lengths from all 10 runs for each simulation experiment were taken to be the estimated measures.

## **5.6 Model calibration**

As previously mentioned, this research aims to reveal how control transitions affect intersection efficiency and how the timing of TORs affect the traffic efficiency at an intersection as the traffic volume increases through VISSIM simulation. For any microscopic traffic models to be useful, it must be correctly calibrated so that it can replicate actual traffic conditions. This section documents the procedures and assumptions used to develop and calibrate the VISSIM simulation for the takeover behavior study. The VISSIM model for each scenario were calibrated to real world conditions, as documented using a variety of field data and reference study sources.

### 5.6.1 Calibration method

According to the description of model development ([Section 5.2 and 5.3](#)), there are 36 simulation models which include six baseline scenarios that don't include a DAS model and no disengagement will occur. All baseline scenarios in the simulation experiment are assumed to be accurate as the field data on intersection traffic operations. Numerous sources of traffic data on urban network or urban intersections are available. Furthermore, calibration measures that can be used for model calibration in this study are presented in [Table 5-4](#). Through calibrating the measures collected both at the intersection level and at the link or route level, the final model with adjusted parameters is used to replicate the temporal and spatial characteristics of an urban street with signalized intersections.

**Table 5-5** Calibration measures, data sources, and calibration threshold

<b>Calibration measures</b>	<b>Areas for calibration</b>	<b>VISSIM output</b>	<b>Calibration threshold</b>
<b>Volume</b> Different targeted inputs must be met for at least 90% of approaches	Intersection approach  Link	Data collection points  Link evaluation	Within $\pm 5\%$ for volume $< 400$ veh/h Within $\pm 8\%$ for $400 \text{ veh/h} < \text{volume} < 600 \text{ veh/h}$ Within $\pm 10\%$ for $600 \text{ veh/h} < \text{volume} < 800 \text{ veh/h}$ Within $\pm 15\%$ for $800 \text{ veh/h} < \text{volume} < 900 \text{ veh/h}$
<b>Travel Times</b> Different targeted travel times must be met for a minimum of 85% routes	Link	Data collection points Node evaluation	Within $\pm 40$ s for routes with theoretical travel time that are less than 360s
<b>Speed</b> Targeted speed around 35 mph must be met for at least 85% of the links or routes	Intersection approach  Link	Data collection points Travel time segments	Speed heat maps were used to qualitatively review the patterns and duration of congestions Average speed of vehicle routes must be within $\pm 11\%$ of design speed
<b>Queue lengths</b> Target queue lengths must be met for at least 85% of the critical locations	Intersection approach Link	Node evaluation Queue counter	Queue spillback from turn lanes Modeled queues qualitatively reflect the impact of input turning movements in the target intersection area

### 5.6.2 Calibration results

According to the calibration methods presented in [Section 5.6.1](#) and the calibration threshold in [Table 5-5](#), the calibration results for all baseline scenarios are summarized in [Table 5-6](#). Overall, the proposed calibration criteria are met. After calibration, on average, 86% of the traffic volumes for starting points of 10 links and 12 intersection approaches were accomplished in all baseline scenarios. In addition, the targeted values of travel times, speed, and queue lengths had better calibration results in all baseline scenarios compared to traffic volumes.

Based on the results obtained in calibration process, the final version of VISSIM models is reasonably calibrated to replicate realistic traffic operations as well as to meet the design standards used in this research. These calibrated baseline models are then used with a deduction of left-turn movements of human driving vehicles and an addition of *cars with automation systems* to simulate control transitions.

**Table 5-6** Summary of calibration results

<b>Calibration measures</b>	<b>Areas used for calibration</b>	<b>Total calibration data points</b>	<b>Percentage</b>	<b>Target met</b>
<b>Volume</b>	Intersection approach (n = 12) Link (n = 10)	22	86%	Yes
<b>Travel Times</b>	Link (n = 10*2)	20	88%	Yes
<b>Speed</b>	Intersection approach (n = 12) Link (n= 10*2)	32	100%	Yes
<b>Queue lengths</b>	Intersection approach (n = 12) Link (n= 10*2)	32	96%	Yes

## Chapter 6 Simulation results and discussions

After all simulation runs, the collected simulation data can be analyzed to investigate the impact of control transitions at a signalized intersection. The traffic network shown in [Figure 5-1](#) contains three signalized intersections, 68 links, and one node. Delays and queues at the westbound and eastbound approaches of intersection IB are analyzed in this research.

### 6.1 Delays and queues

In this research, average vehicle delays are the delay of a vehicle computed by the differences between the theoretical travel time and actual travel time. The theoretical travel time is the travel time that can be achieved if there were no other vehicles or no signal controls or no other causes for stops.

There are two independent variables in this research, which are traffic volume and AV penetration rate. As is shown in [Table 6-1](#), there are six levels in both traffic volume and AV penetration rate. The dependent variable is vehicle delay and queue length. [Figures 6-1](#) and [6-2](#) show the vehicle delays and queue lengths in scenarios with different levels of traffic volume and AV penetration rates. A two-factor analysis of variance (ANOVA) is used to further analyze simulation results of control transitions in different scenarios.

It is hypothesized that there may be difference in delays and queues with the presence of *cars with automation systems* that request drivers to take back control. The simulation results are shown in [Table 6-1](#) and are organized by volume and AV penetration rates. The ANOVA computations are presented in an ANOVA table where the variation is partitioned into that due to the main effect of penetration rates, the main effect of traffic volume, and the interaction effect.

Table 6-1 Delays and queue lengths by traffic volume and AV penetration rate

Volume	Penetration rate	Vehicle Delay (s/veh)	Queue length (ft)
400	0%	7.73	91.56
	10%	9.42	92.35
	30%	10.29	103.28
	50%	11.34	101.47
	70%	12.1	91.52
	100%	9.45	93.76
500	0%	6.96	92.43
	10%	8.42	106.17
	30%	11.91	94.28
	50%	9.83	107.61
	70%	10.78	101.21
	100%	12.15	104.35
600	0%	10.71	102.29
	10%	13.32	106.74
	30%	12.85	111.21
	50%	11.61	119.86
	70%	13.39	116.46
	100%	12.28	115.62
700	0%	12.67	122.64
	10%	13.46	134.71
	30%	14.67	128.86
	50%	15.98	141.49
	70%	15.26	136.82
	100%	16.13	146.53
800	0%	14.21	136.49
	10%	13.87	134.21
	30%	15.86	157.46
	50%	17.07	149.36
	70%	16.69	152.38
	100%	17.43	144.63
900	0%	14.93	168.43
	10%	15.46	155.78
	30%	18.13	149.58
	50%	16.41	163.46
	70%	17.79	157.21
	100%	17.39	156.46

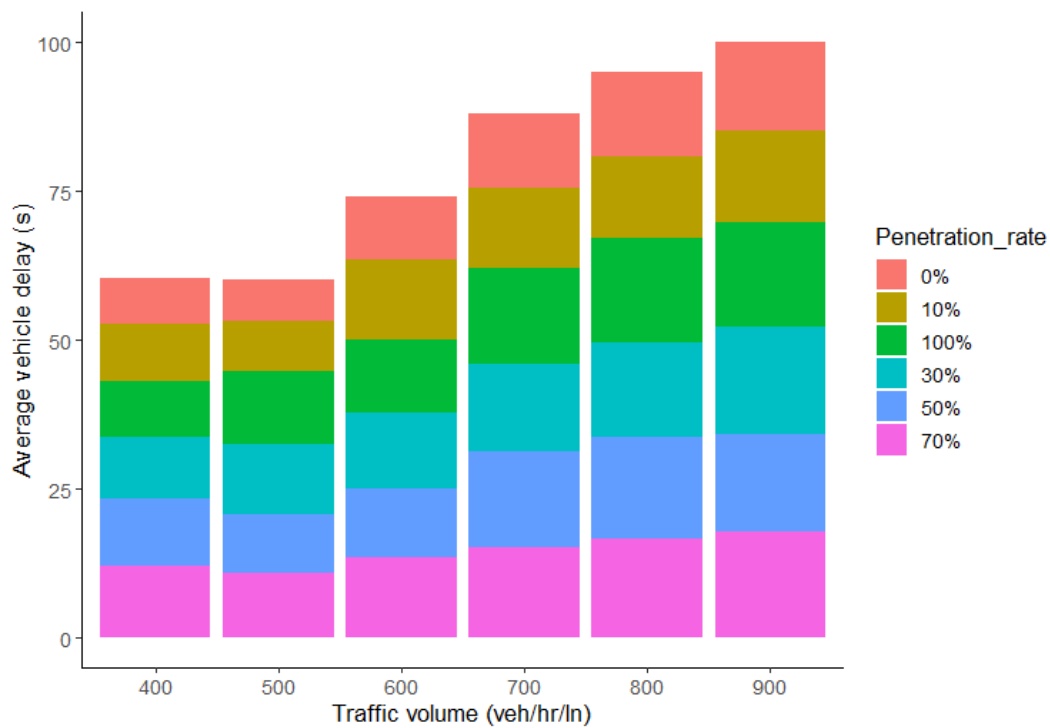


Figure 6-2 Vehicle delays in scenarios with different levels of traffic volume and penetration rate

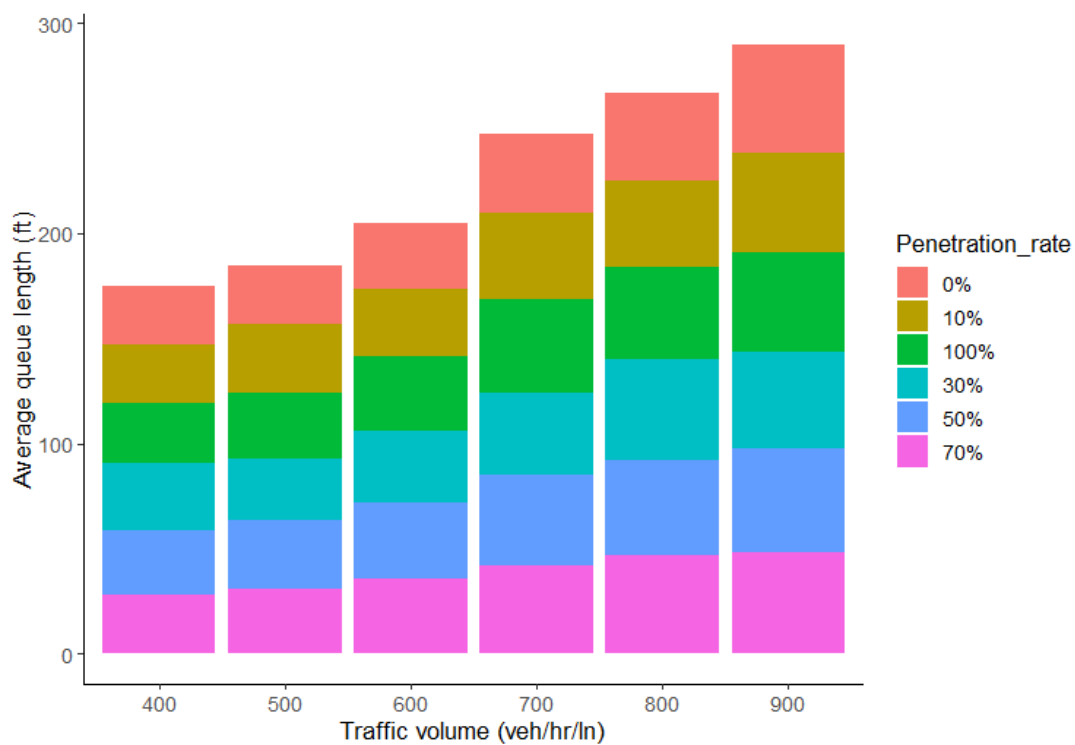


Figure 6-2 Queue lengths in scenarios with different levels of traffic volume and penetration rate

Two two-factor ANOVA models with interaction tests for delays and queue lengths are conducted and discussed individually. There are three statistical tests in the ANOVA tables for delay analysis ([Table 6-2](#)) and for queue length analysis ([Table 6-3](#)), respectively. These three tests correspond to three null hypotheses, which are as following:

- There is no difference in group means at any level of the first independent variable;
- There is no difference in group means at any level of the second independent variable; and
- The effect of one independent variable is independent of the effect of the other independent variable.

Firstly, box plot was created to visualize the data group by the combinations of independent variables, which is shown in [Figure 6-3](#). [Table 6-2](#) contains the main delay of vehicles in each level of traffic volume for different levels of AV penetration rate. Notice in [Figure 5-6](#) that the dot represents actual vehicle delays when the traffic volume changes. The ANOVA analysis for vehicle delays is to evaluate whether there is a difference among the means of vehicle delays in different scenarios. The R function *aov()* was used to do the ANOVA test and R function *summary()* was used to summarize the analysis of variance results. The test results for vehicle delays are presented in [Table 5-8](#). Each row in [Table 5-8](#) shows the main effects of traffic volume, penetration rates, and the interaction effect on vehicle delays.

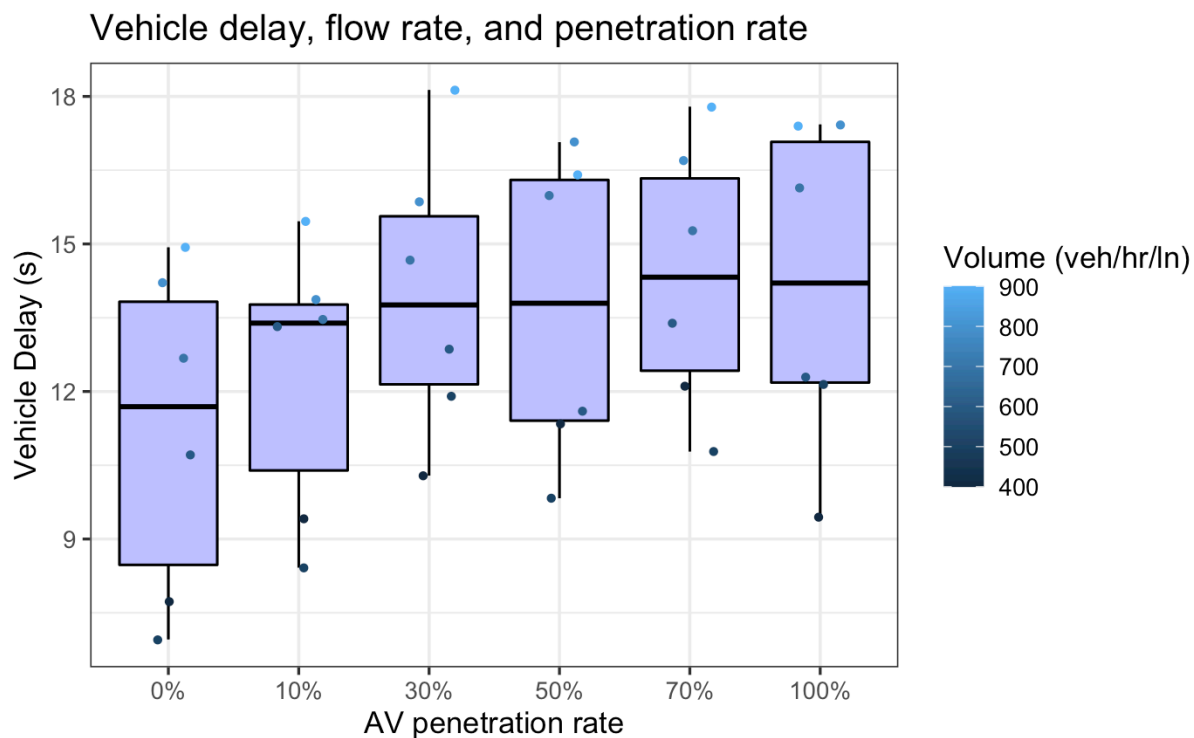


Figure 6-3 Boxplot of vehicle delays in different simulation scenarios

A significant P-value in ANOVA shows that some of the group means are statistically different. In this research, there was a statistically significant effect of traffic volume on average vehicle delays ( $F(1, 24)$ ,  $P\text{-value} < 0.05$ ). Since the main effect of traffic volume is significant ( $p < 0.05$ ), it can be generalized that traffic volume has a significant impact on vehicle delays at signalized intersections with the presence of control transitions between automation systems and human drivers. The change of AV penetration rates was also identified to have a statistically significant impact on vehicle delays. However, the interaction between traffic volume and AV penetration rate does not reach a statistical significance ( $P\text{-value} = 0.887$ ).

Table 6-2 ANOVA table for two-factor ANOVA analysis of vehicle delays

Source of variation	Degree of freedom	Sums of squares	Mean squares	F-value	P-value
Penetration rate	5	46.29	9.26	7.111	0.000331
Volume	1	241	241	185.132	8.89E-13
Volume * Penetration rate	5	2.18	0.44	0.335	0.886709
Residual	24	31.24	1.3		

\*Note: '\*\*\*' indicate statistically significant

In addition, it is unknown which groups are different. Multiple pairwise-comparisons can be performed to identify if means between certain pairs of experiments are statistically significant. R function *TukeyHSD()* was used to compute Tukey Honest Significant Differences (Tukey HSD). The results of the Tukey multiple comparison of means are presented in Table 6-3 and visualized in Figure 6-4. Tukey's testing among six levels of penetration rates requires 15 tests and any adjusted P-value less than 0.05 is honestly significant. The output contains the difference in means, confidence levels, and the adjusted P-values for all pairs. It is found that the differences between scenarios with penetration rate of 0% and of 30%, 50%, 70%, and 100% are large enough to be significant.

Table 6-3 Tukey Test results for Vehicle delays

Pairs	Differences	Lower	Upper	P-adjusted
10%-0%	1.1233	-0.9134	3.1601	0.5416
30%-0%	2.7500	0.7133	4.7867	0.0041
70%-0%	3.1333	1.0966	5.1701	0.0010
50%-0%	2.5050	0.4683	4.5417	0.0099
100%-0%	2.9367	0.8999	4.9734	0.0020
30%-10%	1.6267	-0.4101	3.6634	0.1731
50%-10%	1.3817	-0.6551	3.4184	0.3217
70%-10%	2.0100	-0.0267	4.0467	0.0545
100%-10%	1.8133	-0.2234	3.8501	0.1010
50%-30%	0.2450	-1.7917	2.2817	0.9989
70%-30%	0.3833	-1.6534	2.4201	0.9913
100%-30%	0.1867	-1.8501	2.2234	0.9997
70%-50%	0.6283	-1.4084	2.6651	0.9279
100%-50%	0.4317	-1.6051	2.4684	0.9852
100%-70%	0.1967	-1.8401	2.2334	0.9996

### 95% family-wise confidence level

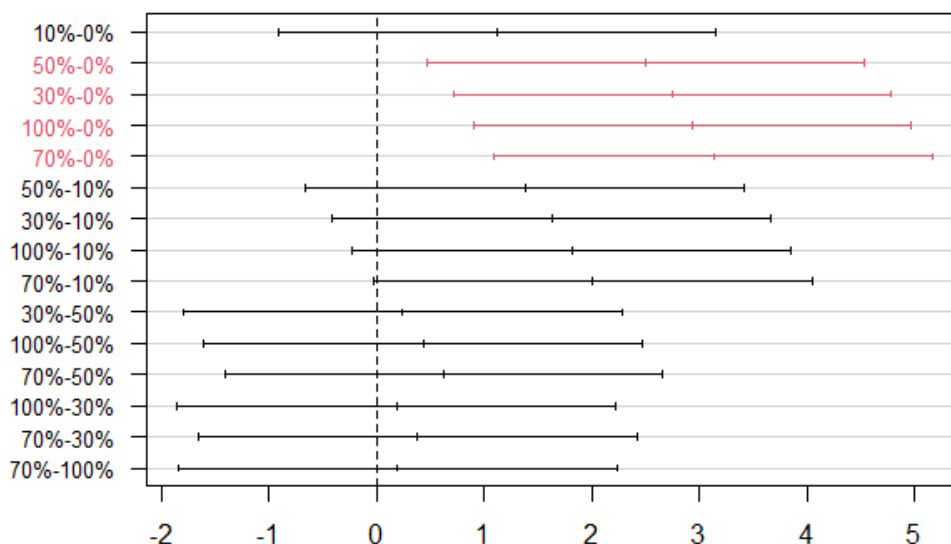


Figure 6-3 Differences in means of vehicle delays between scenarios with different penetration rate

Likewise, the ANOVA test for queue length is also started with a box plot, which is shown in Figure 5-7. The results of ANOVA test of queue lengths in different scenarios are summarized in Table 5-9. The F statistic for the main effect of volume on queue length is 317.55 and is highly statistically significant with the P-value as  $2.45e-15$ . The main effect of penetration rate on queue lengths is not statistically significant (P-value = 0.184). The interaction between traffic volume and AV penetration rate does not reach statistical significance.

Table 6-4 ANOVA table for two-factor ANOVA analysis of queue lengths

Source of variation	Degree of freedom	Sums of squares	Mean squares	F-value	P-value
Penetration rate	5	497	99	1.654	0.184
Volume	1	19058	19058	317.55	$2.45e-15$ ***
Volume * Penetration rate	5	119	24	0.397	0.846
Residual	24	1442	60		

\*Note: '\*\*\*' indicate statistically significant

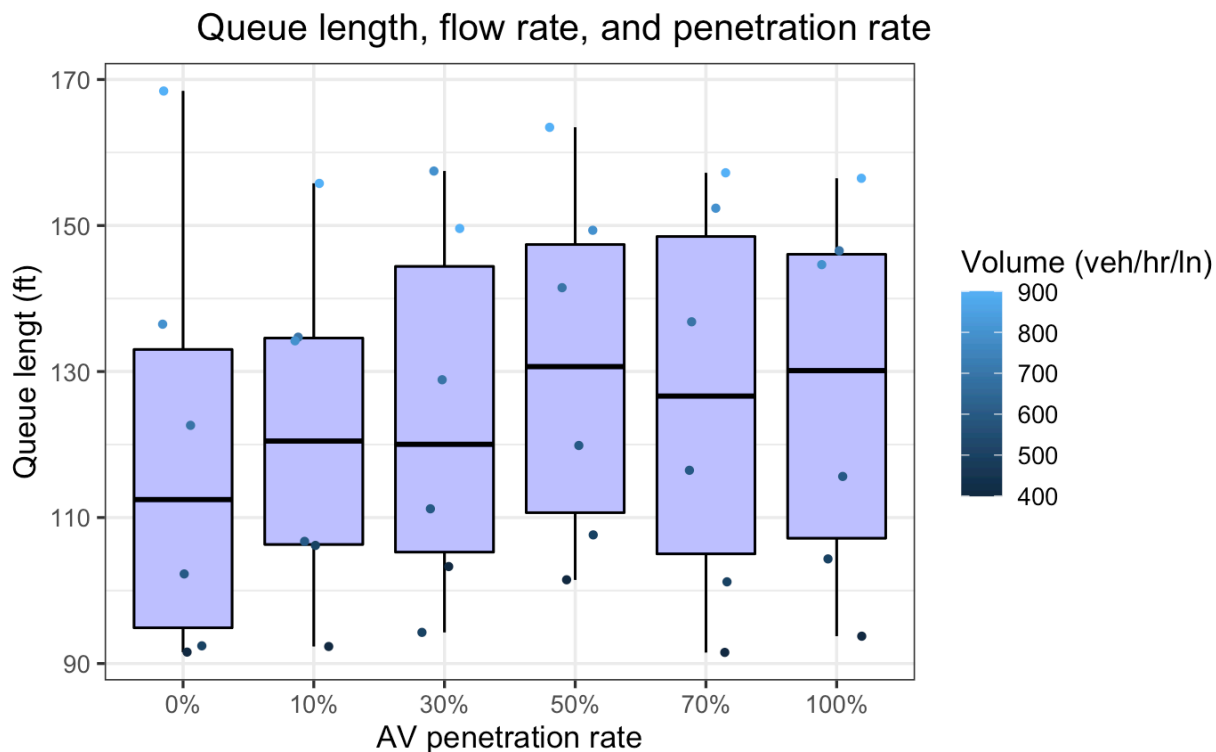


Figure 6-4 Boxplot of vehicle delays in different simulation scenarios

The Tukey HSD test was also conducted for queue lengths in different scenarios. The results are summarized in Table 6-5 and are visualized in Figure 6-6. As mentioned earlier, the HSD is a test statistic that determines if there is a significant difference between groups. It is shown that there is no statistically significant difference in queue lengths in different scenarios.

Table 6-5 Tukey Test results for Vehicle delays

Pairs	Differences	Lower	Upper	P-adjusted
10%-0%	2.6867	-11.1513	16.5247	0.9900
30%-0%	5.1383	-8.6997	18.9764	0.8562
70%-0%	11.5683	-2.2697	25.4064	0.1398
50%-0%	6.9600	-6.8780	20.7980	0.6339
100%-0%	7.9183	-5.9197	21.7564	0.5027
30%-10%	2.4517	-11.3863	16.2897	0.9934
50%-10%	8.8817	-4.9563	22.7197	0.3795
70%-10%	4.2733	-9.5647	18.1114	0.9276
100%-10%	5.2317	-8.6063	19.0697	0.8469
50%-30%	6.4300	-7.4080	20.2680	0.7053
70%-30%	1.8217	-12.0163	15.6597	0.9984
100%-30%	2.7800	-11.0580	16.6180	0.9883

70%-50%	4.6083	-9.2297	18.4464	0.9032
100%-50%	0.9583	-12.8797	14.7964	0.9999
100%-70%	3.6500	-10.1880	17.4880	0.9618

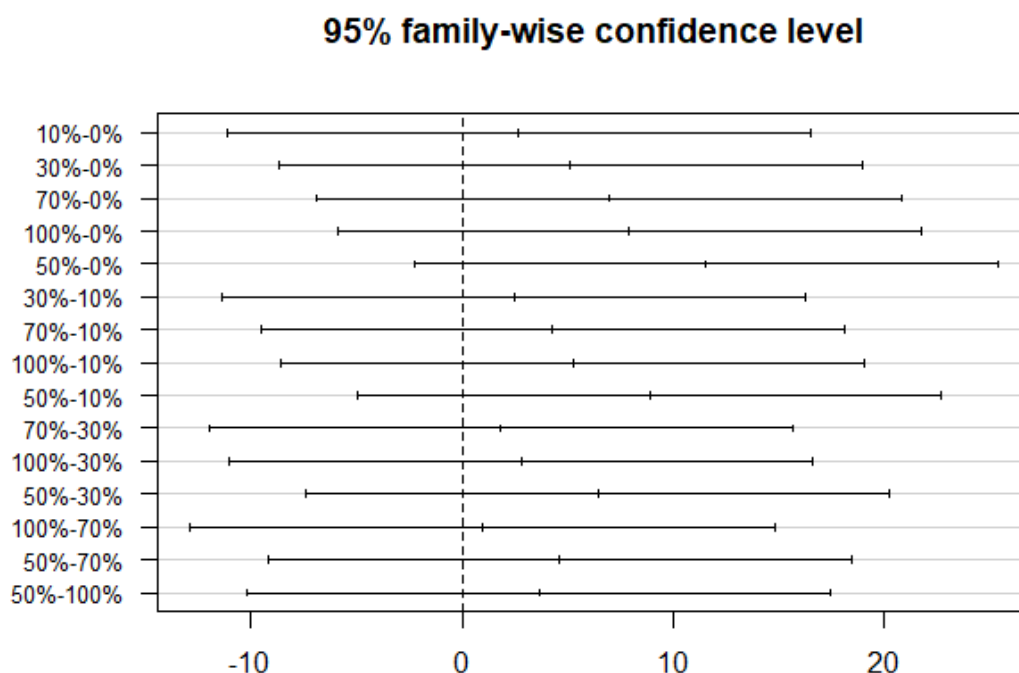


Figure 6-5 Differences in means of queue lengths between scenarios with different penetration rate

## 6.2 Safety

### 6.2.1 Speed variation

Safety cannot be directly quantified using crashes from VISSIM simulations. However, the stability of traffic flow can be used as a surrogate safety indicator. Higher variations in vehicular behaviors generally indicate an increased risk in traffic flow. In this research, variations of speed are used to measure the stability of traffic flow. Lower variations in speed indicates a relatively stable traffic flow. The variation measures of speed are collected by lane types. Table 5-11 shows the standard deviation of speeds for both *left-turn lane* (LL) and shared *through and right-turn lane* (TRL).

It is found that the maximum speed standard deviation for left-turn lanes occurs when traffic volume is 400 veh/h/ln with an AV penetration rate of 50%, which is 5.52 mph. The maximum speed standard deviation for shared through and right-turn lanes occurs when traffic volume is 800 veh/h/ln with an AV penetration rate of 50%, which is 5.88 mph. Based on the data presented in [Table 6-6](#), the average speed standard deviations for the same level of flow rate can also be calculated. It is found that when traffic demand increases from 400 veh/h/ln to 900 veh/h/ln, the average speed standard deviation of traffic flow does not change significantly, and is always in the range of 1.99 to 2.98 mph. Likewise, the average speed standard deviations of traffic flow for the same level of AV penetration rate ranges from 2.40 to 2.66 mph.

**Table 6-6** Standard deviation of speeds for different movements at intersection IB

Volume (veh/h/ln)	AV %	*Speed Std (mph)	Volume (veh/h/ln)	AV %	*Speed Std (mph)
400	0%	LL:1.67	700	0%	LL:1.83
		TRL:2.12			TRL:2.65
	10%	LL:1.11		10%	LL:1.77
		TRL:3.35			TRL:1.56
	30%	LL:2.18		30%	LL:3.35
		TRL:1.06			TRL:3.51
	50%	LL:5.52		50%	LL:3.57
		TRL:3.5			TRL:5.1
	70%	LL:3.59		70%	LL:1.08
		TRL:2.02			TRL:4.5
	100%	LL:3.75		100%	LL:1.43
		TRL:4.69			TRL:2.76
500	0%	LL:1.26	800	0%	LL:1.87
		TRL:0.59			TRL:1.35
	10%	LL:2.24		10%	LL:2.17
		TRL:0.84			TRL:3.5
	30%	LL:2.95		30%	LL:2.38
		TRL:0.61			TRL:1.1
	50%	LL:2.93		50%	LL:5.02
		TRL:2.19			TRL:5.88
	70%	LL:0.62		70%	LL:3.76
		TRL:4.15			TRL:2.08
	100%	LL:4.48		100%	LL:1.84
		TRL:2.67			TRL:2.81
600	0%	LL:0.92	900	0%	LL:0.93

		TRL:2.08			TRL:1.31
	10%	LL:1.29		10%	LL:2.82
		TRL:0.72			TRL:1.1
	30%	LL:2.53		30%	LL:1.28
		TRL:2.05			TRL:1.13
	50%	LL:3.98		50%	LL:2.73
		TRL:2.03			TRL:3.49
	70%	LL:4.88		70%	LL:4.41
		TRL:3.55			TRL:1.53
	100%	LL:4.28		100%	LL:4.74
		TRL:3.45			TRL:3.35

*\*Notes: LL: left-turn lane; TRL: through and right-turn lane*

The impacts of takeover behavior on traffic flow when flow rates changes and when AV penetration rate changes are further investigated in [Figure 6-7](#) and [Figure 6-8](#) respectively. No apparent linear relationship was observed between speed variations and traffic volumes for both LL and TRL movements. When investigating the impact of AV penetration rates on speed variations, two linear models were fitted for both LL and TRL movements, respectively. It can be observed in [Figure 6-8](#) that 23% and 26.6% of the variances of the speed are explained by the changes of AV penetration rates for LL and TRL movements.

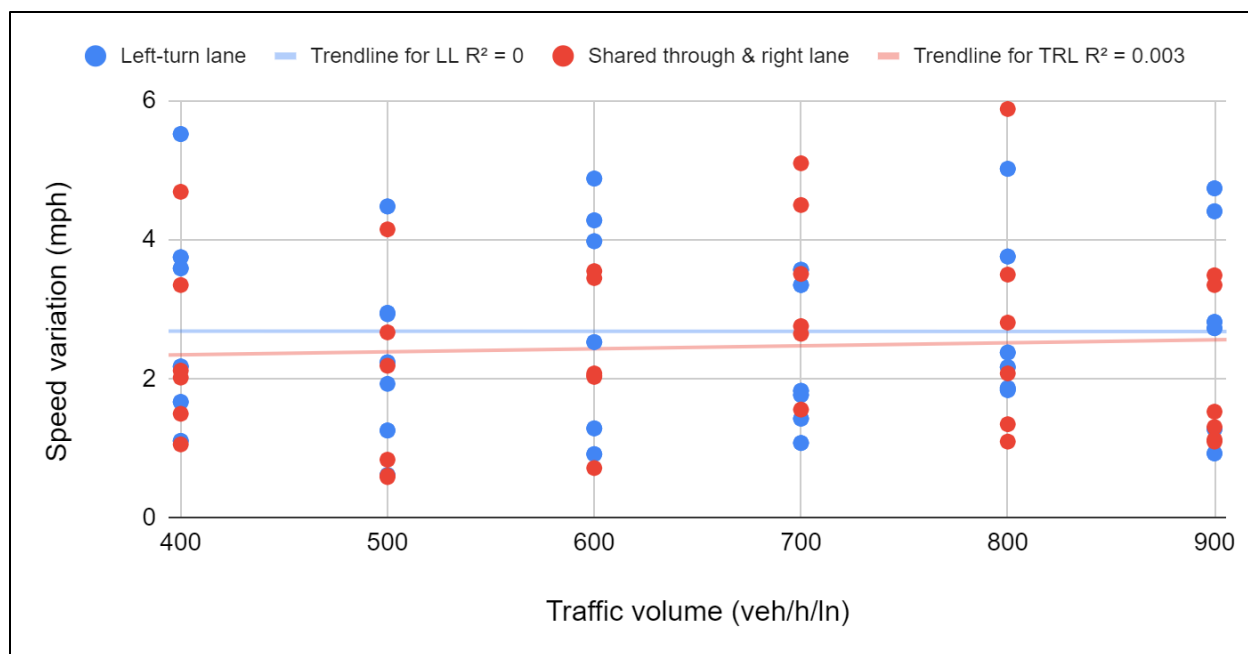


Figure 6-6 Standard deviation of speeds with different flow rates

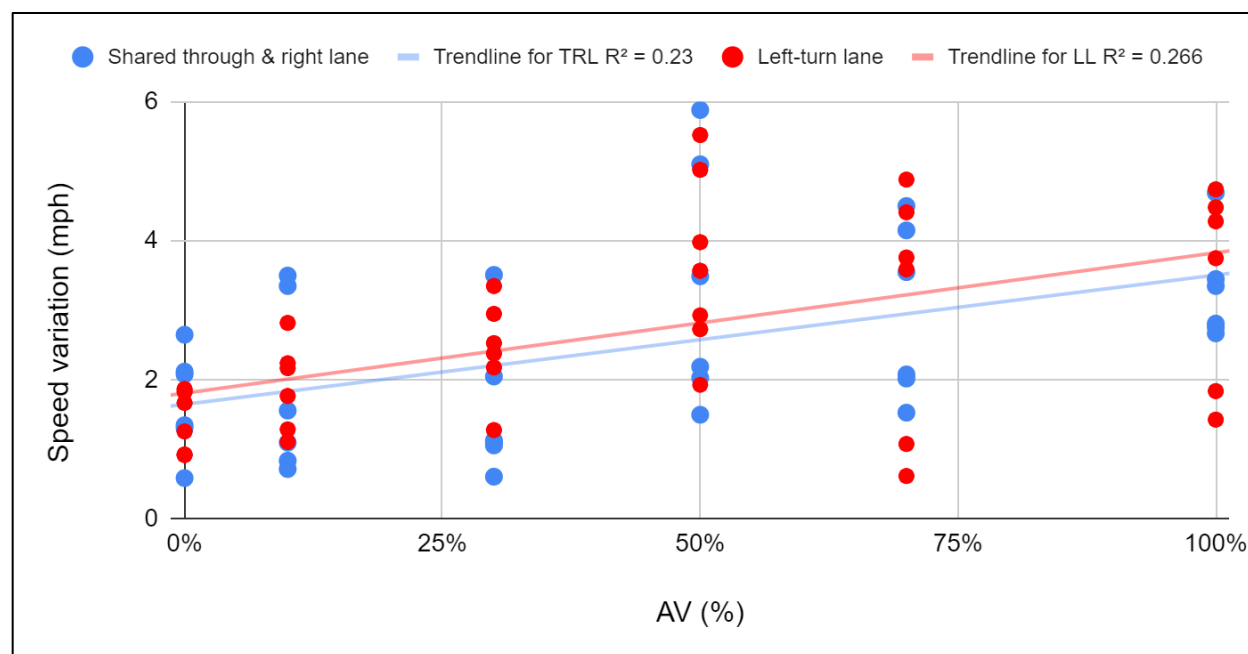


Figure 6-7 Standard deviation of speeds with different AV penetration rates

### 6.2.2 Surrogate safety measures

The software Surrogate Safety Assessment Model (SSAM) is used to conduct intersection conflicts analysis. SSAM identifies conflicts from vehicle trajectory files generated by microscopic simulation, such as VISSIM. In SSAM, six surrogate safety measures are defined for safety assessment, including (1) Time-to-collision (TTC), (2) Post Encroachment time (PET), (3) deceleration rate, (4) Maximum speed, (5) speed differential, and (6) Location of the conflict point (Gettman and Head, 2003). Three types of conflicts were considered in SSAM, including rear-end conflicts, lane-change conflicts, and crossing conflicts. A vehicle interaction is considered as a conflict when TTC or PET exceed predetermined threshold values. Given the definitions of surrogate safety measures and computational algorithms, an event file can be obtained that include a list of conflicts. The details of algorithms computing calculating surrogate safety measures can be reviewed at (Gettman and Head, 2003).

In this research,  $TTC^* = 1.5$  s and  $PET^* = 2.0$  s are used to determine whether an event is a valid conflict event. Ten replications were conducted for each experiment case and the resulting trajectory data were analyzed by SSAM. The simulated traffic conflicts are presented in Table 6-7. According to Table 6-7, the highest number of rear-end conflicts is 51, which occurred when traffic volume is 900 veh/hr/ln and the AV penetration rate is 50%; the highest number of lane-change conflicts is 68, which also occurred when traffic volume is 900 veh/hr/ln and the AV penetration rate is 50%; the highest number of crossing conflicts is 42, which occurred when traffic volume is 900 veh/hr/ln and the AV penetration rate is 100%. When traffic volume is low, rear-end conflicts, lane-change conflict, and crossing conflicts could be zero. The means of conflicts in each level of traffic volume are also computed and are presented in Table 6-8.

Table 6-7 Simulated traffic conflicts in different experimental conditions

Volume (veh/h/ln)	Penetration rate	Rear-end conflicts	Lane-change conflicts	Crossing conflicts	Total conflicts
400	0%	1	0	0	1
	10%	2	1	0	3
	30%	0	2	1	4
	50%	3	5	3	11
	70%	4	3	2	9
	100%	2	3	0	5
500	0%	3	3	1	7
	10%	5	1	0	6
	30%	7	2	7	16
	50%	6	7	6	19
	70%	5	3	3	11
	100%	4	4	5	13
600	0%	8	6	2	16
	10%	6	4	7	17
	30%	7	7	9	23
	50%	11	10	10	31
	70%	16	13	8	37
	100%	9	15	12	36
700	0%	8	11	11	30
	10%	14	9	9	32
	30%	21	12	15	48
	50%	17	18	14	49
	70%	18	13	12	43
	100%	15	12	17	44
800	0%	21	28	25	74
	10%	28	37	19	84
	30%	29	32	31	92
	50%	36	48	34	118
	70%	32	44	27	103
	100%	25	46	24	95
900	0%	33	44	23	100
	10%	31	61	28	120
	30%	45	52	24	121
	50%	51	68	37	156
	70%	37	57	24	118
	100%	46	51	42	139

**Table 6-8** Average traffic conflicts with different levels of traffic volume

<b>Volume (veh/hr/ln)</b>	<b>Rear-end conflicts</b>	<b>Lane-change conflicts</b>	<b>Crossing conflicts</b>	<b>Total conflicts</b>
400	2	2	1	6
500	5	3	4	12
600	10	9	8	27
700	16	13	13	41
800	29	39	27	94
900	41	56	30	126

**Table 6-8** indicates what is expected to happen when traffic increasing from 400 veh/hr/ln to 900 veh/hr/ln, that is rear-end conflicts, lane-change conflicts, crossing conflicts, and total conflicts increase as traffic volume increase.

Linear regression analysis was conducted to identify if simulated traffic conflicts present any correlation: (1) between traffic volumes and traffic conflicts, and (2) between penetration rates and traffic conflicts. The linear regression analysis is presented in Figure 6-8 and Figure 6-9. The  $R^2$  for rear-end conflicts vs. traffic volume is 0.928; for lane-change conflicts vs. traffic volume is 0.848; for crossing conflicts vs. traffic volume is 0.940; for total conflicts vs. traffic volume is 0.905. The high  $R^2$  in the analysis of traffic conflicts in relation to traffic volume indicates that 85% to 94% traffic conflicts were explained by the change of traffic volume. In addition, **Figure 6-7** also indicates that the increase of traffic volume has the greatest impact of the number of rear-end conflicts. According to Figure 6-8, AV penetration rates can only explain about 1% to 2% changes in traffic conflicts. It is intuitive since the incorporation of takeover behavior in VISSIM only model how driver react to the disengagement event in the very beginning of the control transition.

Based on the observations of the traffic conflicts, the following conclusions can be drawn:

- The numbers of rear-end conflicts, lane-change conflicts, crossing conflicts, and total conflicts increase as traffic volume increase; and
- The effect that AV penetration rates have on the numbers of rear-end conflicts, lane-change conflicts, crossing conflicts, and total conflicts is not statistically significant.

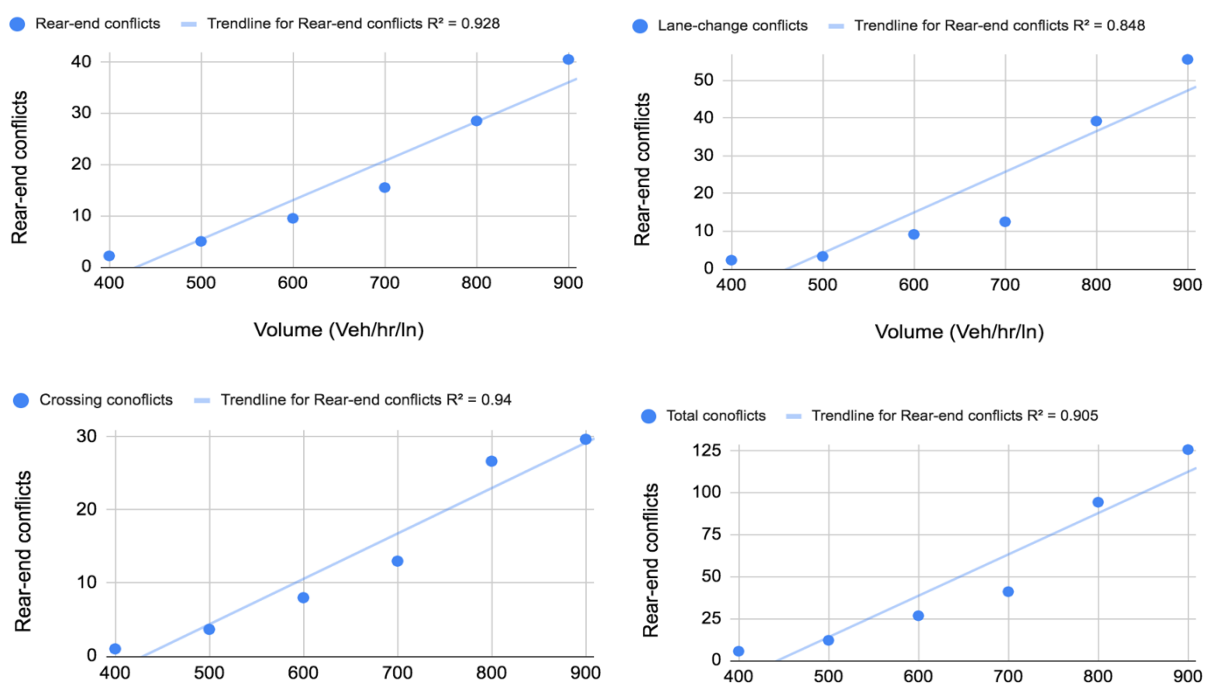


Figure 6-8 Traffic conflicts with different flow rate

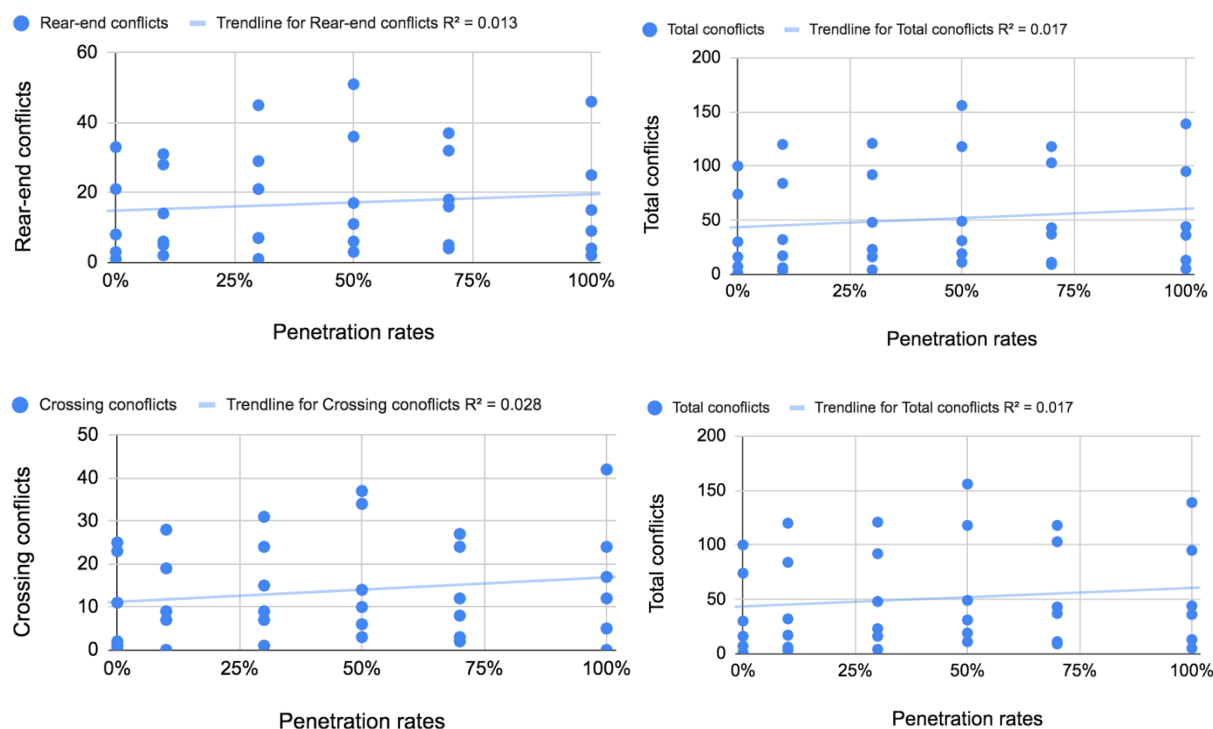


Figure 6-9 Traffic conflicts with different penetration rates

## 6.3 Conclusions

[Chapter 5](#) presented how disengagement-triggering events can be modeled in VISSIM. Traffic model files for both baseline scenario and experiment scenarios can be created by adjusting speed distributions, vehicle composition, driving behavior, and vehicle routes to model an urban network in which the signalized intersections allow permissive left turns. [Section 6.1](#) and [6.2](#) presented the simulation data and analysis of results. In [Section 6.1](#), vehicle delays and queue lengths in different scenarios with different levels of traffic volume and AV penetration rates are first analyzed by the ANOVA test. Then the hypothesis testing was further analyzed by a post hoc analysis that is Tukey's HSD test. Post-hoc analysis usually provides greater insights into the differences between

certain groups and is thus a significant step in data analysis. The list below summarized the main conclusions of [VISSIM simulation work](#):

- (1) The control transition is modeled by reserving one type of vehicle in vehicle inputs, whose behavior were defined according to driving area and will be transitioned from AV\_normal, to AV\_disengaged, and then to Human\_takeover mode if it enters a disengagement-triggering area;
- (2) Traffic volume has a significant impact on vehicle delays at signalized intersections with the presence of control transitions between automation systems and human drivers. The change of AV penetration rates was also identified to have a statistically significant impact on vehicle delays. However, the interaction between traffic volume and AV penetration rate does not reach statistical significance (P-value = 0.887);
- (3) The differences of vehicle delays among scenarios with penetration rate of 0% and of 30%, 50%, 70%, and 100% are large enough to be statistically significant;
- (4) Traffic volume has a statistically significant impact (P-value =  $2.45e-15$ ) on queue lengths at signalized intersections with the presence of control transitions between automation systems and human drivers. The impact that penetration rate has on queue lengths is not statistically significant (P-value = 0.184). The interaction effect on queue lengths between traffic volume and AV penetration rate does not reach statistical significance.
- (5) No statistically significant difference was found in queue lengths in scenarios with different penetration rates;
- (6) No statistically significant difference is found in queue lengths in scenarios with different levels of AV penetration rate;

- (7) No interaction effect between traffic volume and penetration rate was found in the both vehicle delays and queue lengths;
- (8) A higher market penetration rate of cars with automation systems that disengages at permissive left turn signals results in longer delays and longer queues;
- (9) The maximum standard deviation of speed for left-turn lanes occurs when traffic volume is 400 veh/h/ln with an AV penetration rate of 50%, which is 5.52 mph. The maximum speed standard deviation for shared through and right-turn lanes occurs when traffic volume is 800 veh/h/ln with an AV penetration rate of 50%, which is 5.88 mph.
- (10) When traffic demand increases from 400 veh/h/ln to 900 veh/h/ln, the average speed standard deviations of traffic flow does not change significantly and is always in the range of 1.99 to 2.98 mph. Likewise, the average speed standard deviations of traffic flow for the same level of AV penetration rate ranges from 2.40 to 2.66 mph;
- (11) No apparent linear relationship was observed between speed variations and traffic volumes for both LL and TRL movements;
- (12) For LL and TRL movements, 23% and 26.6% of the variances of the speed are explained by the changes of AV penetration rates, respectively;
- (13) No apparent linear relationship was observed between speed variations and traffic volumes for both LL and TRL movements;
- (14) Traffic volume in different scenarios has no direct impact on the speed variations of traffic stream.

## Chapter 7 Contributions and future research

This research thoroughly studies issues related to control transitions based on narrative review ([Chapter 2](#)), meta-regression analysis ([Chapter 3](#)), modeling ([Chapter 4](#)), and simulation ([Chapter 5](#)). The final chapter summarizes main contributions of each part, elaborates on potential engineering applications, and suggests directions for the future research. Overall, this dissertation provides a theoretical foundation of influencing factors of control transitions, computation resources of takeover behavior, and workflow outline for performing a simulation evaluation on control transitions' impact on traffic operations and safety. Detailed conclusions and contributions are also presented at the end of each chapter.

### 7.1 Theoretical contribution

Most driving automation systems to date make the task of driving a vehicle shared between the system and the driver. [Chapter 1](#) and [Chapter 2](#) identify critical issues in a transportation system where vehicles are developed with different levels of automation, drivers are expected to take over control when the automation system reaches the limits of its operational design domain, and the traditional traffic signals at intersections might remain because of human-driven vehicles.

This dissertation theoretically unified control transition related factors and a model used to predict takeover behavior. Existing disengagement-related studies focused on individual disengagement scenarios such as urban roads with a stationary car, highways with two stationary vehicles, highways with a sharp horizontal curve bending to the left, highways with straight and curved sections, highway driving with a lead vehicle suddenly brakes, highways with exit lane on the left side, and missing pavement markings ([Clark et al., 2018](#); [Eriksson and Stanton, 2017](#);

Happee et al., 2017; Li et al., 2019; Madigan et al., 2018; Naujoks et al., 2017b; Petermeijer et al., 2017a; Petermeijer et al., 2017c; Sportillo et al., 2018; Wandtner et al., 2018b). This research utilized results from previous control-transition studies and extended it to predict takeover behavior in new disengagement scenarios. Through meta-regression, DAS modeling, and simulation, it is shown that even though triggering events of disengagements could be very different, drivers' response to TORs is only determined by when to take over control and how much longitudinal and lateral control is needed. There is no previous research that has similarly combined the results of multiple studies and apply them to new scenarios. This research systematically assesses study-level results and then derive high-level summary measures of takeover behavior.

## **7.2 Methodological contribution**

The development of more feasible and reliable driving automation systems when encountering permissive left-turn circumstances cannot be separated from the understanding of drivers' behaviors in automated driving systems. Meta-regression analysis was performed by extracting independent variables that described the disengagement scenario and by designing a TOQ variable that unifies different metrics used in existing studies as a response variable. The methodological contribution of this research is twofold:

- It demonstrated a statistical procedure that combined data from multiple studies focusing on the same question—takeover behavior in control transitions to consolidate research evidence into a quantitative estimates of drivers' takeover behavior; and
- It showed how learned knowledge and quantitative estimates of takeover behavior can be incorporated in simulation.

[Chapter 4](#) described a model framework to capture the interactions of a DAS during control transition in the context of PPLT scenario. The core problem of a DAS in PPLT scenario is how a driver might take back control from an automation system. Based on discussions in [Chapter 3](#) and [Chapter 4](#), it follows that automation disengagement and driver takeover behavior can be simulated by an event-based approach in VISSIM ([Chapter 5](#)). This research conducted XGBoost-based meta-regression analysis, developed a DAS model whose core is a computational model of XGBoost, and implemented the DAS model in VISSIM simulation. The whole process serves as a general framework enabling comprehensive data consolidation and knowledge enhancement and expansion. The unique model calibration method and simulation analysis in this study have potential to be used in practical engineering applications for safety evaluations of signalized intersections.

### **7.3 Engineering significance**

Automated driving systems have the potential to fundamentally change the entirety of future transportation through assisting and replacing human drivers to reduce traffic crashes brought about by human errors. Compared to human drivers, driving automation is expected to perform driving tasks better through quicker reaction times, better recognition, improved judgment, and the elimination of road rage, fatigue driving, distracted driving, and impaired driving. The following three parties are identified to be stakeholders that may interested in the effect of control transitions between an automation system and a human driver:

- Industry
- Academic institutions (such as universities and research institutes)
- Governmental agencies

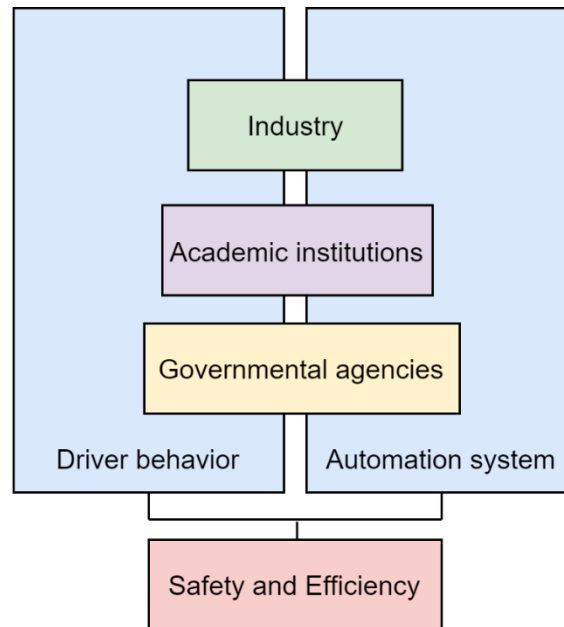


Figure 7-1 Achieving safety and efficiency goal through efforts of stakeholders

One common goal shared by these three parties are to effectively manage the performance of a DAS system before fully self-driving technology arrives so that the DAS system in traffic stream is safe and efficient. As illustrated in Figure 7-1, when trying to achieve an effective DAS system, automobile manufacturers, academic institutions, and governmental agencies have look into both driver behavior and the design of automation systems. This research starts by identifying problems in the process of developing a highly automated driving systems where a driver is expected to take full control of the vehicle if the automation system disengages.

Firstly, the automobile manufactures need to design those ADAS feature in a reliable way such that whenever an automation system disengages, the risk caused by disengagement can be managed by a driver to a tolerable level. The design parameters of the automation system should be reasonable and representative. The lead time, operating speed, and takeover time analyzed in

this research serve as a solid foundation for the testing and validation of any automation feature that may disengage in certain scenarios. The takeover dataset collected and XGBoost model trained in this research can serve as a computational engine for practical applications that need to estimate driver behavior when designing ADAS features.

Considering undergoing development of autonomous driving or advanced automated driving technologies, the approach to event-based DAS modeling explored in this research centers on the development of driver models in the context of disengagement scenarios. AI-based models of vehicle control focus on tasks such as lane keeping and car-following, which emphasize more on vehicle dynamics and pay little attention to driver and thus fail to generalize cases such as takeover behavior after an automation disengagement and NDRTs' engagement during control transitions. Many successes of vehicle behavior models in the research field have exemplified the significance of rigorous modeling for both theoretical elaboration of driving behavior and practical applications in system development.

This research is based on the culmination of several years of related work focusing on control transitions issues in different disengagement-triggering conditions. The influencing factors of takeover behavior have been assessed by XGBoost analysis outside the context of specific disengagement-triggering events as a stand-alone set of features input to a computational model. During the XGBoost training process, it has demonstrated how the XGBoost regression model can account for takeover behavior across a number of empirical studies. It is hoped that both the computational model (XGBoost regression) and the DAS framework model can be extended to other applicable scenarios in the near future. In fact, the disengagement event in urban driving context has unblocked explorations of a number of interesting scenarios. The impact of control

transitions in other specific urban driving scenarios can also be assessed following the same steps described in [Figures 3-6](#) and [4-3](#).

Just as the rapid evolution of electric vehicles, the industry, research institutes, and governmental agencies need to have clear strategies to address issues identified in this research. The next decade promises to be very exciting for the automobile industry and more advanced systems capable of taking control of more and more complex driving tasks will be implemented. Researchers must also be able to solve potential problems in the driver-vehicle interaction and to provide effective solutions to them. The conclusions and methods presented in this research help system designers and technology researchers and innovators in vehicle feature development. This research also provides government agencies with valuable insights on control transition issues to ensure their safe implementations in the real world.

## **7.2 Limitations**

All takeover behavioral data used in this research ([Chapter 3](#)) is collected from studies that conducted driving simulator-based experiments. When using driving behavior data collected from driving simulators, it must acknowledge that there are validity limitations in using driving simulator data to assess real world driving scenarios. Besides, as shown in [Table 2-14](#), different tools (retrofitted vehicles, Tesla, desktop driving simulator, or full-scale driving simulator), different experimental design, different disengagement scenarios, and different behavioral measures were used in different studies. The limitation of comparability due to variations in those studies should be recognized.

Another limitation of this research is the availability of the most up-to-date knowledge on autonomous driving technology: as a potential game changing innovation, most of the technologies

are patented or are still in development, and how automation might occur and how often it occurs depend on the system design and their technology maturity. Meanwhile, this research must make reasonable hypothesis and to rely on conclusions from related works.

Based on a critical review of the key aspects in driving automation systems, traffic control methods, and human-automation interactions, research challenges to address current limitations are identified and future research directions are suggested so as to remove barriers for the realization of reliable and safe driving automation systems in urban environments.

### 7.3 Future research

The findings identified in this research also raised new questions that can be addressed in future research. To start with, one aspect that deserves further investigation is how the modeling procedure presented in this research can be extended to study broader operational conditions. The XGBoost model can to be trained on a dataset that can feature new scenarios of interest.

In addition, future research should also account for distinctive driving behavior of automated vehicles in VISSIM. Currently, this research adopted the driving behavior parameters proposed by (Sukennik, 2018) to model the behavior of *cars with automation systems*. In future, if new driving behavior models become available for *cars with automation systems*, comparative studies can be conducted by implementing different driving behaviors of automated vehicles.

As mentioned before, the simulation scenario in this research is a simplified case. Vehicle delays, queue lengths, and speed variations investigated at the target intersection are a point analysis of the impact that control transitions have on urban traffic operations and safety. A more realistic traffic network or corridor calibrated by field data can be developed to further assess control transitions' impact on traffic operations and safety.

Finally, this research has developed a common procedure for evaluating a broad range of future operational principles. There is a great need for better understanding the relationship between control transitions and traffic operations. It has been pointed out that disengagement events in traffic stream can also be modeled in other ways rather than the event-based approach used in this research. It is also important to develop a robust simulation model that allows for experimentations with more types of driving behaviors. One possible future exploration could be building agent-based models to assess more driver-automation interactions in traffic stream.

## Appendix A Machine learning-based meta-analysis

### Global setting

```

import time
import xgboost as xgb
from sklearn.tree import DecisionTreeRegressor
from sklearn.ensemble import RandomForestRegressor
from sklearn.ensemble import AdaBoostRegressor
from sklearn.linear_model import LinearRegression
from xgboost import plot_tree
from sklearn import tree
import graphviz
from scipy.spatial.distance import pdist
from sklearn.neighbors import DistanceMetric
from sklearn.datasets import load_boston
from sklearn.model_selection import train_test_split, RepeatedKFold
from sklearn.model_selection import cross_val_score, KFold, GridSearchCV
from sklearn.metrics import mean_squared_error
from sklearn.model_selection import train_test_split
from sklearn.metrics import mean_squared_error as MSE
from sklearn.metrics import mean_absolute_error as MAE
from sklearn.metrics import explained_variance_score as r2
from sklearn.metrics import r2_score, make_scorer, accuracy_score
import csv
import numpy as np
import pandas as pd
from collections import defaultdict

import matplotlib.pyplot as plt
import matplotlib.pylab as pylab
params = {'legend.fontsize': 'x-large',
         'figure.figsize': (15, 5),
         'axes.labelsize': 'x-large',
         'axes.titlesize': 'x-large',
         'xtick.labelsize': 'x-large',
         'ytick.labelsize': 'x-large'}
pylab.rcParams.update(params)

#load data
d = pd.read_csv('prepared_xgboost_data.csv')

```

## 1 Data preparation¶

### 1.1 Training and testing

```
d.columns
Index(['ID', 'Sample size', 'Age_mean', 'Age_sd', 'NDRT', 'Lead_time',
      'Modality', 'Speed', 'Takeover', 'TTC', 'Deceleration', 'Angle',
      'Lateral_acceleartion', 'Male_percent', 'Modality_A', 'Modality_V',
      'Modality_H', 'TOQ', 'Group', 'Age_Y', 'Age_M', 'Age_O', 'Age'],
      dtype='object')
X = d[['Age_mean', 'Age_sd', 'NDRT', 'Lead_time', 'Speed',
      #'Takeover', 'TTC', 'deceleration', 'angle',
      'Male_percent', 'Modality_A', 'Modality_V',
      'Modality_H', 'Age_Y', 'Age_M', 'Age_O']]
y = d['TOQ']
X_train, X_test, y_train, y_test=train_test_split(X, y, test_size=0.25)
```

### 2 Model fitting and model selection

- For our regression problem, we considered linear regression, decision tree regression, random forest regression, AdaBoost regression trees, and XGBoost regression.
- We can start with its default parameters.
- We can then set the new parameter values according to the data characteristics.

#### 2.1 Train and compare multiple regression models

```
l_regression = LinearRegression()
dt_regression = DecisionTreeRegressor(criterion = 'mse', max_depth = 4)
rf_regression = RandomForestRegressor(max_depth= 4, random_state=0)
adab_regression = AdaBoostRegressor(DecisionTreeRegressor(max_depth=4),n_estimators=10)
xgb_regression = xgb.XGBRegressor(base_score=0.5,
                                  booster='gbtree',
                                  colsample_bylevel=0.8,
                                  colsample_bynode=0.8, colsample_bytree=0.7, gamma=0, gpu_id=-1,
                                  importance_type='gain', interaction_constraints="",
                                  learning_rate=0.300000012, max_delta_step=0, max_depth=3,
                                  min_child_weight=0.8, monotone_constraints='()',
                                  n_estimators=10, n_jobs=0, num_parallel_tree=1, random_state=0,
                                  reg_alpha=0, reg_lambda=1, scale_pos_weight=1, subsample=1)

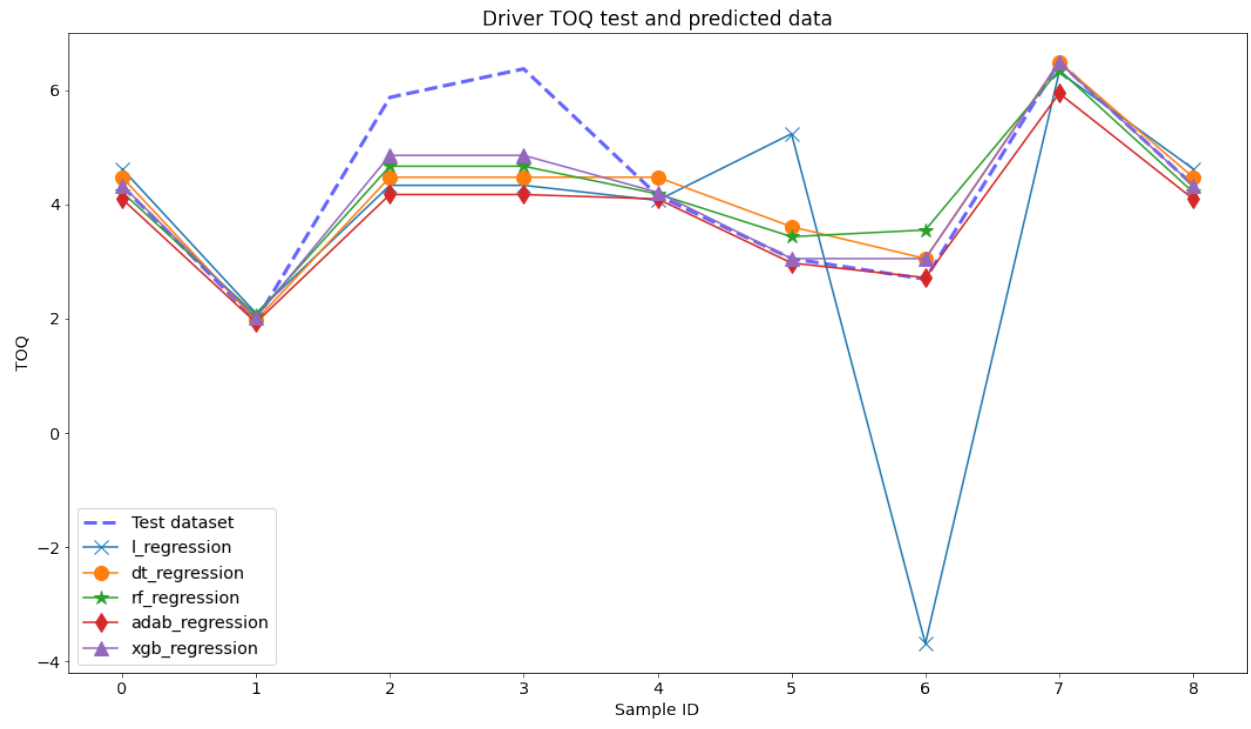
model_names = ['l_regression', 'dt_regression', 'rf_regression', 'adab_regression', 'xgb_regression']
model_algorithms = [l_regression, dt_regression, rf_regression, xgb_regression, adab_regression]
results = defaultdict(list)
linetype = ['x', 'o', '*', 'd', '^']
plt.figure(figsize=(18,10))
x_ax = range(len(y_test))
```

```

plt.plot(x_ax, y_test, label='Test dataset', color="blue", linestyle = '--',alpha = 0.6, linewidth = 3)
i = -1
for name, algorithm in zip(model_names, model_algorithms):
    i += 1
    # model training
    t0 = time.time()
    m = algorithm.fit(X_train, y_train)
    t1 = time.time()
    #print('training_time:%.2f' %(t1-t0))
    # training score
    # testing accuracy
    y_pred = m.predict(X_test)
    print(m,y_pred)
    print('training score:%.2f' % m.score(X_train, y_train))

    m_RMSE = mean_squared_error(y_test, y_pred)**(1/2.0)
    print("RMSE: %.2f" % m_RMSE)
    m_MAE = MAE(y_test, y_pred)
    print("MAE : % f" % (m_MAE))
    m_R2 = r2(y_test, y_pred)
    print("R2 : % f" % (m_R2))
    results[name].append(algorithm.score(X_train, y_train))
    results[name].append(m_RMSE)
    results[name].append(m_MAE)
    results[name].append(m_R2)
    plt.plot(x_ax, y_pred, label=name, marker = linetype[i],markersize=12)
plt.title("Driver TOQ test and predicted data",fontsize=17)
plt.xlabel('Sample ID',fontsize=14)
plt.ylabel('TOQ',fontsize=14)
plt.legend()
plt.savefig('regression.png')
plt.show()

```

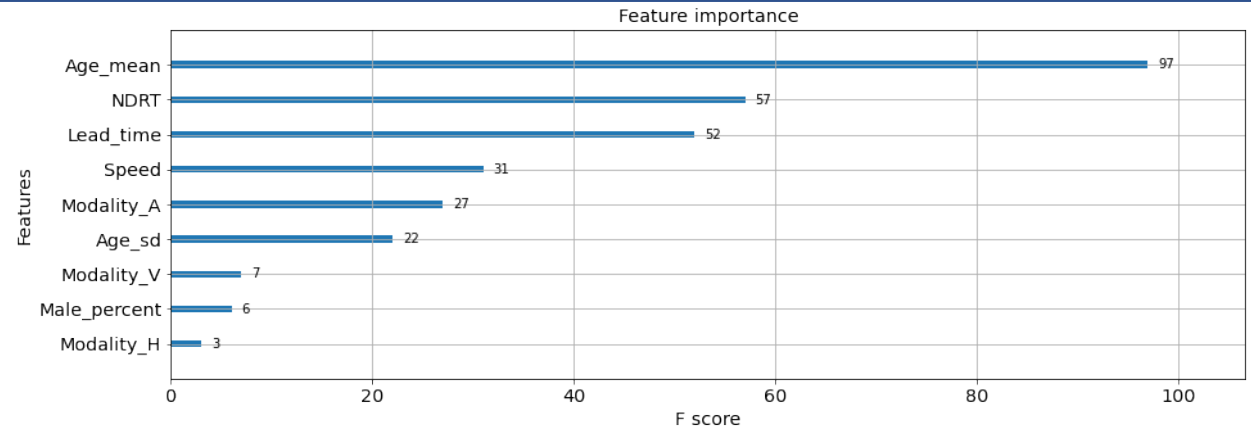


### 2.2 Fit XGBoost model with training data.

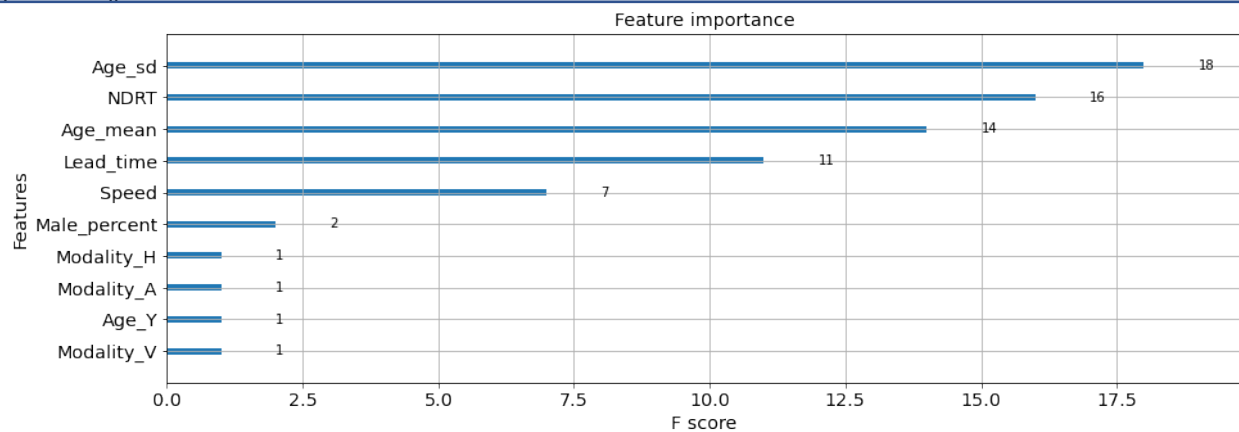
```
m_0 = xgb_r0.fit(X_train, y_train)
score_0 = xgb_r0.score(X_train, y_train)
m_1 = xgb_r1.fit(X_train, y_train)
score_1 = xgb_r1.score(X_train, y_train)
print("Training score of the original model with default parameters in xgboost: ", score_0)
print("Training score of a slightly tuned model: ", score_1)
Training score of the original model with default parameters in xgboost: 0.9920678901069927
Training score of a slightly tuned model: 0.9651487763041269
```

### 2.3 Feature selection using XGBoost

```
xgb.plot_importance(m_0)
plt.show()
```



```
xgb.plot_importance(m_1)
plt.show()
```



```
X_sf = d[['Age_mean', 'Lead_time', 'Speed', 'Age_sd', 'NDRT',
        #'Takeover', 'TTC', 'deceleration', 'angle',
        'Male_percent',
        'Modality_A', 'Modality_V', 'Modality_H']]
y = d['TOQ']

#prepare training and test data with selected features
X_train_sf, X_test_sf, y_train, y_test=train_test_split(X_sf, y, test_size=0.30, random_state= 88)
m_2 = xgb_r1.fit(X_train_sf, y_train)
```

### 3 Fine tune XGBoost

#### General Approach for Parameter Tuning

- Choose a relatively high learning rate. Generally a learning rate of 0.1 works but somewhere between 0.05 to 0.3 should work for different problems. XGBoost has a very useful function called as “cv” which performs cross-validation at each boosting iteration and thus returns the optimum number of trees required.
- Tune tree-specific parameters ( max\_depth, min\_child\_weight, subsample, colsample\_bytree) for decided learning rate and number of trees. Note that we can choose different parameters to define a tree and I’ll take up an example here.
- Tune regularization parameters (gamma, lambda, alpha) for xgboost which can help reduce model complexity and enhance performance.
- Lower the learning rate and decide the optimal parameters .

#### 3.1 Fix learning rate and number of estimators for tuning tree-based parameters

- max\_depth = 5 : This should be between 3-10. We start with 5 but can choose a different number as well. For instance 4-6 can be good starting points.
- min\_child\_weight = 3: A smaller value is chosen because it is a highly imbalanced class problem and leaf nodes can have smaller size groups.

- `gamma = 0` : A smaller value like 0.1-0.2 can also be chosen for starting. This will anyways be tuned later.
- `subsample = 0.8`
- `colsample_bytree = 0.8`: This is a commonly used start value. Typical values range between 0.5-0.9.

Note: all the above are initial estimates and will be tuned later. Let's take the default learning rate of 0.3 here.

```
xgb_regression = xgb.XGBRegressor(verbosity=0,
    learning_rate =0.3,
    n_estimators=15,
    max_depth=5,
    min_child_weight=1,
    gamma=0,
    subsample=0.8,
    colsample_bytree=0.8,
    nthread=4,
    seed=123)
xgb_regression.fit(X_train_sf,y_train)

y_pred= xgb_regression.predict(X_test_sf)

rmse = np.sqrt(mean_squared_error(y_test, y_pred))
print("RMSE: %f" % (rmse))
RMSE: 0.311697
```

### 3.2 Tune max\_depth and min\_child\_weight

We tune these two first as they have the highest impact on model results. To start with, let's set wider ranges and then we will perform another iteration for smaller ranges.

```
Note: Grid search will be used here.
param_test1 = {
    'max_depth':[2,3,4,5,6],
    'min_child_weight':[1,2,3,4,5,6]
}
xgb_regression = xgb.XGBRegressor(verbosity=0,
    learning_rate =0.3,
    n_estimators=15,
    max_depth=5,
    min_child_weight=1,
    gamma=0,
    subsample=0.8,
    colsample_bytree=0.8
    nthread=4,
```



```

fill_value='?',
dtype=object),
'params': [{'max_depth': 2, 'min_child_weight': 1},
{'max_depth': 2, 'min_child_weight': 2},
{'max_depth': 2, 'min_child_weight': 3},
{'max_depth': 2, 'min_child_weight': 4},
{'max_depth': 2, 'min_child_weight': 5},
{'max_depth': 2, 'min_child_weight': 6},
{'max_depth': 3, 'min_child_weight': 1},
{'max_depth': 3, 'min_child_weight': 2},
{'max_depth': 3, 'min_child_weight': 3},
{'max_depth': 3, 'min_child_weight': 4},
{'max_depth': 3, 'min_child_weight': 5},
{'max_depth': 3, 'min_child_weight': 6},
{'max_depth': 4, 'min_child_weight': 1},
{'max_depth': 4, 'min_child_weight': 2},
{'max_depth': 4, 'min_child_weight': 3},
{'max_depth': 4, 'min_child_weight': 4},
{'max_depth': 4, 'min_child_weight': 5},
{'max_depth': 4, 'min_child_weight': 6},
{'max_depth': 5, 'min_child_weight': 1},
{'max_depth': 5, 'min_child_weight': 2},
{'max_depth': 5, 'min_child_weight': 3},
{'max_depth': 5, 'min_child_weight': 4},
{'max_depth': 5, 'min_child_weight': 5},
{'max_depth': 5, 'min_child_weight': 6},
{'max_depth': 6, 'min_child_weight': 1},
{'max_depth': 6, 'min_child_weight': 2},
{'max_depth': 6, 'min_child_weight': 3},
{'max_depth': 6, 'min_child_weight': 4},
{'max_depth': 6, 'min_child_weight': 5},
{'max_depth': 6, 'min_child_weight': 6}],
'split0_test_score': array([-0.94245889, -0.92056283, -1.17855449, -1.14651788, -1.16464744,
-1.10468371, -0.79421058, -0.91640572, -1.15781442, -1.14651788,
-1.16464744, -1.10468371, -0.78725149, -0.91341449, -1.15781442,
-1.14651788, -1.16464744, -1.10468371, -0.79303033, -0.91674564,
-1.15781442, -1.14651788, -1.16464744, -1.10468371, -0.79200763,
-0.91674564, -1.15781442, -1.14651788, -1.16464744, -1.10468371]),
'split1_test_score': array([-0.21035683, -0.66466289, -1.2754679, -1.30270059, -0.64272579,
-0.6855188, -0.59635561, -0.69659788, -1.23887359, -1.30270059,
-0.64272579, -0.6855188, -0.60431161, -0.701104, -1.19129511,
-1.30270059, -0.64272579, -0.6855188, -0.60613996, -0.701104,
-1.19129511, -1.30270059, -0.64272579, -0.6855188, -0.60613996,
-0.701104, -1.19129511, -1.30270059, -0.64272579, -0.6855188 ]),

```

```

'split2_test_score': array([-0.32924678, -0.7331672, -0.78366722, -0.92953401, -1.08658606,
-1.26881116, -0.42979857, -0.66695107, -0.75510595, -0.9304019,
-1.08658606, -1.26881116, -0.43027843, -0.66773192, -0.75510595,
-0.9304019, -1.08658606, -1.26881116, -0.43027843, -0.66773192,
-0.75510595, -0.9304019, -1.08658606, -1.26881116, -0.43027843,
-0.66773192, -0.75510595, -0.9304019, -1.08658606, -1.26881116]),
'split3_test_score': array([-0.45571388, -0.19003662, -0.48148195, -0.22597922, -0.72263102,
-0.46509092, -0.61775814, -0.47338089, -0.41173669, -0.19508305,
-0.72263102, -0.46509092, -0.61736027, -0.3808303, -0.41173669,
-0.19508305, -0.72263102, -0.46509092, -0.61736027, -0.3808303,
-0.41173669, -0.19508305, -0.72263102, -0.46509092, -0.61736027,
-0.3808303, -0.41173669, -0.19508305, -0.72263102, -0.46509092]),
'split4_test_score': array([-1.64759495, -1.7944064, -1.86000927, -1.94807055, -2.11575773,
-2.24245552, -1.43804362, -1.70503197, -1.82271224, -1.94807055,
-2.11575773, -2.24245552, -1.32191085, -1.7036034, -1.82518975,
-1.94807055, -2.11575773, -2.24245552, -1.32191085, -1.7036034,
-1.82518975, -1.94807055, -2.11575773, -2.24245552, -1.32191085,
-1.7036034, -1.82518975, -1.94807055, -2.11575773, -2.24245552]),
'mean_test_score': array([-0.71707427, -0.86056719, -1.11583616, -1.11056045, -1.14646961,
-1.15331202, -0.77523331, -0.89167351, -1.07724858, -1.10455479,
-1.14646961, -1.15331202, -0.75222253, -0.87333682, -1.06822838,
-1.10455479, -1.14646961, -1.15331202, -0.75374397, -0.87400305,
-1.06822838, -1.10455479, -1.14646961, -1.15331202, -0.75353943,
-0.87400305, -1.06822838, -1.10455479, -1.14646961, -1.15331202]),
'std_test_score': array([0.52766446, 0.52533335, 0.46817752, 0.55765374, 0.52475383,
0.61553507, 0.35094115, 0.43027597, 0.47644759, 0.56745213,
0.52475383, 0.61553507, 0.30642627, 0.44843037, 0.47438141,
0.56745213, 0.52475383, 0.61553507, 0.30639009, 0.44849189,
0.47438141, 0.56745213, 0.52475383, 0.61553507, 0.30636414,
0.44849189, 0.47438141, 0.56745213, 0.52475383, 0.61553507]),
'rank_test_score': array([ 1,  6, 20, 19, 21, 26,  5, 10, 14, 15, 21, 26,  2,  7, 11, 15, 21,
 26,  4,  8, 11, 15, 21, 26,  3,  8, 11, 15, 21, 26], dtype=int32)},
{'max_depth': 2, 'min_child_weight': 1},
-0.7170742658539622)

```

Here, we have  $5 \times 6 = 30$  combinations with wider steps between values. The optimal values for `max_depth` and `min_child_weight` are 2 and 1, respectively. Let's go one step deeper and look for optimum values.

### 3.3 Tune gamma

Next we tune gamma by using the parameters already tuned above. gamma controls the minimum loss reduction required to make a further partition on a leaf node of the tree. The larger gamma is, the more conservative the algorithm will be.

XGBoost supports regularization by regularization parameters to penalize the model as it becomes more complex.

gamma: controls whether a given node will split based on the expected reduction in loss after the split. A higher value leads to fewer splits. Supported only for tree-based learners. reg\_alpha: L1 regularization on leaf weights. A large value leads to more regularization. reg\_lambda: L2 regularization on leaf weights and is smoother than L1 regularization. We will first tune gamma and come back to reg\_alpha and reg\_lambda later.

```
xgb_regression = xgb.XGBRegressor(verbosity=0,
    learning_rate=0.1,
    n_estimators=10,
    max_depth=2,
    min_child_weight=1,
    gamma=0,
    subsample=0.8,
    colsample_bytree=0.8,
    nthread=4,
    seed=123)
param_test3 = {'gamma': [0, 0.01, 0.05, 0.1, 0.2, 0.3, 0.4, 0.5]}
grid_search3 = GridSearchCV(estimator = xgb_regression,
    param_grid = param_test3,
    #scoring="r2",
    scoring="neg_root_mean_squared_error",
    n_jobs=4,
    cv=5)

grid_search3.fit(X_train_sf, y_train)
grid_search3.cv_results_, grid_search3.best_params_, grid_search3.best_score_
({'mean_fit_time': array([0.02588873, 0.03407421, 0.03873544, 0.0669899, 0.05812616,
    0.06388497, 0.0688868, 0.0560194 ]),
    'std_fit_time': array([0.01005763, 0.02447646, 0.01978489, 0.00439791, 0.01885385,
    0.00685591, 0.01094218, 0.0112568 ]),
    'mean_score_time': array([0.02224045, 0.02858472, 0.02645292, 0.02833934, 0.02508025,
    0.02428141, 0.0272007, 0.02363753]),
    'std_score_time': array([0.00758065, 0.00533258, 0.00530758, 0.0066716, 0.00349368,
    0.0019218, 0.00549833, 0.00284006]),
    'param_gamma': masked_array(data=[0, 0.01, 0.05, 0.1, 0.2, 0.3, 0.4, 0.5],
    mask=[False, False, False, False, False, False, False, False],
    fill_value='?',
    dtype=object),
    'params': [{'gamma': 0},
    {'gamma': 0.01},
    {'gamma': 0.05},
    {'gamma': 0.1},
```

```

{'gamma': 0.2},
{'gamma': 0.3},
{'gamma': 0.4},
{'gamma': 0.5}],
'split0_test_score': array([-2.35769618, -2.35769618, -2.36006415, -2.36006415, -2.36006415,
-2.36006415, -2.36006415, -2.36006415]),
'split1_test_score': array([-1.52574078, -1.52574078, -1.52574078, -1.52574078, -1.53090985,
-1.53090985, -1.53090985, -1.53090985]),
'split2_test_score': array([-1.68697007, -1.68697007, -1.68697007, -1.68697007, -1.68697007,
-1.69067052, -1.69067052, -1.69067052]),
'split3_test_score': array([-2.04681348, -2.04681348, -2.04681348, -2.06055674, -2.06055674,
-2.06055674, -2.06055674, -2.06055674]),
'split4_test_score': array([-1.73210222, -1.73210222, -1.73210222, -1.73210222, -1.73210222,
-1.7260718 , -1.7260718 , -1.75357384]),
'mean_test_score': array([-1.86986455, -1.86986455, -1.87033814, -1.87308679, -1.87412061,
-1.87365461, -1.87365461, -1.87915502]),
'std_test_score': array([0.29669535, 0.29669535, 0.29747453, 0.29915122, 0.29795561,
0.29808203, 0.29808203, 0.29555098]),
'rank_test_score': array([1, 1, 3, 4, 7, 5, 5, 8], dtype=int32)},
{'gamma': 0},
-1.869864547896928)

```

This shows that the original value of gamma 0 is the optimum one. Before proceeding, it is always good to re-calibrate the number of boosting rounds for the updated parameters.

```

xgb_regression = xgb.XGBRegressor(verbosity=0,
    learning_rate=0.1,
    n_estimators=10,
    max_depth=2,
    min_child_weight=1,
    gamma=0,
    subsample=0.8,
    colsample_bytree=0.8,
    nthread=4,
    seed=123)

```

### 3.4 Tune subsample vs colsample\_bytree

After tuning `n_estimator`, `learning_rate`, and `gamma` the next step would be to tune different `subsample` and `colsample_bytree` values.

```

xgb_regression = xgb.XGBRegressor(verbosity=0,
    learning_rate=0.3,
    n_estimators=10,
    max_depth=2,

```

```

        min_child_weight=1,
        gamma=0,
        subsample=0.8,
        colsample_bytree=0.8,
        nthread=4,
        seed=123)

param_test4 = {'subsample': [0.4,0.5,0.6,0.7,0.8,0.9,1],
               'colsample_bytree': [0.4,0.5,0.6,0.7,0.8,0.9,1]}
grid_search4 = GridSearchCV(estimator = xgb_regression,
                             param_grid = param_test4,
                             #scoring="r2",
                             scoring="neg_root_mean_squared_error",
                             n_jobs=4,
                             cv=5)

grid_search4.fit(X_train_sf,y_train)
grid_search4.cv_results_ , grid_search4.best_params_ , grid_search4.best_score_
({'mean_fit_time': array([0.02401104, 0.02839031, 0.03625879, 0.06129494, 0.04813538,
                          0.05845852, 0.056043 , 0.05582967, 0.05845456, 0.05102868,
                          0.07342143, 0.05962811, 0.05902791, 0.0609838 , 0.0671452 ,
                          0.05867262, 0.06588154, 0.05932074, 0.05786929, 0.05964894,
                          0.06096973, 0.06511326, 0.06704717, 0.05620999, 0.10220819,
                          0.12837429, 0.02295389, 0.01899405, 0.03110919, 0.04112554,
                          0.08053155, 0.06513333, 0.04954982, 0.05600228, 0.06830354,
                          0.06622772, 0.06363144, 0.06672168, 0.068116 , 0.06890159,
                          0.06731286, 0.0625031 , 0.06065059, 0.06258759, 0.05712605,
                          0.0642591 , 0.05952544, 0.05211744, 0.05202317])),
 'std_fit_time': array([0.01321923, 0.0218998 , 0.01932402, 0.00640247, 0.0094431 ,
                        0.00853089, 0.00798951, 0.00955132, 0.01187426, 0.00619858,
                        0.01475219, 0.00897614, 0.01068187, 0.01318507, 0.00841225,
                        0.01086231, 0.01356221, 0.00647474, 0.01377158, 0.0037393 ,
                        0.01264164, 0.01846265, 0.01007461, 0.01155028, 0.0310341 ,
                        0.02121366, 0.00813713, 0.00805909, 0.01929991, 0.02434578,
                        0.05594366, 0.0323223 , 0.00686093, 0.0041766 , 0.01404047,
                        0.0093477 , 0.01109986, 0.01051193, 0.0097402 , 0.01714138,
                        0.00875801, 0.01183351, 0.01248274, 0.00915558, 0.01706628,
                        0.0090715 , 0.00508845, 0.01328112, 0.01024234])),
 'mean_score_time': array([0.03494496, 0.02263417, 0.02610006, 0.0268671 , 0.03109713,
                           0.03133564, 0.03574634, 0.03087144, 0.03437204, 0.03015213,
                           0.0279038 , 0.03000369, 0.02491431, 0.03055835, 0.02875156,
                           0.02643661, 0.03139582, 0.02692924, 0.02734914, 0.033498 ,
                           0.02334223, 0.02817521, 0.02701969, 0.02579355, 0.03342557,
                           0.04823661, 0.00731382, 0.01426029, 0.0268846 , 0.03549519,

```

```

0.0423728 , 0.01905503, 0.01838465, 0.02315688, 0.02681656,
0.02464018, 0.02337346, 0.02567301, 0.02156653, 0.02784753,
0.02416921, 0.02361097, 0.0261476 , 0.02914624, 0.03054495,
0.02767363, 0.03681436, 0.03324165, 0.02745643]),
'std_score_time': array([0.01477914, 0.00289531, 0.00083252, 0.00460025, 0.00305415,
0.00653466, 0.00723589, 0.00676733, 0.00307002, 0.00572064,
0.00468972, 0.00478972, 0.00046948, 0.00466054, 0.005585 ,
0.00222191, 0.00647737, 0.00767324, 0.00390148, 0.00824059,
0.0032644 , 0.00413921, 0.00270272, 0.00416749, 0.00691636,
0.00763115, 0.00437483, 0.0053561 , 0.00909144, 0.01352221,
0.01724874, 0.00416886, 0.00282106, 0.00465836, 0.00410217,
0.00759741, 0.00369999, 0.00433855, 0.00451719, 0.00454294,
0.00584997, 0.00525147, 0.00322359, 0.00536542, 0.00621586,
0.0021428 , 0.00863789, 0.00543495, 0.0086225 ]),
'param_colsample_bytree': masked_array(data=[0.4, 0.4, 0.4, 0.4, 0.4, 0.4, 0.4, 0.5, 0.5, 0.5, 0.5,
0.5, 0.5, 0.5, 0.6, 0.6, 0.6, 0.6, 0.6, 0.6, 0.6, 0.7,
0.7, 0.7, 0.7, 0.7, 0.7, 0.8, 0.8, 0.8, 0.8, 0.8,
0.8, 0.8, 0.9, 0.9, 0.9, 0.9, 0.9, 0.9, 0.9, 0.9, 1, 1, 1,
1, 1, 1, 1],
mask=[False, False, False, False, False, False, False, False,
False, False, False, False, False, False, False, False,
False],
fill_value='?',
dtype=object),
'param_subsample': masked_array(data=[0.4, 0.5, 0.6, 0.7, 0.8, 0.9, 1, 0.4, 0.5, 0.6, 0.7,
0.8, 0.9, 1, 0.4, 0.5, 0.6, 0.7, 0.8, 0.9, 1, 0.4, 0.5,
0.6, 0.7, 0.8, 0.9, 1, 0.4, 0.5, 0.6, 0.7, 0.8, 0.9, 1,
0.4, 0.5, 0.6, 0.7, 0.8, 0.9, 1, 0.4, 0.5, 0.6, 0.7,
0.8, 0.9, 1],
mask=[False, False, False, False, False, False, False, False,
False, False, False, False, False, False, False, False,
False],
fill_value='?',
dtype=object),
'params': [{'colsample_bytree': 0.4, 'subsample': 0.4},
{'colsample_bytree': 0.4, 'subsample': 0.5},

```

```
{'colsample_bytree': 0.4, 'subsample': 0.6},
{'colsample_bytree': 0.4, 'subsample': 0.7},
{'colsample_bytree': 0.4, 'subsample': 0.8},
{'colsample_bytree': 0.4, 'subsample': 0.9},
{'colsample_bytree': 0.4, 'subsample': 1},
{'colsample_bytree': 0.5, 'subsample': 0.4},
{'colsample_bytree': 0.5, 'subsample': 0.5},
{'colsample_bytree': 0.5, 'subsample': 0.6},
{'colsample_bytree': 0.5, 'subsample': 0.7},
{'colsample_bytree': 0.5, 'subsample': 0.8},
{'colsample_bytree': 0.5, 'subsample': 0.9},
{'colsample_bytree': 0.5, 'subsample': 1},
{'colsample_bytree': 0.6, 'subsample': 0.4},
{'colsample_bytree': 0.6, 'subsample': 0.5},
{'colsample_bytree': 0.6, 'subsample': 0.6},
{'colsample_bytree': 0.6, 'subsample': 0.7},
{'colsample_bytree': 0.6, 'subsample': 0.8},
{'colsample_bytree': 0.6, 'subsample': 0.9},
{'colsample_bytree': 0.6, 'subsample': 1},
{'colsample_bytree': 0.7, 'subsample': 0.4},
{'colsample_bytree': 0.7, 'subsample': 0.5},
{'colsample_bytree': 0.7, 'subsample': 0.6},
{'colsample_bytree': 0.7, 'subsample': 0.7},
{'colsample_bytree': 0.7, 'subsample': 0.8},
{'colsample_bytree': 0.7, 'subsample': 0.9},
{'colsample_bytree': 0.7, 'subsample': 1},
{'colsample_bytree': 0.8, 'subsample': 0.4},
{'colsample_bytree': 0.8, 'subsample': 0.5},
{'colsample_bytree': 0.8, 'subsample': 0.6},
{'colsample_bytree': 0.8, 'subsample': 0.7},
{'colsample_bytree': 0.8, 'subsample': 0.8},
{'colsample_bytree': 0.8, 'subsample': 0.9},
{'colsample_bytree': 0.8, 'subsample': 1},
{'colsample_bytree': 0.9, 'subsample': 0.4},
{'colsample_bytree': 0.9, 'subsample': 0.5},
{'colsample_bytree': 0.9, 'subsample': 0.6},
{'colsample_bytree': 0.9, 'subsample': 0.7},
{'colsample_bytree': 0.9, 'subsample': 0.8},
{'colsample_bytree': 0.9, 'subsample': 0.9},
{'colsample_bytree': 0.9, 'subsample': 1},
{'colsample_bytree': 1, 'subsample': 0.4},
{'colsample_bytree': 1, 'subsample': 0.5},
{'colsample_bytree': 1, 'subsample': 0.6},
{'colsample_bytree': 1, 'subsample': 0.7},
```

```
{'colsample_bytree': 1, 'subsample': 0.8},
{'colsample_bytree': 1, 'subsample': 0.9},
{'colsample_bytree': 1, 'subsample': 1}],
'split0_test_score': array([-1.7628876 , -1.30921623, -1.08415269, -1.15259107, -1.1157705 ,
-1.22111069, -1.30638414, -1.60347662, -1.20348606, -0.92818691,
-1.09406079, -1.04096788, -1.24252482, -1.24796196, -1.51044896,
-1.20053664, -0.92818691, -1.12355883, -1.20874163, -1.25336989,
-1.14673176, -1.62570763, -1.28605567, -0.98466808, -1.11358096,
-1.09796477, -1.25034077, -1.17204958, -1.46481198, -1.22589389,
-1.13417624, -1.17671299, -1.09534366, -1.14313029, -1.18624596,
-1.47068842, -1.2353872 , -1.13391814, -1.17671299, -1.09534366,
-1.14799975, -1.1412127 , -1.46592076, -1.21251926, -1.01160365,
-1.03630359, -1.02428154, -1.09351365, -1.1612162 ]),
'split1_test_score': array([-0.59715712, -0.62238519, -0.42385317, -0.48318162, -0.67716608,
-0.76943392, -0.53601463, -0.58261641, -0.84032483, -0.93965168,
-0.82498227, -0.76626622, -0.94274458, -0.69292127, -0.99046458,
-1.01730388, -1.07595132, -0.8357405 , -1.00259158, -0.76466292,
-0.40834191, -1.03440367, -1.06234323, -1.09573312, -0.8713116 ,
-0.347244 , -0.75686897, -0.67331162, -0.91087908, -1.11695939,
-1.01811768, -0.9329267 , -0.37857707, -0.67962895, -0.70594693,
-0.67466594, -0.85896619, -0.92092898, -0.75044675, -0.18404703,
-0.62223933, -0.70514651, -0.65612042, -0.55148708, -0.5053159 ,
-0.4199305 , -0.19318244, -0.51171309, -0.70514651]),
'split2_test_score': array([-0.97199732, -0.79555323, -0.58742926, -0.61797753, -0.62741858,
-0.63345774, -0.74201612, -1.20326674, -1.11663015, -0.7349229 ,
-0.79666944, -0.58782444, -0.73043086, -0.64261989, -1.15696903,
-1.24541975, -0.59035719, -0.69039687, -0.49543637, -0.4653024 ,
-0.77755644, -1.13872372, -1.18769623, -0.68000896, -0.6220898 ,
-0.50421403, -0.49025561, -0.52137989, -1.06143791, -0.94693573,
-0.57484174, -0.66303517, -0.42838537, -0.45107578, -0.51098292,
-1.10870189, -0.94693573, -0.57363219, -0.66303517, -0.42838537,
-0.45107578, -0.5646402 , -1.01583915, -0.95511233, -0.48217436,
-0.59331084, -0.44161474, -0.47033287, -0.51666764]),
'split3_test_score': array([-1.12708027, -0.89339454, -0.40132592, -0.53096956, -0.67622562,
-0.45050122, -0.98289304, -1.0716967 , -0.75242376, -0.66189255,
-0.58044314, -0.51070355, -0.44281561, -0.65896076, -1.0716967 ,
-0.78229733, -0.60100987, -0.6843039 , -0.39170725, -0.5296356 ,
-0.39995164, -1.0569535 , -0.63971385, -0.63338712, -0.55286462,
-0.50025741, -0.3299186 , -0.30370805, -0.90220537, -0.73258763,
-0.83036665, -0.71581645, -0.39094754, -0.42666085, -0.34262408,
-0.8306946 , -0.6209772 , -0.7199182 , -0.88389703, -0.3623849 ,
-0.36999071, -0.40225972, -0.8306946 , -0.62846953, -0.58960229,
-0.88173819, -0.48004918, -0.53230979, -0.40225972]),
'split4_test_score': array([-1.59342646, -1.66367242, -1.54203422, -1.63231579, -1.59290036,
```

```

-1.6035661 , -1.78204042, -1.8566331 , -1.76717212, -1.57336459,
-1.6834196 , -1.53420136, -1.61191996, -1.73089471, -1.9608922 ,
-1.80470867, -1.61271402, -1.48754413, -1.55698818, -1.471161 ,
-1.46572696, -1.76488353, -1.6704591 , -1.65091064, -1.59742587,
-1.62275389, -1.51521598, -1.42146829, -1.77479812, -1.6704591 ,
-1.70437149, -1.63652343, -1.58892687, -1.42863989, -1.36958875,
-1.77479812, -1.69649787, -1.69833135, -1.50120299, -1.44418603,
-1.53226375, -1.60683274, -1.77479812, -1.75123836, -1.67134914,
-1.49867062, -1.44418603, -1.53226375, -1.60056412]),
'mean_test_score': array([-1.21050976, -1.05684432, -0.80775905, -0.88340711, -0.93789623,
-0.93561394, -1.06986967, -1.26353791, -1.13600739, -0.96760373,
-0.99591505, -0.88799269, -0.99408717, -0.99467172, -1.33809429,
-1.21005325, -0.96164386, -0.96430885, -0.931093 , -0.89682636,
-0.83966174, -1.32413441, -1.16925362, -1.00894158, -0.95145457,
-0.81448682, -0.86851999, -0.81838349, -1.22282649, -1.13856715,
-1.05237476, -1.02500295, -0.7764361 , -0.82582715, -0.82307773,
-1.1719098 , -1.07175284, -1.00934577, -0.99505898, -0.7028694 ,
-0.82471387, -0.88401837, -1.14867461, -1.01976531, -0.85200907,
-0.88599075, -0.71666279, -0.82802663, -0.87717084]),
'std_test_score': array([0.42232608, 0.378332 , 0.44196613, 0.4445604 , 0.37242926,
0.41998024, 0.43890326, 0.44077432, 0.35717288, 0.32152167,
0.38048097, 0.37101279, 0.4048431 , 0.43217495, 0.35838633,
0.33914123, 0.37576285, 0.30629923, 0.43696207, 0.39887159,
0.41701043, 0.30819243, 0.33377597, 0.36591914, 0.3787722 ,
0.47895315, 0.44936492, 0.41543683, 0.34333221, 0.31386108,
0.37690587, 0.35554697, 0.48782698, 0.39628543, 0.39307098,
0.40507222, 0.36909043, 0.39284897, 0.30711948, 0.48250061,
0.44553678, 0.43696647, 0.41328972, 0.43561079, 0.45224324,
0.37439614, 0.45378155, 0.41997162, 0.44476401]),
'rank_test_score': array([45, 36, 4, 15, 22, 21, 37, 47, 39, 26, 30, 18, 27, 28, 49, 44, 24,
25, 20, 19, 11, 48, 42, 31, 23, 5, 13, 6, 46, 40, 35, 34, 3, 9,
7, 43, 38, 32, 29, 1, 8, 16, 41, 33, 12, 17, 2, 10, 14],
dtype=int32)},
{'colsample_bytree': 0.9, 'subsample': 0.8},
-0.7028693982744602)

```

Here, it is found that 0.9 was the optimal value for `colsample_bytree` and 0.8 is the optimal value for `subsample`. A careful action is that we try values in 0.02 interval around these two optimal values.

```

xgb_regression = xgb.XGBRegressor(verbosity=0,
    learning_rate =0.3,
    n_estimators=10,
    max_depth=2,
    min_child_weight=1,

```

```

gamma=0,
subsample=0.8,
colsample_bytree=0.8,
nthread=4,
seed=123)

```

```

param_test4 = {'subsample': [0.7,0.76,0.78, 0.8,0.82,0.84,0.86,0.88,0.9,0.92,0.94,0.96],
               'colsample_bytree': [0.72,0.74,0.76,0.78,0.8,0.92,0.94,0.96,0.98]}

```

```

grid_search4 = GridSearchCV(estimator = xgb_regression,
                             param_grid = param_test4,
                             #scoring="r2",
                             scoring="neg_root_mean_squared_error",
                             n_jobs=4,
                             cv=5)

```

```
grid_search4.fit(X_train_sf,y_train)
```

```

grid_search4.cv_results_ , grid_search4.best_params_ , grid_search4.best_score_
({'mean_fit_time': array([0.02234187, 0.02497082, 0.03654051, 0.05481458, 0.04758868,
                          0.06597133, 0.06660638, 0.07431946, 0.06711326, 0.05986271,
                          0.06953979, 0.06021109, 0.06712332, 0.06564665, 0.06804471,
                          0.06846428, 0.07062893, 0.06283197, 0.07027612, 0.05814881,
                          0.06297879, 0.06623044, 0.06885848, 0.05652232, 0.06896038,
                          0.05829268, 0.06784973, 0.07017508, 0.06910124, 0.06851435,
                          0.07165194, 0.06803174, 0.06206713, 0.05519753, 0.07300835,
                          0.06384616, 0.07445803, 0.06367531, 0.06950235, 0.06282907,
                          0.07378926, 0.061443 , 0.07160678, 0.068329 , 0.06913743,
                          0.06683736, 0.07131672, 0.05959945, 0.06326737, 0.06675334,
                          0.07188458, 0.06372705, 0.06708207, 0.0657023 , 0.07001915,
                          0.06681485, 0.07586107, 0.06308994, 0.07158127, 0.06747079,
                          0.06299868, 0.0670712 , 0.07246723, 0.06827979, 0.07055016,
                          0.06707301, 0.06823378, 0.0633112 , 0.06922593, 0.06153517,
                          0.06253729, 0.06647553, 0.07047625, 0.06237845, 0.06336856,
                          0.06335149, 0.06378493, 0.06965208, 0.06748509, 0.06416192,
                          0.06247239, 0.06629686, 0.07111659, 0.06756401, 0.06551042,
                          0.06631064, 0.06828427, 0.0719873 , 0.06437802, 0.0627562 ,
                          0.06869321, 0.06806502, 0.06954699, 0.06293344, 0.06314654,
                          0.06742096, 0.06423264, 0.0671114 , 0.06700315, 0.0672092 ,
                          0.06765904, 0.06658616, 0.06725826, 0.06392102, 0.06534553,
                          0.06092954, 0.0602756 , 0.06412997]),
 'std_fit_time': array([0.01075744, 0.0190639 , 0.0212958 , 0.01730629, 0.0155979 ,
                        0.00971818, 0.0093616 , 0.01751852, 0.0101168 , 0.00938272,
                        0.00980158, 0.0047858 , 0.01335645, 0.0048184 , 0.01318237,
                        0.01025605, 0.00789412, 0.012098 , 0.0098762 , 0.00537514,

```

```
0.00752269, 0.0070476 , 0.01200713, 0.00829822, 0.01237925,
0.0080787 , 0.01205946, 0.00985216, 0.01741896, 0.02154702,
0.0152486 , 0.01125611, 0.00432639, 0.00515357, 0.0108193 ,
0.01010047, 0.01295424, 0.01508381, 0.00932033, 0.00844913,
0.01074358, 0.00700509, 0.01875148, 0.01198903, 0.00627003,
0.01182878, 0.00855626, 0.00956421, 0.01098542, 0.01081546,
0.00664114, 0.00621206, 0.00584754, 0.00351197, 0.01162025,
0.00883645, 0.01548683, 0.01204343, 0.01352806, 0.00688762,
0.01380758, 0.0039645 , 0.01184106, 0.00330969, 0.00571572,
0.00976587, 0.00674952, 0.00411446, 0.01107377, 0.00472081,
0.00723895, 0.00960162, 0.00595773, 0.0142432 , 0.00473827,
0.00704449, 0.01004894, 0.00831155, 0.00762362, 0.00979437,
0.00789206, 0.0087337 , 0.01109029, 0.01466877, 0.01363091,
0.00868543, 0.01451014, 0.00997076, 0.0086693 , 0.0090602 ,
0.00433446, 0.01033957, 0.0117832 , 0.00635127, 0.00553139,
0.00839587, 0.0057123 , 0.0173654 , 0.01068847, 0.01002769,
0.01016578, 0.00654098, 0.01221494, 0.00571576, 0.01349369,
0.00869288, 0.00996556, 0.01118461]],
'mean_score_time': array([0.03043761, 0.02483292, 0.02423148, 0.02861366, 0.03073673,
0.02782226, 0.0260221 , 0.0274972 , 0.02708578, 0.0293324 ,
0.02907505, 0.03212919, 0.02864561, 0.02656703, 0.02618027,
0.02890959, 0.0262691 , 0.02497063, 0.02794418, 0.02533493,
0.02524648, 0.02678137, 0.02670236, 0.02792902, 0.02961359,
0.02396159, 0.02608476, 0.02751431, 0.02692451, 0.02759552,
0.02572894, 0.02575765, 0.02614059, 0.02617168, 0.02431426,
0.02943802, 0.03063316, 0.0291533 , 0.02939343, 0.0252429 ,
0.02623062, 0.02375879, 0.02351151, 0.02464814, 0.02297344,
0.02930145, 0.02435064, 0.02751446, 0.02846198, 0.02608972,
0.02889452, 0.02613664, 0.02877312, 0.02744503, 0.02943301,
0.02568893, 0.02148175, 0.02596793, 0.02304382, 0.02534838,
0.02691402, 0.02919483, 0.0254488 , 0.02686 , 0.02757573,
0.02644744, 0.02747955, 0.03030705, 0.02656212, 0.02728405,
0.02782664, 0.02881432, 0.02833233, 0.02829609, 0.02849884,
0.02663026, 0.02971301, 0.0288321 , 0.0270597 , 0.02685165,
0.02643981, 0.02671041, 0.0297729 , 0.02677631, 0.02541375,
0.02434425, 0.02793174, 0.02609591, 0.02858057, 0.02816148,
0.02917194, 0.02805467, 0.02954979, 0.02664537, 0.02744985,
0.02647276, 0.02745419, 0.02643156, 0.02681336, 0.02343988,
0.02953992, 0.02583227, 0.02661901, 0.02764502, 0.02253036,
0.02985873, 0.02739677, 0.0240314 ]),
'std_score_time': array([0.01610018, 0.00565463, 0.00403194, 0.00441602, 0.00575156,
0.00342729, 0.00146189, 0.00619727, 0.00247171, 0.00253318,
0.00542152, 0.00547613, 0.00539285, 0.00223179, 0.00134845,
0.00691332, 0.00208849, 0.00357782, 0.00373117, 0.00090016,
```





```
{'colsample_bytree': 0.74, 'subsample': 0.78},
{'colsample_bytree': 0.74, 'subsample': 0.8},
{'colsample_bytree': 0.74, 'subsample': 0.82},
{'colsample_bytree': 0.74, 'subsample': 0.84},
{'colsample_bytree': 0.74, 'subsample': 0.86},
{'colsample_bytree': 0.74, 'subsample': 0.88},
{'colsample_bytree': 0.74, 'subsample': 0.9},
{'colsample_bytree': 0.74, 'subsample': 0.92},
{'colsample_bytree': 0.74, 'subsample': 0.94},
{'colsample_bytree': 0.74, 'subsample': 0.96},
{'colsample_bytree': 0.76, 'subsample': 0.7},
{'colsample_bytree': 0.76, 'subsample': 0.76},
{'colsample_bytree': 0.76, 'subsample': 0.78},
{'colsample_bytree': 0.76, 'subsample': 0.8},
{'colsample_bytree': 0.76, 'subsample': 0.82},
{'colsample_bytree': 0.76, 'subsample': 0.84},
{'colsample_bytree': 0.76, 'subsample': 0.86},
{'colsample_bytree': 0.76, 'subsample': 0.88},
{'colsample_bytree': 0.76, 'subsample': 0.9},
{'colsample_bytree': 0.76, 'subsample': 0.92},
{'colsample_bytree': 0.76, 'subsample': 0.94},
{'colsample_bytree': 0.76, 'subsample': 0.96},
{'colsample_bytree': 0.78, 'subsample': 0.7},
{'colsample_bytree': 0.78, 'subsample': 0.76},
{'colsample_bytree': 0.78, 'subsample': 0.78},
{'colsample_bytree': 0.78, 'subsample': 0.8},
{'colsample_bytree': 0.78, 'subsample': 0.82},
{'colsample_bytree': 0.78, 'subsample': 0.84},
{'colsample_bytree': 0.78, 'subsample': 0.86},
{'colsample_bytree': 0.78, 'subsample': 0.88},
{'colsample_bytree': 0.78, 'subsample': 0.9},
{'colsample_bytree': 0.78, 'subsample': 0.92},
{'colsample_bytree': 0.78, 'subsample': 0.94},
{'colsample_bytree': 0.78, 'subsample': 0.96},
{'colsample_bytree': 0.8, 'subsample': 0.7},
{'colsample_bytree': 0.8, 'subsample': 0.76},
{'colsample_bytree': 0.8, 'subsample': 0.78},
{'colsample_bytree': 0.8, 'subsample': 0.8},
{'colsample_bytree': 0.8, 'subsample': 0.82},
{'colsample_bytree': 0.8, 'subsample': 0.84},
{'colsample_bytree': 0.8, 'subsample': 0.86},
{'colsample_bytree': 0.8, 'subsample': 0.88},
{'colsample_bytree': 0.8, 'subsample': 0.9},
{'colsample_bytree': 0.8, 'subsample': 0.92},
```

```
{'colsample_bytree': 0.8, 'subsample': 0.94},
{'colsample_bytree': 0.8, 'subsample': 0.96},
{'colsample_bytree': 0.92, 'subsample': 0.7},
{'colsample_bytree': 0.92, 'subsample': 0.76},
{'colsample_bytree': 0.92, 'subsample': 0.78},
{'colsample_bytree': 0.92, 'subsample': 0.8},
{'colsample_bytree': 0.92, 'subsample': 0.82},
{'colsample_bytree': 0.92, 'subsample': 0.84},
{'colsample_bytree': 0.92, 'subsample': 0.86},
{'colsample_bytree': 0.92, 'subsample': 0.88},
{'colsample_bytree': 0.92, 'subsample': 0.9},
{'colsample_bytree': 0.92, 'subsample': 0.92},
{'colsample_bytree': 0.92, 'subsample': 0.94},
{'colsample_bytree': 0.92, 'subsample': 0.96},
{'colsample_bytree': 0.94, 'subsample': 0.7},
{'colsample_bytree': 0.94, 'subsample': 0.76},
{'colsample_bytree': 0.94, 'subsample': 0.78},
{'colsample_bytree': 0.94, 'subsample': 0.8},
{'colsample_bytree': 0.94, 'subsample': 0.82},
{'colsample_bytree': 0.94, 'subsample': 0.84},
{'colsample_bytree': 0.94, 'subsample': 0.86},
{'colsample_bytree': 0.94, 'subsample': 0.88},
{'colsample_bytree': 0.94, 'subsample': 0.9},
{'colsample_bytree': 0.94, 'subsample': 0.92},
{'colsample_bytree': 0.94, 'subsample': 0.94},
{'colsample_bytree': 0.94, 'subsample': 0.96},
{'colsample_bytree': 0.96, 'subsample': 0.7},
{'colsample_bytree': 0.96, 'subsample': 0.76},
{'colsample_bytree': 0.96, 'subsample': 0.78},
{'colsample_bytree': 0.96, 'subsample': 0.8},
{'colsample_bytree': 0.96, 'subsample': 0.82},
{'colsample_bytree': 0.96, 'subsample': 0.84},
{'colsample_bytree': 0.96, 'subsample': 0.86},
{'colsample_bytree': 0.96, 'subsample': 0.88},
{'colsample_bytree': 0.96, 'subsample': 0.9},
{'colsample_bytree': 0.96, 'subsample': 0.92},
{'colsample_bytree': 0.96, 'subsample': 0.94},
{'colsample_bytree': 0.96, 'subsample': 0.96},
{'colsample_bytree': 0.98, 'subsample': 0.7},
{'colsample_bytree': 0.98, 'subsample': 0.76},
{'colsample_bytree': 0.98, 'subsample': 0.78},
{'colsample_bytree': 0.98, 'subsample': 0.8},
{'colsample_bytree': 0.98, 'subsample': 0.82},
{'colsample_bytree': 0.98, 'subsample': 0.84},
```

```
{'colsample_bytree': 0.98, 'subsample': 0.86},
{'colsample_bytree': 0.98, 'subsample': 0.88},
{'colsample_bytree': 0.98, 'subsample': 0.9},
{'colsample_bytree': 0.98, 'subsample': 0.92},
{'colsample_bytree': 0.98, 'subsample': 0.94},
{'colsample_bytree': 0.98, 'subsample': 0.96}],
'split0_test_score': array([-1.11358096, -0.97763429, -1.10001639, -1.09796477, -1.05104277,
-1.10026288, -1.08301158, -1.08385207, -1.25034077, -1.16076653,
-1.21639456, -1.20032907, -1.11358096, -0.97763429, -1.10001639,
-1.09796477, -1.05104277, -1.10026288, -1.08301158, -1.08385207,
-1.25034077, -1.16076653, -1.21639456, -1.20032907, -1.11358096,
-0.97763429, -1.10001639, -1.09796477, -1.05104277, -1.10026288,
-1.08301158, -1.08385207, -1.25034077, -1.16076653, -1.21639456,
-1.20032907, -1.17671299, -0.99401702, -1.09732995, -1.09534366,
-1.07043105, -1.07800143, -1.07929056, -1.12111204, -1.14313029,
-1.06366899, -1.08382296, -1.0932959 , -1.17671299, -0.99401702,
-1.09732995, -1.09534366, -1.07043105, -1.07800143, -1.07929056,
-1.12111204, -1.14313029, -1.06366899, -1.08382296, -1.0932959 ,
-1.17671299, -0.99906933, -1.09732995, -1.09534366, -1.07043105,
-1.07800143, -1.07929056, -1.12111204, -1.14799975, -1.06366899,
-1.06752785, -1.0932959 , -1.17671299, -0.99906933, -1.09732995,
-1.09534366, -1.07043105, -1.07800143, -1.07929056, -1.12111204,
-1.14799975, -1.06366899, -1.06752785, -1.0932959 , -1.17671299,
-0.99906933, -1.09732995, -1.09534366, -1.07043105, -1.07800143,
-1.07929056, -1.12111204, -1.14799975, -1.06366899, -1.06752785,
-1.0932959 , -1.17671299, -0.99906933, -1.09732995, -1.09534366,
-1.07043105, -1.07800143, -1.07929056, -1.12111204, -1.14799975,
-1.06366899, -1.06752785, -1.0932959 ]),
'split1_test_score': array([-0.8713116 , -0.81423748, -0.33221742, -0.347244 , -0.49271105,
-0.40168283, -0.45031725, -0.44282323, -0.75686897, -0.75381908,
-0.7480585 , -0.78534999, -0.8713116 , -0.81423748, -0.33221742,
-0.347244 , -0.49271105, -0.40168283, -0.45031725, -0.44282323,
-0.75686897, -0.75381908, -0.7480585 , -0.78534999, -0.8713116 ,
-0.81423748, -0.33221742, -0.347244 , -0.49271105, -0.40168283,
-0.45031725, -0.44282323, -0.75686897, -0.75381908, -0.7480585 ,
-0.78534999, -0.9329267 , -0.79714955, -0.35040507, -0.37857707,
-0.43205352, -0.27699849, -0.3242961 , -0.36763796, -0.67962895,
-0.61535246, -0.65201628, -0.65173063, -0.9329267 , -0.79714955,
-0.35040507, -0.37857707, -0.43205352, -0.27699849, -0.3242961 ,
-0.36763796, -0.67962895, -0.61535246, -0.65201628, -0.65173063,
-0.75044675, -0.81214415, -0.16750122, -0.18404703, -0.27762374,
-0.27610083, -0.30694751, -0.30653823, -0.62223933, -0.48758891,
-0.57003506, -0.56975298, -0.75044675, -0.81214415, -0.16750122,
-0.18404703, -0.27762374, -0.27610083, -0.30694751, -0.30653823,
```

```
-0.62223933, -0.48758891, -0.57003506, -0.56975298, -0.75044675,  
-0.81214415, -0.16750122, -0.18404703, -0.27762374, -0.27610083,  
-0.30694751, -0.30653823, -0.62223933, -0.48758891, -0.57003506,  
-0.56975298, -0.75044675, -0.81214415, -0.16750122, -0.18404703,  
-0.27762374, -0.27610083, -0.30694751, -0.30653823, -0.62223933,  
-0.48758891, -0.57003506, -0.56975298)),  
'split2_test_score': array([-0.6220898, -0.48717361, -0.50138114, -0.50421403, -0.46209917,  
-0.4729481, -0.54473443, -0.54968504, -0.49025561, -0.49051749,  
-0.56574639, -0.56544169, -0.6220898, -0.48717361, -0.50138114,  
-0.50421403, -0.46209917, -0.4729481, -0.54473443, -0.54968504,  
-0.49025561, -0.49051749, -0.56574639, -0.56544169, -0.6220898,  
-0.48717361, -0.50138114, -0.50421403, -0.46209917, -0.4729481,  
-0.54473443, -0.54968504, -0.49025561, -0.49051749, -0.56574639,  
-0.56544169, -0.66303517, -0.46910806, -0.48442398, -0.42838537,  
-0.44734306, -0.43537083, -0.53492137, -0.53965007, -0.45107578,  
-0.43007623, -0.52260111, -0.52252268, -0.66303517, -0.46910806,  
-0.48442398, -0.42838537, -0.44734306, -0.43537083, -0.53492137,  
-0.53965007, -0.45107578, -0.43007623, -0.52260111, -0.52252268,  
-0.66303517, -0.47550426, -0.49053583, -0.42838537, -0.44734306,  
-0.45502927, -0.53492137, -0.53965007, -0.45107578, -0.43007623,  
-0.52260111, -0.52252268, -0.66303517, -0.47550426, -0.49053583,  
-0.42838537, -0.44734306, -0.45502927, -0.53492137, -0.53965007,  
-0.45107578, -0.43007623, -0.52260111, -0.52252268, -0.66303517,  
-0.47550426, -0.49053583, -0.42838537, -0.44734306, -0.45502927,  
-0.53492137, -0.53965007, -0.45107578, -0.43007623, -0.52260111,  
-0.52252268, -0.66303517, -0.47550426, -0.49053583, -0.42838537,  
-0.44734306, -0.45502927, -0.53492137, -0.53965007, -0.45107578,  
-0.43007623, -0.52260111, -0.52252268]),  
'split3_test_score': array([-0.55286462, -0.55901694, -0.50025741, -0.50025741, -0.46738444,  
-0.46843921, -0.33589202, -0.40082224, -0.3299186, -0.45749878,  
-0.34032706, -0.34032706, -0.55286462, -0.55901694, -0.50025741,  
-0.50025741, -0.46738444, -0.46843921, -0.33589202, -0.40082224,  
-0.3299186, -0.45749878, -0.34032706, -0.34032706, -0.55286462,  
-0.55901694, -0.50025741, -0.50025741, -0.46738444, -0.46843921,  
-0.33589202, -0.40082224, -0.3299186, -0.45749878, -0.34032706,  
-0.34032706, -0.71581645, -0.57958058, -0.39094754, -0.39094754,  
-0.49543753, -0.45908002, -0.47027485, -0.40596381, -0.42666085,  
-0.39882041, -0.31005834, -0.31005834, -0.71581645, -0.57958058,  
-0.39094754, -0.39094754, -0.49543753, -0.45908002, -0.47027485,  
-0.40596381, -0.42666085, -0.39882041, -0.31005834, -0.31005834,  
-0.88389703, -0.45931356, -0.3623849, -0.3623849, -0.43406605,  
-0.45004295, -0.4957871, -0.52126332, -0.36999071, -0.48606413,  
-0.50506391, -0.50506391, -0.88389703, -0.45931356, -0.3623849,  
-0.3623849, -0.43406605, -0.45004295, -0.4957871, -0.52126332,
```

```
-0.36999071, -0.48606413, -0.50506391, -0.50506391, -0.88389703,  
-0.45931356, -0.3623849 , -0.3623849 , -0.43406605, -0.45004295,  
-0.4957871 , -0.52126332, -0.36999071, -0.48606413, -0.50506391,  
-0.50506391, -0.88389703, -0.45931356, -0.3623849 , -0.3623849 ,  
-0.43406605, -0.45004295, -0.4957871 , -0.52126332, -0.36999071,  
-0.48606413, -0.50506391, -0.50506391)),  
'split4_test_score': array([-1.59742587, -1.52675168, -1.62275389, -1.62275389, -1.62851839,  
-1.55198012, -1.55640157, -1.46936231, -1.51521598, -1.49921314,  
-1.50280715, -1.50280715, -1.59742587, -1.52675168, -1.62275389,  
-1.62275389, -1.62851839, -1.55198012, -1.55640157, -1.46936231,  
-1.51521598, -1.49921314, -1.50280715, -1.50280715, -1.59742587,  
-1.52675168, -1.62275389, -1.62275389, -1.62851839, -1.55198012,  
-1.55640157, -1.46936231, -1.51521598, -1.49921314, -1.50280715,  
-1.50280715, -1.63652343, -1.49228563, -1.58892687, -1.58892687,  
-1.58869688, -1.5023968 , -1.59110088, -1.46562217, -1.42863989,  
-1.41875158, -1.47266882, -1.47266882, -1.63652343, -1.49228563,  
-1.58892687, -1.58892687, -1.58869688, -1.5023968 , -1.59110088,  
-1.46562217, -1.42863989, -1.41875158, -1.47266882, -1.47266882,  
-1.50120299, -1.44495062, -1.44418603, -1.44418603, -1.57176072,  
-1.47812293, -1.47966554, -1.44124527, -1.53226375, -1.47781385,  
-1.4470047 , -1.4470047 , -1.50120299, -1.44495062, -1.44418603,  
-1.44418603, -1.57176072, -1.47812293, -1.47966554, -1.44124527,  
-1.53226375, -1.47781385, -1.4470047 , -1.4470047 , -1.50120299,  
-1.44495062, -1.44418603, -1.44418603, -1.57176072, -1.47812293,  
-1.47966554, -1.44124527, -1.53226375, -1.47781385, -1.4470047 ,  
-1.4470047 , -1.50120299, -1.44495062, -1.44418603, -1.44418603,  
-1.57176072, -1.47812293, -1.47966554, -1.44124527, -1.53226375,  
-1.47781385, -1.4470047 , -1.4470047 ]),  
'mean_test_score': array([-0.95145457, -0.8729628 , -0.81132525, -0.81448682, -0.82035116,  
-0.79906263, -0.79407137, -0.78930898, -0.86851999, -0.87236301,  
-0.87466673, -0.87885099, -0.95145457, -0.8729628 , -0.81132525,  
-0.81448682, -0.82035116, -0.79906263, -0.79407137, -0.78930898,  
-0.86851999, -0.87236301, -0.87466673, -0.87885099, -0.95145457,  
-0.8729628 , -0.81132525, -0.81448682, -0.82035116, -0.79906263,  
-0.79407137, -0.78930898, -0.86851999, -0.87236301, -0.87466673,  
-0.87885099, -1.02500295, -0.86642817, -0.78240668, -0.7764361 ,  
-0.80679241, -0.75036952, -0.79997675, -0.77999721, -0.82582715,  
-0.78533393, -0.8082335 , -0.81005527, -1.02500295, -0.86642817,  
-0.78240668, -0.7764361 , -0.80679241, -0.75036952, -0.79997675,  
-0.77999721, -0.82582715, -0.78533393, -0.8082335 , -0.81005527,  
-0.99505898, -0.83819639, -0.71238758, -0.7028694 , -0.76024492,  
-0.74745948, -0.77932241, -0.78596179, -0.82471387, -0.78904242,  
-0.82244653, -0.82752803, -0.99505898, -0.83819639, -0.71238758,  
-0.7028694 , -0.76024492, -0.74745948, -0.77932241, -0.78596179,
```

```

-0.82471387, -0.78904242, -0.82244653, -0.82752803, -0.99505898,
-0.83819639, -0.71238758, -0.7028694 , -0.76024492, -0.74745948,
-0.77932241, -0.78596179, -0.82471387, -0.78904242, -0.82244653,
-0.82752803, -0.99505898, -0.83819639, -0.71238758, -0.7028694 ,
-0.76024492, -0.74745948, -0.77932241, -0.78596179, -0.82471387,
-0.78904242, -0.82244653, -0.82752803]),
'std_test_score': array([0.3787722 , 0.37127887, 0.48252086, 0.47895315, 0.46187248,
0.45413205, 0.45932514, 0.41895635, 0.44936492, 0.40201708,
0.42622027, 0.42181638, 0.3787722 , 0.37127887, 0.48252086,
0.47895315, 0.46187248, 0.45413205, 0.45932514, 0.41895635,
0.44936492, 0.40201708, 0.42622027, 0.42181638, 0.3787722 ,
0.37127887, 0.48252086, 0.47895315, 0.46187248, 0.45413205,
0.45932514, 0.41895635, 0.44936492, 0.40201708, 0.42622027,
0.42181638, 0.35554697, 0.36136431, 0.48545047, 0.48782698,
0.45770184, 0.46498206, 0.47098267, 0.43684066, 0.39628543,
0.39577336, 0.41751455, 0.41881275, 0.35554697, 0.36136431,
0.48545047, 0.48782698, 0.45770184, 0.46498206, 0.47098267,
0.43684066, 0.39628543, 0.39577336, 0.41751455, 0.41881275,
0.30711948, 0.36600746, 0.48006892, 0.48250061, 0.48826156,
0.45591184, 0.4344476 , 0.42480674, 0.44553678, 0.41505484,
0.37536338, 0.37890454, 0.30711948, 0.36600746, 0.48006892,
0.48250061, 0.48826156, 0.45591184, 0.4344476 , 0.42480674,
0.44553678, 0.41505484, 0.37536338, 0.37890454, 0.30711948,
0.36600746, 0.48006892, 0.48250061, 0.48826156, 0.45591184,
0.4344476 , 0.42480674, 0.44553678, 0.41505484, 0.37536338,
0.37890454, 0.30711948, 0.36600746, 0.48006892, 0.48250061,
0.48826156, 0.45591184, 0.4344476 , 0.42480674, 0.44553678,
0.41505484, 0.37536338, 0.37890454]),
'rank_test_score': array([[100, 91, 56, 59, 62, 45, 42, 39, 85, 88, 94, 97, 100,
91, 56, 59, 62, 45, 42, 39, 85, 88, 94, 97, 100, 91,
56, 59, 62, 45, 42, 39, 85, 88, 94, 97, 107, 83, 27,
19, 50, 13, 48, 25, 73, 29, 52, 54, 107, 83, 27, 19,
50, 13, 48, 25, 73, 29, 52, 54, 103, 79, 5, 1, 15,
9, 21, 31, 69, 35, 65, 75, 103, 79, 5, 1, 15, 9,
21, 31, 69, 35, 65, 75, 103, 79, 5, 1, 15, 9, 21,
31, 69, 35, 65, 75, 103, 79, 5, 1, 15, 9, 21, 31,
69, 35, 65, 75], dtype=int32)),
{'colsample_bytree': 0.92, 'subsample': 0.8},
-0.7028693982744602)

```

Here, we can see the improvement in rmse. So the final parameters are:

- `colsample_bytree: 0.92`
- `subsample: 0.8`

### 3.5 Tune Regularization Parameters

We've tuned gamma before. Next step is to tune other regularization parameter to reduce overfitting. Though many people don't use this parameters much as gamma provides a substantial way of controlling complexity. But we should always try it.

```
xgb_regression = xgb.XGBRegressor(verbosity=0,
    learning_rate =0.1,
    n_estimators=10,
    max_depth=2,
    min_child_weight=1,
    gamma=0,
    subsample=0.8,
    colsample_bytree=0.92,
    nthread=4,
    seed=123)

param_test5 = {'reg_alpha': [0.0001,0.001, 0.01, 0.1, 1,10,100, 1000]}
grid_search5 = GridSearchCV(estimator = xgb_regression,
    param_grid = param_test5,
    #scoring="r2",
    scoring="neg_root_mean_squared_error",
    n_jobs=4,
    cv=5)

grid_search5.fit(X_train_sf,y_train)
grid_search5.cv_results_, grid_search5.best_params_, grid_search5.best_score_
({'mean_fit_time': array([0.02360191, 0.03090887, 0.03145518, 0.05858536, 0.0575839 ,
    0.06168342, 0.05740004, 0.05503716]),
    'std_fit_time': array([0.00408096, 0.02304609, 0.0176919 , 0.00354492, 0.01313541,
    0.01305938, 0.00988973, 0.01071927]),
    'mean_score_time': array([0.02460256, 0.02507486, 0.02672658, 0.02819185, 0.02725749,
    0.02602897, 0.02613659, 0.0254406 ]),
    'std_score_time': array([0.00643058, 0.00313857, 0.0021861 , 0.0025608 , 0.00254516,
    0.00430522, 0.00238913, 0.00465337]),
    'param_reg_alpha': masked_array(data=[0.0001, 0.001, 0.01, 0.1, 1, 10, 100, 1000],
    mask=[False, False, False, False, False, False, False, False],
    fill_value='?',
    dtype=object),
    'params': [{'reg_alpha': 0.0001},
    {'reg_alpha': 0.001},
    {'reg_alpha': 0.01},
    {'reg_alpha': 0.1},
```

```

{'reg_alpha': 1},
{'reg_alpha': 10},
{'reg_alpha': 100},
{'reg_alpha': 1000}],
'split0_test_score': array([-2.3577017 , -2.3577514 , -2.35824856, -2.35141093, -2.41864776,
    -2.87959653, -4.63541223, -4.63541223]),
'split1_test_score': array([-1.52368288, -1.52373738, -1.52428357, -1.54653009, -1.58691669,
    -2.01729806, -3.84824164, -3.84824164]),
'split2_test_score': array([-1.68465221, -1.68471139, -1.68530478, -1.68746556, -1.74699276,
    -2.11836324, -3.81491961, -3.81491961]),
'split3_test_score': array([-2.02970257, -2.02977792, -2.03053148, -2.05975842, -2.185863 ,
    -2.57029067, -4.21319765, -4.21319765]),
'split4_test_score': array([-1.76414302, -1.76417648, -1.76451234, -1.83736731, -1.87740033,
    -1.97477388, -3.14188985, -3.14188985]),
'mean_test_score': array([-1.87197648, -1.87203091, -1.87257615, -1.89650646, -1.96316411,
    -2.31206447, -3.9307322 , -3.9307322 ]),
'std_test_score': array([0.29285948, 0.29286109, 0.29287665, 0.28399587, 0.30090123,
    0.35410331, 0.49373073, 0.49373073]),
'rank_test_score': array([1, 2, 3, 4, 5, 6, 7, 7], dtype=int32)},
{'reg_alpha': 0.0001},
-1.8719764764671498)

```

The values of `reg_alpha` we tried here are very widespread. Now we can vary values closer to the optimum here (0.0001) to see if we can improve model performance.

```

xgb_regression = xgb.XGBRegressor(verbosity=0,
    learning_rate=0.1,
    n_estimators=10,
    max_depth=2,
    min_child_weight=1,
    gamma=0,
    subsample=0.8,
    colsample_bytree=0.92,
    nthread=4,
    seed=123)

param_test6 = {'reg_alpha': [0.00001, 0.00005, 0.0001, 0.0002, 0.0004, 0.0006, 0.001]}
grid_search6 = GridSearchCV(estimator = xgb_regression,
    param_grid = param_test6,
    #scoring="r2",
    scoring="neg_root_mean_squared_error",
    n_jobs=4,
    cv=5)
grid_search6.fit(X_train_sf, y_train)

```

```

grid_search6.cv_results_, grid_search6.best_params_, grid_search6.best_score_
({'mean_fit_time': array([0.02480679, 0.02565174, 0.03140278, 0.04962902, 0.04047127,
0.06541271, 0.0636044 ]),
 'std_fit_time': array([0.01009876, 0.01615063, 0.0201472 , 0.01011704, 0.01403234,
0.01295107, 0.01090667]),
 'mean_score_time': array([0.03001432, 0.02499027, 0.0311058 , 0.03339276, 0.03264608,
0.02313228, 0.01925559]),
 'std_score_time': array([0.01213803, 0.01185257, 0.00335911, 0.00285216, 0.00105785,
0.00402034, 0.00483799]),
 'param_reg_alpha': masked_array(data=[1e-05, 5e-05, 0.0001, 0.0002, 0.0004, 0.0006, 0.001],
mask=[False, False, False, False, False, False, False],
fill_value='?',
dtype=object),
 'params': [{'reg_alpha': 1e-05},
{'reg_alpha': 5e-05},
{'reg_alpha': 0.0001},
{'reg_alpha': 0.0002},
{'reg_alpha': 0.0004},
{'reg_alpha': 0.0006},
{'reg_alpha': 0.001}],
 'split0_test_score': array([-2.35769686, -2.35769884, -2.3577017 , -2.35770738, -2.35771837,
-2.3577294 , -2.3577514 ]),
 'split1_test_score': array([-1.52367736, -1.52367985, -1.52368288, -1.52368887, -1.52370103,
-1.52371323, -1.52373738]),
 'split2_test_score': array([-1.68464635, -1.68464889, -1.68465221, -1.68465885, -1.68467194,
-1.68468523, -1.68471139]),
 'split3_test_score': array([-2.02969501, -2.02969849, -2.02970257, -2.02971089, -2.02972753,
-2.0297444 , -2.02977792]),
 'split4_test_score': array([-1.7641396 , -1.76414114, -1.76414302, -1.76414676, -1.76415412,
-1.76416164, -1.76417648]),
 'mean_test_score': array([-1.87197103, -1.87197344, -1.87197648, -1.87198255, -1.8719946 ,
-1.87200678, -1.87203091]),
 'std_test_score': array([0.29285938, 0.29285938, 0.29285948, 0.29285971, 0.29286004,
0.29286036, 0.29286109]),
 'rank_test_score': array([1, 2, 3, 4, 5, 6, 7], dtype=int32)},
{'reg_alpha': 1e-05},
-1.8719710349325402)

```

We can see that by using `reg_alpha = 1e-05` we slightly improved the negative rmse from `-1.8719764764671498` to `-1.8719710349325402`. Now we can apply this regularization in the model and look at the model performance

```

xgb_regression = xgb.XGBRegressor(verbosity=0,
learning_rate=0.3,
n_estimators=15,

```

```

        max_depth=2,
        min_child_weight=1,
        gamma=0,
        subsample=0.8,
        colsample_bytree=0.92,
        nthread=4,
        rel_alpha = 1e-5,
        seed=123)
data_dmatrix = xgb.DMatrix(data=X,label=y)
parameters = {
    'n_estimator': 15,
    'colsample_bytree': 0.92,
    'min_child_weight': 1,
    'subsample': 0.8,
    'learning_rate': 0.3, #so called `eta` value
    'max_depth': 2,
    'gamma': 0,
    'reg_alpha': 1e-5
}
cv_results = xgb.cv(dtrain=data_dmatrix,
                    params=parameters, nfold=3,
                    early_stopping_rounds=10,
                    metrics="rmse",
                    as_pandas=True,
                    #seed = 123)
cv_results.head()

```

	train-rmse-mean	train-rmse-std	test-rmse-mean	test-rmse-std
0	2.891713	0.261630	3.125655	0.776508
1	2.184249	0.203646	2.516835	0.848750
2	1.650804	0.151039	2.134907	0.960433
3	1.265937	0.113924	1.906052	0.958654
4	1.000663	0.097936	1.814389	0.906569

Again we can see slight improvement in the score.

### 3.6 Tune learning rate and n\_estimators

Lastly, we can try to lower the learning rate and add more trees. We can still use the cv or grid search in this step.

```

xgb_regression = xgb.XGBRegressor(verbosity=0,
                                   max_depth=2,
                                   min_child_weight=1,
                                   gamma=0,

```

```

        subsample=0.8,
        colsample_bytree=0.92,
        nthread=4,
        rel_alpha = 1e-5,
        seed=123)

n_estimators = [10, 12, 14,16, 18, 20,22,24,26,28,30]
learning_rate = [0.01, 0.05, 0.1, 0.2, 0.3, 0.4]
param_grid = dict(learning_rate=learning_rate, n_estimators=n_estimators)

grid_search = GridSearchCV(xgb_regression, param_grid,
                           #scoring="r2",
                           scoring="neg_root_mean_squared_error",
                           n_jobs=-1,
                           cv=5)
grid_result = grid_search.fit(X_train_sf, y_train)
# summarize results
#print("Best: %f using %s" % (grid_result.cv_results_, grid_result.best_params_))
means = grid_result.cv_results_['mean_test_score']
stds = grid_result.cv_results_['std_test_score']
params = grid_result.cv_results_['params']
for mean, stdev, param in zip(means, stds, params):
    print("%f (%f) with: %r" % (mean, stdev, param))
# plot results
scores = np.array(means).reshape(len(learning_rate), len(n_estimators))
for i, value in enumerate(learning_rate):
    plt.plot(n_estimators, scores[i], label='learning_rate: ' + str(value))
plt.legend()
plt.xlabel('n_estimators')
plt.ylabel('neg_root_mean_squared_error')
plt.savefig('n_estimators_vs_learning_rate.png')
-3.617908 (0.467784) with: {'learning_rate': 0.01, 'n_estimators': 10}
-3.558153 (0.461864) with: {'learning_rate': 0.01, 'n_estimators': 12}
-3.499383 (0.456316) with: {'learning_rate': 0.01, 'n_estimators': 14}
-3.445866 (0.453383) with: {'learning_rate': 0.01, 'n_estimators': 16}
-3.390703 (0.449394) with: {'learning_rate': 0.01, 'n_estimators': 18}
-3.335714 (0.444753) with: {'learning_rate': 0.01, 'n_estimators': 20}
-3.281596 (0.440266) with: {'learning_rate': 0.01, 'n_estimators': 22}
-3.231424 (0.434958) with: {'learning_rate': 0.01, 'n_estimators': 24}
-3.181358 (0.431305) with: {'learning_rate': 0.01, 'n_estimators': 26}
-3.136978 (0.427972) with: {'learning_rate': 0.01, 'n_estimators': 28}
-3.094279 (0.427197) with: {'learning_rate': 0.01, 'n_estimators': 30}
-2.661680 (0.372440) with: {'learning_rate': 0.05, 'n_estimators': 10}
-2.465385 (0.355479) with: {'learning_rate': 0.05, 'n_estimators': 12}

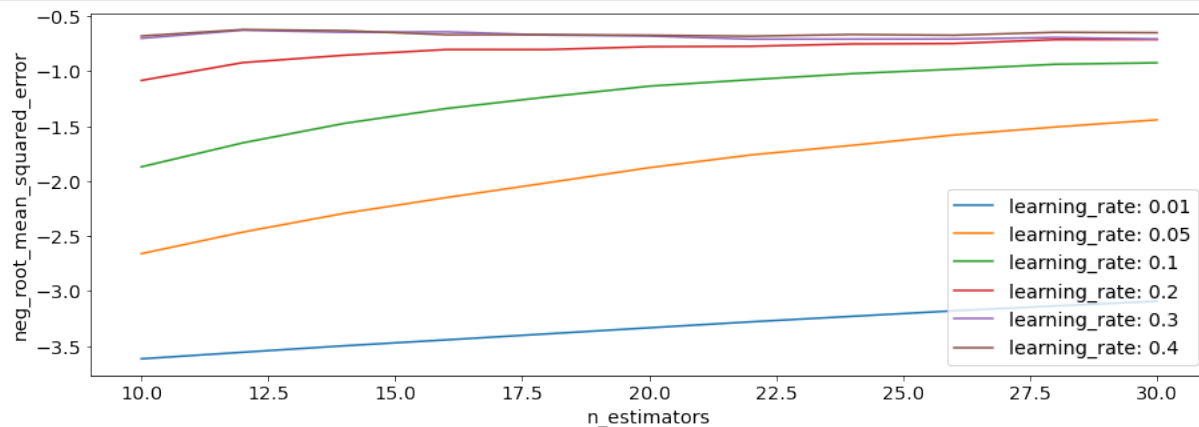
```

-2.294253 (0.338124) with: {'learning\_rate': 0.05, 'n\_estimators': 14}  
-2.151871 (0.321351) with: {'learning\_rate': 0.05, 'n\_estimators': 16}  
-2.016558 (0.317943) with: {'learning\_rate': 0.05, 'n\_estimators': 18}  
-1.879509 (0.304280) with: {'learning\_rate': 0.05, 'n\_estimators': 20}  
-1.763680 (0.293837) with: {'learning\_rate': 0.05, 'n\_estimators': 22}  
-1.676037 (0.280681) with: {'learning\_rate': 0.05, 'n\_estimators': 24}  
-1.581955 (0.285150) with: {'learning\_rate': 0.05, 'n\_estimators': 26}  
-1.509390 (0.277280) with: {'learning\_rate': 0.05, 'n\_estimators': 28}  
-1.444071 (0.280822) with: {'learning\_rate': 0.05, 'n\_estimators': 30}  
-1.871970 (0.292859) with: {'learning\_rate': 0.1, 'n\_estimators': 10}  
-1.653514 (0.268334) with: {'learning\_rate': 0.1, 'n\_estimators': 12}  
-1.476255 (0.256765) with: {'learning\_rate': 0.1, 'n\_estimators': 14}  
-1.341691 (0.257432) with: {'learning\_rate': 0.1, 'n\_estimators': 16}  
-1.235758 (0.273750) with: {'learning\_rate': 0.1, 'n\_estimators': 18}  
-1.138028 (0.286911) with: {'learning\_rate': 0.1, 'n\_estimators': 20}  
-1.078806 (0.316409) with: {'learning\_rate': 0.1, 'n\_estimators': 22}  
-1.023907 (0.344035) with: {'learning\_rate': 0.1, 'n\_estimators': 24}  
-0.983486 (0.353649) with: {'learning\_rate': 0.1, 'n\_estimators': 26}  
-0.938789 (0.342668) with: {'learning\_rate': 0.1, 'n\_estimators': 28}  
-0.925604 (0.342188) with: {'learning\_rate': 0.1, 'n\_estimators': 30}  
-1.086053 (0.389971) with: {'learning\_rate': 0.2, 'n\_estimators': 10}  
-0.923543 (0.410593) with: {'learning\_rate': 0.2, 'n\_estimators': 12}  
-0.856479 (0.435333) with: {'learning\_rate': 0.2, 'n\_estimators': 14}  
-0.804969 (0.429674) with: {'learning\_rate': 0.2, 'n\_estimators': 16}  
-0.805162 (0.424432) with: {'learning\_rate': 0.2, 'n\_estimators': 18}  
-0.779009 (0.398655) with: {'learning\_rate': 0.2, 'n\_estimators': 20}  
-0.775305 (0.421422) with: {'learning\_rate': 0.2, 'n\_estimators': 22}  
-0.754053 (0.415573) with: {'learning\_rate': 0.2, 'n\_estimators': 24}  
-0.750062 (0.416116) with: {'learning\_rate': 0.2, 'n\_estimators': 26}  
-0.714707 (0.413245) with: {'learning\_rate': 0.2, 'n\_estimators': 28}  
-0.713529 (0.419819) with: {'learning\_rate': 0.2, 'n\_estimators': 30}  
-0.702869 (0.482501) with: {'learning\_rate': 0.3, 'n\_estimators': 10}  
-0.628394 (0.476325) with: {'learning\_rate': 0.3, 'n\_estimators': 12}  
-0.647654 (0.466011) with: {'learning\_rate': 0.3, 'n\_estimators': 14}  
-0.643900 (0.438254) with: {'learning\_rate': 0.3, 'n\_estimators': 16}  
-0.672917 (0.413982) with: {'learning\_rate': 0.3, 'n\_estimators': 18}  
-0.681688 (0.381370) with: {'learning\_rate': 0.3, 'n\_estimators': 20}  
-0.710273 (0.389748) with: {'learning\_rate': 0.3, 'n\_estimators': 22}  
-0.710050 (0.348189) with: {'learning\_rate': 0.3, 'n\_estimators': 24}  
-0.708881 (0.318710) with: {'learning\_rate': 0.3, 'n\_estimators': 26}  
-0.695204 (0.286448) with: {'learning\_rate': 0.3, 'n\_estimators': 28}  
-0.709375 (0.285527) with: {'learning\_rate': 0.3, 'n\_estimators': 30}  
-0.681213 (0.433918) with: {'learning\_rate': 0.4, 'n\_estimators': 10}  
-0.623439 (0.394930) with: {'learning\_rate': 0.4, 'n\_estimators': 12}

```

-0.632964 (0.376784) with: {'learning_rate': 0.4, 'n_estimators': 14}
-0.670227 (0.334145) with: {'learning_rate': 0.4, 'n_estimators': 16}
-0.669563 (0.333634) with: {'learning_rate': 0.4, 'n_estimators': 18}
-0.674693 (0.297409) with: {'learning_rate': 0.4, 'n_estimators': 20}
-0.683293 (0.317645) with: {'learning_rate': 0.4, 'n_estimators': 22}
-0.667943 (0.312992) with: {'learning_rate': 0.4, 'n_estimators': 24}
-0.674831 (0.323050) with: {'learning_rate': 0.4, 'n_estimators': 26}
-0.647932 (0.305646) with: {'learning_rate': 0.4, 'n_estimators': 28}
-0.651709 (0.320892) with: {'learning_rate': 0.4, 'n_estimators': 30}

```



### 3.7 Save final model

Both functions `save_model` and `dump_model` save the model, the difference is that in `dump_model` we can save feature name and save tree in text format.

```

final_model = xgb_regression = xgb.XGBRegressor(verbosity=0,
        n_estimators = 20,
        learning_rate = 0.3,
        max_depth=2,
        min_child_weight=1,
        gamma=0,
        subsample=0.8,
        colsample_bytree=0.92,
        nthread=4,
        rel_alpha = 1e-5,
        seed=123)
final_model.fit(X_train_sf, y_train)
XGBRegressor(base_score=0.5, booster='gbtree', colsample_bylevel=1,
        colsample_bynode=1, colsample_bytree=0.92, gamma=0, gpu_id=-1,
        importance_type='gain', interaction_constraints='',
        learning_rate=0.3, max_delta_step=0, max_depth=2,
        min_child_weight=1, missing=nan, monotone_constraints=''),

```

```

n_estimators=20, n_jobs=4, nthread=4, num_parallel_tree=1,
random_state=123, reg_alpha=0, reg_lambda=1, rel_alpha=1e-05,
scale_pos_weight=1, seed=123, subsample=0.8, tree_method='exact',
validate_parameters=1, verbosity=0)
final_model.save_model('final_model.json')

```

#### 4. Make predictions

Next, we can make predictions using the test dataset and then check the prediction accuracy. Here, we'll use RMSE, MAE, and R2 as accuracy metrics.

```

y_pred = final_model.predict(X_test_sf)
mse = mean_squared_error(y_test, y_pred)
print("MSE: %.2f" % mse)
MSE: 3.35
print("RMSE: %.2f" % (mse**(1/2.0)))
RMSE: 1.83
MSE: 0.15
RMSE: 0.39
cv = KFold(n_splits=10, shuffle=True, random_state=123)
kf_cv_scores = cross_val_score(m_2, X, y, scoring='neg_root_mean_squared_error', cv=cv, n_j
obs=-1, error_score='raise')
print('RMSE/neg_root_mean_squared_error: mean %.3f std %.3f' % (np.mean(kf_cv_scores
), np.std(kf_cv_scores)))
RMSE/neg_root_mean_squared_error: mean -0.557 std 0.434

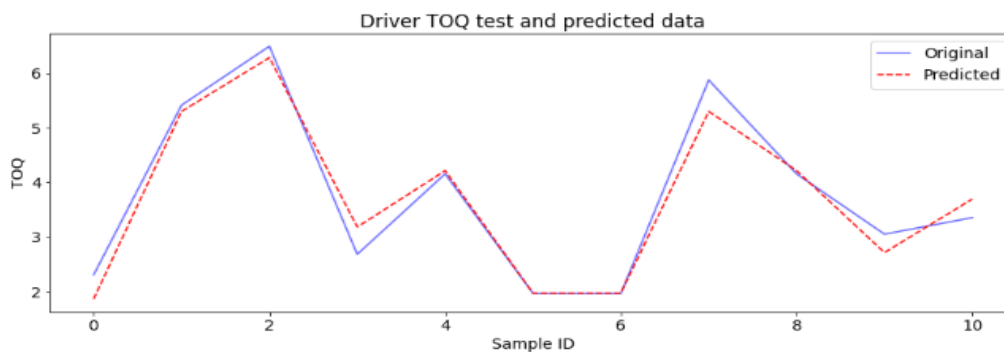
```

Finally, we can visualize the original and predicted test data

```

x_ax = range(len(y_test))
plt.plot(x_ax, y_test, label="Original", color="blue", alpha = 0.6)
plt.plot(x_ax, y_pred, label="Predicted", color="red", linestyle='--')
plt.title("Driver TOQ test and predicted data",fontsize=17)
plt.xlabel('Sample ID',fontsize=14)
plt.ylabel('TOQ',fontsize=14)
plt.legend()
plt.show

```



## References

- AASHTO, 2001. A Policy on geometric design of highways and streets, American Association of State Highway and Transportation Officials.
- Ahn, H., Del Vecchio, D., 2018. Safety Verification and Control for Collision Avoidance at Road Intersections. *IEEE Trans. Automat. Contr.* 63, 630–642. <https://doi.org/10.1109/TAC.2017.2729661>
- AiMotive, 2018. AiMotive Disengagement Report.
- Alhajyaseen, W.K.M., 2015. The Integration of Conflict Probability and Severity for the Safety Assessment of Intersections. *Arab. J. Sci. Eng.* 40, 421–430. <https://doi.org/10.1007/s13369-014-1553-1>
- Alonso, J., Milanés, V., Pérez, J., Onieva, E., González, C., de Pedro, T., 2011. Autonomous vehicle control systems for safe crossroads. *Transp. Res. Part C Emerg. Technol.* 19, 1095–1110. <https://doi.org/10.1016/J.TRC.2011.06.002>
- Amezquita-Semprun, K., Pradeep, Y.C., Del Rosario, M., Chen, W., Zhao, Z., Chen, P.C.Y., 2018. A Practical Evaluation of the Stimuli-Induced Equilibrium Point for Assistance Ramp Merging Systems, in: 2018 IEEE International Conference on Intelligence and Safety for Robotics (ISR). IEEE, pp. 417–422. <https://doi.org/10.1109/IISR.2018.8535947>
- Apple, 2018a. Apple Disengagement Cover Letter.
- Apple, 2018b. Apple Annual Report of Autonomous Vehicle Disengagement.
- Apple, 2018c. Apple disengagement report.
- Audi, 2017. Automated driving at a new level: The Audi AI traffic jam pilot | Audi MediaCenter [WWW Document]. URL <https://www.audi-mediacycenter.com/en/techday-piloted-driving-the-traffic-jam-pilot-in-the-new-audi-a8-9276/automated-driving-at-a-new-level-the-audi-ai-traffic-jam-pilot-9283> (accessed 3.17.19).
- Aurora, 2018. Aurora Innovation Disengagement Report 2018.
- AutoX, 2018. AutoX Disengagement Report.
- Azimi, R., Bhatia, G., Rajkumar, R., Mudalige, P., 2015. Ballroom Intersection Protocol: Synchronous Autonomous Driving at Intersections, in: 2015 IEEE 21st International Conference on Embedded and Real-Time Computing Systems and Applications. IEEE, pp. 167–175. <https://doi.org/10.1109/RTCSA.2015.20>
- Azimi, R., Bhatia, G., Rajkumar, R., Mudalige, P., 2013. V2V-Intersection Management at Roundabouts. *SAE Int. J. Passeng. Cars - Mech. Syst.* 6, 2013-01–0722. <https://doi.org/10.4271/2013-01-0722>
- Azimi, R., Bhatia, G., Rajkumar, R.R., Mudalige, P., 2014. STIP: Spatio-temporal intersection protocols for autonomous vehicles, in: 2014 ACM/IEEE International Conference on Cyber-Physical Systems (ICCPS). IEEE, pp. 1–12. <https://doi.org/10.1109/ICCPS.2014.6843706>
- Baber, J., Kolodko, J., Noel, T., Parent, M., Vlacic, L., 2005. Cooperative autonomous driving -

- Intelligent vehicles sharing city roads cooperative autonomous driving. *IEEE Robot. Autom. Mag.* 12, 44–49. <https://doi.org/10.1109/MRA.2005.1411418>
- Baber, Jonathan, Kolodko, J., Noël, T., Parent, M., Vlacic, L., 2005. Cooperative autonomous driving: Intelligent vehicles sharing city roads. *IEEE Robot. Autom. Mag.* <https://doi.org/10.1109/MRA.2005.1411418>
- Bahram, M., Wolf, A., Aeberhard, M., Wollherr, D., 2014. A prediction-based reactive driving strategy for highly automated driving function on freeways, in: *2014 IEEE Intelligent Vehicles Symposium Proceedings*. IEEE, pp. 400–406. <https://doi.org/10.1109/IVS.2014.6856503>
- Baidu, 2018. Baidu Disengagement Report.
- Banerjee, S.S., Jha, S., Cyriac, J., Kalbarczyk, Z.T., Iyer, R.K., 2018. Hands Off the Wheel in Autonomous Vehicles?: A Systems Perspective on over a Million Miles of Field Data, in: *2018 48th Annual IEEE/IFIP International Conference on Dependable Systems and Networks (DSN)*. IEEE, pp. 586–597. <https://doi.org/10.1109/DSN.2018.00066>
- Banks, V.A., Eriksson, A., O’Donoghue, J., Stanton, N.A., 2018. Is partially automated driving a bad idea? Observations from an on-road study. *Appl. Ergon.* 68, 138–145. <https://doi.org/10.1016/J.APERGO.2017.11.010>
- Bansal, P., Kockelman, K.M., 2017. Forecasting Americans’ long-term adoption of connected and autonomous vehicle technologies. *Transp. Res. Part A Policy Pract.* 95, 49–63. <https://doi.org/10.1016/J.TRA.2016.10.013>
- Barth, M., Boriboonsomsin, K., Wu, G., 2014. Vehicle Automation and Its Potential Impacts on Energy and Emissions. pp. 103–112. [https://doi.org/10.1007/978-3-319-05990-7\\_10](https://doi.org/10.1007/978-3-319-05990-7_10)
- Barthauer, M., 2019. Presorting and presignaling: A new intersection operation mode for autonomous and human-operated vehicles. *Transp. Res. Procedia* 37, 179–186. <https://doi.org/10.1016/J.TRPRO.2018.12.181>
- Bashiri, M., Jafarzadeh, H., Fleming, C., 2018a. PAIM: Platoon-based Autonomous Intersection Management.
- Bashiri, M., Jafarzadeh, H., Fleming, C.H., 2018b. PAIM: Platoon-based Autonomous Intersection Management, in: *2018 21st International Conference on Intelligent Transportation Systems (ITSC)*. IEEE, pp. 374–380. <https://doi.org/10.1109/ITSC.2018.8569782>
- Bazilinskyy, P., Petermeijer, S.M., Petrovych, V., Dodou, D., de Winter, J.C.F., 2018. Take-over requests in highly automated driving: A crowdsourcing survey on auditory, vibrotactile, and visual displays. *Transp. Res. Part F Traffic Psychol. Behav.* 56, 82–98. <https://doi.org/10.1016/J.TRF.2018.04.001>
- Bellem, H., Thiel, B., Schrauf, M., Krems, J.F., 2018. Comfort in automated driving: An analysis of preferences for different automated driving styles and their dependence on personality traits. *Transp. Res. Part F Traffic Psychol. Behav.* 55, 90–100. <https://doi.org/10.1016/J.TRF.2018.02.036>
- Beller, J., Heesen, M., Vollrath, M., 2013a. Improving the driver-automation interaction: An approach using automation uncertainty. *Hum. Factors.* <https://doi.org/10.1177/0018720813482327>

- Beller, J., Heesen, M., Vollrath, M., 2013b. Improving the Driver–Automation Interaction. *Hum. Factors J. Hum. Factors Ergon. Soc.* 55, 1130–1141. <https://doi.org/10.1177/0018720813482327>
- Belwadi, A., Loeb, H., Shen, M., Shaikh, S., Ward McIntosh, C., 2018. Emergency Autonomous to Manual Takeover in a Driving Simulator: Teen vs. Adult Drivers – A Pilot Study. *SAE Tech. Pap. Ser. 1*, 1–4. <https://doi.org/10.4271/2018-01-0499>
- Bencloucif, A.M., Nguyen, A.-T., Sentouh, C., Popieul, J.-C., 2019. Cooperative Trajectory Planning for Haptic Shared Control between Driver and Automation in Highway Driving. *IEEE Trans. Ind. Electron.* 1–1. <https://doi.org/10.1109/TIE.2019.2893864>
- Bernhaupt, R., Cronel, M., Manciet, F., Martinie, C., Palanque, P., 2015. Transparent automation for assessing and designing better interactions between operators and partly-autonomous interactive systems, in: *Proceedings of the 5th International Conference on Application and Theory of Automation in Command and Control Systems*. ACM, pp. 129–139.
- Bichiou, Y., Rakha, H.A., 2018a. Developing an Optimal Intersection Control System for Automated Connected Vehicles. *IEEE Trans. Intell. Transp. Syst.* <https://doi.org/10.1109/TITS.2018.2850335>
- Bichiou, Y., Rakha, H.A., 2018b. Real-time optimal intersection control system for automated/cooperative vehicles. *Int. J. Transp. Sci. Technol.* <https://doi.org/10.1016/j.ijtst.2018.04.003>
- BMW, 2018. BMW Disengagement Report.
- Boelhouwer, A., van den Beukel, A.P., van der Voort, M.C., Martens, M.H., 2019. Should I take over? Does system knowledge help drivers in making take-over decisions while driving a partially automated car? *Transp. Res. Part F Traffic Psychol. Behav.* 60, 669–684. <https://doi.org/10.1016/J.TRF.2018.11.016>
- Borojeni, S.S., Boll, S.C.J., Heuten, W., Bühlhoff, H.H., Chuang, L., 2018a. Feel the Movement: Real Motion Influences Responses to Take-over Requests in Highly Automated Vehicles, in: *Proceedings of the 2018 CHI Conference on Human Factors in Computing Systems - CHI '18*. ACM Press, New York, New York, USA, pp. 1–13. <https://doi.org/10.1145/3173574.3173820>
- Borojeni, S.S., Chuang, L., Heuten, W., Boll, S., 2016. Assisting Drivers with Ambient Take-Over Requests in Highly Automated Driving, in: *Proceedings of the 8th International Conference on Automotive User Interfaces and Interactive Vehicular Applications - Automotive'UI 16*. ACM Press, New York, New York, USA, pp. 237–244. <https://doi.org/10.1145/3003715.3005409>
- Borojeni, S.S., Weber, L., Heuten, W., Boll, S., 2018b. From reading to driving: priming mobile users for take-over situations in highly automated driving, in: *Proceedings of the 20th International Conference on Human-Computer Interaction with Mobile Devices and Services - MobileHCI '18*. ACM Press, New York, New York, USA, pp. 1–12. <https://doi.org/10.1145/3229434.3229464>
- Bosch, Mercedes-Benz, 2018. Reinventing Safety: A Joint Approach to Automated Driving Systems 1–42.

- Bosetti, P., Da Lio, M., Saroldi, A., 2015. On Curve Negotiation: From Driver Support to Automation. *IEEE Trans. Intell. Transp. Syst.* 16, 2082–2093. <https://doi.org/10.1109/TITS.2015.2395819>
- Bourelly, A., Naurois, C.J. De, Zran, A., Rampillon, F., Vercher, J.L., 2018. Impact of a long autonomous driving phase on take-over performance. *Pap. Present. 6th Int. Conf. Driv. Distraction Ina*.
- Braunagel, C., Kasneci, E., Stolzmann, W., Rosenstiel, W., 2015. Driver-Activity Recognition in the Context of Conditionally Autonomous Driving, in: 2015 IEEE 18th International Conference on Intelligent Transportation Systems. IEEE, pp. 1652–1657. <https://doi.org/10.1109/ITSC.2015.268>
- Brehmer, C.L., Kacir, K.C., Noyce, D.A., Manser, M.P., 2003. Evaluation of Traffic Signal Displays for Protected-Permissive Left Turn Control. NCHRP Rep. 493.
- Broen, N.L., Chiang, D.P., 1996. Braking Response Times for 100 Drivers in the Avoidance of an Unexpected Obstacle as Measured in a Driving Simulator. *Proc. Hum. Factors Ergon. Soc. Annu. Meet.* 40, 900–904. <https://doi.org/10.1177/154193129604001807>
- Brown, A., Gonder, J., Repac, B., 2014. An Analysis of Possible Energy Impacts of Automated Vehicles. pp. 137–153. [https://doi.org/10.1007/978-3-319-05990-7\\_13](https://doi.org/10.1007/978-3-319-05990-7_13)
- Buckley, L., Kaye, S.-A., Pradhan, A.K., 2018. A qualitative examination of drivers' responses to partially automated vehicles. *Transp. Res. Part F Traffic Psychol. Behav.* 56, 167–175. <https://doi.org/10.1016/J.TRF.2018.04.012>
- California Department of Motor Vehicle, 2017. Final Statement of Reasons, California Department of Motor Vehicle.
- California DMV, 2018. DMV Posts 2017 Autonomous Vehicle Disengagement Reports Online [WWW Document]. URL [https://www.dmv.ca.gov/portal/dmv/detail/pubs/newsrel/2018/2018\\_09](https://www.dmv.ca.gov/portal/dmv/detail/pubs/newsrel/2018/2018_09) (accessed 3.28.19).
- California DMV, 2014. Autonomous Vehicles Testing Regulations.
- Carlino, D., Boyles, S.D., Stone, P., 2013. Auction-based autonomous intersection management, in: IEEE Conference on Intelligent Transportation Systems, Proceedings, ITSC. <https://doi.org/10.1109/ITSC.2013.6728285>
- Carsten, O., Martens, M.H., 2018. How can humans understand their automated cars? HMI principles, problems and solutions. *Cogn. Technol. Work* 1–18. <https://doi.org/10.1007/s10111-018-0484-0>
- Casner, S.M., Hutchins, E.L., Norman, D., 2016. The challenges of partially automated driving. *Commun. ACM* 59, 70–77. <https://doi.org/10.1145/2830565>
- CGTN, 2016. Shocking footage: Fatal Tesla crash in China triggers suspicion of auto-drive [WWW Document]. URL [https://www.youtube.com/watch?v=CgLE\\_ZLLaxw](https://www.youtube.com/watch?v=CgLE_ZLLaxw)
- Chang, H., 2014. System and method for reducing driving skill atrophy.
- Chen, L., Englund, C., 2016. Cooperative Intersection Management: A Survey. *IEEE Trans. Intell. Transp. Syst.* <https://doi.org/10.1109/TITS.2015.2471812>
- Chen, L., Negenborn, R.R., Hopman, H., 2018. Intersection Crossing of Cooperative Multi-vessel

- Systems. IFAC-PapersOnLine. <https://doi.org/10.1016/j.ifacol.2018.07.062>
- Chen, P., Zeng, W., Yu, G., Wang, Y., 2017. Surrogate Safety Analysis of Pedestrian-Vehicle Conflict at Intersections Using Unmanned Aerial Vehicle Videos. *J. Adv. Transp.* 2017, 1–12. <https://doi.org/10.1155/2017/5202150>
- Chen, T., Chen, L., Xu, X., Cai, Y., Jiang, H., Sun, X., 2019a. Passive fault-tolerant path following control of autonomous distributed drive electric vehicle considering steering system fault. *Mech. Syst. Signal Process.* 123, 298–315. <https://doi.org/10.1016/J.YMSSP.2019.01.019>
- Chen, T., Chen, L., Xu, X., Cai, Y., Sun, X., 2019b. Simultaneous path following and lateral stability control of 4WD-4WS autonomous electric vehicles with actuator saturation. *Adv. Eng. Softw.* 128, 46–54. <https://doi.org/10.1016/J.ADVENGSOFT.2018.07.004>
- Chen, T., Guestrin, C., 2016. XGBoost: A scalable tree boosting system. *Proc. ACM SIGKDD Int. Conf. Knowl. Discov. Data Min.* 13-17-Aug, 785–794. <https://doi.org/10.1145/2939672.2939785>
- Chu, D., Deng, Z., He, Y., Wu, C., Sun, C., Lu, Z., 2017. Curve speed model for driver assistance based on driving style classification. *IET Intell. Transp. Syst.* 11, 501–510. <https://doi.org/10.1049/iet-its.2016.0294>
- Chu, D., Yang, J., Lu, L., He, Y., Wu, C., Zhang, C., 2018. Curve Speed Model Considering Coupled Effect Vehicle and Road for Preventions of Rollover and Sideslip, in: 2018 21st International Conference on Intelligent Transportation Systems (ITSC). IEEE, pp. 1358–1363. <https://doi.org/10.1109/ITSC.2018.8569277>
- Cicchino, J.B., 2017. Effectiveness of forward collision warning and autonomous emergency braking systems in reducing front-to-rear crash rates. *Accid. Anal. Prev.* 99, 142–152. <https://doi.org/10.1016/J.AAP.2016.11.009>
- Clark, J.R., Stanton, N.A., Revell, K.M.A., 2018. Conditionally and highly automated vehicle handover: A study exploring vocal communication between two drivers. *Transp. Res. Part F Traffic Psychol. Behav.* <https://doi.org/10.1016/J.TRF.2018.06.008>
- Cook, R.I., Woods, D.D., Mccolligan, E., Howie, M.B., 1991. Cognitive consequences of clumsy automation on high workload, high consequence human performance.
- Cools, R., 2010. N-Back Test BT - Encyclopedia of Psychopharmacology, in: Stolerman, I.P. (Ed.), . Springer Berlin Heidelberg, Berlin, Heidelberg, p. 822. [https://doi.org/10.1007/978-3-540-68706-1\\_1625](https://doi.org/10.1007/978-3-540-68706-1_1625)
- Correa, A., Maerivoet, S., Mintsis, E., Wijnbenga, A., Sepulcre, M., Rondinone, M., Schindler, J., Gozálvez, J., 2018. Management of Transitions of Control in Mixed Traffic with Automated Vehicles, in: 2018 16th International Conference on Intelligent Transportation Systems Telecommunications (ITST). IEEE, pp. 1–7. <https://doi.org/10.1109/ITST.2018.8566961>
- Cramer, S., Klohr, J., 2019. Announcing Automated Lane Changes: Active Vehicle Roll Motions as Feedback for the Driver. *Int. J. Human-Computer Interact.* 1–16. <https://doi.org/10.1080/10447318.2018.1561790>
- Cui, J., Liew, L.S., Sabaliauskaite, G., Zhou, F., 2018. A Review on Safety Failures, Security Attacks, and Available Countermeasures for Autonomous Vehicles. *Ad Hoc Networks.* <https://doi.org/10.1016/J.ADHOC.2018.12.006>

- Damböck, D., Farid, M., Tönert, L., Bengler, K., 2012. Übernahmezeiten beim hochautomatisierten Fahren. *Tagung Fahrerassistenz* 5, 1–12.
- de Beaucorps, P., Streubel, T., Verroust-Blondet, A., Nashashibi, F., Bradai, B., Resende, P., 2017. Decision-making for automated vehicles at intersections adapting human-like behavior, in: *2017 IEEE Intelligent Vehicles Symposium (IV)*. IEEE, pp. 212–217. <https://doi.org/10.1109/IVS.2017.7995722>
- De Boer, R., Dekker, S., De Boer, R., Dekker, S., 2017. Models of Automation Surprise: Results of a Field Survey in Aviation. *Safety* 3, 20. <https://doi.org/10.3390/safety3030020>
- De Boer, R.J., Hurts, K., 2017. Automation Surprise: Results of a Field Survey of Dutch Pilots. *Aviat. Psychol. Appl. Hum. Factors* 7, 28–41. <https://doi.org/10.1027/2192-0923/a000113>
- de Winter, Joost C F, Happee, R., Martens, M.H., Stanton, N. a., 2014. Effects of adaptive cruise control and highly automated driving on workload and situation awareness: A review of the empirical evidence. *Transp. Res. Part F Traffic Psychol. Behav.* 27, 196–217. <https://doi.org/10.1016/j.trf.2014.06.016>
- de Winter, Joost C.F., Happee, R., Martens, M.H., Stanton, N.A., 2014. Effects of adaptive cruise control and highly automated driving on workload and situation awareness: A review of the empirical evidence. *Transp. Res. Part F Traffic Psychol. Behav.* 27, 196–217. <https://doi.org/10.1016/J.TRF.2014.06.016>
- Dehais, F., Peysakhovich, V., Scannella, S., Fongue, J., Gateau, T., 2015. Automation surprise in aviation: Real-time solutions, in: *Proceedings of the 33rd Annual ACM Conference on Human Factors in Computing Systems*. ACM, pp. 2525–2534.
- Department for Transport, U.K., 2018. The Highway Code - Guidance - GOV.UK [WWW Document]. GOV.UK. URL <https://www.gov.uk/guidance/the-highway-code> (accessed 3.19.19).
- Dixit, V. V., Chand, S., Nair, D.J., 2016. Autonomous vehicles: disengagements, accidents and reaction times. *PLoS One* 11, e0168054.
- Dogan, E., Honnêt, V., Masfrand, S., Guillaume, A., 2019. Effects of non-driving-related tasks on takeover performance in different takeover situations in conditionally automated driving. *Transp. Res. Part F Traffic Psychol. Behav.* 62, 494–504. <https://doi.org/10.1016/J.TRF.2019.02.010>
- Dogan, E., Rahal, M.-C., Deborne, R., Delhomme, P., Kemeny, A., Perrin, J., 2017. Transition of control in a partially automated vehicle: Effects of anticipation and non-driving-related task involvement. *Transp. Res. Part F Traffic Psychol. Behav.* 46, 205–215. <https://doi.org/10.1016/J.TRF.2017.01.012>
- Dresner, K., Stone, P., 2008. A Multiagent Approach to Autonomous Intersection Management. *J. Artif. Intell. Res.* 31, 591–656. <https://doi.org/10.1613/jair.2502>
- Dresner, K., Stone, P., 2007. Sharing the road: Autonomous vehicles meet human drivers, in: *IJCAI International Joint Conference on Artificial Intelligence*. <https://doi.org/10.1.1.65.6962>
- Dresner, K., Stone, P., 2005. Multiagent traffic management: An Improved Intersection Control Mechanism, in: *Proceedings of the Fourth International Joint Conference on Autonomous Agents and Multiagent Systems - AAMAS '05*. ACM Press, New York, New York, USA, p.

471. <https://doi.org/10.1145/1082473.1082545>
- Drive AI, 2018. Drive AI disengagement report.
- Du, Z., HomChaudhuri, B., Pisu, P., 2018. Hierarchical distributed coordination strategy of connected and automated vehicles at multiple intersections. *J. Intell. Transp. Syst. Technol. Planning, Oper.* <https://doi.org/10.1080/15472450.2017.1407930>
- Dukic, T., Ahlstrom, C., Patten, C., Kettwich, C., Kircher, K., 2013. Effects of electronic billboards on driver distraction. *Traffic Inj. Prev.* 14, 469–76. <https://doi.org/10.1080/15389588.2012.731546>
- Efrati, A., 2018. Waymo’s Big Ambitions Slowed by Tech Trouble — The Information [WWW Document]. *Inf. URL* <https://www.theinformation.com/articles/waymos-big-ambitions-slowed-by-tech-trouble> (accessed 3.12.19).
- Endsley, M.R., 2017. Autonomous Driving Systems: A Preliminary Naturalistic Study of the Tesla Model S. *J. Cogn. Eng. Decis. Mak.* <https://doi.org/10.1177/1555343417695197>
- Epple, S., Roche, F., Brandenburg, S., 2018. The Sooner the Better: Drivers’ Reactions to Two-Step Take-Over Requests in Highly Automated Driving. *Proc. Hum. Factors Ergon. Soc. Annu. Meet.* 62, 1883–1887. <https://doi.org/10.1177/1541931218621428>
- Eriksson, A., Petermeijer, S.M., Zimmermann, M., de Winter, J.C.F., Bengler, K.J., Stanton, N.A., 2019. Rolling Out the Red (and Green) Carpet: Supporting Driver Decision Making in Automation-to-Manual Transitions. *IEEE Trans. Human-Machine Syst.* 49, 20–31. <https://doi.org/10.1109/THMS.2018.2883862>
- Eriksson, A., Stanton, N.A., 2017. Takeover Time in Highly Automated Vehicles: Noncritical Transitions to and From Manual Control. *Hum. Factors J. Hum. Factors Ergon. Soc.* 59, 689–705. <https://doi.org/10.1177/0018720816685832>
- Essa, M., Sayed, T., 2018. Traffic conflict models to evaluate the safety of signalized intersections at the cycle level. *Transp. Res. Part C Emerg. Technol.* 89, 289–302. <https://doi.org/10.1016/J.TRC.2018.02.014>
- Etemad, A., 2015. Automated Driving - What is possible today? from EU FP7- Proj. Adapt.
- Fagnant, D.J., Kockelman, K., 2015. Preparing a nation for autonomous vehicles: opportunities, barriers and policy recommendations. *Transp. Res. Part A Policy Pract.* 77, 167–181. <https://doi.org/10.1016/J.TRA.2015.04.003>
- Fajardo, D., Au, T.-C., Waller, S.T., Stone, P., Yang, D., 2011. Automated Intersection Control: Performance of Future Innovation Versus Current Traffic Signal Control. *Transp. Res. Rec. J. Transp. Res. Board* 2259, 223–232. <https://doi.org/10.3141/2259-21>
- Favarò, F., Eurich, S., Nader, N., 2018. Autonomous vehicles’ disengagements: Trends, triggers, and regulatory limitations. *Accid. Anal. Prev.* 110, 136–148. <https://doi.org/10.1016/J.AAP.2017.11.001>
- Fayazi, S.A., Vahidi, A., 2018. Mixed-Integer Linear Programming for Optimal Scheduling of Autonomous Vehicle Intersection Crossing. *IEEE Trans. Intell. Veh.* <https://doi.org/10.1109/tiv.2018.2843163>
- Feldhütter, A., Hecht, T., Kalb, L., Bengler, K., 2019. Effect of prolonged periods of conditionally

- automated driving on the development of fatigue: with and without non-driving-related activities. *Cogn. Technol. Work* 21, 33–40. <https://doi.org/10.1007/s10111-018-0524-9>
- Feng, Y., Head, K.L., Khoshmagham, S., Zamanipour, M., 2015. A real-time adaptive signal control in a connected vehicle environment. *Transp. Res. Part C Emerg. Technol.* <https://doi.org/10.1016/j.trc.2015.01.007>
- Feng, Y., Yu, C., Liu, H.X., 2018. Spatiotemporal intersection control in a connected and automated vehicle environment. *Transp. Res. Part C Emerg. Technol.* 89, 364–383. <https://doi.org/10.1016/J.TRC.2018.02.001>
- Fethi, D., Nemra, A., Louadj, K., Hamerlain, M., 2018. Simultaneous localization, mapping, and path planning for unmanned vehicle using optimal control. *Adv. Mech. Eng.* 10, 168781401773665. <https://doi.org/10.1177/1687814017736653>
- FHWA, 2018. Intersection Safety - Safety | Federal Highway Administration [WWW Document]. URL <https://safety.fhwa.dot.gov/intersection/conventional/signalized/> (accessed 11.3.18).
- Fitts, P.M., 1951. Human engineering for an effective air-navigation and traffic-control system.
- Fletcher, L., Apostoloff, N., Chen, J., Zelinsky, A., 2001. Computer vision for vehicle monitoring and control, in: *Proc. Australian Conference on Robotics and Automation*.
- Ford Motor Company, 2018. A Matter of Trust.
- Forster, Y., Naujoks, F., Neukum, A., Huestegge, L., 2017. Driver compliance to take-over requests with different auditory outputs in conditional automation. *Accid. Anal. Prev.* 109, 18–28. <https://doi.org/10.1016/J.AAP.2017.09.019>
- Friedrich, B., 2016. The Effect of Autonomous Vehicles on Traffic, in: *Autonomous Driving*. Springer Berlin Heidelberg, Berlin, Heidelberg, pp. 317–334. [https://doi.org/10.1007/978-3-662-48847-8\\_16](https://doi.org/10.1007/978-3-662-48847-8_16)
- Galluppi, O., Formentin, S., Novara, C., Savaresi, S.M., 2017. Nonlinear stability control of autonomous vehicles: a MIMO D2-IBC solution. *IFAC-PapersOnLine* 50, 3691–3696. <https://doi.org/10.1016/J.IFACOL.2017.08.563>
- Geiselman, E.E., Johnson, C.M., Buck, D.R., Patrick, T., 2013. Flight deck automation: A call for context-aware logic to improve safety. *Ergon. Des.* 21, 13–18.
- Gettman, D., Head, L., 2003. Surrogate safety measures from traffic simulation models, final report. The Center.
- Glander, K.-H., Rooij, L. van, 2018. How much automation do we really need? Springer Vieweg, Wiesbaden, pp. 19–30. [https://doi.org/10.1007/978-3-658-21444-9\\_2](https://doi.org/10.1007/978-3-658-21444-9_2)
- GM Cruise, 2018. GM Cruise Disengagement Report.
- Gold, C., Berisha, I., Bengler, K., 2015a. Utilization of Drivetime – Performing Non-Driving Related Tasks While Driving Highly Automated. *Proc. Hum. Factors Ergon. Soc. Annu. Meet.* 59, 1666–1670. <https://doi.org/10.1177/1541931215591360>
- Gold, C., Damböck, D., Lorenz, L., Bengler, K., 2013. “Take over!” How long does it take to get the driver back into the loop? *Proc. Hum. Factors Ergon. Soc. Annu. Meet.* 57, 1938–1942. <https://doi.org/10.1177/1541931213571433>

- Gold, C., Happee, R., Bengler, K., 2018. Modeling take-over performance in level 3 conditionally automated vehicles. *Accid. Anal. Prev.* 116, 3–13. <https://doi.org/10.1016/J.AAP.2017.11.009>
- Gold, C., Körber, M., Hohenberger, C., Lechner, D., Bengler, K., 2015b. Trust in Automation – Before and After the Experience of Take-over Scenarios in a Highly Automated Vehicle. *Procedia Manuf.* 3, 3025–3032. <https://doi.org/10.1016/J.PROMFG.2015.07.847>
- Gold, C., Körber, M., Lechner, D., Bengler, K., 2016. Taking over Control from Highly Automated Vehicles in Complex Traffic Situations. *Hum. Factors* 58, 642–652. <https://doi.org/10.1177/0018720816634226>
- Gold, C., Lorenz, L., Bengler, K., 2014. Influence of Automated Brake Application on Take-Over Situations in Highly Automated Driving Scenarios, in: *Proceedings of the FISITA 2014 World Automotive Congress*. KIVI, Engineering Society.
- Goodrich, M. a., Boer, E.R., 2003. Model-Based Human-Centered Task Automation: A Case Study in ACC System Design. *IEEE Trans. Syst. Man, Cybern. Part A Systems Humans.* 33, 325–336. <https://doi.org/10.1109/TSMCA.2003.817040>
- Goodrich, M.A., Boer, E.R., 2000. Designing human-centered automation: trade-offs in collision avoidance system design. *IEEE Trans. Intell. Transp. Syst.* 1, 40–54. <https://doi.org/10.1109/6979.869020>
- Grace, K., Salvatier, J., Dafoe, A., Zhang, B., Evans, O., 2018. Viewpoint: When Will AI Exceed Human Performance? Evidence from AI Experts. *J. Artif. Intell. Res.* 62, 729–754. <https://doi.org/10.1613/jair.1.11222>
- Gregoire, J., Bonnabel, S., De La Fortelle, A., 2014. Priority-based coordination of robots.
- Guler, S.I., Menendez, M., Meier, L., 2014. Using connected vehicle technology to improve the efficiency of intersections. *Transp. Res. Part C Emerg. Technol.* 46, 121–131.
- Guo, C., Sentouh, C., Popieul, J.-C., Haué, J.-B., 2019. Predictive shared steering control for driver override in automated driving: A simulator study. *Transp. Res. Part F Traffic Psychol. Behav.* 61, 326–336. <https://doi.org/10.1016/J.TRF.2017.12.005>
- Guo, H., Cao, D., Chen, H., Sun, Z., Hu, Y., 2019. Model predictive path following control for autonomous cars considering a measurable disturbance: Implementation, testing, and verification. *Mech. Syst. Signal Process.* 118, 41–60. <https://doi.org/10.1016/J.YMSSP.2018.08.028>
- Guo, Y., Liu, P., Wu, Y., Chen, J., 2018. Evaluating how right-turn treatments affect right-turn-on-red conflicts at signalized intersections. *J. Transp. Saf. Secur.* 1–22. <https://doi.org/10.1080/19439962.2018.1490368>
- Guo, Y., Ma, J., Xiong, C., Li, X., Zhou, F., Hao, W., 2019. Joint optimization of vehicle trajectories and intersection controllers with connected automated vehicles: Combined dynamic programming and shooting heuristic approach. *Transp. Res. Part C Emerg. Technol.* 98, 54–72. <https://doi.org/10.1016/J.TRC.2018.11.010>
- Güzel, M.S., 2013. Autonomous Vehicle Navigation Using Vision and Mapless Strategies: A Survey. *Adv. Mech. Eng.* 5, 234747. <https://doi.org/10.1155/2013/234747>

- Happee, R., Gold, C., Radlmayr, J., Hergeth, S., Bengler, K., 2017. Take-over performance in evasive manoeuvres. *Accid. Anal. Prev.* 106, 211–222. <https://doi.org/10.1016/J.AAP.2017.04.017>
- Harris, D., Li, W.-C., 2017. Decision making in aviation.
- Hassan, A.A., Rakha, H.A., 2014. A Fully-Distributed Heuristic Algorithm for Control of Autonomous Vehicle Movements at Isolated Intersections. *Int. J. Transp. Sci. Technol.* 3, 297–309. <https://doi.org/10.1260/2046-0430.3.4.297>
- Hausknecht, M., Au, T.-C., Stone, P., 2011. Autonomous Intersection Management: Multi-intersection optimization, in: 2011 IEEE/RSJ International Conference on Intelligent Robots and Systems. IEEE, pp. 4581–4586. <https://doi.org/10.1109/IROS.2011.6094668>
- HCM, 2010. Highway capacity manual 2010, Transportation Research Board, National Research Council. [https://doi.org/10.1061/\(ASCE\)HY.1943-7900.0000746](https://doi.org/10.1061/(ASCE)HY.1943-7900.0000746).
- Heikoop, D.D., de Winter, J.C.F., van Arem, B., Stanton, N.A., 2018. Effects of mental demands on situation awareness during platooning: A driving simulator study. *Transp. Res. Part F Traffic Psychol. Behav.* 58, 193–209. <https://doi.org/10.1016/J.TRF.2018.04.015>
- Honda, 2018. Honda Disengagement Report.
- Hu, X., Chen, L., Tang, B., Cao, D., He, H., 2018. Dynamic path planning for autonomous driving on various roads with avoidance of static and moving obstacles. *Mech. Syst. Signal Process.* 100, 482–500. <https://doi.org/10.1016/J.YMSSP.2017.07.019>
- Hubmann, C., Becker, M., Althoff, D., Lenz, D., Stiller, C., 2017. Decision making for autonomous driving considering interaction and uncertain prediction of surrounding vehicles, in: 2017 IEEE Intelligent Vehicles Symposium (IV). IEEE, pp. 1671–1678. <https://doi.org/10.1109/IVS.2017.7995949>
- Ilgin Guler, S., Menendez, M., Meier, L., 2014. Using connected vehicle technology to improve the efficiency of intersections. *Transp. Res. Part C Emerg. Technol.* 46, 121–131. <https://doi.org/10.1016/J.TRC.2014.05.008>
- Jamson, A.H., Merat, N., Carsten, O.M.J., Lai, F.C.H., 2013. Behavioural changes in drivers experiencing highly-automated vehicle control in varying traffic conditions. *Transp. Res. Part C Emerg. Technol.* 30, 116–125. <https://doi.org/10.1016/J.TRC.2013.02.008>
- Jang, C., Cho, S., Jeong, S., Suhr, J.K., Jung, H.G., Sunwoo, M., 2017. Traffic light recognition exploiting map and localization at every stage. *Expert Syst. Appl.* 88, 290–304. <https://doi.org/10.1016/J.ESWA.2017.07.003>
- Jarosch, O., Bellem, H., Bengler, K., 2019. Effects of Task-Induced Fatigue in Prolonged Conditional Automated Driving. *Hum. Factors J. Hum. Factors Ergon. Soc.* 001872081881622. <https://doi.org/10.1177/0018720818816226>
- Jarosch Oliverand Bengler, K., 2019. Is It the Duration of the Ride or the Non-driving Related Task? What Affects Take-Over Performance in Conditional Automated Driving?, in: Bagnara Sebastianoand Tartaglia, R. and A.S. and A.T. and F.Y. (Ed.), *Proceedings of the 20th Congress of the International Ergonomics Association (IEA 2018)*. Springer International Publishing, Cham, pp. 512–523.

- Jason Brownlee, 2018. XGBoost with Python.
- Kalb, L., Streit, L., Bengler, K., 2018. Multimodal Priming of Drivers for a Cooperative Take-Over, in: 2018 21st International Conference on Intelligent Transportation Systems (ITSC). IEEE, pp. 1029–1034. <https://doi.org/10.1109/ITSC.2018.8569619>
- Kalra, N., Paddock, S.M., 2016. Driving to safety: How many miles of driving would it take to demonstrate autonomous vehicle reliability? *Transp. Res. Part A Policy Pract.* 94, 182–193. <https://doi.org/10.1016/J.TRA.2016.09.010>
- Kamijo, S., Gu, Y., Hsu, L.-T., 2015. Autonomous Vehicle Technologies :Localization and Mapping. *IEICE ESS Fundam. Rev.* 9, 131–141. [https://doi.org/10.1587/essfr.9.2\\_131](https://doi.org/10.1587/essfr.9.2_131)
- Kellerman, A., 2019. The Internet city : people, companies, systems and vehicles.
- Kellerman, A., 2018. Automated and autonomous spatial mobilities.
- Kerschbaum, P., Lorenz, L., Bengler, K., 2014. Highly automated driving with a decoupled steering wheel. *Proc. Hum. Factors Ergon. Soc. Annu. Meet.* 58, 1686–1690. <https://doi.org/10.1177/1541931214581352>
- Kim, B., Kim, D., Park, S., Jung, Y., Yi, K., 2016. Automated Complex Urban Driving based on Enhanced Environment Representation with GPS/map, Radar, Lidar and Vision. *IFAC-PapersOnLine* 49, 190–195. <https://doi.org/10.1016/J.IFACOL.2016.08.029>
- Kim, J., Jo, K., Kim, D., Chu, K., Sunwoo, M., 2013. Behavior and Path Planning Algorithm of Autonomous Vehicle AI in Structured Environments. *IFAC Proc. Vol.* 46, 36–41. <https://doi.org/10.3182/20130626-3-AU-2035.00053>
- Kim, J., Kim, H.-S., Kim, W., Yoon, D., 2018. Take-over performance analysis depending on the drivers' non-driving secondary tasks in automated vehicles, in: 2018 International Conference on Information and Communication Technology Convergence (ICTC). IEEE, pp. 1364–1366. <https://doi.org/10.1109/ICTC.2018.8539431>
- Kirkpatrick, K., 2015. The moral challenges of driverless cars. *Commun. ACM.* <https://doi.org/10.1145/2788477>
- Knodler, M., Noyce, D., Kacir, K., Brehmer, C., 2007a. Analysis of Driver and Pedestrian Comprehension of Requirements for Permissive Left-Turn Applications. *Transp. Res. Rec. J. Transp. Res. Board.* <https://doi.org/10.3141/1982-10>
- Knodler, M., Noyce, D., Kacir, K., Brehmer, C., 2007b. Evaluation of Flashing Yellow Arrow in Traffic Signal Displays with Simultaneous Permissive Indications. *Transp. Res. Rec. J. Transp. Res. Board.* <https://doi.org/10.3141/1918-06>
- Knodler, M.A., Noyce, D.A., Kacir, K.C., Brehmer, C.L., 2005. Evaluation of Traffic Signal Displays for Protected-Permissive Left-Turn Control Using Driving Simulator Technology. *J. Transp. Eng.* [https://doi.org/10.1061/\(asce\)0733-947x\(2005\)131:4\(270\)](https://doi.org/10.1061/(asce)0733-947x(2005)131:4(270))
- Ko, S.M., Ji, Y.G., 2018. How we can measure the non-driving-task engagement in automated driving: Comparing flow experience and workload. *Appl. Ergon.* 67, 237–245. <https://doi.org/10.1016/J.APERGO.2017.10.009>
- Köhn, T., Gottlieb, M., Schermann, M., Krcmar, H., 2019. Improving take-over quality in automated driving by interrupting non-driving tasks, in: *Proceedings of the 24th International*

- Conference on Intelligent User Interfaces - IUI '19. ACM Press, New York, New York, USA, pp. 510–517. <https://doi.org/10.1145/3301275.3302323>
- Kolodko, J., Vlacic, L., 2003. Cooperative Autonomous Driving at the Intelligent Control Systems Laboratory. *IEEE Intell. Syst.* <https://doi.org/10.1109/MIS.2003.1217622>
- Koopman, P., Wagner, M., 2016. Challenges in Autonomous Vehicle Testing and Validation. *SAE Int. J. Transp. Saf.* 4, 2016-01–0128. <https://doi.org/10.4271/2016-01-0128>
- Körper, M., Baseler, E., Bengler, K., 2018a. Introduction matters: Manipulating trust in automation and reliance in automated driving. *Appl. Ergon.* 66, 18–31. <https://doi.org/10.1016/J.APERGO.2017.07.006>
- Körper, M., Baseler, E., Bengler, K., 2018b. Introduction matters: Manipulating trust in automation and reliance in automated driving. *Appl. Ergon.* 66, 18–31. <https://doi.org/10.1016/J.APERGO.2017.07.006>
- Körper, M., Bengler, K., 2014. Potential individual differences regarding automation effects in automated driving, in: *ACM International Conference Proceeding Series.* <https://doi.org/10.1145/2662253.2662275>
- Körper, M., Gold, C., Lechner, D., Bengler, K., 2016. The influence of age on the take-over of vehicle control in highly automated driving. *Transp. Res. Part F Traffic Psychol. Behav.* 39, 19–32. <https://doi.org/10.1016/J.TRF.2016.03.002>
- Körper, M., Weißgerber, T., Blaschke, C., Farid, M., Kalb, L., 2015. Prediction of take-over time in highly automated driving by two psychometric tests. *DYNA.* <https://doi.org/10.15446/dyna.v82n193.53496>
- Kraft, A.-K., Naujoks, F., Wörle, J., Neukum, A., 2018. The impact of an in-vehicle display on glance distribution in partially automated driving in an on-road experiment. *Transp. Res. Part F Traffic Psychol. Behav.* 52, 40–50. <https://doi.org/10.1016/J.TRF.2017.11.012>
- Kye, D.-K., Kim, S.-W., Seo, S.-W., 2015. Decision making for automated driving at unsignalized intersection, in: *2015 15th International Conference on Control, Automation and Systems (ICCAS).* IEEE, pp. 522–525. <https://doi.org/10.1109/ICCAS.2015.7364974>
- Landman, A., Groen, E.L., van Paassen, M.M. (René), Bronkhorst, A.W., Mulder, M., 2017a. Dealing With Unexpected Events on the Flight Deck: A Conceptual Model of Startle and Surprise. *Hum. Factors J. Hum. Factors Ergon. Soc.* 59, 1161–1172. <https://doi.org/10.1177/0018720817723428>
- Landman, A., Groen, E.L., Van Paassen, M.M., Bronkhorst, A.W., Mulder, M., 2017b. The influence of surprise on upset recovery performance in airline pilots. *Int. J. Aerosp. Psychol.* 27, 2–14.
- Le Vine, S., Zolfaghari, A., Polak, J., 2015. Autonomous cars: The tension between occupant experience and intersection capacity. *Transp. Res. Part C Emerg. Technol.* 52, 1–14. <https://doi.org/10.1016/J.TRC.2015.01.002>
- Lee, J., Park, B., 2012. Development and Evaluation of a Cooperative Vehicle Intersection Control Algorithm Under the Connected Vehicles Environment. *IEEE Trans. Intell. Transp. Syst.* 13, 81–90. <https://doi.org/10.1109/TITS.2011.2178836>

- Lee, J., Park, B. (Brian), Malakorn, K., So, J. (Jason), 2013. Sustainability assessments of cooperative vehicle intersection control at an urban corridor. *Transp. Res. Part C Emerg. Technol.* 32, 193–206. <https://doi.org/10.1016/J.TRC.2012.09.004>
- Lee, J.D., McGehee, D. V, Brown, T.L., Reyes, M.L., 2002. Driver distraction, warning algorithm parameters, and driver response to imminent rear-end collisions in a high-fidelity driving simulator.
- Lerner, N.D., 1993. Brake Perception-Reaction Times of Older and Younger Drivers. *Proc. Hum. Factors Ergon. Soc. Annu. Meet.* 37, 206–210. <https://doi.org/10.1177/154193129303700211>
- Levin, M.W., Boyles, S.D., 2016. A multiclass cell transmission model for shared human and autonomous vehicle roads. *Transp. Res. Part C Emerg. Technol.* 62, 103–116. <https://doi.org/10.1016/J.TRC.2015.10.005>
- Levin, M.W., Boyles, S.D., 2015. Intersection auctions and reservation-based control in dynamic traffic assignment. *Transp. Res. Rec. J. Transp. Res. Board* 35–44.
- Levin, M.W., Rey, D., 2017. Conflict-point formulation of intersection control for autonomous vehicles. *Transp. Res. Part C Emerg. Technol.* 85, 528–547. <https://doi.org/10.1016/J.TRC.2017.09.025>
- Levinson, J., Montemerlo, M., Thrun, S., 2007. Map-Based Precision Vehicle Localization in Urban Environments, in: *Robotics: Science and Systems III*. <https://doi.org/10.15607/RSS.2007.III.016>
- Li, P. (Taylor), Zhou, X., 2017. Recasting and optimizing intersection automation as a connected-and-automated-vehicle (CAV) scheduling problem: A sequential branch-and-bound search approach in phase-time-traffic hypernetwork. *Transp. Res. Part B Methodol.* 105, 479–506. <https://doi.org/10.1016/J.TRB.2017.09.020>
- Li, S., Blythe, P., Guo, W., Namdeo, A., 2019. Investigation of older drivers' requirements of the human-machine interaction in highly automated vehicles. *Transp. Res. Part F Traffic Psychol. Behav.* 62, 546–563. <https://doi.org/10.1016/J.TRF.2019.02.009>
- Li, Y., Hu, Z., Hu, Y., Chu, D., 2018. Integration of vision and topological self-localization for intelligent vehicles. *Mechatronics* 51, 46–58. <https://doi.org/10.1016/J.MECHATRONICS.2018.02.012>
- Li, Z., Chitturi, M. V., Zheng, D., Bill, A.R., Noyce, D.A., 2013. Modeling Reservation-Based Autonomous Intersection Control in VISSIM. *Transp. Res. Rec. J. Transp. Res. Board* 2381, 81–90. <https://doi.org/10.3141/2381-10>
- Liu, T., Zhou, H., Itoh, M., Kitazaki, S., 2018. The Impact of Explanation on Possibility of Hazard Detection Failure on Driver Intervention under Partial Driving Automation, in: *2018 IEEE Intelligent Vehicles Symposium (IV)*. IEEE, pp. 150–155. <https://doi.org/10.1109/IVS.2018.8500521>
- Liu, W., Kim, S.-W., Pendleton, S., Ang, M.H., 2015. Situation-aware decision making for autonomous driving on urban road using online POMDP, in: *2015 IEEE Intelligent Vehicles Symposium (IV)*. IEEE, pp. 1126–1133. <https://doi.org/10.1109/IVS.2015.7225835>
- Liu, Y., Ozguner, U., 2007. Human Driver Model and Driver Decision Making for Intersection Driving, in: *2007 IEEE Intelligent Vehicles Symposium*. IEEE, pp. 642–647.

<https://doi.org/10.1109/IVS.2007.4290188>

- Lorenz, L., Kerschbaum, P., Schumann, J., 2014. Designing take over scenarios for automated driving. *Proc. Hum. Factors Ergon. Soc. Annu. Meet.* 58, 1681–1685. <https://doi.org/10.1177/1541931214581351>
- Louw, T., Markkula, G., Boer, E., Madigan, R., Carsten, O., Merat, N., 2017. Coming back into the loop: Drivers' perceptual-motor performance in critical events after automated driving. *Accid. Anal. Prev.* 108, 9–18. <https://doi.org/10.1016/j.aap.2017.08.011>
- Louw, T., Merat, N., Jamson, H., 2015. Engaging with Highly Automated Driving: To be or Not to be in the Loop?
- Lu, J.J., Chen, S., Ge, X., Pan, F., 2013. A programmable calculation procedure for number of traffic conflict points at highway intersections. *J. Adv. Transp.* 47, 692–703. <https://doi.org/10.1002/atr.190>
- Lulu Chang, Luke Dormehl, 2018. 6 self-driving car crashes that tapped the brakes on the autonomous revolution [WWW Document]. URL <https://www.digitaltrends.com/cool-tech/most-significant-self-driving-car-crashes/> (accessed 3.10.19).
- Lv, C., Cao, D., Zhao, Y., Auger, D.J., Sullman, M., Wang, H., Dutka, L.M., Skrypchuk, L., Mouzakitis, A., 2018. Analysis of autopilot disengagements occurring during autonomous vehicle testing. *IEEE/CAA J. Autom. Sin.* 5, 58–68.
- Madigan, R., Louw, T., Merat, N., 2018. The effect of varying levels of vehicle automation on drivers' lane changing behaviour. *PLoS One* 13, e0192190. <https://doi.org/10.1371/journal.pone.0192190>
- Makarem, L., Gillet, D., 2011. Decentralized Coordination of Autonomous Vehicles at intersections. *IFAC Proc. Vol.* 44, 13046–13051. <https://doi.org/10.3182/20110828-6-IT-1002.02529>
- Mauro, R., Loukopoulou, L., Trippe, J., 2017. Understanding Pilots' Explanations of Automation Surprises. 19th Int. Symp. Aviat. Psychol.
- McCall, J.C., Achler, O., Trivedi, M.M., 2004. Design of an instrumented vehicle test bed for developing a human centered driver support system, in: *IEEE Intelligent Vehicles Symposium, 2004*. IEEE, pp. 483–488. <https://doi.org/10.1109/IVS.2004.1336431>
- Melcher, V., Rauh, S., Diederichs, F., Widlroither, H., Bauer, W., 2015. Take-Over Requests for Automated Driving. *Procedia Manuf.* 3, 2867–2873. <https://doi.org/10.1016/J.PROMFG.2015.07.788>
- Menendez-Romero, C., Sezer, M., Winkler, F., Dornhege, C., Burgard, W., 2018. Courtesy Behavior for Highly Automated Vehicles on Highway Interchanges, in: *2018 IEEE Intelligent Vehicles Symposium (IV)*. IEEE, pp. 943–948. <https://doi.org/10.1109/IVS.2018.8500407>
- Merat, N., A. Jamson, H., Lai, F., Carsten, O., 2014a. Human Factors of Highly Automated Driving: Results from the EASY and CityMobil Projects. pp. 113–125. [https://doi.org/10.1007/978-3-319-05990-7\\_11](https://doi.org/10.1007/978-3-319-05990-7_11)
- Merat, N., Jamson, A.H., Lai, F.C.H., Carsten, O., 2012. Highly Automated Driving, Secondary Task Performance, and Driver State. *Hum. Factors J. Hum. Factors Ergon. Soc.* 54, 762–771.

<https://doi.org/10.1177/0018720812442087>

- Merat, N., Jamson, A.H., Lai, F.C.H., Daly, M., Carsten, O.M.J., 2014b. Transition to manual: Driver behaviour when resuming control from a highly automated vehicle. *Transp. Res. Part F Traffic Psychol. Behav.* <https://doi.org/10.1016/j.trf.2014.09.005>
- Mercedes Benz, 2018. Mercedes Benz Disengagement Report.
- Mersky, A.C., Samaras, C., 2016. Fuel economy testing of autonomous vehicles. *Transp. Res. Part C Emerg. Technol.* 65, 31–48. <https://doi.org/10.1016/J.TRC.2016.01.001>
- Michael, J.B., Godbole, D.N., Lygeros, J., Sengupta, R., 1998. Capacity Analysis of Traffic Flow Over a Single-Lane Automated Highway System\*. *ITS J. - Intell. Transp. Syst. J.* 4, 49–80. <https://doi.org/10.1080/10248079808903736>
- Middlesworth, V.M., Dresner, K., Stone, P., 2008. Replacing the stop sign: Unmanaged intersection control for autonomous vehicles. *Int. Conf. Auton. Agents Multiagent Syst.* <https://doi.org/10.1145/1402821.1402886>
- Milakis, D., Snelder, M., van Arem, B., van Wee, B., de Almeida Correia, G.H., 2017. Development and transport implications of automated vehicles in the Netherlands: scenarios for 2030 and 2050. *Eur. J. Transp. Infrastruct. Res.* 17.
- Mirheli, A., Hajibabai, L., Hajbabaie, A., 2018. Development of a signal-head-free intersection control logic in a fully connected and autonomous vehicle environment. *Transp. Res. Part C Emerg. Technol.* <https://doi.org/10.1016/j.trc.2018.04.026>
- Mirheli, A., Tajalli, M., Hajibabai, L., Hajbabaie, A., 2019. A consensus-based distributed trajectory control in a signal-free intersection. *Transp. Res. Part C Emerg. Technol.* 100, 161–176. <https://doi.org/10.1016/J.TRC.2019.01.004>
- Moon, S., Yi, K., 2008. Human driving data-based design of a vehicle adaptive cruise control algorithm. *Veh. Syst. Dyn.* 46, 661–690. <https://doi.org/10.1080/00423110701576130>
- Morando, M.M., Tian, Q., Truong, L.T., Vu, H.L., 2018. Studying the Safety Impact of Autonomous Vehicles Using Simulation-Based Surrogate Safety Measures. *J. Adv. Transp.* 2018, 1–11. <https://doi.org/10.1155/2018/6135183>
- Müller, E.R., Carlson, R.C., Junior, W.K., 2016. Intersection control for automated vehicles with MILP. *IFAC-PapersOnLine.* <https://doi.org/10.1016/j.ifacol.2016.07.007>
- MUTCD, 2009. Manual on Uniform Traffic Control Devices for streets and highways, Federal Highway Administration (FHWA). <https://doi.org/10.1360/zd-2013-43-6-1064>
- Naujoks, F., Forster, Y., Wiedemann, K., Neukum, A., 2017a. A Human-Machine Interface for Cooperative Highly Automated Driving, in: Stanton, N.A., Landry, S., Di Bucchianico, G., Vallicelli, A. (Eds.), *Advances in Human Aspects of Transportation*. Springer International Publishing, Cham, pp. 585–595.
- Naujoks, F., Höfling, S., Purucker, C., Zeeb, K., 2018. From partial and high automation to manual driving: Relationship between non-driving related tasks, drowsiness and take-over performance. *Accid. Anal. Prev.* 121, 28–42. <https://doi.org/10.1016/J.AAP.2018.08.018>
- Naujoks, F., Purucker, C., Neukum, A., 2016. Secondary task engagement and vehicle automation – Comparing the effects of different automation levels in an on-road experiment. *Transp. Res.*

- Part F Traffic Psychol. Behav. 38, 67–82. <https://doi.org/10.1016/J.TRF.2016.01.011>
- Naujoks, F., Purucker, C., Wiedemann, K., Marberger, C., 2019. Noncritical State Transitions During Conditionally Automated Driving on German Freeways: Effects of Non-Driving Related Tasks on Takeover Time and Takeover Quality. *Hum. Factors J. Hum. Factors Ergon. Soc.* 001872081882400. <https://doi.org/10.1177/0018720818824002>
- Naujoks, F., Purucker, C., Wiedemann, K., Neukum, A., Wolter, S., Steiger, R., 2017b. Driving performance at lateral system limits during partially automated driving. *Accid. Anal. Prev.* 108, 147–162. <https://doi.org/10.1016/J.AAP.2017.08.027>
- Navya, 2018. Navya Safety Report The Autonom Era.
- Nguyen, A.-T., Sentouh, C., Popieul, J.-C., 2018. Fuzzy steering control for autonomous vehicles under actuator saturation: Design and experiments. *J. Franklin Inst.* 355, 9374–9395. <https://doi.org/10.1016/J.JFRANKLIN.2017.11.027>
- Nguyen, A.-T., Sentouh, C., Popieul, J.-C., 2017. Driver-Automation Cooperative Approach for Shared Steering Control Under Multiple System Constraints: Design and Experiments. *IEEE Trans. Ind. Electron.* 64, 3819–3830. <https://doi.org/10.1109/TIE.2016.2645146>
- NHTSA, 2013. National Highway Traffic Safety Administration Preliminary Statement of Policy Concerning Automated Vehicles. *Natl. Highw. Traffic Saf. Adm.* 14.
- Nilsson, J., Brännström, M., Fredriksson, J., Coelingh, E., 2016. Longitudinal and Lateral Control for Automated Yielding Maneuvers. *IEEE Trans. Intell. Transp. Syst.* <https://doi.org/10.1109/TITS.2015.2504718>
- Nilsson, J., Sjöberg, J., 2013. Strategic decision making for automated driving on two-lane, one way roads using model predictive control, in: 2013 IEEE Intelligent Vehicles Symposium (IV). IEEE, pp. 1253–1258. <https://doi.org/10.1109/IVS.2013.6629638>
- NIO USA, 2018. NIO Disengagement Report.
- Nissan, 2018. Nissan Disengagement Report.
- Noh, S., 2019. Decision-Making Framework for Autonomous Driving at Road Intersections: Safeguarding Against Collision, Overly Conservative Behavior, and Violation Vehicles. *IEEE Trans. Ind. Electron.* 66, 3275–3286. <https://doi.org/10.1109/TIE.2018.2840530>
- Noh, S., An, K., 2018. Decision-Making Framework for Automated Driving in Highway Environments. *IEEE Trans. Intell. Transp. Syst.* 19, 58–71. <https://doi.org/10.1109/TITS.2017.2691346>
- Norman, D.A., 1990. The ‘problem’ with automation: inappropriate feedback and interaction, not ‘over-automation.’ *Philos. Trans. R. Soc. London. B, Biol. Sci.* 327, 585–593.
- Noyce, D.A., Bill, A.R., A., J.M., 2014. Evaluation of the Flashing Yellow Arrow (FYA) Permissive Left-Turn in Shared Yellow Signal Sections. Transportation Research Board, Washington, D.C. <https://doi.org/10.17226/22246>
- NTSB, 2018a. Preliminary Report HWY18MH010.
- NTSB, 2018b. Preliminary Report: Highway Hwy18Fh011 8–11.
- NTSB, 2018c. Preliminary Report: Highway HWY18FH013, NTSB.

- NTSB, 2017. Highway Accident Report Collision Between a Car Operating With Automated Vehicle Control Systems and a Tractor-Semitrailer Truck. <https://doi.org/10.1093/jicru/ndl025>
- Nullman, 2018. Nullmax Disengagement Report.
- Nuro, 2018a. Delivering Safety : Nuro ' s Approach 1–33.
- Nuro, 2018b. Nuro Disengagement Report.
- NVIDIA, 2018. Self-driving Safety Report 2018 1–20.
- Ohn-Bar, E., Trivedi, M.M., 2016. Looking at Humans in the Age of Self-Driving and Highly Automated Vehicles. *IEEE Trans. Intell. Veh.* 1, 90–104. <https://doi.org/10.1109/TIV.2016.2571067>
- Olaverri-Monreal, C., Kumar, S., Diaz-Alvarez, A., 2018. Automated Driving: Interactive Automation Control System to Enhance Situational Awareness in Conditional Automation, in: 2018 IEEE Intelligent Vehicles Symposium (IV). IEEE, pp. 1698–1703. <https://doi.org/10.1109/IVS.2018.8500367>
- Olfati-Saber, R., Fax, J.A., Murray, R.M., 2007. Consensus and cooperation in networked multi-agent systems. *Proc. IEEE*. <https://doi.org/10.1109/JPROC.2006.887293>
- Open source, n.d. XGBoost Python Package [WWW Document]. 2020. URL [https://xgboost.readthedocs.io/en/latest/python/python\\_intro.html](https://xgboost.readthedocs.io/en/latest/python/python_intro.html) (accessed 1.1.21).
- Pampel, S.M., Large, D.R., Burnett, G., Matthias, R., Thompson, S., Skrypchuk, L., 2019. Getting the driver back into the loop: the quality of manual vehicle control following long and short non-critical transfer-of-control requests: *TI:NS. Theor. Issues Ergon. Sci.* 1–19. <https://doi.org/10.1080/1463922X.2018.1463412>
- Pan, F., Zhang, L., Lu, J., Zhao, J.J., Wang, F., 2013. A Method for Determining the Number of Traffic Conflict Points Between Vehicles at Major–Minor Highway Intersections. *Traffic Inj. Prev.* 14, 424–433. <https://doi.org/10.1080/15389588.2012.713148>
- Papadoulis, A., Quddus, M., Imprialou, M., 2019. Evaluating the safety impact of connected and autonomous vehicles on motorways. *Accid. Anal. Prev.* 124, 12–22. <https://doi.org/10.1016/J.AAP.2018.12.019>
- Parasuraman, R., Riley, V., 1997. Humans and Automation: Use, Misuse, Disuse, Abuse. *Hum. Factors J. Hum. Factors Ergon. Soc.* 39, 230–253. <https://doi.org/10.1518/001872097778543886>
- Peng, Z., Wen, G., Rahmani, A., Yu, Y., 2015. Distributed consensus-based formation control for multiple nonholonomic mobile robots with a specified reference trajectory. *Int. J. Syst. Sci.* <https://doi.org/10.1080/00207721.2013.822609>
- Perdomo López, D., Sharon, G., Stone, P., Gregoire, J., Bonnabel, S., De La Fortelle, A., Levin, M.W., Boyles, S.D., VanMiddlesworth, M., Dresner, K., Stone, P., 2017. Replacing the stop sign: Unmanaged intersection control for autonomous vehicles, in: *Proceedings of the 7th International Joint Conference on Autonomous Agents and Multiagent Systems-Volume 3. International Foundation for Autonomous Agents and Multiagent Systems*, pp. 151–167.
- Pérez-Marín, A.M., Guillen, M., 2019. Semi-autonomous vehicles: Usage-based data evidences of

- what could be expected from eliminating speed limit violations. *Accid. Anal. Prev.* 123, 99–106. <https://doi.org/10.1016/J.AAP.2018.11.005>
- Perronnet, F., Abbas-Turki, A., El Moudni, A., 2013. A sequenced-based protocol to manage autonomous vehicles at isolated intersections, in: *16th International IEEE Conference on Intelligent Transportation Systems (ITSC 2013)*. IEEE, pp. 1811–1816. <https://doi.org/10.1109/ITSC.2013.6728491>
- Petermeijer, S., Bazilinsky, P., Bengler, K., de Winter, J., 2017a. Take-over again: Investigating multimodal and directional TORs to get the driver back into the loop. *Appl. Ergon.* 62, 204–215. <https://doi.org/10.1016/J.APERGO.2017.02.023>
- Petermeijer, S., Cieler, S., de Winter, J.C.F., 2017b. Comparing spatially static and dynamic vibrotactile take-over requests in the driver seat. *Accid. Anal. Prev.* 99, 218–227. <https://doi.org/10.1016/J.AAP.2016.12.001>
- Petermeijer, S., Doubek, F., de Winter, J., 2017c. Driver response times to auditory, visual, and tactile take-over requests: A simulator study with 101 participants, in: *2017 IEEE International Conference on Systems, Man, and Cybernetics (SMC)*. IEEE, pp. 1505–1510. <https://doi.org/10.1109/SMC.2017.8122827>
- Pfleging, B., Rang, M., Broy, N., 2016. Investigating user needs for non-driving-related activities during automated driving, in: *Proceedings of the 15th International Conference on Mobile and Ubiquitous Multimedia - MUM '16*. ACM Press, New York, New York, USA, pp. 91–99. <https://doi.org/10.1145/3012709.3012735>
- Phantom AI, 2018. Phantom AI Disengagement Report.
- PlusAi, 2018. PlusAi Disengagement Report.
- Politis, I., Langdon, P., Adebayo, D., Bradley, M., Clarkson, P.J., Skrypchuk, L., Mouzakitis, A., Eriksson, A., Brown, J.W.H., Revell, K., Stanton, N., 2018. An Evaluation of Inclusive Dialogue-Based Interfaces for the Takeover of Control in Autonomous Cars, in: *23rd International Conference on Intelligent User Interfaces, IUI '18*. ACM, New York, NY, USA, pp. 601–606. <https://doi.org/10.1145/3172944.3172990>
- Pony AI, 2018. Pony.ai Disengagement Report.
- Qi, Y., Guoguo, A., 2017. Pedestrian safety under permissive left-turn signal control. *Int. J. Transp. Sci. Technol.* 6, 53–62. <https://doi.org/10.1016/J.IJTST.2017.05.002>
- Qian, X., Gregoire, J., Moutarde, F., De La Fortelle, A., 2014. Priority-based coordination of autonomous and legacy vehicles at intersection, in: *17th International IEEE Conference on Intelligent Transportation Systems (ITSC)*. IEEE, pp. 1166–1171. <https://doi.org/10.1109/ITSC.2014.6957845>
- Qiu, F., 2018. Distributed event-triggered consensus control for multi-agent systems. *UPB Sci. Bull. Ser. A Appl. Math. Phys.*
- Quack, T.M., Reiter, M., Abel, D., 2017. Digital Map Generation and Localization for Vehicles in Urban Intersections using LiDAR and GNSS Data. *IFAC-PapersOnLine* 50, 251–257. <https://doi.org/10.1016/J.IFACOL.2017.08.042>
- Qualcomm, 2018. Qualcomm Disengagement Report.

- Radlmayr, J., Gold, C., Lorenz, L., Farid, M., Bengler, K., 2014. How traffic situations and non-driving related tasks affect the take-over quality in highly automated driving, in: Proceedings of the Human Factors and Ergonomics Society. <https://doi.org/10.1177/1541931214581434>
- Rahman, M.S., Abdel-Aty, M., Lee, J., Rahman, M.H., 2019. Safety benefits of arterials' crash risk under connected and automated vehicles. *Transp. Res. Part C Emerg. Technol.* 100, 354–371. <https://doi.org/10.1016/J.TRC.2019.01.029>
- Rankin, A., Woltjer, R., Field, J., 2016. Sensemaking following surprise in the cockpit—a reframing problem. *Cogn. Technol. Work* 18, 623–642.
- Rapier, R., 2017. Waymo Tests Its Self-Driving Cars In My Town. Here Are The Odd Things I've Seen. [WWW Document]. Forbes. URL <https://www.forbes.com/sites/rrapier/2017/11/12/waymo-tests-its-self-driving-cars-in-my-town-here-are-the-odd-things-ive-seen/#4b9a8d094e4a> (accessed 3.12.19).
- Ren, C., Zhang, W., Qin, L., Sun, B., 2018. Queue Spillover Management in a Connected Vehicle Environment. *Futur. Internet.* <https://doi.org/10.3390/fi10080079>
- Reschka, A., Bohmer, J.R., Saust, F., Lichte, B., Maurer, M., 2012. Safe, dynamic and comfortable longitudinal control for an autonomous vehicle, in: 2012 IEEE Intelligent Vehicles Symposium. IEEE, pp. 346–351. <https://doi.org/10.1109/IVS.2012.6232159>
- Rios-Torres, J., Malikopoulos, A.A., 2017a. A survey on the coordination of connected and automated vehicles at intersections and merging at highway on-ramps. *IEEE Trans. Intell. Transp. Syst.* 18, 1066–1077.
- Rios-Torres, J., Malikopoulos, A.A., 2017b. Automated and cooperative vehicle merging at highway on-ramps. *IEEE Trans. Intell. Transp. Syst.* 18, 780–789.
- Roadstar.ai, 2018. Roadstar.ai Disengagement Report.
- Rodrigues de Campos, G., Falcone, P., Hult, R., Wymeersch, H., Sjoberg, J., 2017. Traffic coordination at road intersections: Autonomous decision-making algorithms using model-based heuristics. *IEEE Intell. Transp. Syst. Mag.* 9, 8–21. <https://doi.org/10.1109/MITS.2016.2630585>
- Roosbehani, H., Rudaz, S., Gillet, D., 2009. On decentralized navigation schemes for coordination of multi-agent dynamical systems, in: Conference Proceedings - IEEE International Conference on Systems, Man and Cybernetics. <https://doi.org/10.1109/ICSMC.2009.5346068>
- Roper, D.H., 1987. Los Angeles, 1984 Olympic Games, in: Transportation Research Board Special Report. National Academy Press, 500 Fifth Street, NW Washington, DC United States 20001, pp. 107–116.
- SAE International, 2018. Taxonomy and Definitions for Terms Related to Driving Automation Systems for On-Road Motor Vehicles.
- SAIC Motors, 2018. SAIC Motors Disengagement Report.
- Saito, T., Wada, T., Sonoda, K., 2018. Control Authority Transfer Method for Automated-to-Manual Driving Via a Shared Authority Mode. *IEEE Trans. Intell. Veh.* 3, 198–207. <https://doi.org/10.1109/TIV.2018.2804167>

- Sander, U., Lubbe, N., 2018. The potential of clustering methods to define intersection test scenarios: Assessing real-life performance of AEB. *Accid. Anal. Prev.* 113, 1–11. <https://doi.org/10.1016/J.AAP.2018.01.010>
- Saraoglu, M., Hart, F., Morozov, A., Janschek, K., 2018. Fault-Tolerant Path Planning in Networked Vehicle Systems in Presence of Communication Failures. *IFAC-PapersOnLine* 51, 82–87. <https://doi.org/10.1016/J.IFACOL.2018.12.015>
- Schartmüller, C., Riener, A., Wintersberger, P., Frison, A.-K., 2018. Workaholic: On Balancing Typing- and Handover-performance in Automated Driving, in: *Proceedings of the 20th International Conference on Human-Computer Interaction with Mobile Devices and Services, MobileHCI '18*. ACM, New York, NY, USA, pp. 16:1–16:12. <https://doi.org/10.1145/3229434.3229459>
- Schepperle, H., Böhm, K., 2008. Auction-Based Traffic Management: Towards Effective Concurrent Utilization of Road Intersections, in: *2008 10th IEEE Conference on E-Commerce Technology and the Fifth IEEE Conference on Enterprise Computing, E-Commerce and E-Services*. IEEE, pp. 105–112. <https://doi.org/10.1109/CECandEEE.2008.88>
- Schepperle, H., Böhm, K., 2007. Agent-Based Traffic Control Using Auctions, in: *Cooperative Information Agents XI*. Springer Berlin Heidelberg, Berlin, Heidelberg, pp. 119–133. [https://doi.org/10.1007/978-3-540-75119-9\\_9](https://doi.org/10.1007/978-3-540-75119-9_9)
- Schepperle, H., Böhm, K., Forster, S., 2008. Traffic Management Based on Negotiations between Vehicles – A Feasibility Demonstration Using Agents BT - *Agent-Mediated Electronic Commerce and Trading Agent Design and Analysis*, in: Collins, J., Faratin, P., Parsons, S., Rodriguez-Aguilar, J.A., Sadeh, N.M., Shehory, O., Sklar, E. (Eds.), . Springer Berlin Heidelberg, Berlin, Heidelberg, pp. 90–104.
- Schwalk, M., Kalogerakis, N., Maier, T., 2015. Driver Support by a Vibrotactile Seat Matrix – Recognition, Adequacy and Workload of Tactile Patterns in Take-over Scenarios During Automated Driving. *Procedia Manuf.* 3, 2466–2473. <https://doi.org/10.1016/J.PROMFG.2015.07.507>
- Sefati, M., Chandiramani, J., Kreiskoether, K., Kampker, A., Baldi, S., 2017. Towards tactical behaviour planning under uncertainties for automated vehicles in urban scenarios, in: *2017 IEEE 20th International Conference on Intelligent Transportation Systems (ITSC)*. IEEE, pp. 1–7. <https://doi.org/10.1109/ITSC.2017.8317819>
- Sentouh, C., Nguyen, A.-T., Benloucif, M.A., Popieul, J.-C., 2018. Driver-Automation Cooperation Oriented Approach for Shared Control of Lane Keeping Assist Systems. *IEEE Trans. Control Syst. Technol.* 1–17. <https://doi.org/10.1109/TCST.2018.2842211>
- Seppelt, B.D., Lee, J.D., 2019. Keeping the driver in the loop: Dynamic feedback to support appropriate use of imperfect vehicle control automation. *Int. J. Hum. Comput. Stud.* 125, 66–80. <https://doi.org/10.1016/J.IJHCS.2018.12.009>
- Seppelt, B.D., Lee, J.D., 2015. Modeling Driver Response to Imperfect Vehicle Control Automation. *Procedia Manuf.* 3, 2621–2628. <https://doi.org/10.1016/J.PROMFG.2015.07.605>
- SF Motors, 2018. SF Motors Disengagement Report.

- Shao, Y., Mohd Zulkefli, M.A., Sun, Z., Huang, P., 2019. Evaluating connected and autonomous vehicles using a hardware-in-the-loop testbed and a living lab. *Transp. Res. Part C Emerg. Technol.* 102, 121–135. <https://doi.org/10.1016/J.TRC.2019.03.010>
- Sharon, G., Stone, P., 2017. A protocol for mixed autonomous and human-operated vehicles at intersections, in: *International Conference on Autonomous Agents and Multiagent Systems*. Springer, pp. 151–167.
- Shen, S., Neyens, D.M., 2017. Assessing drivers' response during automated driver support system failures with non-driving tasks. *J. Safety Res.* 61, 149–155. <https://doi.org/10.1016/J.JSR.2017.02.009>
- Sheridan, T.B., Vámos, T., Aida, S., 1983. Adapting automation to man, culture and society. *Automatica* 19, 605–612. [https://doi.org/10.1016/0005-1098\(83\)90024-9](https://doi.org/10.1016/0005-1098(83)90024-9)
- Sheridan, T.B., Verplank, W.L., 1978. Human and Computer Control of Undersea Teleoperators.
- Shum, A., Morris, K., Khajepour, A., 2015. Direction-dependent optimal path planning for autonomous vehicles. *Rob. Auton. Syst.* 70, 202–214. <https://doi.org/10.1016/J.ROBOT.2015.02.003>
- Solís-Marcos, I., Ahlström, C., Kircher, K., 2018. Performance of an Additional Task During Level 2 Automated Driving: An On-Road Study Comparing Drivers With and Without Experience With Partial Automation. *Hum. Factors J. Hum. Factors Ergon. Soc.* 60, 778–792. <https://doi.org/10.1177/0018720818773636>
- Sportillo, D., Paljic, A., Ojeda, L., 2018. Get ready for automated driving using Virtual Reality. *Accid. Anal. Prev.* 118, 102–113. <https://doi.org/10.1016/J.AAP.2018.06.003>
- Stanton, N. a., Young, M., McCaulder, B., 1997. Drive-by-wire: The case of driver workload and reclaiming control with adaptive cruise control. *Saf. Sci.* 27, 149–159. [https://doi.org/10.1016/S0925-7535\(97\)00054-4](https://doi.org/10.1016/S0925-7535(97)00054-4)
- Stanton, N. a., Young, M.S., 1998. Vehicle automation and driving performance 37–41. <https://doi.org/10.1080/001401398186568>
- Stanton, N.A., 2019. Thematic issue: driving automation and autonomy. *Theor. Issues Ergon. Sci.* 20, 215–222. <https://doi.org/10.1080/1463922X.2018.1541112>
- Starsky Robotics, 2018. Starsky Robotics – Voluntary Safety Self-Assessment 1–21.
- Stern, R.E., Cui, S., Delle Monache, M.L., Bhadani, R., Bunting, M., Churchill, M., Hamilton, N., Hauley, R., Pohlmann, H., Wu, F., Piccoli, B., Seibold, B., Sprinkle, J., Work, D.B., 2018. Dissipation of stop-and-go waves via control of autonomous vehicles: Field experiments. *Transp. Res. Part C Emerg. Technol.* 89, 205–221. <https://doi.org/10.1016/J.TRC.2018.02.005>
- Strand, N., Nilsson, J., Karlsson, I.C.M., Nilsson, L., 2014. Semi-automated versus highly automated driving in critical situations caused by automation failures. *Transp. Res. Part F Traffic Psychol. Behav.* 27, 218–228. <https://doi.org/10.1016/J.TRF.2014.04.005>
- Sukennik, P., 2018. Micro-simulation guide for automated vehicles. *Eur. Union's Horiz.* 2020 1–29.
- Sun, W., Zheng, J., Liu, H.X., 2017. A capacity maximization scheme for intersection management

- with automated vehicles. *Transp. Res. Procedia* 23, 121–136. <https://doi.org/10.1016/J.TRPRO.2017.05.008>
- Talebpour, A., Mahmassani, H.S., 2016. Influence of connected and autonomous vehicles on traffic flow stability and throughput. *Transp. Res. Part C Emerg. Technol.* 71, 143–163. <https://doi.org/10.1016/J.TRC.2016.07.007>
- Telenav Inc, 2018. Telenav Dsiengagement Report.
- Tesla, 2016. Tesla model S manual 2016.
- Tettamanti, T., Varga, I., Szalay, Z., 2016. Impacts of Autonomous Cars from a Traffic Engineering Perspective. *Period. Polytech. Transp. Eng.* 44, 244–250. <https://doi.org/10.3311/PPtr.9464>
- Törő, O., Bécsi, T., Aradi, S., Gáspár, P., 2017. Cooperative object detection in road traffic. *IFAC-PapersOnLine* 50, 264–269. <https://doi.org/10.1016/J.IFACOL.2017.08.044>
- Toyota, 2018. Toyota Disengagement Report.pdf.
- Tsianos, K.I., Lawlor, S., Rabbat, M.G., 2012. Consensus-based distributed optimization: Practical issues and applications in large-scale machine learning, in: 2012 50th Annual Allerton Conference on Communication, Control, and Computing, Allerton 2012. <https://doi.org/10.1109/Allerton.2012.6483403>
- Uber, 2018. Uber Disengagement Report.
- Uber Advanced Technologies Group, 2018. A Principled Approach To Safety 1–70.
- Udelv, 2018. Udelv Disengagement Report.
- Van Den Beukel, A.P., Van Der Voort, M.C., 2013. The influence of time-criticality on Situation Awareness when retrieving human control after automated driving. *IEEE Conf. Intell. Transp. Syst. Proceedings, ITSC 2000–2005*. <https://doi.org/10.1109/ITSC.2013.6728523>
- van den Beukel, A.P., van der Voort, M.C., Eger, A.O., 2016. Supporting the changing driver's task: Exploration of interface designs for supervision and intervention in automated driving. *Transp. Res. Part F Traffic Psychol. Behav.* 43, 279–301. <https://doi.org/10.1016/J.TRF.2016.09.009>
- Vogelpohl, T., Kühn, M., Hummel, T., Vollrath, M., 2018. Asleep at the automated wheel—Sleepiness and fatigue during highly automated driving. *Accid. Anal. Prev.* <https://doi.org/10.1016/J.AAP.2018.03.013>
- Volvo, 2018a. Volvo XC90 Owner's Manual, Volvo. <https://doi.org/10.1049/ic.2011.0006>
- Volvo, 2018b. Volvo V90 Owner's Manual, Volvo. <https://doi.org/10.1049/ic.2011.0006>
- Wada, T., 2018. Simultaneous achievement of driver assistance and skill development in shared and cooperative controls. *Cogn. Technol. Work.* <https://doi.org/10.1007/s10111-018-0514-y>
- Wan, J., Wu, C., 2018a. The Effects of Vibration Patterns of Take-Over Request and Non-Driving Tasks on Taking-Over Control of Automated Vehicles. *Int. J. Human-Computer Interact.* 34, 987–998. <https://doi.org/10.1080/10447318.2017.1404778>
- Wan, J., Wu, C., 2018b. The Effects of Lead Time of Take-Over Request and Nondriving Tasks on Taking-Over Control of Automated Vehicles. *IEEE Trans. Human-Machine Syst.* 48, 582–

591. <https://doi.org/10.1109/THMS.2018.2844251>
- Wandtner, B., Schmidt, G., Schömig, N., Kunde, W., 2018a. Non-driving related tasks in highly automated driving - Effects of task modalities and cognitive workload on take-over performance, in: AmE 2018 - Automotive Meets Electronics; 9th GMM-Symposium. pp. 1–6.
- Wandtner, B., Schömig, N., Schmidt, G., 2018b. Secondary task engagement and disengagement in the context of highly automated driving. *Transp. Res. Part F Traffic Psychol. Behav.* 58, 253–263. <https://doi.org/10.1016/J.TRF.2018.06.001>
- Wandtner, B., Schömig, N., Schmidt, G., 2018c. Effects of Non-Driving Related Task Modalities on Takeover Performance in Highly Automated Driving. *Hum. Factors J. Hum. Factors Ergon. Soc.* 60, 870–881. <https://doi.org/10.1177/0018720818768199>
- Wandtner, B., Schömig, N., Schmidt, G., 2018d. Effects of Non-Driving Related Task Modalities on Takeover Performance in Highly Automated Driving. *Hum. Factors J. Hum. Factors Ergon. Soc.* 60, 870–881. <https://doi.org/10.1177/0018720818768199>
- Wang, J., Soffker, D., 2018. Bridging Gaps Among Human, Assisted, and Automated Driving With DVIs: A Conceptual Experimental Study. *IEEE Trans. Intell. Transp. Syst.* 1–13. <https://doi.org/10.1109/TITS.2018.2858179>
- Wang, L., Zhang, Y., Wang, J., 2017. Map-Based Localization Method for Autonomous Vehicles Using 3D-LIDAR. *IFAC-PapersOnLine* 50, 276–281. <https://doi.org/10.1016/J.IFACOL.2017.08.046>
- Wang, P., Chan, C.-Y., 2018. Autonomous Ramp Merge Maneuver Based on Reinforcement Learning with Continuous Action Space. *arXiv Prepr. arXiv1803.09203*.
- Wang, P., Chan, C.-Y., Fortelle, A. de La, 2018. A Reinforcement Learning Based Approach for Automated Lane Change Maneuvers, in: 2018 IEEE Intelligent Vehicles Symposium (IV). IEEE, pp. 1379–1384. <https://doi.org/10.1109/IVS.2018.8500556>
- Wang, X., Abdel-Aty, M., 2008. Analysis of left-turn crash injury severity by conflicting pattern using partial proportional odds models. *Accid. Anal. Prev.* 40, 1674–1682. <https://doi.org/10.1016/J.AAP.2008.06.001>
- Wang, Y., Ding, H., Yuan, J., Chen, H., 2019. Output-feedback triple-step coordinated control for path following of autonomous ground vehicles. *Mech. Syst. Signal Process.* 116, 146–159. <https://doi.org/10.1016/J.YMSSP.2018.06.011>
- Wang, Z., Zheng, R., Kaizuka, T., Nakano, K., 2019. Relationship Between Gaze Behavior and Steering Performance for Driver–Automation Shared Control: A Driving Simulator Study. *IEEE Trans. Intell. Veh.* 4, 154–166. <https://doi.org/10.1109/TIV.2018.2886654>
- Wang, Z., Zheng, R., Kaizuka, T., Nakano, K., 2018. Driver-Automation Shared Control: Modeling Driver Behavior by Taking Account of Reliance on Haptic Guidance Steering, in: 2018 IEEE Intelligent Vehicles Symposium (IV). IEEE, pp. 144–149. <https://doi.org/10.1109/IVS.2018.8500671>
- Waymo, 2018a. On the road to Fully Self-driving - Waymo Safety Report. Waymo Saf. Rep. <https://doi.org/10.1016/B978-0-08-037539-7.50012-0>

- Waymo, 2018b. Waymo Disengagement Report.
- Waymo, whatasimpleton, 2018. Update: Waymo responded to Red light video : SelfDrivingCars [WWW Document]. URL [https://www.reddit.com/r/SelfDrivingCars/comments/7z9ncy/update\\_waymo\\_responded\\_to\\_red\\_light\\_video/?st=jt6jgd4v&sh=9830b000](https://www.reddit.com/r/SelfDrivingCars/comments/7z9ncy/update_waymo_responded_to_red_light_video/?st=jt6jgd4v&sh=9830b000) (accessed 3.12.19).
- Wei, J., Dolan, J.M., 2009. A robust autonomous freeway driving algorithm, in: 2009 IEEE Intelligent Vehicles Symposium. IEEE, pp. 1015–1020. <https://doi.org/10.1109/IVS.2009.5164420>
- WeRide, 2018. WeRide Disengagement Report.
- Wiedemann, K., Naujoks, F., Wörle, J., Kenntner-Mabiala, R., Kaussner, Y., Neukum, A., 2018. Effect of different alcohol levels on take-over performance in conditionally automated driving. *Accid. Anal. Prev.* 115, 89–97. <https://doi.org/10.1016/J.AAP.2018.03.001>
- Wiener, E.L., 1989. Human factors of advanced technology (glass cockpit) transport aircraft.
- Wintersberger, P., Riener, A., Schartmüller, C., Frison, A.-K., Weigl, K., 2018. Let me finish before I take over: Towards attention aware device integration in highly automated vehicles. 10th ACM Int. Conf. Automot. User Interfaces Interact. Veh. Appl. *AutomotiveUI 2018* 53–65. <https://doi.org/10.1145/3239060.3239085>
- Wright, T.J., Agrawal, R., Samuel, S., Wang, Y., Zilberstein, S., Fisher, D.L., 2018. Effective cues for accelerating young drivers' time to transfer control following a period of conditional automation. *Accid. Anal. Prev.* 116, 14–20. <https://doi.org/10.1016/J.AAP.2017.10.005>
- Wu, J., Abbas-Turki, A., El Moudni, A., 2012. Cooperative driving: An ant colony system for autonomous intersection management. *Appl. Intell.* <https://doi.org/10.1007/s10489-011-0322-z>
- Wu, Y., Abdel-Aty, M., Park, J., Zhu, J., 2018. Effects of crash warning systems on rear-end crash avoidance behavior under fog conditions. *Transp. Res. Part C Emerg. Technol.* 95, 481–492. <https://doi.org/10.1016/J.TRC.2018.08.001>
- Wu, Y., Boyle, L.N., 2015. Drivers' engagement level in Adaptive Cruise Control while distracted or impaired. *Transp. Res. Part F Traffic Psychol. Behav.* 33, 7–15. <https://doi.org/10.1016/J.TRF.2015.05.005>
- Wu, Y., Kihara, K., Takeda, Y., Sato, T., Akamatsu, M., Kitazaki, S., 2019. Effects of scheduled manual driving on drowsiness and response to take over request: A simulator study towards understanding drivers in automated driving. *Accid. Anal. Prev.* 124, 202–209. <https://doi.org/10.1016/J.AAP.2019.01.013>
- Xinli Geng, Huawei Liang, Hao Xu, Biao Yu, Maofei Zhu, 2016. Human-driver speed profile modeling for autonomous vehicle's velocity strategy on curvy paths, in: 2016 IEEE Intelligent Vehicles Symposium (IV). IEEE, pp. 755–760. <https://doi.org/10.1109/IVS.2016.7535472>
- Xu, B., Li, S.E., Bian, Y., Li, S., Ban, X.J., Wang, J., Li, K., 2018. Distributed conflict-free cooperation for multiple connected vehicles at unsignalized intersections. *Transp. Res. Part C Emerg. Technol.* <https://doi.org/10.1016/j.trc.2018.06.004>

- Yamamoto, D., Suganuma, N., 2015. Localization for autonomous driving on urban road, in: 2015 International Conference on Intelligent Informatics and Biomedical Sciences (ICIIBMS). IEEE, pp. 452–453. <https://doi.org/10.1109/ICIIBMS.2015.7439488>
- Yang, K., Guler, S.I., Menendez, M., 2016. Isolated intersection control for various levels of vehicle technology: Conventional, connected, and automated vehicles. *Transp. Res. Part C Emerg. Technol.* 72, 109–129. <https://doi.org/10.1016/J.TRC.2016.08.009>
- Yang, Y., Gerlicher, M., Bengler, K., 2018. How does relaxing posture influence take-over performance in an automated vehicle? *Proc. Hum. Factors Ergon. Soc. Annu. Meet.* 62, 696–700. <https://doi.org/10.1177/1541931218621157>
- Yoon, S.H., Ji, Y.G., 2019. Non-driving-related tasks, workload, and takeover performance in highly automated driving contexts. *Transp. Res. Part F Traffic Psychol. Behav.* 60, 620–631. <https://doi.org/10.1016/J.TRF.2018.11.015>
- Yoon, S.H., Kim, Y.W., Ji, Y.G., 2019. The effects of takeover request modalities on highly automated car control transitions. *Accid. Anal. Prev.* 123, 150–158. <https://doi.org/10.1016/J.AAP.2018.11.018>
- You, C., Lu, J., Filev, D., Tsiotras, P., 2019. Advanced planning for autonomous vehicles using reinforcement learning and deep inverse reinforcement learning. *Rob. Auton. Syst.* 114, 1–18. <https://doi.org/10.1016/J.ROBOT.2019.01.003>
- Young, M.S., Stanton, N.A., 2002. Malleable Attentional Resources Theory: A New Explanation for the Effects of Mental Underload on Performance. *Hum. Factors J. Hum. Factors Ergon. Soc.* 44, 365–375. <https://doi.org/10.1518/0018720024497709>
- Yu, C., Feng, Y., Liu, H.X., Ma, W., Yang, X., 2018. Integrated optimization of traffic signals and vehicle trajectories at isolated urban intersections. *Transp. Res. Part B Methodol.* 112, 89–112. <https://doi.org/10.1016/J.TRB.2018.04.007>
- Yun, H., Lee, J.W., Yang, H.D., Yang, J.H., 2018. Experimental Design for Multi-modal Take-over Request for Automated Driving, in: International Conference on Human-Computer Interaction. Springer, pp. 418–425.
- Zakharenko, R., 2016. Self-driving cars will change cities. *Reg. Sci. Urban Econ.* 61, 26–37. <https://doi.org/10.1016/J.REGSCIURBECO.2016.09.003>
- Zeeb, K., Buchner, A., Schrauf, M., 2016. Is take-over time all that matters? The impact of visual-cognitive load on driver take-over quality after conditionally automated driving. *Accid. Anal. Prev.* 92, 230–239. <https://doi.org/10.1016/J.AAP.2016.04.002>
- Zeeb, K., Buchner, A., Schrauf, M., 2015. What determines the take-over time? An integrated model approach of driver take-over after automated driving. *Accid. Anal. Prev.* 78, 212–221. <https://doi.org/10.1016/j.aap.2015.02.023>
- Zeeb, K., Härtel, M., Buchner, A., Schrauf, M., 2017. Why is steering not the same as braking? The impact of non-driving related tasks on lateral and longitudinal driver interventions during conditionally automated driving. *Transp. Res. Part F Traffic Psychol. Behav.* 50, 65–79. <https://doi.org/10.1016/J.TRF.2017.07.008>
- Zhang, D., Xiao, Q., Wang, J., Li, K., 2013. Driver curve speed model and its application to ACC speed control in curved roads. *Int. J. Automot. Technol.* 14, 241–247.

<https://doi.org/10.1007/s12239-013-0027-x>

- Zhang, F., Gonzales, J., Li, S.E., Borrelli, F., Li, K., 2018. Drift control for cornering maneuver of autonomous vehicles. *Mechatronics* 54, 167–174. <https://doi.org/10.1016/J.MECHATRONICS.2018.05.009>
- Zhang, K., Xie, C., Wang, Y., Wang, M., Fortelle, A., Zhang, W., Duan, Z., Zhang, K., Xie, C., Wang, Y., Wang, M., De La Fortelle, A., Zhang, W., Duan, Z., 2018. Service-Oriented Cooperation Policies for Intelligent Ground Vehicles Approaching Intersections. *Appl. Sci.* 8, 1647. <https://doi.org/10.3390/app8091647>
- Zhang, W., Guhathakurta, S., Fang, J., Zhang, G., 2015. Exploring the impact of shared autonomous vehicles on urban parking demand: An agent-based simulation approach. *Sustain. Cities Soc.* 19, 34–45. <https://doi.org/10.1016/J.SCS.2015.07.006>
- Zhao, W., Ngoduy, D., Shepherd, S., Liu, R., Papageorgiou, M., 2018. A platoon based cooperative eco-driving model for mixed automated and human-driven vehicles at a signalised intersection. *Transp. Res. Part C Emerg. Technol.* 95, 802–821. <https://doi.org/10.1016/J.TRC.2018.05.025>
- Zhou, Y., Cholette, M.E., Bhaskar, A., Chung, E., 2018a. Optimal Vehicle Trajectory Planning With Control Constraints and Recursive Implementation for Automated On-Ramp Merging. *IEEE Trans. Intell. Transp. Syst.* 1–12. <https://doi.org/10.1109/TITS.2018.2874234>
- Zhou, Y., Cholette, M.E., Bhaskar, A., Chung, E., 2018b. Automated On-Ramp Merging and Gap Development with Speed Constraints – A State-Constrained Optimal Control Approach, in: 2018 Annual American Control Conference (ACC). IEEE, pp. 4975–4982. <https://doi.org/10.23919/ACC.2018.8430796>
- Zohdy, I.H., Kamalanathsharma, R.K., Rakha, H., 2012. Intersection management for autonomous vehicles using iCACC, in: IEEE Conference on Intelligent Transportation Systems, Proceedings, ITSC. <https://doi.org/10.1109/ITSC.2012.6338827>
- Zohdy, I.H., Rakha, H.A., 2016. Intersection Management via Vehicle Connectivity: The Intersection Cooperative Adaptive Cruise Control System Concept. *J. Intell. Transp. Syst.* 20, 17–32. <https://doi.org/10.1080/15472450.2014.889918>
- Zoox, 2018a. Safety Innovation At Zoox 1–30.
- Zoox, 2018b. Zoox Disengagement Report.